Analysis of Swine Leukocyte Antigen Peptide Binding Profiles and the Identification of T cell Epitopes by Tetramer Staining

Pedersen, Lasse Eggers

Publication date:
2012

Document Version
Publisher's PDF, also known as Version of record

Analysis of Swine Leukocyte Antigen Peptide Binding Profiles and the Identification of T cell Epitopes by Tetramer Staining

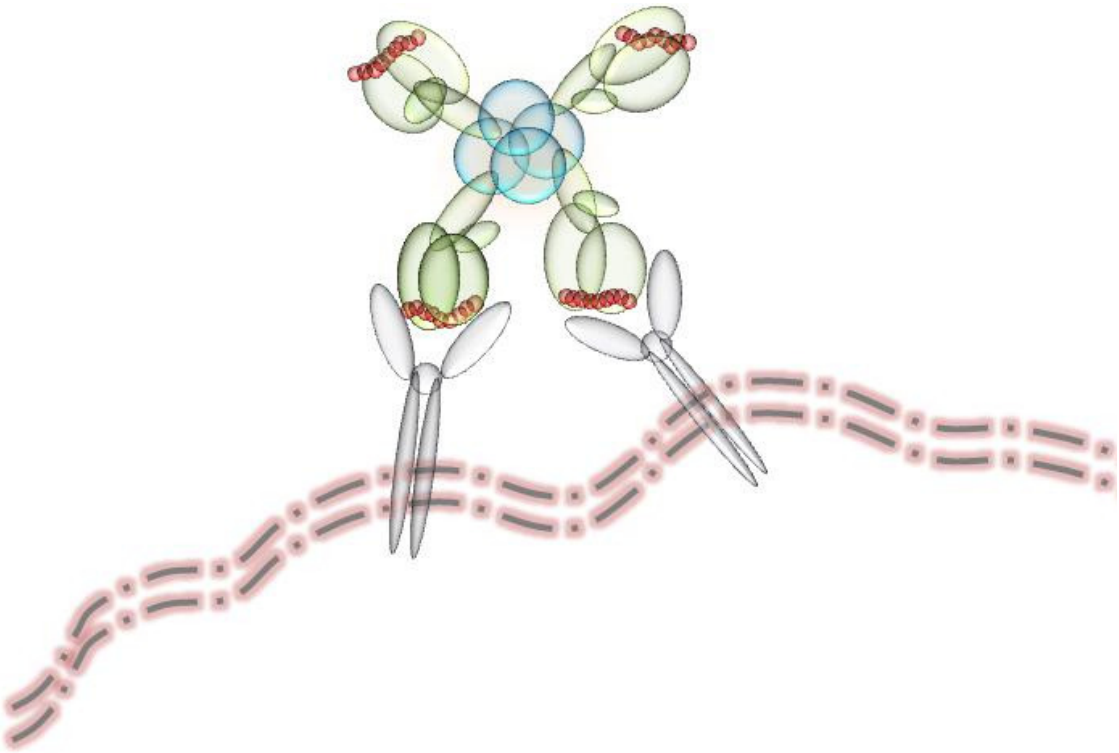

PhD Thesis

Lasse Eggers Pedersen

2012

DTU Vet
National Veterinary Institute

„Think Big About Small Things"

Lasse Eggers Pedersen, September 2003

Supervisors:

Professor Gregers Jungersen

Section for Immunology and Vaccinology

National Veterinary Institute

Technical University of Denmark

Professor Søren Buus

Department of International Health, Immunology and Microbiology

Faculty of Health and medical Sciences

University of Copenhagen

Dr. William T. Golde

Foreign Animal Disease Unit

Plum Island Animal Disease Center, Agricultural Research Service

United States Department of Agriculture, United States Department of Homeland Security

Assessment committee:

Professor Peter M. H. Heegaard (chairperson)

Section for Immunology and Vaccinology

National Veterinary Institute

Technical University of Denmark

Professor Armin Saalmüller

Institute for Immunology

University of Veterinary Medicine Vienna

Professor Søren Skov

Laboratory of Immunology

Faculty of Life Sciences

University of Copenhagen

Front page artwork; Sketch animation of an SLA class I tetramer recognized by T cell receptors at the cell surface, by Lasse Eggers Pedersen, December 2012.

Analysis of Swine Leukocyte Antigen Peptide Binding Profiles and the Identification of T cell Epitopes by Tetramer Staining

Table of Contents

Preface

I clearly remember my first encounter with the Major Histocompatibility Complex (MHC) class I protein. It was during the final year of my bachelor's degree program in biochemistry and I was attending a course in Protein Science. My group decided to work with the MHC molecule because it was obvious that here was a protein with a striking functionality. What I did not know was how it was related to immunology. In fact I did not know anything about immunology at that time. Choosing the MHC molecule as our model in protein science turned out to be the spark from which my passion for immunology burn strongly today.

After the course I was hooked on MHC, and decided to contact Professor Søren Buus, whom I would later find was one of the world leading experts in this field. This was how I really got the appetite for immunology and fortunately, Prof. Søren Buus agreed to let me into his Laboratory of Experimental Immunology at the University of Copenhagen to do my bachelor's, and later

my Master's degrees in Biochemistry. For reasons that I do not know, Søren had just recently put his interest into porcine MHC molecules, and hence he had his student (me) produce, characterize and analyze Swine Leukocyte Antigen (SLA) proteins; The porcine MHC class I molecules. Those three years of working with SLA introduced me to different areas of protein science, biochemistry and not least immunology. Surrounded by extremely skilled and professional people I was taught not only how to navigate in a laboratory but also how to design, set up and adjust techniques to fit different experimental approaches on the way in trying to solve scientific questions and problems that I have encountered, and hopefully will continue to encounter throughout my career.

Graduating from the University of Copenhagen I found myself being a "still-wet-behind-the-ears" but fairly well trained post Master's scientist with a granted fellowship to go and work for the United States Department of Homeland Security (DHS) and Department of Agriculture (USDA). Through Prof. Søren Buus I got connected with Dr. William T. Golde and Prof. Gregers Jungersen. These three scientists turned out to play a major role in my future research and education as my PhD thesis mentors. A scientific collaboration forged between the Technical University of Denmark (DTU), the University of Copenhagen (KU) and the USDA at Plum Island Animal Disease Center (PIADC) in New York, USA, where I moved to and lived for a year and a half to perform part of my thesis research. The rest of the research and work was carried out in Copenhagen, Denmark at KU and DTU.

The research presented in this Ph.D. thesis was performed in the Section for Immunology and Vaccinology, National Veterinary Institute, Technical University of Denmark, Copenhagen, at the Institute of International Health, Immunology and Microbiology (ISIM), University of Copenhagen, Denmark and at the United States Department of Homeland Security, Plum Island Animal Disease Center, New York, USA in the period 2009 - 2012.
The project was funded by the Danish Council for Independent Research, Technology and Production Sciences (274-09-0281) in collaboration with the Agricultural Research Service, USDA (CRIS #1940-32000-053-00D) and the United States National Institutes of Health (NIH) (HHSN266200400025C).

The thesis consists of eight chapters starting with an introduction to the field of immunology seeing the MHC class I molecule as the focal point, followed by chapter 2 which describes specific methodological approaches and other considerations. Chapters 3 – 6 are devoted to the four manuscripts which constitute the backbone of this thesis. These chapters also include respective results as well as general discussion. Chapter 7 discusses the SLA tetramer work related to paper IV and influenza tetramer staining experiments performed at DTU. The eighth and final chapter concerns general conclusions on the topic and thesis work as well as perspectives.

This thesis includes four manuscripts (I – IV):

- Paper I **Pedersen LE**, Harndahl M, Rasmussen M, Lamberth K, Golde WT, Lund O, Nielsen M, Buus S. *Porcine major histocompatibility complex (MHC) class I molecules and analysis of their peptide-binding specificities*. Immunogenetics. 2011 Dec;63(12):821-34. doi: 10.1007/s00251-011-0555-3.
- Paper II **Pedersen LE**, Harndahl M, Nielsen M, Patch JR, Jungersen G, Buus S, Golde WT. *Identification of peptides from foot-and-mouth disease virus structural proteins bound by class I swine leukocyte antigen (SLA) alleles, SLA-1*0401 and SLA-2*0401*. Animal Genetics. 2012 Sep 18. doi: 10.1111/j.1365-2052.2012.02400.x.
- Paper III **Pedersen LE**, Rasmussen M, Harndahl M, Nielsen M, Buus S, Jungersen G. *An analysis of affinity and stability in the identification of peptides bound by Swine Leukocyte Antigens (SLA) combining matrix- and NetMHCpan based peptide selection*. Manuscript ready for submission to Immunogenetics.
- Paper IV Patch JR, **Pedersen LE**, Toka FN, Moraes M, Grubman MJ, Nielsen M, Jungersen G, Buus S, Golde W.T. *Induction of foot-and-mouth disease virus-specific cytotoxic T cell killing by vaccination*. Clinical and Vaccine Immunology: CVI. 2011 Feb;18(2):280-8.

Figure 1 illustrates the relation between the four manuscripts.

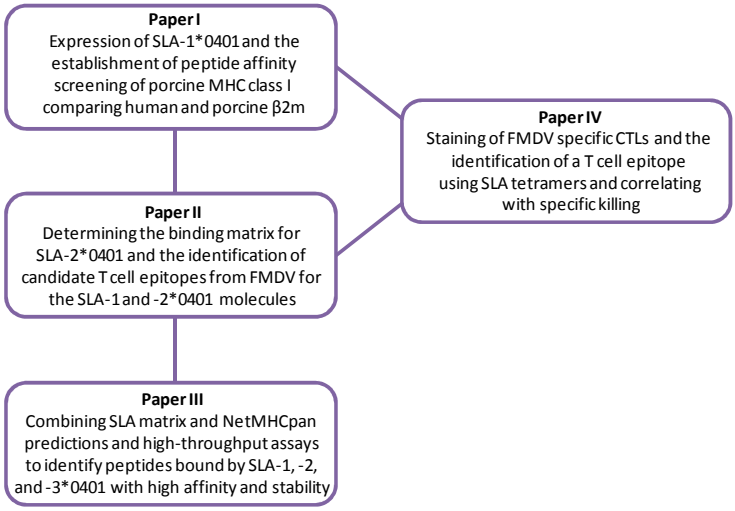

Figure 1. Diagram illustrating how the manuscripts of this thesis are related.

Acknowledgements

I have learned that great things are rarely achieved alone. For the past three years I have crossed paths and thoughts with a lot of interesting people. My path has taken me from Copenhagen to New York, dropping by Baltimore, further educating myself in Minneapolis, learning about livestock viruses in Barcelona, presenting research in Tokyo, expanding my horizon in Edinburgh before returning to Copenhagen. All the people that I have met on this journey deserve a thank you for all the interesting discussions, for sharing of research ideas as well as results, for opening their doors, for listening to opinions and for contributing to my development and education as a scientist as well as a person.

I would like to thank my mentor and main advisor Prof. Gregers Jungersen for welcoming me into his group at DTU, for making this project possible and for always being supportive and taking his time to reflect on and help with ongoing projects and scientific problems.

My two co-advisors deserve special thanks as well;

Prof. Søren Buus for teaching me that serious work often produce serious results and for reminding me that science is far from always easy, nor logic.

Dr. William Golde for letting me into his laboratory as well as into his family, for all the scientific discussions and exciting experimental setups made possible by him and for putting an honor in being my mentor.

A big thank you goes to my science buddy and good friend Michael Rasmussen. Thank you for being critical upon my results and data analysis as well as for discussing interesting topics about anything under the sun. Our Friday afternoons at Mikkeller's brew house has not only been fun but also inspiring.

I thank all the people in the Section for Immunology and Vaccinology, National Veterinary Institute, DTU for their kind help in the laboratory as well as in regard to general issues and problems, for advice and lunch time conversations, and for making me feel as part of a social, diverse and very professional group of people, all connected by veterinary science. I owe Ulla Riber, Dorte Fink Vadekær and Panchale Olsen a special thanks for their help with flow cytometry, SLA typing and peptide affinity tests, respectively.

I also thank the Buus group at the Institute of International Health, Immunology and Microbiology (ISIM), University of Copenhagen for always providing help and expertise when needed. Particularly, I thank Mikkel Harndahl for his help with our high-throughput peptide binding experiments as well as discussing the data output with me. The same goes for Morten Nielsen of the Center for Biological Sequence Analysis, DTU, without whose contributions and knowledge this thesis work would not have been what it is today.

All the people who are, or have been, part of the Golde group at PIADC in New York, during the time that I have been working there deserve a warm thank you for always making me feel welcome and as a part of the team, and for helping me with the continuous porcine tetramer work that we have been performing on and off for the past three years. Special thanks goes to Jared Patch for numerous discussions on different scientific topics, for escorting me in the BSL-3 facility before I got my Select Agent Clearance from FBI and for coming early and staying late on the island with me whenever it was needed.

Last but not least, I would like to thank my friends and family. Without them none of this would ever have been possible. I would like to thank my friends for sharing my enthusiasm, frustration and laughs, and I would like to thank you, my mom and dad, for always believing in and supporting me, for telling me how good I am and for never letting me doubt how proud you are of me. A warm thank you goes to my sister Rikke as well, for always listening to what I have to say and for sharing ideas. Finally, I would like to thank my wife, my love, my life, Kristina for her limitless support and patience with me. You are always there when I need you the most.
It has been three intense years, which have required some sacrifice but also given me a tremendous insight in the field of immunology as well as in myself. I am looking forward to seeing all of you again now that my thesis is written and published.

Thank You

Copenhagen, December 2012.
Lasse Eggers Pedersen

Summary

The immune system has evolved in such a way that it is capable of specifically distinguishing between *self* and *non-self* structures. Combining this with the ability to memorize and strongly prepare for all pathogens that it has previously encountered, is essential for the proper and effective function of the immune system, and provides the cornerstone for vaccine design. In all vertebrate animals, $CD8^+$ cytotoxic T lymphocytes (CTLs) survey the intracellular environment for signs of invasion by pathogenic organisms such as viruses and bacteria. CTLs survey major histocompatibility complex (MHC) class I molecules, which are highly polymorphic peptide receptors which select and present endogenously derived peptides to circulating CTLs. Peptides that are recognized by CTLs in the context of MHC are epitopes, and represent a small sample of the pathogen proteome, making it possible for the immune system to specifically identify and react upon non-self peptide fragments unique only to the foreign intruder. The

polymorphism of the MHC molecule effectively individualizes the immune response of each member of any given species. Moreover, responding T cells recognize antigen ligands, *only* in the context of peptide:MHC:β_2m (pMHC) complex.

The gene encoding the MHC is one of the most polymorphic regions of the genome known. Despite thousands of different human leukocyte antigen (HLA) variants identified, each member of a species only inherits and expresses a few of these MHC alleles. The "MHC fingerprint" of an individual can be identified by defining MHC alleles. This is classically called "tissue typing" and is done by analyzing the reactivity of peripheral blood cells with sera unique to MHC alleles. Such knowledge is paramount to analysis of the immune response regarding MHC restriction and CTL recognition of pathogen-specific proteins.

Most of the polymorphism of MHC proteins is resident in the peptide binding groove. Hence, each MHC is unique in the way it binds peptides, and by inference it individualizes the entire T cell repertoire of the host. In this way, the diversity of MHC within a species makes immune escape almost impossible for any intruding pathogen.

Characterization of the SLA class I and class II gene products and their peptide binding capacity defines the T cell epitopes of any given pathogen proteome.

To date the analysis of MHC peptide interactions, strength (affinity) and stability of the peptide:MHC complex, has been extensively reported in mice and humans, whereas data for livestock animals such as the pig is rather limited. This thesis describes adapting and applying analytical approaches, originally developed for man and mice to understand porcine MHC class I peptide binding characteristics in relation to immune responses to vaccination or infection. Applying proven technologies to newly produced, recombinant swine leukocyte antigen (SLA) class I proteins yielded a body of data for peptide:SLA:β_2m (pSLA) complex affinity and stability. Mapping the SLA proteins for their peptide binding requirements along with the identification of their cognate virally derived peptides, made it possible to explore the nature of the SLA proteins and the roles they play in establishing adaptive immunity. The development of SLA tetramers, enabled investigation of the specific CTL response elicited as a result of immunization against foot-and-mouth-disease virus (FMDV) and swine influenza A virus. These studies resulted in the identification of T cell epitopes from both viruses.

As SLA:peptide binding data accumulates in these and similar studies, it becomes possible for collaborators at Center for Biological Sequence Analysis (CBS), DTU, to further strengthen the *NetMHCpan* algorithm. This prediction tool now has the capacity for the selection of peptide candidates to be bound by human (HLA), bovine (bovine leukocyte antigen (BoLA)) and swine (SLA) MHC proteins.

Expanding the knowledge of porcine MHC class I molecules, mapping their peptide binding matrices, and producing tetramers as well as improving today's state-of-the-art method for SLA peptide prediction will modernize immunological science of livestock species. These approaches and results should lead to accelerated development of vaccines with increased efficacy due to optimal activation of cell-mediated immune responses with minimal adverse events.

Resumé (Danish summary)

Immunsystemet har udviklet sig på en sådan måde, at det er i stand til specifikt at skelne mellem *selv* og *ikke-selv* strukturer. Ved at kombinere dette med evnen til effektivt at huske og forberede sig imod samtlige patogener, som det tidligere er stødt på, er af afgørende betydning for et korrekt og effektivt fungerende immunsystem og er selve grundstenen i ethvert design af vacciner. I alle hvirveldyr overvåger kroppens $CD8^+$ cytotoksiske T-lymfocytter (CTL'er) det intracellulære miljø i søgen efter tegn på invasion af udefrakommende patogene organismer såsom virus og bakterier. CTL'er overvåger major histocompatibilitets kompleks (MHC) klasse I molekyler, som er stærkt polymorfe peptid-receptorer, der udvælger og præsenterer endogent afledte peptider til cirkulerende CTL'er. Peptider, der genkendes af CTL'er i samspil med MHC molekylet, er såkaldte epitoper og repræsenterer et lille fragment af det patogene proteom, hvilket gør det muligt for immunsystemet specifikt at identificere og reagere imod fremmede peptid fragmenter, som er unikke for den invaderende patogen. MHC molekylets polymorfi er det, der individualiserer immunresponset for hvert enkelt individ i en given art. Endvidere genkender kroppens T-celler kun antigene peptid ligander, når de fremstår som del af det trimere peptid:MHC:β_2m (pMHC) kompleks.

Genet der koder for MHC er kendt som en af de mest polymorfe regioner i genomet. Til trods for eksistensen af tusindvis af forskellige humane leukocyt antigen (HLA) varianter, arver og udtrykker hvert medlem af en art kun et par stykker af disse MHC alleler. Selve "MHC fingeraftrykket" udtrykt af et individ, kan identificeres ved at definere MHC alleler. Den unikke MHC allel kan fastslås ved en metode, traditionelt kendt som ”vævstypebestemmelse”, som foretages ved at analysere perifere blod cellers reaktivitet overfor vævstypnings-sera. En sådan viden er afgørende, for at kunne analysere et immunrespons i forhold til MHC restriktion og CTL genkendelse af patogen-specifikke proteiner.

Størstedelen af MHC proteinets polymorfi er lokaliseret i den peptidbindende kløft. Derfor er hvert enkelt MHC molekyle unikt i måden det binder peptid-antigener på og som følge heraf individualiseres også hele individets T-celle repertoire via MHC. På denne måde er de enkelte MHC molekylers forskellighed indenfor en bestemt art medvirkende til, at det stort set er umuligt for indtrængende patogener, at undslippe immun systemets søgelys.

Karakterisering af individuelle SLA klasse I- og klasse II gen produkter og deres unikke peptid bindende kriterier definerer T-celle epitoper fra ethvert givent patogen proteom.

Til dato er analysen af MHC klasse I molekylets evne til at binde og præsentere peptider, både i form af bindingsstyrke (affinitet) og stabilitet af peptid:MHC komplekset, blevet omfattende beskrevet i både mus og mennesker. Sådanne data er stadig relativt begrænsede for landbrugs dyr såsom svin. Denne ph.d. afhandling beskriver hvorledes analytiske tilgange, der oprindeligt er udviklet til mennesker og mus, kan tilpasses og anvendes i grise, for at opnå en bedre forståelse af de porcine MHC klasse I molekylers peptid-bindings karakteristika i forbindelse med immun responser rejst imod vaccinering eller infektion. En sådan anvendelse af tidligere afprøvede analyse metoder sammen med nyligt producerede, rekombinante SLA klasse I proteiner, førte til en betydelig mængde data for peptid:SLA:β_2m (pSLA) kompleksets affinitet og stabilitet. Kortlægning af SLA proteinernes bindingsmotiver samt identifikationen af matchende virale peptider, gjorde det muligt at undersøge beskaffenheden af de forskellige SLA proteiner samt de roller, de spiller i etableringen af adaptiv immunitet. Udviklingen af pSLA-baserede tetramerer muliggjorde endvidere studier af specifikke CTL responser fremkaldt som

et resultat af immunisering mod mund- og klovesyge virus (MKS) og svine influenza A virus. Disse undersøgelser resulterede i identifikationen af T-celle epitoper fra begge virus.
Med stadigt stigende mængder peptid bindings data for de forskellige SLA molekyler, opnået igennem disse samt andres studier, er det muligt for vores samarbejdspartnere på Center for Biologisk Sekvensanalyse (CBS), DTU, yderligere at styrke og forbedre den peptid forudsigende algoritme *NetMHCpan*. Denne forudsigelses algoritme er nu i stand til at udpege peptid kandidater til binding af både humane (HLA), kvæg (BoLA) og svine (SLA) MHC proteiner.

Ved at udvide kendskabet til porcine MHC klasse I molekyler, kortlægge deres peptid bindings motiver og producere pSLA baserede tetramerer, samt forbedre nutidens aktuelle tekniske niveau indenfor metoder til at forudsige SLA peptid binding, kan vi modernisere immunologisk videnskabelige studier i landbrugs dyr. Disse fremgangsmåder og resultater må forventes at føre til en fremskyndet og forbedret udvikling af vacciner med forøget effektivitet, på grund af optimal aktivering af det cellemedierede immunrespons med tilhørende minimale bivirkninger.

Abbreviations

(In order of appearance)

MHC	Major Histocompatibility Complex
SLA	Swine Leukocyte Antigen
DHS	Department of Homeland Security
USDA	United States Department of Agriculture
DTU	Technical University of Denmark
KU	University of Copenhagen
PIADC	Plum Island Animal Disease Center
ISIM	Institute of International Health, Immunology and Microbiology
NIH	National Institutes of Health
CTLs	Cytotoxic T Lymphocytes
pMHC	peptide:MHC:beta-2-microglobulin *or* peptide:MHC:β_2m
HLA	Human Leukocyte Antigen

FMDV	Foot-and-Mouth-Disease Virus
CBS	Center for Biological Sequence analysis
BoLA	Bovine Leukocyte Antigen
DC	Dendritic Cell
NK	Natural Killer cell
Ab	Antibody
Ig	Immunoglobulin
T_h	T Helper cell
T_{reg}	Regulatory T cell
PRRs	Pattern-Recognition Receptors
BCR	B Cell Receptor
TCR	T Cell Receptor
IL	Interleukin
IFN	Interferon
TAP	Transporter associated with Antigen Processing
IPD	Immune Polymorphism Database
ER	Endoplasmic Reticulum
PLC	Peptide Loading Complex
IFN	Interferon
TNF	Tumor Necrosis Factor
HA	Hemagglutinin
NA	Neuraminidase
ORF	Open Reading Frame
VPg	Viral Protein genome-linked
UTR	Untranslated Region
IRES	Internal Ribosome Entry Site
FMD	Foot-and-mouth Disease
AA	Amino Acid
UK	United Kingdom
OIE	Office International des Epizooties

DIVA	Differentiating Infected from Vaccinated Animals
Ad5	Adenovirus 5
PRRSV	Porcine Reproductive and Respiratory Syndrome Virus
ASFV	African Swine Fever Virus
VSV	Vesicular Stomatitis Virus
PCR-SSP	PCR Sequence-Specific Primers
PBMCs	Peripheral Blood Mononuclear Cells
ELISA	Enzyme-Linked Immunosorbent Assay
LOCI	Luminescent Oxygen Channeling Immunoassay
SPA	Scintillation Proximity Assay
PK15	Porcine Kidney cell line 15
TCID50	Tissue Culture Infective Dose 50% pathological change
BoLA	Bovine Leukocyte Antigen
APC	Allophycocyanin
BV421	Brilliant Violet
EBV	Epstein-Barr Virus
CMV	Cytomegalovirus
SIP	Synthetic Immunogenic Protein
Ad-SIP	Adenovirus Vaccine Vectored SIP
CAF	Cationic Adjuvant System
ISCOMs	Immune Stimulatory Complexes

List of Figures

1. Introduction

1.1. THE IMMUNE SYSTEM

In a world in which we are constantly exposed to pathogenic microbes and viruses it is astounding how rarely we actually get ill. The primary reason for this is the immune system, which consists of an array of different cells and mechanisms that form the body's defense system. The ability of the immune system to successfully overcome incessant pathogenic invasions relies on its aptitude to sense and evaluate microbial threats leading to the control and/or elimination of the intruding pathogen with minimal collateral host tissue destruction and alteration of homeostasis (Goldszmid and Trinchieri 2012). Protection of the host against the different responses of its own immune system is achieved by various levels of tight regulation (Banchereau et al. 2012, Germain 2012, Murray and Smale 2012). The immune system of vertebrates is often divided into two main arms; the *innate* and the *adaptive* immune systems (Messaoudi et al. 2011). These systems rely on different immune cells generated in the bone marrow from a common precursor (Figure 2), which display various functions. It is a delicate balance between these two branches, and a coordinated action of their respective

cells, which underlies the immunologic function and success on which the host overall health depends.

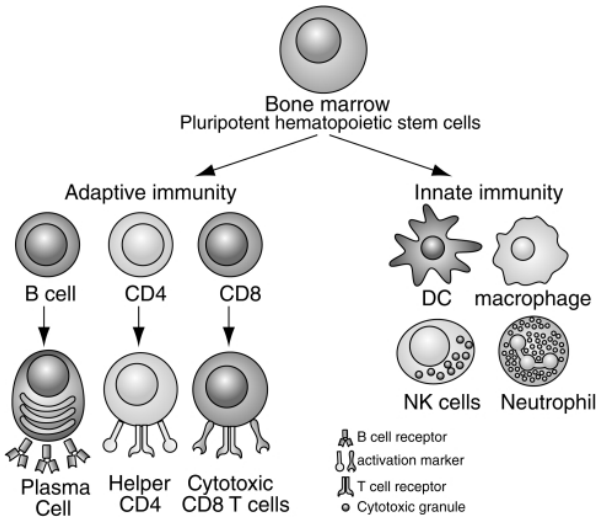

Figure 2. Key cellular components of the adaptive and innate branches of the immune system. Dendritic cells (DC), natural killer cells (NK). The figure is adapted from (Messaoudi et al. 2011).

Traditionally, the immune response has been characterized by the type of antibodies (Ab) produced and their ability to mediate a range of functions. Different antigens and differential regulation of B cell stimulation, proliferation and differentiation into plasma cells (Shapiro-Shelef and Calame 2005) leads to the production of Abs of various immunoglobulin (Ig) isotypes. These different isotypes mediate effector functions such as neutralization, complement fixation and opsonization of pathogens. With notable exceptions, the humoral immune response is controlled by T lymphocytes that regulate B cell responses via the cytokines they produce. This includes the T helper (T_h) subsets, T_{h1}, T_{h2}, T_{h17}, Th_{21}, and the $CD4^+/CD25^+/Foxp3^+$ regulatory T cells (T_{reg}). In addition to the effector function mediated by B cells, a principal T cell effector function is mediated by the $CD8^+$ cytotoxic T lymphocyte (CTL) lineage. These cells are critical in anti-viral responses as they detect and kill virus infected cells. A detailed overview of the different cells, cell stages and primary cytokines involved in the induction and regulation of the innate and adaptive immune responses is illustrated in Figure 3 (Thakur et al. 2012).

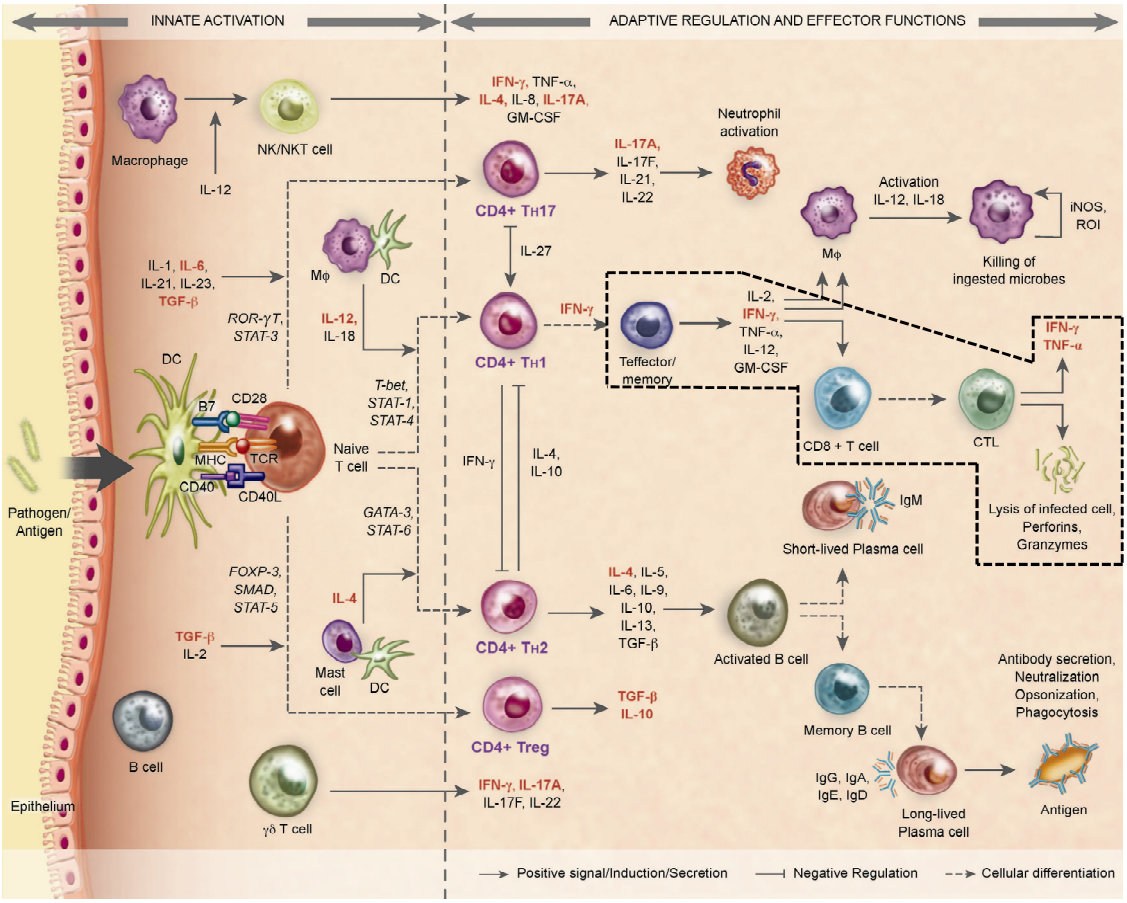

Figure 3. Illustration of the different cells and cell stages involved in the induction and regulation of the innate and adaptive immune responses. The figure was published in July 2012 by (Thakur et al. 2012), the author of this thesis being co-author. For clarification, the primary focus of this thesis has been framed (dashed line square).

1.1.1. Innate Immunity

The innate immune response is the body's first and primary line of defense against pathogenic intruders, and provides immediate responses to a given infection, but without the establishment of long lasting protection. The primary line of defense consists of mechanical barriers like the gut and skin which are difficult for pathogens to penetrate.

The primary leukocytes mediating innate responses are the NK cells, mast cells, eosinophils and basophils, also including the phagocytic cells; macrophages, dendritic cells and neutrophils (Murphy et al. 2008). Two key functions of the innate immune system are the capacity to broadly recognize and respond to conserved microbial products that are distinctive for non-eukaryotic cells, mediated by germline encoded pattern-recognition receptors (PRRs), and recruitment of adaptive immune cells to the site of infection by the induction and production of cytokines (Janeway, Jr. 1989, Medzhitov 2007).

1.1.2. Adaptive Immunity

In contrast to the innate immune system, the adaptive immune system is not immediate, and it takes time for specialized cells to be stimulated and proliferate in response to an infection. Compared to the innate immunity that relies on germline-encoded receptors to detect the presence of pathogens, the adaptive immune system utilizes a highly diverse set of antigen receptors generated through somatic recombination of gene segments, thereby creating huge numbers of B cell receptors (BCR) and antibodies with different specificities (Baranov and Eppel' 1984, Tonegawa 1983). The antigen receptor on T cells, the T cell receptor (TCR), can be nearly as diverse with specificities exceeding 10^{15} (Davis and Bjorkman 1988, Messaoudi et al. 2011, Schatz 2004, Tonegawa 1983). TCR diversity is dependent on inexact recombination of gene segments during T cell development (Robins et al. 2009). The difference in antigen recognition by BCRs and TCRs lies in the way B cells directly recognize antigens, whereas T cells recognize antigens (*non-self*) in *association* with MHC (*self*), hereby combining the two (Danilova 2012). Such MHC restriction is particularly important during the development and maturation of primary lymphocytes in the thymus where T cells are forced to walk the fine line of *positive selection* (Anderson and Takahama 2012, Bevan 1977, Kisielow et al. 1988). In the bone marrow, auto-reactive B cells on the other hand, are *negatively selected* leading to apoptosis (Gay et al. 1993, Hartley et al. 1993). B cell subsets are involved in the humoral immunity by producing antibodies while T cells are responsible for the cellular immunity and regulatory functions (Danilova 2012). TCR genomic rearrangements enable the adaptive immune response to produce receptors capable of covering the extremely diverse pathogenic pool by recognition of nearly any possible molecular structure.

During T cell development, positive selection ensures that T cells, expressing TCRs with self MHC:peptide binding of a low level of affinity, receive sufficient signal to survive and further develop. At this point T cells expressing a TCR stimulated by self MHC:peptide complexes, i.e. *auto-reactive*, undergo negative selection resulting in induced apoptosis.

Mature, naïve T cells leave the thymus and start to patrol the lymphatic system of the host in a constant search for pMHC complexes suitable for their specialized TCR. Upon encounter of a

pMHC complex presenting a foreign peptide antigen the T cell goes from being naïve to becoming activated, undergoing proliferation and eventually exiting the lymphatic system in high numbers. From there they migrate to the site of infection to clear the pathogenic invaders. Once the immediate infection has been cleared most of the activated effector cells will die off, whereas a minor subset of activated T cells will survive, and dependent on cytokine signals, such as interleukin (IL)-12 or interferon (IFN)-α at distinct stages of the response, become resting *memory* T cells (Mescher et al. 2006, Parish and Kaech 2009). These cells keep an elevated precursor frequency of the activated T cells, capable of functioning as fast responders to any subsequent similar infection.

1.2. MHC CLASS I AND THE SWINE LEUKOCYTE ANTIGEN

A large gene family exists in all vertebrates that encode the major histocompatibility complex (MHC) cell surface molecules. These proteins are sub divided into three classes of molecules, I, II and III. In humans, non-human primates and livestock animals, the focus is commonly set on the MHC class I and II proteins. Also encoded in this gene locus are several other proteins such as the transporter associated with antigen processing (TAP1 and TAP2), tapasin, MHC II DM and DR, which are involved in the processing and load of antigen into the MHC binding groove (Cresswell et al. 1999, Wijdeven et al. 2012).

The MHC class I proteins are encoded by a highly polymorphic gene cluster in most jawed vertebrates (Ho et al. 2009c, Ujvari and Belov 2011). They are important protein determinants in immune responses to infectious diseases and vaccines, as well as to autoimmunity and in graft acceptance/rejection (Horton et al. 2004, Kelley et al. 2005, Singer et al. 1997). This region was originally discovered through genetic studies of transplant *incompatibility* and the related function of these proteins to create *histocompatibility*, or "self" identification through cell surface expression of these highly polymorphic proteins (Gorer et al. 1948). The MHC class I molecules are glycosylated, membrane-anchored proteins found on almost every nucleated cell in vertebrates.

The MHC class I trimeric complex is made up of a heavy chain protein of approximately 43 kDa, simultaneously non-covalently bound to the stabilizing subunit protein light chain, β_2m of 12 kDa, and exogenous peptide (Cresswell et al. 1973, Grey et al. 1973). The heavy chain is made

up of three alpha domains, α_1, α_2 and α_3 in addition to a membrane spanning domain and a small cytosolic C-terminal tail (Figure 4). Most of the sequence variation is found in the α_1 and α_2 domains which are responsible for the binding of exogenous peptides within the MHC class I *peptide binding groove*, whereas the α_3 domain and β_2m are far more conserved expressing homology to immune globulin domains (Bjorkman et al. 1987a, Bjorkman et al. 1987b, Orr et al. 1979). The higher conservancy of the α_3 domain is most likely due to its role in the interaction with the CTL surface expressed co-receptor CD8 (Salter et al. 1989).

In pigs the MHC is termed swine leukocyte antigen (SLA). The existence of the SLA complex was clearly established more than 40 years ago (Vaiman et al. 1970, Viza et al. 1970), and it was later determined that the SLA region extends for 2.0 Mbp on chromosome 7 (Chardon et al. 2000). Six different loci encode the classical (SLA-1, SLA-2, SLA-3) and non-classical (SLA-6, SLA-7, SLA-8) SLA class I molecules (Ho et al. 2009b, Kusza et al. 2011). The SLA molecules are highly polymorphic and extensive comparisons of the classical SLA class I and human MHC class I genes (*HLA-A*, *HLA-B*, and *HLA-C*) have concluded, that there are more sequence homology amongst the SLA genes than between any of these SLA loci and any HLA class I gene (Smith et al. 2005). Furthermore, the overall genomic organization of the SLA class I region is quite different from that of the HLA class I region (Lunney et al. 2009). As a result, the SLA class I genes were assigned with numbers to avoid the implications that any loci were more homologous to the genes of the HLA system. The non-classical class I genes are categorized so because of their *limited* polymorphism and slight variations in the 3' end specific of the cytoplasmic tail compared to the three classical genes (Chardon et al. 2001). All SLA allele sequences reported to date are publicly available at the Immune Polymorphism Database (IPD)-MHC (http://www.ebi.ac.uk/ipd/mhc/sla/index.html).

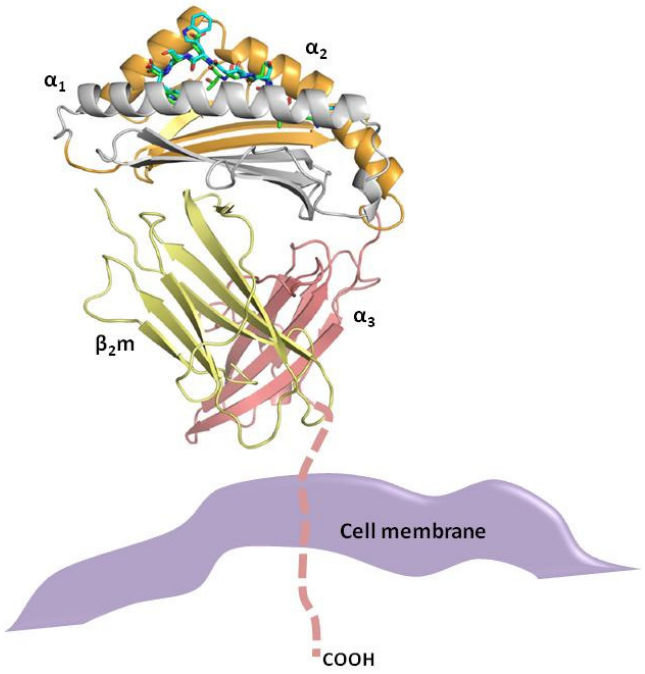

Figure 4. Membrane bound SLA-1*0401 molecule illustrated with two different peptides bound (swine influenza A- (blue) and *Ebola* virus-derived (green)). The α_1, α_2, and α_3 domains are displayed in grey, orange and pink, respectively, forming the heavy chain. The stabilizing subunit light chain, β_2m, is shown in yellow. The membrane spanning domain and cytoplasmic C-terminal (COOH) tail is illustrated by the dotted line. The figure is modified from (Zhang et al. 2011).

The diversity in peptide ligand binding of the SLA proteins has been shown to influence swine adaptive immune traits (Mallard et al. 1989a, Mallard et al. 1989b), vaccine responsiveness (Lumsden et al. 1993, Rothschild et al. 1984) and disease resistance (Lacey et al. 1989, Madden et al. 1990). Like the HLA molecules of humans, the SLA class I molecules of swine form a binding groove which can be divided into six pockets responsible for binding of the individual peptide antigen residues. These pockets are termed A, B, D, C, E and F and are responsible for the binding of peptide residues P1, P2, P3, P6, P7 and P9, respectively (Madden 1995, Zhang et al. 2011). The peptide specificity between different class I molecules is extremely diverse and is defined by structural requirements such as the presence of certain amino acids in specific positions of the peptide, especially at the peptide termini which account for most of the peptide-MHC interactions by hydrogen bonds between the peptide backbone and the MHC binding groove (Madden et al. 1992). These residues are often referred to as *anchor positions* and define the binding motif of each individual MHC class I molecule.

For most MHCs, the critical residues for peptide binding are the P2 and P9 (or C-terminus if the peptide is not a 9mer) of the peptide (Kubo et al. 1994). The side chains at P1, P4 and P5 of the peptide generally protrude toward the solvent and away from the peptide binding groove making them available for TCR recognition, whereas the P2, P3, P6 and P9 side chains face into the groove and stay shielded from the TCR. The A and F pocket structures are well conserved among many class I molecules. In comparison, those of the B through E pockets differ greatly between heavy chains with respect to size and chemical nature (Matsumura et al. 1992), sometimes leading to alternative peptide anchors in one of these pockets.

Degradation of cytosolic proteins predominantly by the proteasome, generates peptides of both self and non-self origin depending on the status of the cell. Such peptides are actively transported into the lumen of the *Endoplasmic Reticulum* (ER) by the TAP1 and TAP2 and loaded onto the MHC class I in symphony with components of a multi molecular unit termed the peptide loading complex (PLC) (Dalchau et al. 2011, Elliott and Williams 2005). Once a peptide has been bound, the mature pMHC complex is being released from the PLC in the ER and into the *Golgi Apparatus* from where it is transported to the cell surface. At the surface pMHC complexes can be scanned by circulating $CD8^+$ CTLs. In such a way, pSLA complexes constantly signal the cell's current state of integrity to the immune system of the host. Upon recognition of foreign, non-self peptides, specific CTLs become activated to kill the infected or transformed cell (Bevan 1995, Doherty and Zinkernagel 1975, Harty et al. 2000), even though a given peptide:MHC complex is estimated to be present at the cell surface at 10 - 400 copies per cell (Hunt et al. 1992).

The high number of SLA class I molecules and the level of polymorphism observed ensure the diversity between different alleles. The number of MHC loci varies among species. Humans and swine can express up to six different MHC class I molecules if they are heterozygous at all three class I loci. However, the presence of duplicated loci leading to copy number variance of some loci of classical SLA class I genes has been suggested to occur among SLA haplotypes (Ho et al. 2009b, Ho et al. 2010b). Such duplication leads to encoding of more than two class I alleles of a gene in animals heterozygous for that particular locus (Ho et al. 2010b, Tanaka-Matsuda et al. 2009). Altogether, such SLA heterozygosity increases immune-competence in that a greater

variety of antigens are likely to be presented leading to a more robust immune response (Penn et al. 2002).

1.3. MONITORING CYTOTOXIC $CD8^+$ T CELL FREQUENCY AND EFFECTOR FUNCTION – GOING FROM MICE AND MEN TO CATTLE AND PIG

Section 1.3 of this thesis is modified from section 3.2 in a paper previously published in Vaccine (Thakur et al. 2012) with the thesis author as a coauthor including the responsibility for the writing of section 3.2.

In recent years the scientific fields of immunology and biochemistry have seen great advances in the ability to detect and isolate antigen-specific $CD8^+$ CTLs (Altman et al. 1996, Dunbar et al. 1998, Romero et al. 1998). Successive modifications of methods like the recombinant MHC tetramer approach for staining of specific CTLs (Altman et al. 1996, Leisner et al. 2008), peptide affinity ELISA (Sylvester-Hvid et al. 2002), cytokine sensitive ELISpot assays (Hutchings et al. 1989, Malyguine et al. 2007) and the use of chimeric molecules and transgenic animals (Choi et al. 2002), have all contributed to the increasing amount of data describing cytotoxic immune responses during infection and vaccination.

A major function of immune-activated CTLs is the exocytosis of cytotoxic proteins such as pore forming proteins (perforins), serine proteases (granzymes), and cytokines such as IFN-γ, tumor necrosis factor (TNF)-α and interleukin (IL)-2 (Zuber et al. 2005). Such components, revealing the state of activation for individual CTLs, provide a relatively simple set of cytokines that can be used to monitor and define both CTL frequency and function in responses against infections that require T cells for protection (Seder et al. 2008). A potential drawback of using cytokines as a measure for cell activation and function is that the secretion of many cytokines such as IFN-γ is not necessarily indicative of CTL function, because they can be released by non-cytotoxic cells involved in the innate and adaptive immune responses (Figure 3). An assay measuring the secretion of molecules associated with lytic activity or the level of killing of specific target cells by CTLs provides a better approach for assessment of cytotoxic T cell function. Present and future approaches combining one such assay with highly specific MHC tetramer staining of CTLs and additional flow cytometry-based intracellular staining assays are state-of-the-art and could be applicable to models of almost any species of interest.

1.4. MHC CLASS I TETRAMERS

MHC tetramers have been described for mouse (Lemke et al. 2011), human (Altman et al. 1996, Leisner et al. 2008) and bovine (Norimine et al. 2006). These complexes are four recombinant MHC molecules loaded with synthetic peptides that are bound (usually through the Biotin–Streptavidin interaction) to a fluorescent tag (Figure 5). They have been well known for more than a decade (Altman et al. 1996), and being readily combined with functional assays they are becoming more important as a tool in monitoring immune responses and in the enumeration and characterization of T cells (Altman and Davis 2003, Wooldridge et al. 2009, Xu and Screaton 2002). Although some interaction of T cells with MHC monomers and dimers can be detected, reproducible staining is best obtained with tetramers due to the higher avidity (Klenerman et al. 2002). Up to three of the four MHC monomers in a tetramer can be recognized and bound simultaneously by TCRs on the surface of the same antigen specific T cell thereby increasing the tetramer-CTL interaction. Furthermore, tetramers themselves might bind each other to form higher-order oligomers (Klenerman et al. 2002), which could further elevate the magnitude of staining depending on the corresponding level of structural hindrance resulting from random oligomerization. With the correct tetramers, antigen-specific CTLs can be directly enumerated *ex vivo* from peripheral blood samples although in cases of very low *in vivo* frequencies *in vitro* manipulations such as cell enrichment, cell expansion, and/or prolonged antigen stimulation may enhance the individual frequencies for more detailed analyses (Addo et al. 2003, Kiepiela et al. 2004, Leisner et al. 2008, Schmidt et al. 2009). However, such *in vitro* manipulations may hinder the accuracy of monitoring the natural existence and frequency of CTL responses elicited by infection or vaccination (Schmidt et al. 2009, thor Straten et al. 2000).

One main disadvantage of tetramers is their single-specificity which is a problem when analyzing outbred animals and infections with certain viruses for which immunodominant peptides do not exist. In cases where a complex set of epitopes might be targeted by T cells, it would be necessary to perform analysis using several different class I tetramers produced with several different peptide epitope candidates to obtain multiple specificities. Furthermore, in the case of HLA and SLA, the limited number of recombinant MHC molecules available, and scarce details of their peptide binding preferences, restricts the usage of MHC tetramers (Saalmuller 2006).

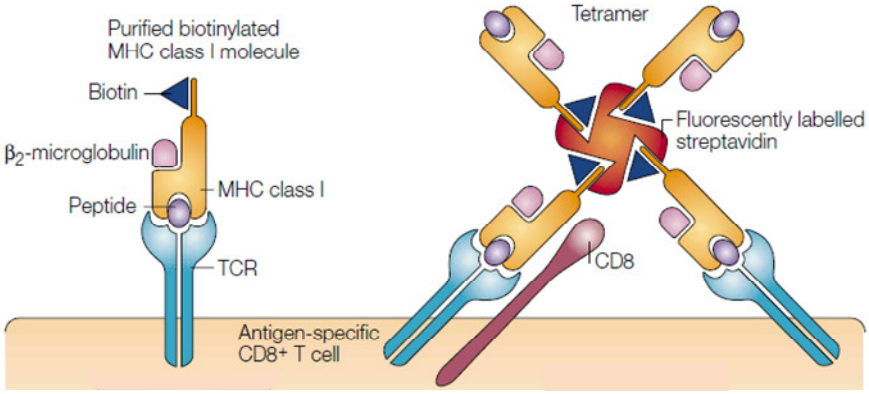

Figure 5. The basic construction of an MHC class I monomer and tetramer recognized by TCRs at the surface of an antigen-specific, $CD8^+$ T cell. The fluorescently labeled streptavidin enables detection of CTLs that specifically bind the pMHC tetrameric complex with higher avidity as compared to the lower affinity of the monomer. Figure modified from (Klenerman et al. 2002).

Despite the established importance of virus-specific, CTL-mediated killing of virus infected cells and the possibility to quantify induced CTLs by tetramer staining, the MHC heterogeneity of any outbred population, and the exclusive specificity of the MHC tetramer with the corresponding TCR, has so far made it difficult to use tetramer staining as an immunological correlate of protection by validation of specific $CD8^+$ CTLs (Thakur et al. 2012). Tetramer stained CTLs are, however, important immune markers of the effects of vaccination as different vaccines or vaccine strategies can be directly evaluated for their induction of peptide antigen-specific $CD8^+$ CTL subsets. In addition, adoptive transfer of human CTLs specifically purified by tetramer staining has been shown to induce protection against cytomegalovirus (Cobbold et al. 2005). Furthermore, tetramers should allow the investigation of different T cell recognition patterns with pMHC complexes for example by comparing peptides of different lengths.

1.5. FOOT-AND-MOUTH-DISEASE AND SWINE INFLUENZA A VIRUS – OUTBREAK, TREATMENT AND CONTROL

The focus of this PhD project has been set on two of the most contagious and costly viral infections that occasionally devastate the agricultural world, foot-and-mouth disease virus and swine influenza A virus.

1.5.1. Swine Influenza A Virus

The swine influenza A virus strains are negative-sense, single-stranded RNA viruses of the family *Orthomyxoviridae* (Beigel and Bray 2008). The most common influenza A virus strains circulating worldwide are the H1N1, H3N2, and H1N2 distinguished by their divergence in the two major glycoproteins hemagglutinin (HA) and neuraminidase (NA) (Brown et al. 1997, Campanini et al. 2010, Olsen 2002, Richt et al. 2003). HA and NA display a fine balance playing important roles in the influenza A replication cycle. HA mediates docking of the virions to their target cells through binding to sialic acid (which is covalently linked to the terminal galactose of an oligosaccharide, a glycoprotein or glycolipid). NA then functions by cleaving sialic acid from galactose to avoid virion docking on non-respiratory epithelial cells as well as to release newly formed virions from the surface of infected cells (Figure 6) (Beigel and Bray 2008, Jo et al. 2007, Olsen 2002, Richt et al. 2003).

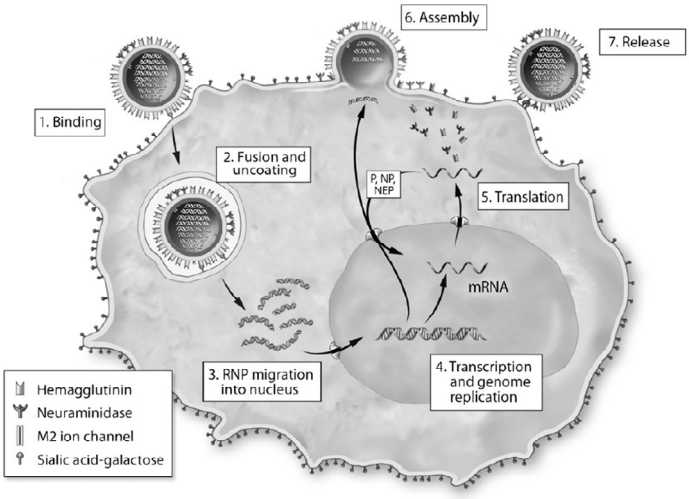

Figure 6. Replication of influenza A virus by initial docking of the virion to the surface of the target epithelial cell via HA-Sialic acid-galactose interactions (**1**), followed by endocytosis, HA cleavage, and fusion of the viral and endosomal membranes (**2**) which leads to the release and formation of ribonucleoprotein (RNP) particles into the cell cytoplasm and further migration to the nucleus (**3**). Transcription and genome replication takes place within the nucleus (**4**) resulting in translation of mRNA and the generation of nascent viral components such as HA and NA (**5**), and culminating in the virion assembly and release at the cell membrane (**6** + **7**). The figure is modified from (Beigel and Bray 2008).

Swine may play an important role in influenza ecology because they express viral receptors that support infection with avian, swine and human influenza viruses, and by that act as mixing vessel for new influenza A virus re-assortments, which may have the potential to be

transmitted to other hosts, including humans (Kida et al. 1994, Kundin 1970, Torremorell et al. 2012, Trebbien et al. 2011). Influenza A virus is mostly transmitted directly through pig-to-pig contact and via aerosols. Seasonal influenza outbreaks greatly affect the meat and agricultural industries every year due to illness, lowered meat production and in worst cases death within animal herds.

The respiratory disease associated with influenza A virus has a global effect on swine as well as birds and humans (Webster et al. 1992) leading to seasonal high demands of Oseltamivir - also known as Tamiflu - which is the only currently available drug used in the prophylaxis of the disease (Saxena et al. 2012). To avoid the risk of resistance and because of the greatly increased price of the active compound of Tamiflu (shikimic acid), it is relevant to find alternative approaches for the prevention and treatment of swine influenza, making it extremely important to seek a better understanding of the immune response against influenza in swine, as well as of the different mechanisms of transmission within pigs and across species (Torremorell et al. 2012). Furthermore, in depth investigation and monitoring of porcine immune responses elicited by new vaccines and by natural disease would contribute to improved testing and development of future vaccines and vaccine delivery approaches.

1.5.2. Foot-and-Mouth Disease Virus (FMDV)

Foot-and-mouth disease virus is a member of the aphthovirus family of *Picornaviridae*. The genome consists of a positive stranded RNA molecule which encodes a single polyprotein that can be processed into four structural and nine non-structural proteins by virally encoded proteases, including $3C^{Pro}$ and L^{Pro} (Guzman et al. 2008, Racaniello V.R. 2006, Stanway et al. 2005). The FMDV genome is surrounded by a densely packed icosahedral arrangement of 60 protomers, each consisting of the four structural proteins VP1, VP2, VP3 and VP4 encoded in the P1 region (Figure 7) (Grubman and Baxt 2004, Rueckert and Wimmer 1984).

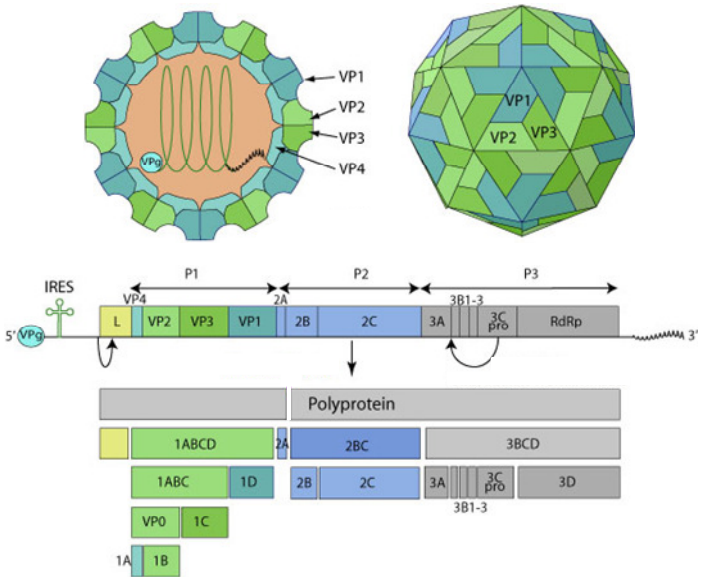

Figure 7. The FMDV virion (top) and the linear single-stranded RNA genome (bottom). The linear single-stranded RNA genome is composed of a single open reading frame (ORF) encoding a polyprotein. The genomic RNA has a linked viral protein (VPg) at its 5' end. The long untranslated region (UTR) at the 5' end contains an internal ribosome entry site (IRES). The P1 region encodes the structural proteins (VP1 – VP4), whereas The P2 and P3 regions encode the nonstructural proteins associated with replication. The N-terminal leader protease (L^{Pro}) is encoded in addition to the 3C protease ($3C^{Pro}$). This figure is modified from the Swiss Institute of Bioinformatics (viralzone.expasy.org).

FMD is a highly contagious disease of cloven-hoofed animals including livestock such as cattle, sheep, goats and swine. It is characterized by development of oral and pedal vesicles that result in high morbidity but mortality is low. However, infection in young animals may be lethal (Golde et al. 2005, Grubman and Baxt 2004, Pacheco et al. 2005). Devastating outbreaks such as the one experienced in the United Kingdom (UK) in 2001 resulted in the slaughter of over 4 million animals and an estimated total loss to the UK economy of between US$ 12.3 and 13.8 billion (Scudamore and Harris 2002, Thompson et al. 2002).

Today, outbreaks that appear in previously *FMD-free* countries, such as in the UK, are controlled by inhibition of animal movement followed by slaughter of infected as well as in-contact animals (stamping out) and completed by decontamination (Pacheco et al. 2005). Such methods are expensive in terms of lost agricultural production and export. In addition to this there is also a considerable expense in the killing and burning of millions of animals, which generally lead to public concern (Figure 8).

Along with the environmental problems raised by the need to eliminate these animals, such factors underline the needs for alternative and better ways of controlling and dealing with FMD. Although effective vaccines are currently available as chemically inactivated whole virus antigen in adjuvant (Doel 2003), the use of vaccination is most often a decision of last resort. The reason for this is that countries choosing to vaccinate animals (instead of stamping out) are subjects to a prolonged loss of export markets for livestock and livestock products due to a minimum of 6 months before regaining a status as FMD-free. Until recently this period was a full 12 months in accordance with the previous version of the International Animal Health Code of the Office International des Epizooties (OIE), which made the choice of vaccination further unfavorable (Golde et al. 2005). In comparison, at present a country can get classified as FMD-free by documentation of an absence of disease for 3 consecutive months when clearing an outbreak by slaughter and decontamination.

Figure 8. Over four millions animals infected by FMDV were culled and burned during the 2001 outbreak in the UK in an attempt to control and eradicate the virus. This picture was taken in North Cumbria, UK, one of the worst affected areas in the country. Foto: Murdo Mcleod (www.guardian.co.uk).

Focusing more research on the control of FMDV and the development of further improved vaccines and effective outbreak response programs, could ultimately lead to a state where vaccination to *prevent* the disease, thereby saving millions of animals (and billions of US$), would not just be a goal but an achievement.

Assays based on sensitive detection of antibodies against non-structural FMDV proteins, and hence capable of differentiating infected from vaccinated animals (DIVA), have been developed and are still being improved and redesigned for enhanced specificity and sensitivity (Brocchi et

al. 2006, Clavijo et al. 2004, Gao et al. 2012, Muller et al. 2010, Sorensen et al. 2005). Furthermore, the OIE recommends that FMDV vaccines are composed of inactivated and purified virus to remove non-structural viral proteins (Muller et al. 2010), thereby enabling assay specificity for detection of non-structural protein-specific antibodies unique only to infection and *not* to vaccination. One candidate for such a next-generation FMDV vaccine is the "empty capsid" platform comprised of a replication-defective human adenovirus 5 (Ad5) viral vector with the FMDV P1 capsid and $3C^{Pro}$ precursor inserted (Grubman et al. 2010). Compatible with present diagnostic tests, this vaccine strategy has DIVA capability as well as being effective in swine (Mayr et al. 1999, Mayr et al. 2001, Moraes et al. 2002) and cattle (Pacheco et al. 2005). A limitation is seen for the vaccine (as for killed-virus vaccines and natural infection in general) in that the neutralizing Abs raised against the vaccine strain of choice do not provide cross-serotype protection. Due to such a requirement for vaccine efficacy, the lack of cross-serotype protection limits the value of vaccination during outbreak or in disease eradication (Rodriguez and Grubman 2009). Improved DIVA assays and vaccines would facilitate the process of future vaccination programs to be preferred choices in the prevention, as well as control of FMD outbreaks.

Previous work has demonstrated that vaccination of swine with wild type ($3C^{Pro}$ *intact*) adeno-vectored FMDV containing the strain A24 P1, 2A and strain A12 3C coding sequence (Ad5A24) resulted in the generation of protective anti-FMDV antibodies (Moraes et al. 2002). These experiments showed that swine vaccinated with a single dose of the Ad5A24 were completely protected against a following challenge with FMDV. In comparison, the two control groups, which were vaccinated with either a vesicular stomatitis virus G protein gene vectored by Ad5 (Ad5VSV-G) or with PBS alone, both developed characteristic signs of foot-and-mouth disease (FMD). In addition, mutation of the $3C^{Pro}$, specifically an amino acid change (C163S), resulted in inhibition of the processing of P1 into mature capsid proteins and a reduced production of anti-FMDV antibodies (Grubman et al. 1995, Patch et al. 2011). These data illustrate that $3C^{Pro}$ is needed for successful structural capsid processing and virion assembly, which again is required for proper induction of an anti-FMDV antibody response. A simplified illustration of the viral FMDV replication cycle is shown in figure 9.

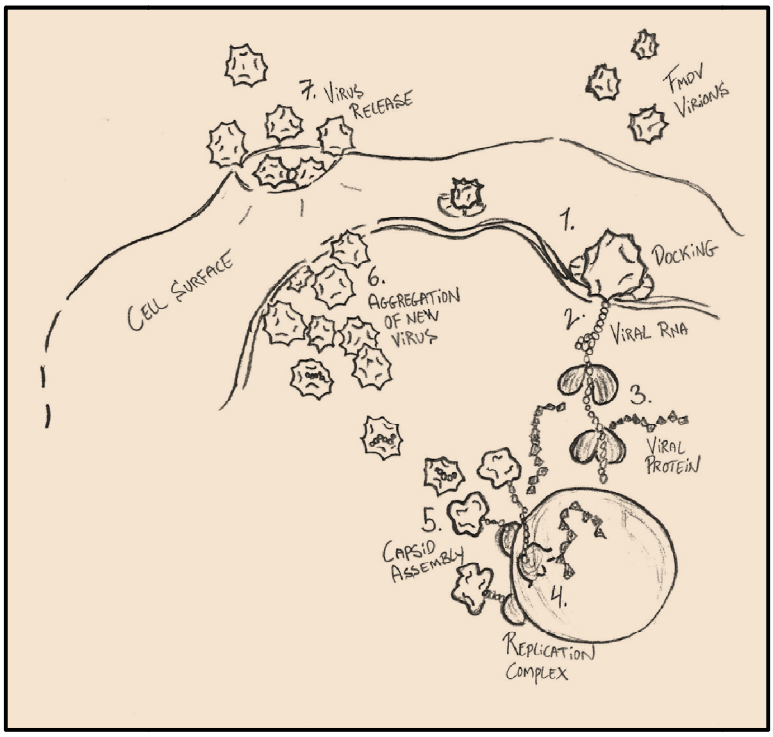

Figure 9. Illustration of the FMDV replication cycle. FMDV virus dock to the cell surface (**1**) and release the viral RNA into the cytosol (**2**) leading to viral takeover of the cells own replication machinery and the generation of new viral proteins (**3**), as well as viral RNA within the replication complexes associated with new vesicles from the *Endoplasmic Reticulum* (**4**). New viral RNA forms the genomes of virus particles which become surrounded by newly forming capsids (**5**). Once assembled the newly produced virus particles are transported to the cell membrane, causing aggregation, and eventually rupture of the cell (**6**), hereby releasing millions of new virus particles capable of infecting healthy cells of the host (**7**). Figure illustration made by the author.

Development of vaccines focusing on the activation of an FMDV specific CTL response have been somewhat neglected partly due to observations done in the early events after FMDV infection, indicating a reduction of cell surface pMHC class I complex expression (Sanz-Parra et al. 1998). Other reasons for CTLs being neglected in the context of FMDV infection could also be that neutralizing Abs have been demonstrated to be central players in protection against the disease (Mayr et al. 2001, Moraes et al. 2002), and technical difficulties in developing the appropriate assays for monitoring such CTLs specific for FMDV. Despite this, development of more specific assays for the analysis of vaccine induced CTL responses could reveal a promising effect of such CTLs in the clearance of virus from the infected host. Furthermore, the ability of CTLs to recognize peptide epitopes that would otherwise remain hidden to neutralizing antibodies makes them interesting candidates for enhancing FMDV immunity.

1.6. SLA TISSUE TYPING

Knowing which SLA alleles that are commonly occuring within a herd, a country or even on a global scale can be of great importance in regard to vaccine development and the establishment of immune protection in swine through broad coverage, highly specific, subunit based vaccination against viruses such as the previously mentioned swine influenza virus and FMDV. These technologies can also be applied to addressing other important viral diseases of swine such as porcine reproductive and respiratory syndrome virus (PRRSV), African swine fever virus (ASFV) and vesicular stomatitis virus (VSV).

Because of the extensive polymorphic nature of SLA genes, it is necessary to have very accurate and sensitive typing methods to distinguish the different alleles (Ho et al. 2009c). Historically the most important means for determining SLA class I antigen specificities was serological typing using alloanti-sera (Kristensen 1988, Renard et al. 1988). This is compromised by the lack of typing sera with documented specificities, limiting SLA characterization. Since MHC molecules occasionally differ by sites inaccessible to antibody binding, and often share similar (outer) epitopes, SLA typing sera are limited in identifying specific expression patterns. A combination of sera is usually required to differentiate between animals, and most such typing reagents are directed against an entire haplotype rather than individual alleles, further complicating precise identification of particular SLA alleles. Hence the need for a more sensitive and highly specific typing system, enabling the examination of SLA class I allelic diversities in outbred populations, emerged.

Today, such needs are met by the application of DNA-based typing methods using low- and high-resolution PCR sequence-specific primers (PCR-SSP). These allow high-throughput identification of individual SLA class I alleles, and overall SLA haplotype screening of pig herds and breeds of interest for class I (Essler et al. 2012, Ho et al. 2006, Ho et al. 2009c, Ho et al. 2009a, Martens et al. 2003) and class II alleles (Ho et al. 2010a). The principle of allele-specific primer design is to identify primers where the 3’ end of one or both primers covers polymorphic sites unique to their allele, thereby enabling the identification of that exact allele using that particular pair of primers (Martens et al. 2003). To design site-specific primers, one must know the DNA sequences of the different SLA alleles present in the swine herd or

population being studied. This limits the sequence-based typing approach to alleles with known sequences. SLA allele sequences reported to date are publicly available at the IPD-MHC (http://www.ebi.ac.uk/ipd/mhc/sla/index.html). As of November 2012, there are 131 class I (SLA-1, SLA-2, SLA-3 (all classical class Ia), and SLA-6 (non-classical class Ib)) alleles officially designated (Table 1) with a total of 31 class I high-resolution haplotypes assigned at the allele level, which puts the SLA system among the most well characterized MHC systems in non-primate species (Ho et al. 2012).

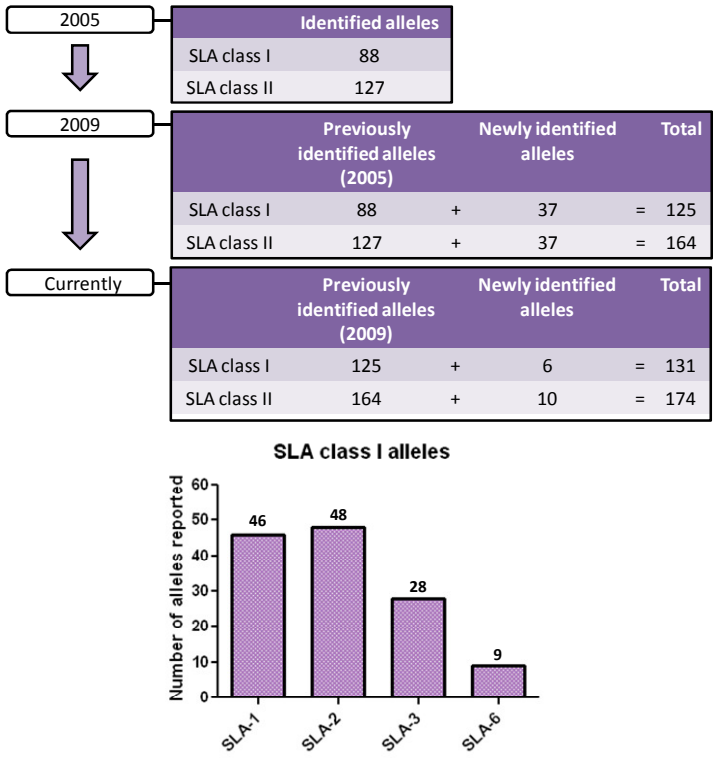

Table 1. Statistics of the current SLA sequence database displaying the number of newly identified alleles since 2005. The total number reported for each allele group is indicated in the lower graph. The table was modified and used with approval from the corresponding author (Ho et al. 2012).

The relevance of SLA typing can be linked to the SLA peptide ligand binding and presentation (Lunney et al. 2009). An initial step in identifying virally derived T cell epitopes, that generate a protective T cell response against infection in pigs, is to identify which SLA alleles are expressed by the animals and which peptides they bind and present. Once candidate peptides or proteins have been identified, they may be used to specifically target, activate and/or monitor T cells mediating immunity through subunit based vaccination or synthetically designed pSLA

multimers. Highly specific vaccines based on detailed information about SLA peptide binding and presentation could become useful in preventing the outbreaks of viruses such as swine influenza and FMDV, hereby limiting the almost inevitable financial losses and animal suffering, which are associated with such outbreaks.

2. Methodological Setup and Considerations

This chapter describes the methods and experimental approaches used throughout the PhD project, but not explicitly described in the respective manuscripts. General and detailed materials and methods sections for all methods and approaches of my PhD work can be found in the individual manuscripts presented in this thesis, Paper I – IV.

2.1. PEPTIDE-SLA CLASS I AFFINITY MEASURES

In the studies performed throughout this PhD project the affinities of hundreds of different peptides for binding by the three SLA class I molecules, SLA-1*0401, SLA-2*0401 and SLA-3*0401 have been measured. The assay initially used for this was an enzyme-linked immunosorbent assay (ELISA) previously developed for HLA (Sylvester-Hvid et al. 2002) and through this project adapted to SLA (Paper I – III). The ELISA as such was first described in 1971 and is based on specific Abs capturing antigen which is then detected by an enzyme conjugated detection Ab in symphony with a substrate to give a visible signal (Engvall and Perlmann 1971, Van Weemen and Schuurs 1971). Today the use of monoclonal Abs with various specificities is common practice in most laboratories allowing for an extremely broad range of antigen detection measures. The ELISA used in this project was based on the capture of biotinylated SLA molecules followed by the detection of human β_2m using a monoclonal Ab (Figure 10A). This assay principle is based on data showing the affinity between β_2m and the MHC heavy chain is enhanced in the presence of bound peptide ligand (Elliott et al. 1991). Hence β_2m is only stably folded with SLA class I when there is peptide binding. This results in no detection of peptide-empty SLA molecules in the assay. Due to the lack of a monoclonal Ab specific for porcine β_2m we decided to build the assay with human β_2m. This decision was based on the findings that both human and porcine β_2m show equal capacity to support the folding of pMHC

class I complexes irrelevant of the heavy chain expressing an HLA or SLA α_3 domain as presented in Paper I (Figure 4 + 5) of this thesis. The amount of peptide needed to fully saturate half of the SLA molecules made available will give the affinity constant (K_D) of each peptide tested once correlated to a pre-folded HLA-A*02:01 standard curve based on non-linear curve regression (Figure 10B).

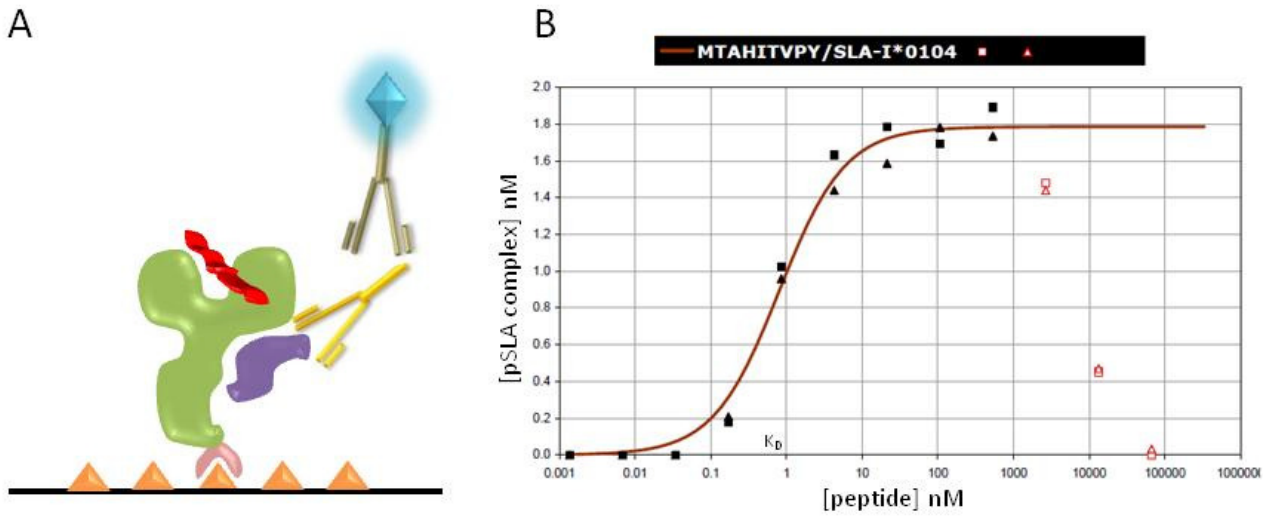

Figure 10. Illustration of the SLA peptide affinity ELISA setup (**A**) and an example of curve-fitting to peptide dose/response titrations, and the corresponding pSLA complex formation (**B**). The ELISA plate is covered with streptavidin (orange) which bind the biotin (pink) linked to the SLA heavy chain molecule (green) with bound peptide (red) and the co-bound stabilizing subunit protein β_2m (purple). β_2m-specific primary Ab (yellow) captures correctly formed pSLA complex made visible by detection via an enzyme (glowing blue) conjugated detection Ab (grey). The peptide dose/response curve illustrates a peptide (MTAHITVPY) bound with extremely high affinity (K_D, 0.8 nM) as presented in Paper II of this thesis.

2.2. HOMOGENOUS PEPTIDE AFFINITY AND pSLA COMPLEX STABILITY ASSAYS

Luminescent oxygen channeling immunoassay (LOCI) is a technology which enables high throughput, homogenous screening of peptide-MHC class I interactions, among a wide range of other rapid, and quantitative determination possibilities. The technology itself was first described in the nineties (Ullman et al. 1994, Ullman et al. 1996), and the assay consists of two primary components, donor- and acceptor beads, the latter emitting a signal when brought into close proximity with excited donor beads (Figure 11).

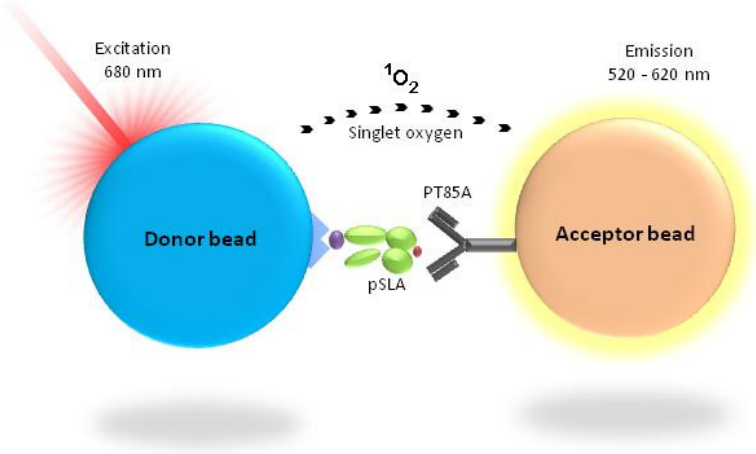

Figure 11. The LOCI principle. Biotinylated pSLA (green) is bound to a streptavidin coated donor bead (blue) and captured by an anti SLA monoclonal Ab (PT85A, black) which is conjugated to an acceptor bead (orange).

The donor beads contain a blue-green colored photosensitizing agent, phthalocyanine, which converts ambient oxygen into singlet oxygen upon illumination at 680 nm. The lifetime of singlet oxygen in water is very short (4 µs), hence it can only travel approximately 200 nm before returning to its ground state. This enables acceptor beads to become activated only when brought into close proximity of the donor bead, resulting in a chemiluminescent signal via the PT85A monoclonal Ab capture of correctly folded pSLA complex at the surface of the streptavidin conjugated donor beads (Figure 11). The resulting light emission from activated acceptor beads is at a higher energy than the light used for excitation, which result in very low background signals and a high signal-to-background ratio. In addition to this, the beads are bioactive and can easily be conjugated with Abs or other proteins (such as streptavidin). Furthermore, the homogenous nature of the LOCI assay leaves out the washing steps needed in-between steps for the ELISAs. Altogether, such assay qualities make the LOCI preferable to use in present and future peptide-SLA affinity analyses. To measure the assay signal an instrument like the EnVision® or EnSpire™ (Perkin Elmer Life Sciences) multilabel reader is needed. The LOCI technology was adapted to screen for peptide:SLA affinities having biotinylated heavy chain proteins and an SLA-specific Ab available and adjusted to the assay. LOCI based peptide affinity analysis is described and presented for the SLA-2*0401 and SLA-3*0401 molecules in paper III.

In addition to the affinity, which is a measure for the likeliness of a given peptide to be bound by the MHC class I molecule, accompanying stability measures of pSLA complexes were included. The stability of pMHC has been proposed to be a better determinant of immunogenicity than the actual binding affinity (Busch and Pamer 1998, Harndahl et al. 2012, Mullbacher et al. 1999, van der Burg et al. 1996). To measure such stabilities we used a radiolabeled-based scintillation proximity assay (SPA). The first SPA emerged in the late 1970s (Hart and Greenwald 1979a, Hart and Greenwald 1979b) making the technology commercially available. By radio-labeling porcine β_2m with the ^{125}I isotope we were able to develop a high throughput, homogenous assay for measuring pSLA complex stabilities. Such stability measures are based on the energy transfer between β-particles from the iodine isotope and the scintillation material imbedded in streptavidin coated FlashPlates which bind biotinylated peptide:SLA:^{125}I-β_2m complexes. Upon peptide binding by the SLA molecule, ^{125}I-labeled β_2m will co-bind, which will bring the β_2m close to the scintillation material in the plate, hereby activating it by the emitted electrons (β-particles). Activation of the plate then results in a positive signal read-out (Figure 12).

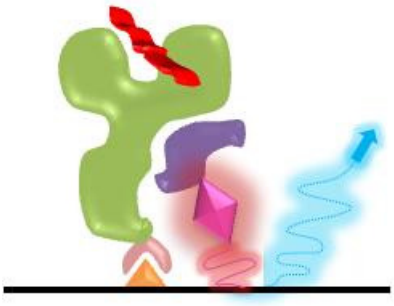

Figure 12. Illustration of the SPA principle. All components are the same as described in Figure 10 with the exception of the β_2m now being labeled with ^{125}I (glowing pink) and the signal emitted from the activated scintillation material (glowing blue).

The ^{125}I isotope was chosen partly due to its short ranged electron emitters, hence only labeled ^{125}I-β_2m brought in close proximity of the FlashPlate scintillation material by the streptavidin-biotin interaction, will lead to signal in the reader. Electrons emitted from unbound ^{125}I-β_2m will be absorbed by the surroundings. The dissociation of ^{125}I-β_2m is used as a measure of the stability of the pSLA complex. Excess of un-labeled β_2m is added to the sample when steady-state of the complex folding reaction is reached, and just prior to sample measurement. This is

done to ensure that dissociated peptide:SLA:^{125}I-β_2m complex is only re-associated by support of un-labeled β_2m, not leading to a false high stability by regeneration of measurable peptide:SLA:^{125}I-β_2m complexes. Samples are measured continuously in a TopCount NXT liquid scintillation counter for 24 hours at 37^{o}C. The assay and the corresponding stability data achieved for SLA-1*0401, SLA-2*0401 and SLA-3*0401 is presented and discussed in detail in Paper III.

2.3. DESIGNING NEGATIVE CONTROL PEPTIDES FOR THE PRODUCTION AND USE OF pSLA TETRAMERS

Critical to interpreting tetramer binding data is the capacity to measure background signal. In order to address this, two peptides derived from the VP35 region of the Sudan *Ebola* virus and from the *Vibrio Cholera* bacteria, respectively were used as nonspecific controls. The binding prediction for the peptides with two SLA molecules, SLA-1*0401 and SLA-2*0401, and *in vitro* ELISA affinity tests, revealed both peptides as being strongly bound as presented in Paper II. The idea was to produce tetramers using these peptides as negative controls when staining PBMCs. It was based on the presumption that animals under study had never encountered either *Ebola* or *Cholera*, and therefore should not be expected to recognize such tetramers, leading to positive staining of their CTLs. This approach was most successful using the *Ebola* peptide, leading to relatively low false positive background staining. Using the *Ebola* peptide construct as the reference tetramer was effective, as presented in details in Paper IV. Considering the binding and overall conformation of pMHC complex, combining it with recognition by the TCR being based on the peptide and MHC protein, it follows that the smaller the AAs of the peptide, the less available would the peptide residues be for TCR identification. Following this logic, better control peptides for tetramer formation could be designed resulting in less false-positive tetramer staining. Synthetic 9mer peptides were designed based on three criteria; (i) satisfying the residue preferences inherent in the SLA-1*0401 binding matrix anchor positions P2 and P9, (ii) be comprised of as many alanines or glycines as possible, and (iii) be ranked as strong binders by the *NetMHCpan* algorithm. Following these criteria, five such peptides were synthesized and tested for affinity binding by SLA-1*0401. Three of the five peptides had high binding affinities of 19, 40 and 104 nM. The two peptides with the highest

affinities were included in the tetramer experiments to provide a “null” tetramer. From those studies we observed that the peptide ASYGAGAGY was consistent in exibiting low signal in the flow cytometry analysis of T cell staining. This peptide is currently our best option as a negative control in the tetramer experiments.

2.4. VACCINATION TRIALS AGAINST FMDV USING A T CELL SPECIFIC VACCINE CONSTRUCT

Performing the vaccination and boosting trials presented in Paper IV we compared two different vaccine constructs which differed in the functionality of the $3C^{pro}$ as described above. The reason for using a $3C^{pro}$ mutated version (C163S) of the original vaccine construct was in an attempt to specifically induce a CTL response. We hypothesized that a stronger CTL response would be induced by such an “FMDV-T activating” vaccine, as opposed to the FMDV-B activating construct displaying a functional $3C^{pro}$ protein. The hypothesis was based on previously published data showing that the mutated and inactivated protease lacks the ability to successfully cleave the FMDV P1 protein into the sub-proteins (VP1 – 4) which form the viral capsid, hereby enabling the virus to leave the cell. Instead, viral protein would stay captured inside the cells leading to proteasome degradation and elevated availability of various FMDV P1 derived peptides for MHC class I load in the ER, and presentation at the cell surface. The work described in Paper IV presents the approaches made to test this hypothesis and the outcome of the experiments.

3. Paper I

Porcine major histocompatibility complex (MHC) class I molecules and analysis of their peptide-binding specificities

Pedersen LE, Harndahl M, Rasmussen M, Lamberth K, Golde WT, Lund O, Nielsen M, Buus S.

Immunogenetics. 2011 Dec:63(12):821-34. doi: 10.1007/s00251-011-0555-3

The work presented in this manuscript was focused on the production of the SLA-1*0401 molecule and the porcine β_2m stabilizing subunit protein. Generating chimeric human/swine MHC-molecules by systemically transferring domains of the frequently expressed SLA-1*0401 onto a HLA-I molecule (HLA-A*11:01), enabled us to analyze the peptide-binding characteristics of these molecules and validate the effects of pMHC complex formation supported by either human or porcine β_2m.

In this study we demonstrated that the approaches developed for the "Human MHC Project" can be successfully applied to other species such as pigs. Furthermore, we here presented the complete PSCPL mapped binding motif for one of the most common SLA molecules worldwide, and showed that pMHC complex formation can be equally supported by human as well as porcine β_2m, regardless of the α_3 domain of the heavy chain being of human or porcine origin. In addition, we demonstrate the successful use of a pan-specific predictor of peptide:MHC class I binding, the *NetMHCpan*, in predicting the specificities of the SLA-1*0401 molecule.

Immunogenetics (2011) 63:821–834
DOI 10.1007/s00251-011-0555-3

ORIGINAL PAPER

Porcine major histocompatibility complex (MHC) class I molecules and analysis of their peptide-binding specificities

Lasse Eggers Pedersen · Mikkel Harndahl · Michael Rasmussen · Kasper Lamberth · William T. Golde · Ole Lund · Morten Nielsen · Soren Buus

Received: 25 March 2011 / Accepted: 20 June 2011 / Published online: 8 July 2011

Abstract In all vertebrate animals, $CD8^+$ cytotoxic T lymphocytes (CTLs) are controlled by major histocompatibility complex class I (MHC-I) molecules. These are highly polymorphic peptide receptors selecting and presenting endogenously derived epitopes to circulating CTLs. The polymorphism of the MHC effectively individualizes the immune response of each member of the species. We have recently developed efficient methods to generate recombinant human MHC-I (also known as human leukocyte antigen class I, HLA-I) molecules, accompanying peptide-binding assays and predictors, and HLA tetramers for specific CTL staining and manipulation. This has enabled a complete mapping of all HLA-I specificities ("the Human MHC Project"). Here, we demonstrate that these approaches can be applied to other species. We systematically transferred domains of the frequently expressed swine MHC-I molecule, SLA-1*0401, onto a HLA-I molecule (HLA-A*11:01), thereby generating recombinant human/swine chimeric MHC-I molecules as well as the intact SLA-1*0401 molecule. Biochemical peptide-binding assays and positional scanning combinatorial peptide libraries were used to analyze the peptide-binding motifs of these molecules. A pan-specific predictor of peptide–MHC-I binding, *NetMHCpan*, which was originally developed to cover the binding specificities of all known HLA-I molecules, was successfully used to predict the specificities of the SLA-1*0401 molecule as well as the porcine/human chimeric MHC-I molecules. These data indicate that it is possible to extend the biochemical and bioinformatics tools of the Human MHC Project to other vertebrate species.

Keywords Recombinant MHC · Peptide specificity · Binding predictions

Electronic supplementary material The online version of this article (doi:10.1007/s00251-011-0555-3) contains supplementary material, which is available to authorized users.

L. E. Pedersen · M. Harndahl · M. Rasmussen · K. Lamberth · S. Buus (✉)
Laboratory of Experimental Immunology,
Faculty of Health Sciences, University of Copenhagen,
Panum 18.3.12, Blegdamsvej 3B,
2200 Copenhagen, Denmark
e-mail: sbuus@sund.ku.dk

W. T. Golde
Plum Island Animal Disease Center,
Agricultural Research Service, USDA,
Greenport, NY, USA

O. Lund · M. Nielsen
Center for Biological Sequence Analysis,
Technical University of Denmark,
Copenhagen, Denmark

Introduction

Major histocompatibility complex class I (MHC-I) molecules are found in all vertebrate animals where they play a crucial role in generating specific cellular immune responses against viruses and other intracellular pathogens. They are highly polymorphic proteins that bind 8–11 amino acid long peptides derived from the intracellular protein metabolism. The resulting heterotrimeric complexes—consisting of the MHC-I heavy chain, the monomorphic light chain, beta-2 microglobulin (β_2m), and specifically bound peptides—are translocated to the cell surface where they displayed as target structures for peptide-specific, MHC-I-restricted CTLs. If a peptide of foreign origin is detected, the T cells may become activated and kill the infected target cell.

MHC-I is extremely polymorphic. In humans, more than 3,400 different human leukocyte antigen class I (HLA-I) molecules have been registered (as of January 2011), and this number is currently growing rapidly as more efficient HLA typing techniques are employed worldwide. The polymorphism of the MHC-I molecule is concentrated in and around the peptide-binding groove, where it determines the peptide-binding specificity. Due to this polymorphism, it is highly unlikely that any two individuals will share the same set of HLA-I molecules thereby presenting the same peptides and generating T cell responses of the same specificities—something, that otherwise would give microorganisms a strong evolutionary chance of escape. Rather, this polymorphism can be seen as diversifying peptide presentation thereby individualizing T cell responses and reducing the risk that escape variants of microorganisms might evolve.

In 1999, we proposed that all human MHC specificities should be mapped ("the Human MHC Project") as a preamble for the application of MHC information and technologies in humans (Buus 1999). Since then, we have developed large-scale tools that are generally applicable towards this goal: production, analysis, prediction and validation of peptide–MHC interactions (Ferre et al. 2003; Harndahl et al. 2009; Hoof et al. 2009; Larsen et al. 2005; Lundegaard et al. 2008; Nielsen et al. 2003, 2007; Ostergaard et al. 2001; Pedersen et al. 1995; Stranzl et al. 2010; Stryhn et al. 1996), and a "one-pot, read-and-mix" HLA-I tetramer technology for specific T cell analysis (Leisner et al. 2008). Here, we demonstrate that many of these tools can be transferred to other vertebrate animals as exemplified by an important livestock animal, the pig. We have successfully generated a recombinant swine leukocyte antigen I (SLA-I) protein, SLA-1*0401, one of the most common SLA molecules of swine (Smith et al. 2005). Using this protein, we have developed the accompanying biochemical peptide-binding assays and demonstrated that the immunoinformatics tools originally developed to cover all HLA-I molecules, despite the evolutionary distance, can be applied to SLA-I molecules. We suggest that the "human MHC project" can be extended to cover other species of interest.

Materials and methods

Peptides and peptide libraries

All peptides were purchased from Schafer-N, Denmark (www.schafer-n.com). Briefly, they were synthesized by standard 9-fluorenylmethyloxycarbonyl (Fmoc) chemistry, purified by reversed-phase high-performance liquid chromatography (to at least >80% purity, frequently 95–99% purity), validated by mass spectrometry, and quantitated by weight.

Positional scanning combinatorial peptide libraries (PSCPL) peptides were synthesized using standard solid-phase Fmoc chemistry on 2-chlorotrityl chloride resins. Briefly, an equimolar mixture of 19 of the common Fmoc amino acids (excluding cysteine) was prepared for each synthesis and used for coupling in 8 positions, whereas a single type of Fmoc amino acid (including cysteine) was used in one position. This position was changed in each synthesis starting with the N-terminus and ending with the C-terminus. In one synthesis, the amino acid pool was used in all nine positions. The library therefore consisted of $20 \times 9+1=181$ individual peptide libraries:

- Twenty PSCPL sublibraries describing position 1: AX_8, CX_8, DX_8, …. YX_8
- Twenty PSCPL sublibraries describing position 2: XAX_7, XCX_7, XDX_7, …. XYX_7
- etc
- Twenty PSCPL sublibraries describing position 9: X_8A, X_8C, X_8D, …. X_8Y
- A completely random peptide library: X_9

X denotes the random incorporation of amino acids from the mixture, whereas the single letter amino acid abbreviation is used to denote identity of the fixed amino acid.

The peptides in each synthesis were cleaved from the resin in trifluoroacetic acid/1,2-ethanedithiol/triisopropylsilane/water 95:2:1:3 *v/v/v/v*, precipitated in cold diethylether, and extracted with water before desalting on C18 columns, freeze drying, and weighting.

Recombinant constructs encoding chimeric and SLA-1*0401 molecules

A synthetic gene encoding a transmembrane-truncated fragment encompassing residues 1 to 275 of human HLA-A*11:01 alpha chain followed by a FXa–BSP–HAT tag (FXa = factor Xa cleavage site comprised of the amino acid sequence IEGR, BSP = biotinylation signal peptide, HAT = histidine affinity tag for purification purposes; see Online Resource 1) had previously been generated and inserted into the pET28 expression plasmid (Novagen) (Ferre et al. 2003). Synthetic genes encoding the corresponding fragments of the SLA-1*0401 alpha chain ($\alpha_1\alpha_2$) and α_3, respectively, (Sullivan et al. 1997) were purchased from GenScript. To exchange domains and generate chimeric human/swine MHC-I gene constructs, a type II restriction endonuclease-based cloning strategy (SeamLess® Stratagene; Cat#214400, Revision#021003a), with modifications, was used. All primers were purchased HPLC-purified from Eurofins MWG Operon (Ebersberg, Germany), and all PCR amplifications were performed in a DNA Engine Dyad

PCR instrument (MJ Research, MN, USA). All constructs were validated by DNA sequencing. The following MHC-I heavy chain constructs were made HHH, HHP, HPP, PHP, and PPP, where the first, second, and third letter indicates domains α_1 (positions 1–90), α_2 (positions 91–181), and α_3 (positions 182–275), respectively, and H indicates that the domain is of HLA-A*11:01 origin, whereas P indicates that it is of SLA-1*0401 origin.

Constructs were transformed into DH5α cells, cloned, and sequenced (ABI Prism 3100Avant, Applied Biosystems) (Hansen et al. 2001). Validated constructs of interest were transformed into an *Escherichia coli* production cell line, BL21(DE3), containing the pACYC184 expression plasmid (Avidity, Denver, USA) containing an isopropyl-β-d-1-thiogalactopyranoside (IPTG)-inducible BirA gene to express biotin-ligase. This leads to almost complete in vivo biotinylation of the desired product (Leisner et al. 2008).

Expression of recombinant proteins

To maintain the pET28-derived plasmids, the media was supplemented with kanamycin (50 μg/ml) throughout the expression cultures. When appropriate, the media was further supplemented with chloroamphenicol (20 μg/ml) to maintain the BirA containing pACYC184 plasmid. *E. coli* BL21(DE3) cells transformed with appropriate plasmids were grown for 5 h at 30°C, and a 10-ml sample adjusted to $OD_{(600)}$=1 was then transferred to a 2-l fed-batch fermentor (LabFors®). To induce protein expression, IPTG (1 mM) was added at $OD_{(600)}$~25 and the culture was continued for an additional 3 h at 42°C (for in vivo biotinylation of the product, the induction media was further supplemented with biotin (Sigma #B4501, 125 μg/ml)). Samples were analyzed by reducing sodium dodecyl sulfate polyacrylamide gel electrophoresis (SDS-PAGE) before and after IPTG induction. At the end of the induction culture, protease inhibitor (PMSF, 80 μg/l) was added, and cells were lysed in a cell disrupter (Constant Cell Disruptor Systems set at 2,300 bar) and the released inclusion bodies were isolated by centrifugation (Sorval RC6, 20 min, 17,000×*g*). The inclusion bodies were washed twice in PBS, 0.5% NP-40 (Sigma), and 0.1% deoxycholic acid (Sigma) and extracted into urea–Tris buffer (8 M urea, 25 mM Tris, pH 8.0), and any contaminating DNA was precipitated with streptomycin sulfate (1% *w*/*v*).

MHC class I heavy chain purification

The dissolved MHC-I proteins were purified by Ni^2+/IDA metal chelating affinity column chromatography followed by Q-Sepharose ion exchange column chromatography, hydrophobic interaction chromatography, and eventually by Superdex-200 size exclusion chromatography. Fractions containing MHC-I heavy chain molecules were identified by A280 absorbance and SDS-PAGE and pooled. Throughout purification and storage, the MHC-I heavy chain proteins were dissolved in 8 M urea to keep them denatured. Note that the MHC-I heavy chain proteins at no time were exposed to reducing conditions. This allowed purification of highly active pre-oxidized moieties as previously described (Ostergaard et al. 2001). Protein concentrations were determined by bicinchoninic acid assay. The degree of biotinylation (usually >95%) was determined by a gel-shift assay (Leisner et al. 2008). The pre-oxidized, denatured proteins were stored at −20°C in Tris-buffered 8 M urea.

Recombinant constructs encoding human and porcine beta-2 microglobulin

Recombinant human β_2m was expressed and purified as described elsewhere (Ostergaard et al. 2001), (Ferre et al. 2003). Using a previously reported *E. coli* codon-optimized gene encoding human β_2m as template (Pedersen et al. 1995), a gene encoding porcine β_2m was generated by multiple rounds of site-directed mutagenesis (QuikChange® Stratagene, according to the manufacturer's instructions) (Online Resource 2). Briefly, the genes encoding human or pig β_2m were N-terminally fused to a histidine affinity encoding tag (HAT) followed by a restriction enzyme encoding tag (FXa), inserted into the pET28 vector and expressed in inclusion bodies in *E. coli*. The fusion proteins were extracted into 8 M urea, purified by immobilized metal affinity chromatography (IMAC), and refolded by dilution. The fusion tags were then removed by FXa restriction protease digestion. The liberated intact and native human or pig β_2m were purified by IMAC and gel filtration chromatography, analyzed by SDS-PAGE analysis, concentrated, and stored at −20°C until use (Fig. 1).

Purification and refolding of recombinant porcine β_2m proteins

Porcine β_2m was purified in the same way as human β_2m (Ostergaard et al. 2001; Ferre et al. 2003). Briefly, the urea-dissolved β_2m protein was purified by Ni^2+/IDA metal chelating affinity column chromatography, refolded by drop-wise dilution into an excess refolding buffer under stirring (25 mM Tris, 300 mM urea, pH 8.00), and then concentrated (VivaFlow, 10 kDa). The refolded product was purified by Ni^2+/IDA metal chelating affinity column chromatography again (this time in aqueous buffer, i.e., without urea). Fractions containing HAT-pβ_2m were iden-

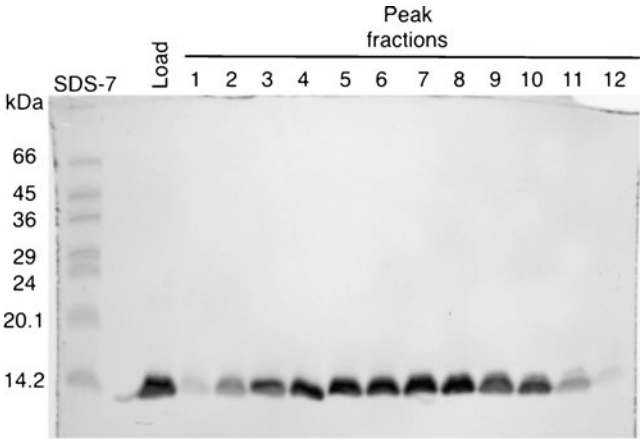

Fig. 1 SDS-PAGE analysis of peak fractions from size exclusion chromatography of porcine β_2m (11.4 kDa) after removal of histidine affinity tag (HAT) by FXa protease digestion. Samples were mixed 1:1 in non-reducing SDS sample buffer and loaded onto a 15% polyacrylamide gel

tified by SDS-PAGE and pooled. Removal of the HAT tag was performed by cleavage with factor Xa restriction protease (FXa) followed by renewed purified by Ni^2+/IDA metal chelating affinity and Superdex200 gel filtration column chromatography, concentrated by spin ultrafiltration (10 kDa), mixed 1:1 with glycerol, and stored at −20°C.

SDS-PAGE analysis

Protein samples were mixed 1:1 in SDS sample buffer (4% SDS, 17.4% glycerol, 0.003% bromophenol blue, 0.125 M Tris, 8 mM IAA (iodoacetamide)) with or without reducing agent (2-mercaptoethanol) as indicated, boiled for 3 min, spun at 20,000×*g* for 1 min, and loaded onto a 12% or 15% running gel with a 5% stacking gel. Gels were run at 180 V, 40 mA for 50 min.

Peptide–MHC class I interaction measured by radioassay and spun column chromatography

A HLA-A*11:01-binding peptide, KVFPYALINK (non-natural consensus sequence A3CON1 (Sette et al. 1994)), was radiolabeled with iodine (^{125}I) using a chloramine-T procedure (Hunter and Greenwood 1962). Dose titrations of MHC-I heavy chains (HHH or HHP) were diluted into refolding buffer (Tris–maleate–PBS) and mixed with β_2m (human or porcine) and radiolabeled peptide, and incubated at 18°C overnight. Then binding of radiolabeled peptide to MHC-I was determined in duplicate by Sephadex™ G50 spun column gel chromatography as previously described (Buus et al. 1995). MHC bound peptide eluted in the excluded volume, whereas free peptide was retained on the microcolumn. Both fractions were counted by gamma spectroscopy, and the fraction peptide bound was calculated as excluded radioactivity divided by total radioactivity.

To examine the affinity of the interaction, increasing concentrations of unlabeled competitor peptide were added. When conducted under limiting concentrations of MHC-I molecule, the concentration of competitor peptide needed to effect 50% inhibition of the interaction, the IC_{50}, is an approximation of the affinity of the interaction between MHC-I and the competitor peptide.

Peptide–MHC class I interaction measured by an enzyme-linked immunosorbent assay

Peptide–MHC-I interaction was also measured in a modified version of a previously described enzyme-linked immunosorbent assay (ELISA) (Sylvester-Hvid et al. 2002). Briefly, denatured biotinylated recombinant MHC-I heavy chains were diluted into a renaturation buffer containing β_2m and graded concentrations of the peptide to be tested and incubated at 18°C for 48 h allowing equilibrium to be reached. We have previously demonstrated that denatured MHC molecules can de novo fold efficiently, however, only in the presence of appropriate peptide. The concentration of peptide–MHC complexes generated was measured in a quantitative sandwich ELISA (using streptavidin as capture layer and the monoclonal anti-β_2m antibody, BBM1, as detection layer) and plotted against the concentration of peptide offered (Sylvester-Hvid et al. 2002). A prefolded, biotinylated FLPSDYFPSV/HLA-A*02:01 (Kast et al. 1994) complex was used as standard. Because the effective concentration of MHC (3–5 nM) used in these assays is below the equilibrium dissociation constant (K_D) of most high-affinity peptide–MHC interactions, the peptide concentration, ED_{50}, leading to half-saturation of the MHC is a reasonable approximation of the affinity of the interaction.

Using peptide libraries to perform an unbiased analysis of MHC specificity

The experimental strategy of PSCPL has previously been described (Stryhn et al. 1996). The construction of the sublibraries and the ELISA-driven quantitative measurements of MHC interaction are as given above.

Briefly, the relative binding (RB) affinity of each PSCPL sublibrary was determined as RB (PSCPL)=ED_{50} (X_9)/ED_{50} (PSCPL) (where ED_{50} is the concentration needed to half-saturate a low concentration of MHC-I molecules) and normalized so that the sum of the RB values of the 20 naturally occurring amino acids equals 20 (since peptides with a given amino acid in a given position are 20 times more frequent in the corresponding PSCPL sublibrary than

in the completely random X_9 library). A RB value above 2 was considered as the corresponding position and amino acid being favored, whereas a RB value below 0.5 was considered as being unfavorable (these thresholds represent the 95% confidence intervals). An anchor position (AP) value was calculated by the equation $\sum(RB-1)^2$. A primary anchor position is characterized by one or few amino acids being strongly preferred and many amino acids being unacceptable. We have arbitrarily defined anchor residues as having an AP value above 15 (Lamberth et al. 2008). The peptide–SLA-I*0401 binding activity of each sublibrary was determined using previously published biochemical binding assay (ELISA) (Sylvester-Hvid et al. 2002) (with the modifications described above).

Sequence logos

Sequences logos describing the predicted binding motif for each MHC molecule were calculated as described by Rapin et al. (2010). In short, the binding affinity for a set of 1,000,000 random natural 9mer peptides was predicted using the *NetMHCpan* method, and the 1% strongest binding peptides were selected for construction of a position-specific scoring matrix (PSSM). The PSSM was constructed as previously described (Nielsen et al. 2004) including pseudo-count correction for low counts. Next, sequence logos were generated from the amino acid frequencies identified in the PSSM construction. For each position, the frequency of all 20 amino acids is displayed as a stack of letters. The total height of the stack represents the sequence conservation (the information content), while the individual height of the symbols relates to the relative frequency of that particular symbol at that position. Letter shown upside-down are underrepresented compared to the background (for details see Rapin et al. (2010)).

MHC distance trees

MHC distance trees were derived from correlations between predicted binding affinities. For each allelic MHC-I molecule, the binding affinity was predicted for a set of 200,000 random natural peptides using the *NetMHCpan* method. Next, the distance between any two alleles was defined, as $D=1-\mathrm{PCC}$, where PCC is the Pearson correlation between the subset of peptides within the superset of top 10% best binding peptides for each allele. In this measure, two molecules that share a similar binding specificity will have a distance close to 0 whereas two molecules with non-overlapping binding specificities would have a distance close to 2. Using bootstrap, 100 such distance trees were generated, and branch bootstrap values and the consensus tree were calculated.

Results

Generation of chimeric MHC class I molecules

We have previously generated highly active, recombinant human MHC-I (HLA-I) molecules and accompanying high-throughput assays and bioinformatics prediction resources. Here, we transfer the underlying approaches to an important domesticated livestock animal, the pig, and its MHC system, the SLAs. MHC-I molecules are composed of a unique and highly variable distal peptide-binding platform consisting of the alpha 1 (α_1) and alpha 2 (α_2) domains of the MHC-I heavy chain (HC) and a much more conserved proximal immunoglobulin-like membrane attaching stalk consisting of the alpha 3 (α_3) domain of the HC non-covalently associated with the soluble MHC-I light chain (β_2m).

A priori, the establishment of recombinant SLA molecules is complicated by the lack of validated reagents. Any failure could therefore be caused either by real technical problems in generating SLA molecules, or merely by a lack of information about strong peptide binders to the SLA in question. To reduce this uncertainty, we decided to migrate from human to pig MHC-I in a step-wise manner and generate an intermediary chimeric MHC-I molecule composed of a well-known human peptide-binding platform attached to a SLA stalk, which might allow us to assess whether we could generate a functional SLA stalk consisting of SLA-1*0401 α_3 HC and pig β_2m. To this end, we used the $\alpha_1\alpha_2$ domains of the HLA-A*11:01 molecule, which we expected should be able to bind a known high-affinity HLA-A*11:01-binding peptide (KVFPYALINK). This peptide could be ^{125}I radiolabeled and used in a very robust peptide-binding assay testing whether the human stalk could be replaced with the corresponding SLA stalk. Once that had been successfully established, the entire SLA-1*0401 molecule would be constructed and tested.

We have previously expressed and purified the extracellular segment spanning positions 1–275 of the human HLA-A*11:01 in a denatured and pre-oxidized version that rapidly refold and bind appropriate target peptides (Ostergaard et al. 2001; Ferre et al. 2003). Codon-optimized genes encoding the corresponding segments of SLA-1*0401 ($\alpha_1\alpha_2$) and SLA-1*0401 (α_3) were constructed as described in the "Materials and methods" section and used to replace the HLA-A*11:01 gene segment in the above construct generating a new construct allowing for the expression of SLA-1*0401. For the generation of HLA-A*11:01/SLA-1*0401 chimeras, the genes encoding α_1 (spanning positions 1–90), α_2 (spanning positions 91–181), and/or α_3 (spanning positions 182–275) domains of HLA-A*11:01 and SLA-1*0401 were exchanged using Seam-Less and touch-down cloning strategies. Genes encoding

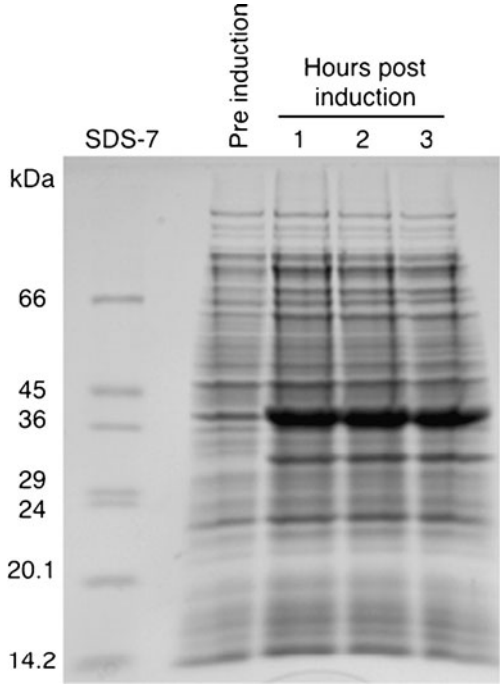

Fig. 2 SDS-PAGE analysis of cell lysates of SLA-1*0401 expression in *E. coli* before and after induction with IPTG. Samples were mixed 1:1 in a reducing SDS sample buffer and loaded onto a 12% polyacrylamide gel

the extracellular segments 1–275 of the above natural or chimeric MHC-I molecules were C-terminally fused to a biotinylation tag (as indicated for SLA-1*0401 in Online Resource 1), inserted into pET28, and expressed in inclusion bodies in *E. coli* (Fig. 2 shows SDS-PAGE of lysates of recombinant *E. coli* before and 3 h after IPTG induction). The fusion proteins were extracted into 8 M urea (without any reducing agents), purified by ion exchange, hydrophobic and gel filtration chromatography (all conducted in 8 M urea, without any reducing agents) (Fig. 3 shows SDS-PAGE of the purified SLA-1*0401 after gel filtration), concentrated, and stored in urea at −20°C.

Testing a chimeric molecule consisting of a SLA-1*0401 stalk and a HLA-A*11:01 peptide-binding platform—comparing human versus porcine β_2m

To test the proximal immunoglobulin-like membrane attaching SLA stalk, we generated recombinant porcine β_2m and a chimeric human/porcine MHC-I heavy chain molecule where the $\alpha_1\alpha_2$ were derived from the human HLA-A*11:01, and the α_3 was derived from the porcine SLA-1*0401. Since this construct contains the entire peptide-binding platform of HLA-A*11:01, we reasoned that the binding of the HLA-A*11:01 restricted peptide, KVFPYALINK, could be used as a functional readout of the refolding, activity, and assembly of the entire chimeric molecule including the porcine SLA stalk. For comparison, we tested the supportive capacity of human β_2m and folding ability of the entirely human HLA-A*11:01. A total of four combinations could therefore be tested: porcine or human β_2m in combination with either HHP or HHH (where the first letter indicates the origin of the α_1 domain (*H*uman HLA-A*11:01 or *P*orcine SLA-1*0401), the second letter the origin of the α_2 domain, and the third letter the origin of the α_3 domain). A concentration–titration of heavy chain was added to a fixed excess concentration (3 μM) of β_2m and a fixed trace concentration (23 nM) of radiolabeled peptide. As shown in Figs. 4 and 5, the four combinations gave almost the same heavy chain dose titration with a half-saturation occurring around 1–2 nM heavy chain. Porcine β_2m supported folding of the chimeric (HHP) α chain slightly better than it supported folding of the human (HHH) α chain. Human β_2m

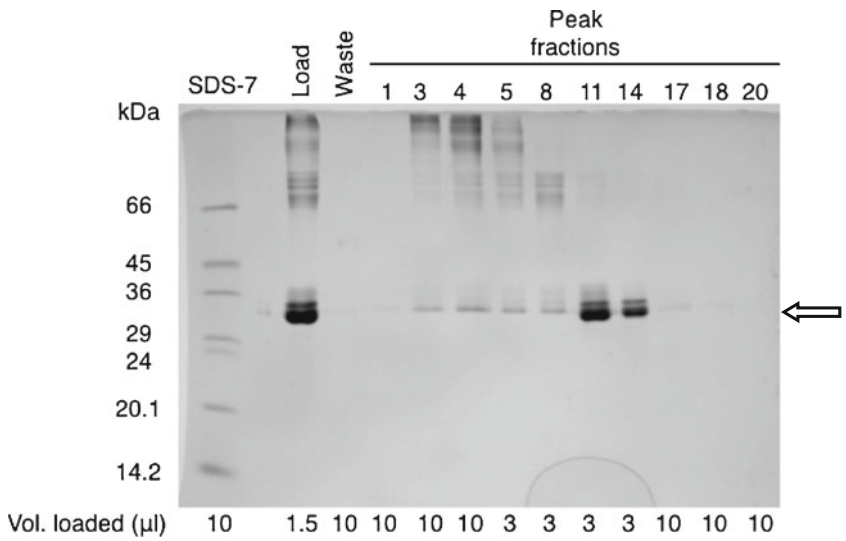

Fig. 3 SDS-PAGE analysis of size exclusion chromatography peak fractions from SLA-1*0401 purification. Fraction numbers are shown above each lane. Samples were mixed 1:1 in non-reducing SDS sample buffer and loaded onto a 12% polyacrylamide gel. Lanes were loaded with different volumes, indicated below each lane, to avoid overloading. An *arrow* indicates the band representing purified SLA-1*0401-BSP-HAT heavy chain (36,675 Da)

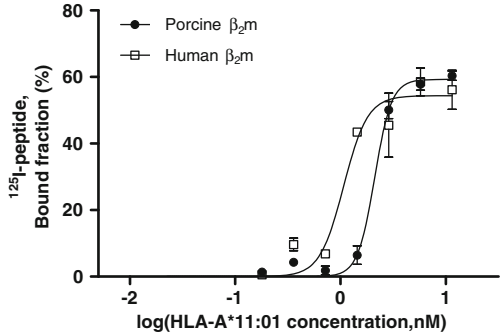

Fig. 4 HLA-A*11:01 complex formation with a known HLA-A*11:01-binding peptide (KVFPYALINK) using either human (*open squares*) or porcine (*filled circles*) β_2m. The affinity of HLA-A*11:01 to porcine and human β_2m was determined as 2.11 nM (95% confidence interval, 1.96 to 2.27) and 1.07 nM (95% confidence interval, 0.871 to 1.32), respectively

supported folding of HHP and HHH equally well. Thus, a recombinant SLA stalk can fold and support peptide binding of the peptide-binding platform. These results also suggest that human β_2m can support folding and peptide binding of porcine MHC-I heavy chain molecules.

Using a positional scanning combinatorial peptide library approach to perform an unbiased analysis of the specificity of SLA-1*0401 and human–pig chimeric MHC class I molecules

Using human β_2m to support folding, the recombinant SLA-1*0401 and human–pig chimeric MHC-I molecule were tested for peptide binding. We have previously described how PSCPL can be used to perform an unbiased analysis of MHC-I molecules (Stryhn et al. 1996). A PSCPL consists of 20 sublibraries for each position where one of each of the 20 natural amino acids have been locked and all other positions contain random amino acids. Analyzing how much of each PSCPL sublibrary is needed to support MHC-I folding (see examples in Fig. 6) and comparing each sublibrary with a completely random library, the effect of any amino acid in any position can be examined and expressed as a RB value. Further, an AP value calculated as the sum of squared deviations of RB values for each position can be used to identify the most prominent anchor position (see "Materials and methods" for calculations). Thus, the specificity of a nonamer binding MHC-I molecule can be analyzed comprehensively with 9×20+1 completely random library=181 sublibraries (Stryhn et al. 1996).

Here, this approach was used to perform a complete experimental analysis of SLA-1*0401 and a limited analysis of the chimeric HPP and PHP molecules. A nonamer PSCPL analysis of SLA-1*0401 can be seen in Table 1. AP values identified positions 9, 3, and 2 (in that order of importance) as the anchor positions of SLA-1*0401. In position 9, the amino acid preferences were dominated by the large and bulky aromatic tyrosine (Y), tryptophane (W), and phenylalanine (F), all having RB values above 4 (Table 1). In the almost equally important position 3, preferences for negatively charged amino acids glutamic acid (E) and aspartic acid (D) were observed. In the lesser important position 2, the most preferred amino acids were the hydrophobic amino acids valine (V), isoleucine (I), and leucine (L), followed by the polar amino acids threonine (T) and serine (S).

Finally, a very limited PSCPL analysis was performed for the two chimeric human HLA-A*11:01/porcine SLA-1*0401 MHC-I molecules, HPP and PHP (Table 2). For both chimeric molecules, it could be demonstrated that position 9 is a strong anchor position. The positively charged amino acids, arginine (R) and lysine (K), were preferred in position 9 of the chimeric HPP molecule, whereas the aromatic amino acid, tyrosine (Y), was exclusively preferred in position 9 of the chimeric PHP molecule.

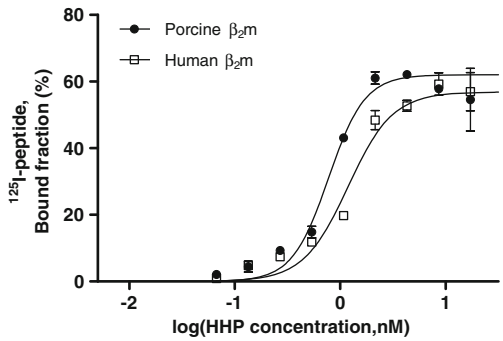

Fig. 5 MHC-I complex formation of the chimeric class I molecule HHP (HLA-A*11:01 ($\alpha_1\alpha_2$), SLA-1*0401 (α_3)) with a known HLA-A*11:01-binding peptide (KVFPYALINK), and human (*open squares*) versus porcine β_2m (*filled circles*). The affinity of HHP to porcine and human β_2m was determined as 0.774 nM (95% confidence interval, 0.630 to 0.951) and 1.19 nM (95% confidence interval, 0.958 to 1.47), respectively

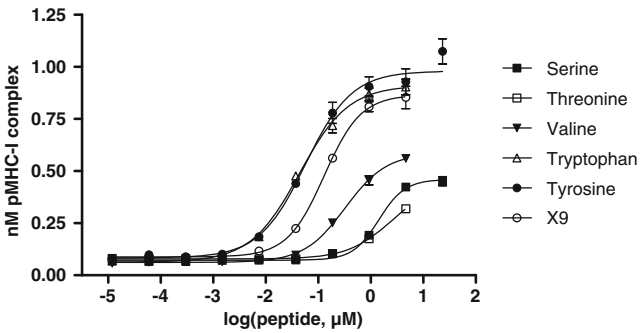

Fig. 6 PSCPL position 9 sublibrary analysis of the SLA-1*0401 peptide-binding motif. The amino acids valine, serine, and threonine are disfavored in position 9, evident by a decrease in affinity compared to the reference peptide (X9), whereas the large and bulky amino acids tryptophan and tyrosine are favored as seen by an increase in affinity compared to the reference peptide

Table 1 Binding motif of the SLA-1*0401 allele determined by PSCPL strategy

SLA-1*0401	Amino acid position in peptide								
	1	2	3	4	5	6	7	8	9
A	1.7	0.8	1.6	1.1	0.8	*0.4*	1.7	0.7	*0.0*
C	0.8	*0.2*	*0.4*	**2.7**	1.1	1.0	0.7	1.7	*0.0*
D	*0.4*	0.7	**7.7**	**2.1**	0.8	*0.1*	0.5	1.8	*0.0*
E	1.6	*0.0*	**2.8**	0.6	1.0	1.4	0.9	0.9	*0.2*
F	*0.4*	*0.2*	0.8	*0.0*	1.0	1.1	1.1	1.1	**5.8**
G	0.5	*0.3*	*0.1*	1.5	1.1	1.4	*0.0*	1.0	*0.0*
H	0.5	*0.2*	*0.1*	*0.1*	1.3	**2.4**	0.5	0.7	*0.4*
I	0.7	**3.4**	*0.3*	0.8	0.8	0.9	0.7	0.9	*0.3*
K	1.1	*0.2*	*0.1*	*0.4*	*0.4*	1.2	0.4	0.9	*0.0*
L	0.6	**2.1**	*0.2*	0.6	1.0	1.7	1.0	1.2	0.6
M	1.7	1.9	1.0	1.2	1.4	1.4	1.2	1.4	0.7
N	1.4	0.5	0.6	1.4	1.9	0.7	1.0	1.9	*0.0*
P	*0.0*	*0.0*	*0.1*	1.6	0.5	1.1	1.9	1.2	1.1
Q	1.0	0.9	*0.2*	1.0	0.5	*0.4*	0.8	0.7	*0.0*
R	**2.3**	*0.0*	*0.1*	0.6	**2.4**	0.9	1.0	0.5	*0.2*
S	1.8	**2.4**	1.8	1.1	0.8	1.5	1.6	0.7	*0.0*
T	1.4	**2.5**	1.6	0.7	0.9	0.5	2.0	0.7	*0.0*
V	1.1	**3.7**	*0.3*	0.5	0.7	0.8	0.9	0.6	0.8
W	*0.3*	*0.0*	*0.2*	0.6	1.0	0.8	0.6	1.4	**5.6**
Y	0.6	*0.0*	*0.5*	1.3	0.6	*0.2*	1.6	*0.3*	**4.3**
Sum	20	20	20	20	20	20	20	20	20
AP value	7	28	57	8	4	6	5	4	67

The normalized relative binding (RB) value indicates whether an amino acid is favored (RB>2, bold numbers) or disfavored (RB<0.5, italic numbers) in a given peptide position. The anchor position (AP) value is given by the equation $\sum(\mathrm{RB}-1)^2$. The important anchor positions 2, 3, and 9 for SLA-1*0401 are underlined

The positively charged amino acids, arginine (R) and lysine (K), were preferred in position 9 of the chimeric HPP molecule similar to the position 9 specificity of the HLA-A*11:01 molecule. In contrast, the aromatic amino acid tyrosine (Y) was preferred in position 9 of the chimeric PHP molecule similar to the position 9 specificity of the SLA-1*0401 molecule.

Using *NetMHCpan* to predict peptides that bind to SLA-1*0401 or to human–pig chimeric MHC class I molecules

Our recently described neural network-driven bioinformatics predictor, *NetMHCpan* (version 2.0), has been trained on about 88,000 peptide-binding data points representing more than 80 different MHC-I molecules (primarily HLA-A and HLA-B molecules). We have previously shown that *NetMHCpan* is an efficient tool to identify peptides that bind to HLA molecules where no prior data exist (Nielsen et al. 2007) and demonstrated that *NetMHCpan* can be extended to MHC-I molecules of other species[1] (Hoof et al. 2009). We applied *NetMHCpan* to our peptide repository of about 10,000 peptides, which over the past decade have been selected to scan infectious agents (e.g., SARS and influenza, Sylvester-Hvid et al. 2004; Wang et al. 2010), improve coverage of MHC-I specificities (e.g., Buus et al. 2003; Christensen et al. 2003), etc. We extracted 29 peptides as predicted binders to either the SLA-1*0401, the HPP, or the PHP human/porcine chimeric class I molecules (some of the peptides were predicted to bind to two or even all three of these molecules). All these peptide–MHC-I combinations were tested for binding (Table 3); 13 of 14 peptides bound to the SLA-1*0401 molecule with an affinity (IC_{50} value) better than 500 nM (6 with an affinity less than 50 nM); all 13 peptides tested on the PHP molecule were strong binders with IC_{50} values below 50 nM; and 3 of 12 peptides tested on the HPP molecule bound with an affinity better than 500 nM. Of the 39 peptide–MHC-I combinations tested, 20 (51%) were found to be good binders, 9 (23%) were average binders, and 10 (26%) did not bind well (Table 3). This is in stark contrast to the 0.5% frequency of binders among randomly selected peptides (Yewdell and Bennink 1999).

Next, the *NetMHCpan* method was used to generate PSSMs and sequence logos from the corresponding amino acid frequencies as described by Nielsen et al. (2004). For each position, the frequencies of all 20 amino acids were displayed as a stack of letters showing the sequence conservation/information content (the height of the entire

[1] A preliminary report of SLA-1*0401 binding was given in Hoof et al. (2009).

Table 2 Comparison of PSCPL derived binding motifs for the three MHC-I heavy chains HPP, PHP, and PPP ($h\alpha_1p\alpha_2p\alpha_3$, $p\alpha_1h\alpha_2p\alpha_3$, and SLA-I*0401) regarding peptide positions 2 and 9

Molecule: HPP Position in peptide			Molecule: PPP Position in peptide			Molecule: PHP Position in peptide		
Amino acid	2	9	Amino acid	2	9	Amino acid	2	9
A	*0.3*	*0.4*	A	0.8	*0.0*	A	1.0	*0.0*
C	*0.2*	*0.4*	C	*0.2*	*0.0*	C	*0.0*	*0.0*
D	*0.2*	*0.4*	D	0.7	*0.0*	D	*0.0*	*0.0*
E	*0.2*	*0.4*	E	0.0	*0.2*	E	*0.0*	*0.0*
F	*0.0*	*0.4*	F	*0.2*	**5.8**	F	*0.1*	0.5
G	*0.2*	*0.4*	G	*0.3*	*0.0*	G	*0.4*	*0.0*
H	*0.2*	*0.4*	H	*0.2*	*0.4*	H	*0.2*	0.5
I	**2.4**	*0.4*	I	**3.4**	*0.3*	I	**2.7**	*0.1*
K	*0.2*	**2.3**	K	*0.2*	*0.0*	K	*0.1*	*0.0*
L	*0.0*	*0.4*	L	**2.1**	0.6	L	1.8	*0.4*
M	**5.3**	*0.4*	M	1.9	0.7	M	**2.1**	0.7
N	*0.0*	*0.4*	N	0.5	*0.0*	N	*0.2*	*0.0*
P	*0.2*	*0.4*	P	*0.0*	1.1	P	*0.0*	0.7
Q	*0.0*	*0.4*	Q	0.9	*0.0*	Q	1.1	*0.0*
R	*0.2*	**9.6**	R	*0.0*	*0.2*	R	*0.2*	*0.0*
S	**3.4**	*0.4*	S	**2.4**	*0.0*	S	**2.8**	*0.0*
T	**4.8**	*0.4*	T	**2.5**	*0.0*	T	**3.6**	*0.0*
V	1.6	*0.4*	V	**3.7**	0.8	V	**3.3**	*0.3*
W	*0.2*	*0.4*	W	*0.0*	**5.6**	W	*0.1*	*0.2*
Y	*0.2*	*0.4*	Y	*0.0*	**4.3**	Y	*0.2*	**16.5**
Sum	20	20	Sum	20	20	Sum	20	20
AP value	51	81	AP value	28	67	AP value	30	254

RB and AP values are defined as described in Table 1

stack) and the relative frequency of amino acids (the height of the individual amino acids). Figure 7 shows a specificity tree clustering of the SLA-1*0401 molecule compared to prevalent representatives of the 12 common HLA supertypes that *NetMHCpan* originally intended to cover (Lund et al. 2004). By this token, SLA-1*0401 most closely resembles that of HLA-A*01:01.

The limited PSCPL analysis of the chimeric MHC-I molecules revealed strong P9 signals with specificities that seemed to be determined by the origin of the α_1 domain: the HPP chimera showed an HLA-A*11:01-like P9 specificity, whereas the PHP chimera showed a SLA-1*0401/HLA-A*01:01-like specificity. Since the *NetMHCpan* predictor successfully captured these chimeric specificities (see above), we reasoned that the predictor might also be used to perform in silico dissection of these specificities and used the P9 specificity as an example of such an in silico analysis. The *NetMHCpan* predictor considers a pseudo-sequence consisting of 34 polymorphic positions, which contain residues that are within 4.0 Å of the atoms of bound nonamer peptides (Nielsen et al. 2007). Of the 34 positions of the pseudo-sequence, 10 delineates the P9 binding pocket; however, only 3 of these, positions 74, 77, and 97, differ between SLA-1*0401 and HLA-A*11:01. To explore the effect of these three residues, we performed in silico experiments where we examined single substitutions Y74D, G77D, and S97I (the letter before the position number indicates the SLA-A*0401 single letter residue, whereas the letter after indicates the HLA-A*11:01 residue) as well as the corresponding triple substitution (YGS-DDI). As described above, PSSMs were generated for each of the in silico molecules followed by a specificity tree clustering (including SLA-A*0401, HLA-A*01:01, and HLA-A*11:01). Figure 8 shows this tree along with the sequence logo plots showing the predicted binding specificity of each in silico MHC-I molecule. Albeit the Y74D and G77D single substitutions showing some of the positively charged P9 peptide residue preference of HLA-A*11:01, they still clustered with HLA-A*01:01. In contrast, the in silico (YGS-DDI) triple substitution clustered with the HLA-A*11:01. This suggests that the *NetMHCpan* method is capable of defining the residues of the F pocket that determine the specificity of position 9.

Discussion

We have previously suggested that the specificities of the entire human MHC-I system should be solved ("the human

Table 3 Peptide sequences and in vitro determined K_D values for the three different MHC molecules PPP (SLA-1*0401) (top), PHP ($p\alpha_1 h\alpha_2 p\alpha_3$) (middle), and HPP ($h\alpha_1 p\alpha_2 p\alpha_3$) (bottom), respectively

Peptide #	Sequence	Affinity (K_D, nM)
PPP		
1	HSNASTLLY	452
2	SSMNSFLLY	192
3	YSAEALLPY	202
4	MTFPVSLEY	15
5	MSSAAHLLY	103
6	STFATVLEY	32
7	MTAASYARY	16
8	HTSALSLGY	163
9	ASYQFQLPY	8
10	YANMWSLMY	386
11	STYQPLPLY	38
12	HTAAPWGSY	Non-binder
13	ITMVNSLTY	169
14	ATAAATEAY	5
PHP		
1	HSNASTLLY	5
2	SSMNSFLLY	2
4	MTFPVSLEY	1
5	MSSAAHLLY	1
6	STFATVLEY	3
9	ASYQFQLPY	1
13	ITMVNSLTY	2
15	STMPLSWMY	1
16	HMMAVTLFY	11
17	KTFEWGVFY	6
18	ATNNLGFMY	1
19	ATATWFQYY	3
20	ITMVNSLTY	2
HPP		
2	SSMNSFLLY	Non-binder
4	MTFPVSLEY	Non-binder
6	STFATVLEY	Non-binder
21	FSFGGFTFK	Non-binder
22	KVFDKSLLY	Non-binder
23	ATFSVPMEK	Non-binder
24	RVMPVFAFK	17
25	AVYSSSMVK	127
26	AVARPFFAK	231
27	GSYFSGFYK	Non-binder
28	LTFLHTLYK	Non-binder
29	MTMRRRLFK	Non-binder

The NetMHCpan percentage of success for predicting binders for the PPP, PHP, and HPP heavy chains were 93%, 100%, and 33%, respectively

MHC", Buus 1999; Lauemoller et al. 2000). However, due to the extreme polymorphism of the MHCs, any attempt to address the specificity of the entire MHC system is a significant experimental undertaking. During the past decade, we have established a series of technologies to support a general solution of human MHC class I and II specificities. For MHC-I, this includes (1) a highly efficient *E. coli* expression system for production of recombinant human and mouse MHC-I molecules (both heavy chain and light chain (β_2m) molecules) (Pedersen et al. 1995; Ostergaard et al. 2001), (2) a purification system for obtaining the highly active pre-oxidized MHC-I heavy chain species (Ferre et al. 2003), (3) a high-throughput homogenous peptide–MHC-I binding assay for obtaining large data sets on peptide–MHC-I interactions (Harndahl et al. 2009), (4) a positional scanning combinatorial peptide library approach for a robust and unbiased analysis of the specificity of any MHC-I molecule (Stryhn et al. 1996), (5) an immunobioinformatics approach to generate predictors of the peptide–MHC-I interaction, *NetMHCpan*, that allows predictions to be made for any human MHC-I molecules, HLA-I, even those that have not yet been covered by existing data set (Hoof et al. 2009; Nielsen et al. 2007), and finally (6) we have demonstrated that pre-oxidized MHC-I molecules can be used to generate MHC-I tetramers in a simple "one-pot, mix-and-read" manner (Leisner et al. 2008). Here, we propose that the next goal should be to extend the overall approach to MHC-I molecules of other species of interest. Mouse and rats have been extensively studied in the past, but much less reagents and information have accrued for the MHC-I molecules of other species. Here, we have used an important livestock animal, the pig, as a model system and demonstrated that it indeed is possible to transfer the original human approach to other species.

Before attempting to generate a recombinant version of the entire porcine SLA-1*0401 molecule, we grafted the more conserved membrane-proximal "stalk" (the immunoglobulin-like class I heavy chain α_3 and β_2m domains) of porcine SLA-1*0401 onto the peptide-binding domain of HLA-A*11:01 generating a chimeric human/porcine MHC-I molecule. This chimeric molecule retained the peptide-binding specificity of the HLA-A*11:01 molecule, and it clearly demonstrated that the recombinant porcine stalk was functional and, by inference, also properly folded. It also suggests that the peptide-binding specificity of the distal domains do not crucially depend upon the identity of the proximal stalk. Further, comparing the ability of human and porcine β_2m to support MHC-I complex formation using either a human or a porcine MHC-I stalk, we demonstrated that every combination (porcine β_2m/human-α_3, porcine β_2m/porcine-α_3, human β_2m/human-α_3, and human β_2m/porcine-α_3) showed al-

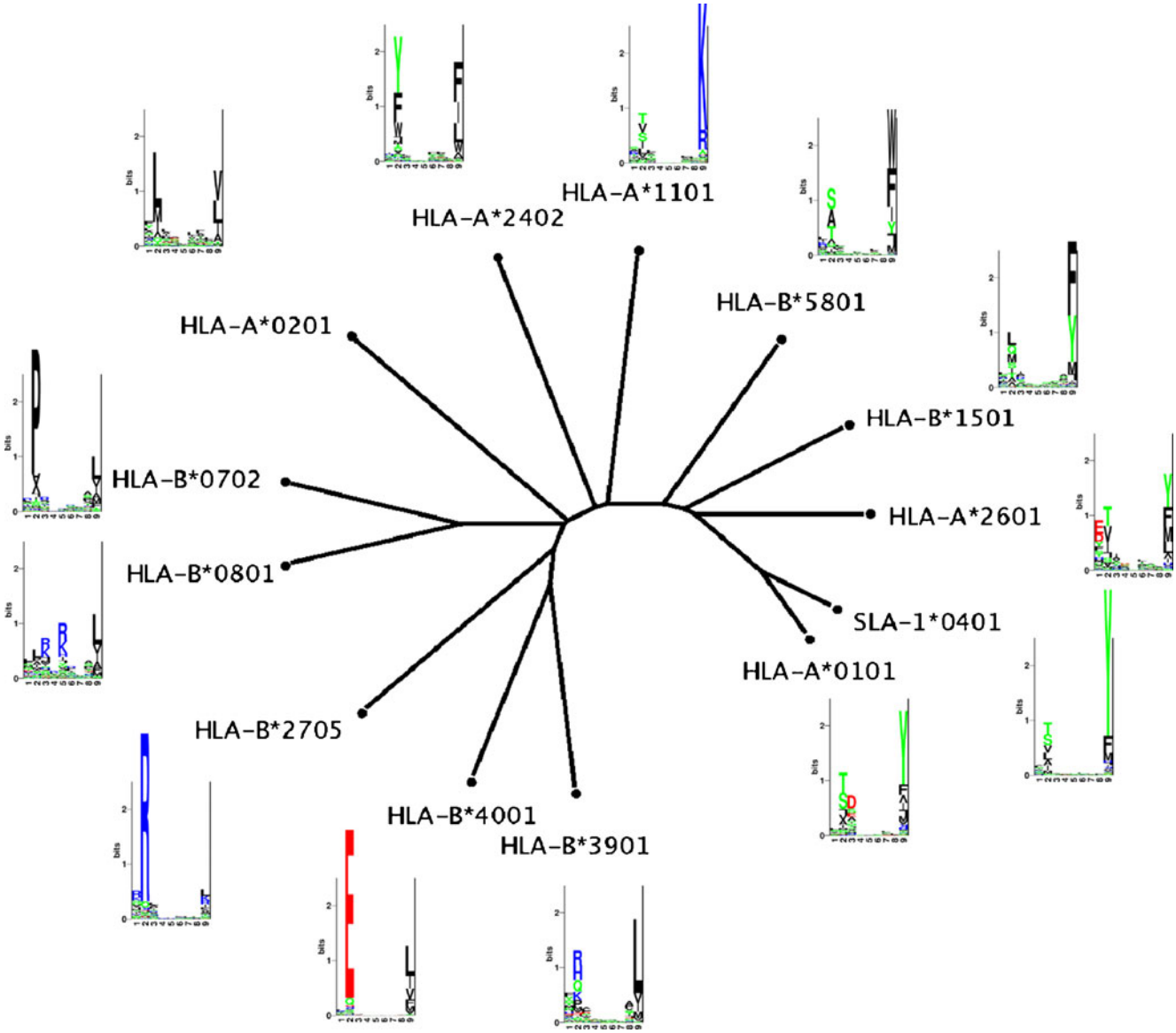

Fig. 7 Specificity tree clustering of the SLA-1*0401 molecule compared to prevalent representatives of the 12 common HLA supertypes (Lund et al. 2004). The distance between any two MHC molecules and the consensus tree is calculated as described in "Materials and methods". All branch points in the tree have bootstrap values of 100%. Sequence logos of the predicted binding specificity are shown for each molecule. In the logo, acidic amino acids [DE] are shown in *red*, basic amino acids [HKR] in *blue*, hydrophobic amino acids [ACFILMPVW] in *black*, and neutral amino acids [GNQSTY] in *green*. The axis of the LOGOs indicates in all case positions one through nine of the motif, and the y-axis the information content (see Materials and methods)

most the same heavy chain dose titration with identical half-saturations. These results illustrate the ability for porcine and human β_2m to support complex formation of SLA molecules and vice versa and suggest evolutionary that the stalk is quite conserved.

Next, we generated the entire SLA-1*0401 heavy chain and succeeded in generating complexes using human β_2m as the light chain and PCSPL as peptide donors. The latter solved the a priori problem of not knowing which peptides would be needed to support proper folding of SLA-1*0401, and it did so in an unbiased manner. Furthermore, this approach is highly efficient since it readily establishes a complete matrix representing the amino acid preference for each amino acid and each position of a nonamer peptide. The specificity of SLA-1*0401 shows two primary anchors: one in positions 9 with a preference for aromatic amino acids and another in position 3 with a preference for negatively charged amino acids. In addition, the SLA-1*0401 features a secondary anchor in position 2 with hydrophobic or polar amino acid preferences.

An alternative approach to solve the problem of identifying peptides that support folding of MHC-I molecules of so far unknown specificity is to use our recently developed pan-specific predictor, *NetMHCpan*. The successful use of this predictor to initiate peptide-binding studies was recently

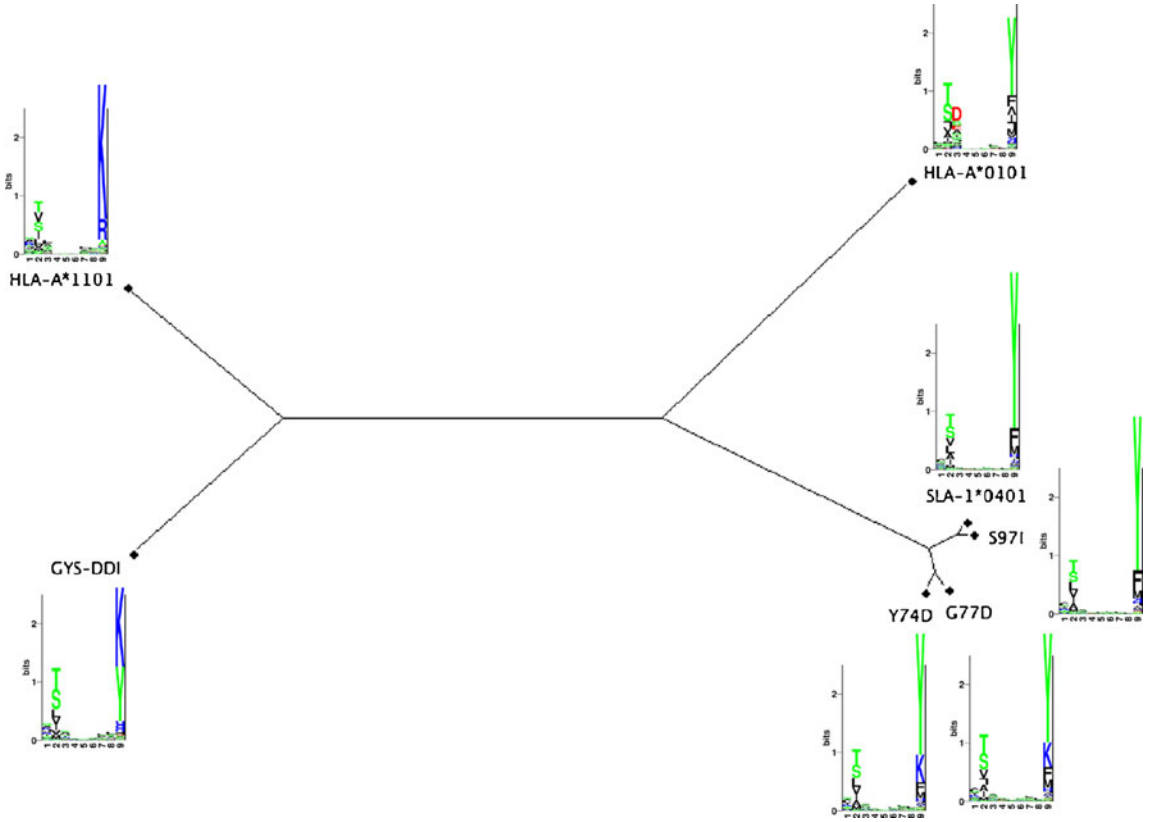

Fig. 8 Comparison of specific in silico mutations of the SLA-1*0401 molecule and comparison with the two HLA molecules: HLA-A*11:01 and HLA-A*01:01. The distance between any two MHC molecules and the consensus tree is calculated as described in "Materials and methods". All branch points in the tree have bootstrap values of 100%. The SLA-1*0401 mutations are indicated as Y74D, G77D, and S97I, where the letter before the position number indicates the SLA-1*0401 single letter residue and the letter after indicates the HLA-A*11:01 residue. YGS-DDI is the corresponding triple substitution. Sequence logos are calculated and visualized as described in Fig. 7. The axis of the LOGOs indicates in all case positions one through nine of the motif, and the y-axis the information content (see Materials and methods)

demonstrated for HLA-A*3001 (Lamberth et al. 2008). Although originally developed to cover all HLA-A and HLA-B molecules, it has also been shown to extend to MHC-I molecules of other species (Hoof et al. 2009). Here, we demonstrate that the *NetMHCpan* predictor is capable of extracting MHC-I sequence information across species and correctly relate this to peptide binding even in the absence of any available data for the specific query MHC-I molecule, i.e., the SLA-1*0401 as well as the chimeric HPP ($h\alpha_1p\alpha_2p\alpha_3$) and PHP ($p\alpha_1h\alpha_2p\alpha_3$) molecules. It is not clear why binding of the PHP chimera was more efficiently predicted than binding of the HPP chimera. One could speculate that *NetMHCpan* has not captured the effect of the different positions of the pseudo-sequence equally well and not all positions and pockets (and by inference—not all chimeric molecules) are therefore predicted equally well.

Using the *NetMHCpan* predictor to cluster SLA-1*0401 and representative molecules of 12 human HLA supertypes according to predicted peptide-binding specificities, the SLA-1*0401 specificity closely resembled that of HLA-A*01:01 (IEDB, http://www.immuneepitope.org/MHCalleleId/142, accessed March 9th 2011). This result was also obvious from an inspection of the PSCPL analysis of the SLA-1*0401. The PSCPL analysis of the P9 specificity of the SLA-1*0401 and the two chimeric molecules suggested that the P9 specificity primarily was determined by the α_1 domain. This contention was further strengthened by a *NetMHCpan*-driven in silico analysis of the residues delineating the F pocket, which interacts with P9. This suggests that *NetMHCpan* can be used to design and interpret detailed experiments addressing the structure–function relationship of peptide–MHC-I interaction. In the case of SLA-1*0401, *NetMHCpan* suggests that Y74, G77, and S97 play a prominent role in defining the P9 F pocket. Whereas the *NetMHCpan* readily captured the P9 anchor residue of SLA-1*0401, it did not capture the P3 anchor (at least not in the 2.4 version). We surmise that this shortcoming is due to insufficient examples of the use of P3 anchors within the currently available peptide–MHC-I binding data. Inspecting the pseudo-sequence of SLA-1*0401 and HLA-A*01:01 vs. HLA-A*11:01 suggests that the presence of an arginine in position 156 might

explain the preference for negatively charged amino acid residues in P3. Future *NetMHCpan*-guided experiments could pointedly address this question, and the resulting data could complement existing data and be used to update and improve the *NetMHCpan* predictor.

All in all the two complementary approaches, PSCPL and *NetMHCpan*, agreed on the specificity of the SLA-1*0401 molecule, as well as of the two chimeric MHC-I molecules. Thus, the specificity of SLA-1*0401 appear to be well established. This specificity has successfully been used to search for foot-and-mouth disease virus (FMDV)-specific CTL epitopes in FMDV-vaccinated, SLA-1*0401-positive pigs, and the recombinant SLA-1*0401 molecules have been used to generate corresponding tetramers and stain pig CTLs (Patch et al. 2011). In conclusion, we here present a set of methods that can be used to generate functional recombinant MHC-I molecules, map their specificities and identify MHC-I-restricted epitopes, and eventually generate peptide–MHC-I tetramers for validation of CTL responses. This suite of methods is not only applicable to humans, but potentially to any species of interest.

Acknowledgments We thank Lise Lotte Bruun Nielsen, Anne Caroline Schmiegelow, and Iben Sara Pedersen for their expert experimental support. This work was in part supported by the Danish Council for Independent Research, Technology and Production Sciences (274-09-0281) and by the National Institute of Health (NIH) (HHSN266200400025C).

References

Buus S (1999) Description and prediction of peptide-MHC binding: the 'human MHC project'. Curr Opin Immunol 11:209–213

Buus S, Stryhn A, Winther K, Kirkby N, Pedersen LO (1995) Receptor–ligand interactions measured by an improved spun column chromatography technique. A high efficiency and high throughput size separation method. Biochim Biophys Acta 1243:453–460

Buus S, Lauemoller SL, Worning P, Kesmir C, Frimurer T, Corbet S, Fomsgaard A, Hilden J, Holm A, Brunak S (2003) Sensitive quantitative predictions of peptide-MHC binding by a 'Query by Committee' artificial neural network approach. Tissue Antigens 62:378–384

Christensen JK, Lamberth K, Nielsen M, Lundegaard C, Worning P, Lauemoller SL, Buus S, Brunak S, Lund O (2003) Selecting informative data for developing peptide–MHC binding predictors using a query by committee approach. Neural Comput 15:2931–2942

Ferre H, Ruffet E, Blicher T, Sylvester-Hvid C, Nielsen LL, Hobley TJ, Thomas OR, Buus S (2003) Purification of correctly oxidized MHC class I heavy-chain molecules under denaturing conditions: a novel strategy exploiting disulfide assisted protein folding. Protein Sci 12:551–559

Hansen NJ, Pedersen LO, Stryhn A, Buus S (2001) High-throughput polymerase chain reaction cleanup in microtiter format. Anal Biochem 296:149–151

Harndahl M, Justesen S, Lamberth K, Roder G, Nielsen M, Buus S (2009) Peptide binding to HLA class I molecules: homogenous, high-throughput screening, and affinity assays. J Biomol Screen 14:173–180

Hoof I, Peters B, Sidney J, Pedersen LE, Sette A, Lund O, Buus S, Nielsen M (2009) NetMHCpan, a method for MHC class I binding prediction beyond humans. Immunogenetics 61:1–13

Hunter W, Greenwood F (1962) Preparation of iodine-131 labelled human growth hormone of high specific activity. Nature 194:495–496

Kast WM, Brandt RM, Sidney J, Drijfhout JW, Kubo RT, Grey HM, Melief CJ, Sette A (1994) Role of HLA-A motifs in identification of potential CTL epitopes in human papillomavirus type 16 E6 and E7 proteins. J Immunol 152:3904–3912

Lamberth K, Roder G, Harndahl M, Nielsen M, Lundegaard C, Schafer-Nielsen C, Lund O, Buus S (2008) The peptide-binding specificity of HLA-A*3001 demonstrates membership of the HLA-A3 supertype. Immunogenetics 60:633–643

Larsen MV, Lundegaard C, Lamberth K, Buus S, Brunak S, Lund O, Nielsen M (2005) An integrative approach to CTL epitope prediction: a combined algorithm integrating MHC class I binding, TAP transport efficiency, and proteasomal cleavage predictions. Eur J Immunol 35:2295–2303

Lauemoller SL, Kesmir C, Corbet SL, Fomsgaard A, Holm A, Claesson MH, Brunak S, Buus S (2000) Identifying cytotoxic T cell epitopes from genomic and proteomic information: "the human MHC project". Rev Immunogenet 2:477–491

Leisner C, Loeth N, Lamberth K, Justesen S, Sylvester-Hvid C, Schmidt EG, Claesson M, Buus S, Stryhn A (2008) One-pot, mix-and-read peptide–MHC tetramers. PLoS One 3:e1678

Lund O, Nielsen M, Kesmir C, Petersen AG, Lundegaard C, Worning P, Sylvester-Hvid C, Lamberth K, Roder G, Justesen S, Buus S, Brunak S (2004) Definition of supertypes for HLA molecules using clustering of specificity matrices. Immunogenetics 55:797–810

Lundegaard C, Lamberth K, Harndahl M, Buus S, Lund O, Nielsen M (2008) NetMHC-3.0: accurate web accessible predictions of human, mouse and monkey MHC class I affinities for peptides of length 8–11. Nucleic Acids Res 36:W509–W512

Nielsen M, Lundegaard C, Worning P, Lauemoller SL, Lamberth K, Buus S, Brunak S, Lund O (2003) Reliable prediction of T-cell epitopes using neural networks with novel sequence representations. Protein Sci 12:1007–1017

Nielsen M, Lundegaard C, Worning P, Hvid CS, Lamberth K, Buus S, Brunak S, Lund O (2004) Improved prediction of MHC class I and class II epitopes using a novel Gibbs sampling approach. Bioinformatics 20:1388–1397

Nielsen M, Lundegaard C, Blicher T, Lamberth K, Harndahl M, Justesen S, Roder G, Peters B, Sette A, Lund O, Buus S (2007) NetMHCpan, a method for quantitative predictions of peptide binding to any HLA-A and -B locus protein of known sequence. PLoS One 2:e796

Ostergaard PL, Nissen MH, Hansen NJ, Nielsen LL, Lauenmoller SL, Blicher T, Nansen A, Sylvester-Hvid C, Thromsen AR, Buus S (2001) Efficient assembly of recombinant major histocompatibility complex class I molecules with preformed disulfide bonds. Eur J Immunol 31:2986–2996

Patch JR, Pedersen LE, Toka FN, Moraes M, Grubman MJ, Nielsen M, Jungersen G, Buus S, Golde WT (2011) Induction of foot-and-mouth disease virus-specific cytotoxic T cell killing by vaccination. Clin Vaccine Immunol 18:280–288

Pedersen LO, Stryhn A, Holter TL, Etzerodt M, Gerwien J, Nissen MH, Thogersen HC, Buus S (1995) The interaction of beta 2-microglobulin (beta 2m) with mouse class I major histocompatibility antigens and its ability to support peptide binding. A comparison of human and mouse beta 2m. Eur J Immunol 25:1609–1616

Rapin N, Hoof I, Lund O, Nielsen M (2010) The MHC motif viewer: a visualization tool for MHC binding motifs. Curr. Protoc. Immunol. Chapter 18:Unit 18.17

Sette A, Sidney J, del Guercio MF, Southwood S, Ruppert J, Dahlberg C, Grey HM, Kubo RT (1994) Peptide binding to the most frequent HLA-A class I alleles measured by quantitative molecular binding assays. Mol Immunol 31:813–822

Smith DM, Lunney JK, Martens GW, Ando A, Lee JH, Ho CS, Schook L, Renard C, Chardon P (2005) Nomenclature for factors of the SLA class-I system, 2004. Tissue Antigens 65:136–149

Stranzl T, Larsen MV, Lundegaard C, Nielsen M (2010) NetCTLpan: pan-specific MHC class I pathway epitope predictions. Immunogenetics 62:357–368

Stryhn A, Pedersen LO, Romme T, Holm CB, Holm A, Buus S (1996) Peptide binding specificity of major histocompatibility complex class I resolved into an array of apparently independent subspecificities: quantitation by peptide libraries and improved prediction of binding. Eur J Immunol 26:1911–1918

Sullivan JA, Oettinger HF, Sachs DH, Edge AS (1997) Analysis of polymorphism in porcine MHC class I genes: alterations in signals recognized by human cytotoxic lymphocytes. J Immunol 159:2318–2326

Sylvester-Hvid C, Kristensen N, Blicher T, Ferre H, Lauemoller SL, Wolf XA, Lamberth K, Nissen MH, Pedersen LO, Buus S (2002) Establishment of a quantitative ELISA capable of determining peptide–MHC class I interaction. Tissue Antigens 59:251–258

Sylvester-Hvid C, Nielsen M, Lamberth K, Roder G, Justesen S, Lundegaard C, Worning P, Thomadsen H, Lund O, Brunak S, Buus S (2004) SARS CTL vaccine candidates; HLA supertype-, genome-wide scanning and biochemical validation. Tissue Antigens 63:395–400

Wang M, Larsen MV, Nielsen M, Harndahl M, Justesen S, Dziegiel MH, Buus S, Tang ST, Lund O, Claesson MH (2010) HLA class I binding 9mer peptides from influenza A virus induce CD4 T cell responses. PLoS One 5:e10533

Yewdell JW, Bennink JR (1999) Immunodominance in major histocompatibility complex class I-restricted T lymphocyte responses. Annu Rev Immunol 17:51–88

4. Paper II

Identification of peptides from foot-and-mouth disease virus structural proteins bound by class I swine leukocyte antigen (SLA) alleles, SLA-1*0401 and SLA-2*0401

Pedersen LE, Harndahl M, Nielsen M, Patch JR, Jungersen G, Buus S, Golde WT.

Anim Genet. 2012 Sep 18. doi: 10.1111/j.1365-2052.2012.02400.x

This manuscript describes the determination of the complete SLA-2*0401 binding motif and apply such PSCPL determined amino acid preferences, expressed by both SLA-1*0401 and SLA-2*0401, to *NetMHCpan* based predictions. Followed by *in vitro* peptide binding analyses these studies lead to the identification of several high-affinity binding peptides derived from FMDV. The analyses and methods presented provide the characterization of potential T cell epitopes in response to threatening diseases such as FMDV.

ANIMAL GENETICS Immunogenetics, Molecular Genetics and Functional Genomics

doi: 10.1111/j.1365-2052.2012.02400.x

Identification of peptides from foot-and-mouth disease virus structural proteins bound by class I swine leukocyte antigen (SLA) alleles, SLA-1*0401 and SLA-2*0401

L. E. Pedersen*[†,‡], M. Harndahl[†], M. Nielsen[§], J. R. Patch*, G. Jungersen[‡], S. Buus[†] and W. T. Golde*

*Foreign Animal Disease Unit, Plum Island Animal Disease Center, Agricultural Research Service, USDA, Greenport, NY, USA. [†]Laboratory of Experimental Immunology, Faculty of Health Sciences, University of Copenhagen, Copenhagen N., 2200, Denmark. [‡]National Veterinary Institute, Technical University of Denmark, Copenhagen, Denmark. [§]Center for Biological Sequence Analysis, Technical University of Denmark, Copenhagen, Denmark.

Summary

Characterization of the peptide-binding specificity of swine leukocyte antigen (SLA) class I and II molecules is critical to the understanding of adaptive immune responses of swine toward infectious pathogens. Here, we describe the complete binding motif of the SLA-2*0401 molecule based on a positional scanning combinatorial peptide library approach. By combining this binding motif with data achieved by applying the NetMHCpan peptide prediction algorithm to both SLA-1*0401 and SLA-2*0401, we identified high-affinity binding peptides. A total of 727 different 9mer and 726 different 10mer peptides within the structural proteins of foot-and-mouth disease virus (FMDV), strain A24 were analyzed as candidate T-cell epitopes. Peptides predicted by the NetMHCpan were tested in ELISA for binding to the SLA-1*0401 and SLA-2*0401 major histocompatibility complex class I proteins. Four of the 10 predicted FMDV peptides bound to SLA-2*0401, whereas five of the nine predicted FMDV peptides bound to SLA-1*0401. These methods provide the characterization of T-cell epitopes in response to pathogens in more detail. The development of such approaches to analyze vaccine performance will contribute to a more accelerated improvement of livestock vaccines by virtue of identifying and focusing analysis on bona fide T-cell epitopes.

Keywords binding motif, prediction, SLA, T-cell epitope

Introduction

The major histocompatibility complex class I (MHC I) molecules are highly polymorphic proteins that bind 8 to 11 amino acid (AA) peptides derived from the intracellular protein metabolism. In humans, such MHC class I molecules are referred to as human leukocyte antigens (HLA) and in swine are termed swine leukocyte antigens (SLA). These integral membrane proteins are found on all nucleated cells in vertebrates and play a crucial role in the cell-mediated immune response against viruses, other intracellular pathogens and transformed cells (cancer). When an endogenous peptide engages in a productive interaction with a MHC class I heavy chain and the non-polymorphic MHC I-stabilizing subunit molecule, beta-2-microglobulin (β_2m), they generate a heterotrimeric peptide/MHC/β_2m (pMHC) complex that is displayed at the cell surface. When surface-exposed MHC complexes incorporate foreign peptides, derived from a virus for instance, these complexes serve as targets for the T-cell receptor (TCR) on $CD8^+$, MHC I-restricted, peptide-specific, cytotoxic T lymphocytes (CTLs). In this way, endogenous peptides are constantly presented on the cell surface, signaling the cell's current state of integrity to the immune system of the host. If the peptide presented is of foreign origin, T cells may become activated and kill the infected or transformed cell (Doherty & Zinkernagel 1975; Zinkernagel & Doherty 1975; Bevan 1995; Harty *et al.* 2000).

Address for correspondence

W.T. Golde, Plum Island Animal Disease Center, Agricultural Research Service, USDA, PO Box 848, Greenport, NY 11944, USA.
E-mail: william.golde@ars.usda.gov

Accepted for publication 19 June 2012

The effect of polymorphism of the MHC I molecule is reflected in the different peptide-binding motifs that different class I molecules have, with peptide-binding anchor positions (APs) typically in positions 1, 2, 3 and 9 (Sette & Sidney 1999; Lamberth *et al.* 2008). More than 5400 different HLA-I alleles have been registered according to the IMGT/HLA database (http://www.ebi.ac.uk/imgt/hla/stats.html), and this number is growing rapidly as more efficient HLA typing techniques are employed worldwide. The same has been seen for SLA typing in recent years, with highly specific primer-based typing systems being used with success for both class I and class II genes in inbred as well as outbred pigs (Ho *et al.* 2006, 2010a,b; Yeom *et al.* 2010). As such, there is an equivalent need for biochemical data. However, characterizing the peptide-binding motif for each of these alleles is not feasible. Rather, application of the NetMHCpan peptide-binding predictor algorithm (Nielsen *et al.* 2007; Hoof *et al.* 2009) developed from the extensive human database available provides a method for quantitative predictions of peptide binding to any MHC protein. Thus, potential peptides that will bind can be reduced from hundreds (or even thousands) to a more dexterous number that can be tested.

Previously, we reported that the bioinformatics tools originally developed to cover all HLA-I molecules, despite the evolutionary distance, can be applied to SLA-I molecules (Hoof *et al.* 2009; Pedersen *et al.* 2011). Here, we have used the NetMHCpan predictor to predict peptides likely to be bound by the SLA-1*0401 and SLA-2*0401 molecules using a NetMHCpan rank score threshold of 2.00%. In this way, we were able to limit the number of possible peptides derived from the structural proteins of foot-and-mouth disease virus (FMDV), strain A24, from more than 700 to <16. Furthermore, by comparing the sequences of these peptides with the AA binding preferences exhibited by the SLA molecule in question, we were able to further reduce the number of peptides to be tested. The final peptide candidates were then analyzed *in vitro* for the ability to induce the formation of pMHC complexes with a high enough affinity to allow proper folding using the recombinant SLA-1*0401 and SLA-2*0401 class I heavy chains.

Through the production of recombinant SLA molecules, mapping of their peptide-binding motifs using universal peptide libraries, that is, the positional scanning combinatorial peptide libraries (PSCPL) (Stryhn *et al.* 1996; Lamberth *et al.* 2008), and the screening of AA sequences from FMDV structural proteins for possible peptide/MHC matches using NetMHCpan (Hoof *et al.* 2009), we were able to identify several *in vitro* binding peptides and characterize the SLA-2*0401 binding motif. Such data add to the knowledge of the binding characteristics for SLA molecules in general and could eventually lead to further insight into specific viral-derived peptides that induce porcine CTLs during infection. The result of taking these approaches is a rapid and accurate capacity to identify T-cell epitopes and the subsequent ability to measure specific T-cell immunity following vaccination or infection (Patch *et al.* 2011).

Materials and methods

Recombinant construct encoding the SLA-2*0401 protein

SLA-2*0401 recombinant protein was produced using a previously described standard expression system (Pedersen *et al.* 2011). Briefly, a transmembrane, truncated fragment encompassing residues 1–276 of the SLA-2*0401 alpha chain (Genscript, Appendix S1) followed by an FXa-BSP-HAT tag (FXa = factor Xa cleavage site comprising the AA sequence IEGR = I (isoleucine), E (glutamine acid), G (glycine), R (arginine), BSP = biotinylation signal peptide, HAT = histidine affinity tag for purification purposes) was inserted into a pET28a expression vector (Novagen). The construct was transformed into DH5α cells and sequenced (ABI Prism 3100Avant; Applied Biosystems) (Hansen *et al.* 2001). The validated construct of interest was transformed into an *Escherichia coli* (E. coli) production cell line, BL21 (DE3), containing the pACYC184 expression plasmid (Avidity) with an IPTG (Isopropyl-beta-D-thiogalactoside)-inducible BirA gene to express biotin-ligase. This leads to almost complete *in vivo* biotinylation of the desired product (Schmidt *et al.* 2009).

Expression and purification of recombinant SLA-2*0401 and human beta-2 microglobulin

SLA-2*0401 heavy chain proteins were produced as previously described (Pedersen *et al.* 2011). *E. coli* BL21(DE3) cells containing the SLA proteins were lyzed in a cell disrupter (Constant Cell Disruptor Systems set at 2300 bar), and the released inclusion bodies were isolated by centrifugation (Sorval RC6, 20 min, 17 000 ***g***). The inclusion bodies were washed twice in PBS, 0.5% NP-40 (Sigma), 0.1% deoxycholic acid (DOC; Sigma) and extracted into urea–Tris buffer (8 M urea, 25 mM Tris, pH 8.0). SLA-2*0401 heavy chain proteins extracted in 8 M urea were purified as previously described for the SLA-1*0401 molecule (Pedersen *et al.* 2011). In brief, this was carried out by successive immobilized metal adsorption, hydrophobic interaction, and Superdex-200 size exclusion chromatography. Throughout purification and storage, the MHC I heavy chain proteins were dissolved in 8 M urea to keep them denatured. The pre-oxidized, denatured proteins were stored at −20 °C in Tris-buffered 8 M urea. Recombinant human β_2m was expressed and purified as described elsewhere (Ostergaard *et al.* 2001; Ferre *et al.* 2003). Complexing the porcine alpha chains with human β_2m and peptide allowed the application of the ELISA for class I MHC folding using mouse anti-human β_2m, as described below and previously (Pedersen *et al.* 2011). Reagents for porcine β_2m are not available.

Published 2012. This article is a U.S. Government work and is in the public domain in the USA., doi: 10.1111/j.1365-2052.2012.02400.x

Peptides and peptide libraries

All peptides were purchased from Schafer-N. Briefly, they were synthesized by standard 9-fluorenylmethyloxycarbonyl (Fmoc) chemistry, purified by reverse-phase high-performance liquid chromatography (to at least >80% purity, frequently 95–99% purity), validated by mass spectrometry and quantitated by weight.

PSCPL peptides were used to determine the SLA-2*0401-binding motif. The experimental strategy of PSCPL has previously been described for both HLA (Stryhn *et al.* 1996) and SLA (Pedersen *et al.* 2011) proteins. Briefly, pools of random peptides with a single fixed AA in a fixed peptide position for every AA in every peptide position were used to determine the MHC-binding pocket motif of the MHC I protein. PSCPL peptides were used in a quantitative ELISA as described for the SLA-1*0401 molecule (Pedersen *et al.* 2011). The relative binding (RB) affinity of each PSCPL sublibrary was determined as RB (PSCPL) = $ED_{50}(X_9)$/ED_{50}(PSCPL) and normalized, so that the sum of the RB values of the 20 naturally occurring AA equaled 20 (ED_{50} being the concentration needed to half-saturate a low concentration of MHC class I molecules). Anchor position values were calculated by the equation $\sum(RB - 1)^2$.

PSCPL peptides were synthesized using standard solid-phase Fmoc chemistry on 2-chlorotrityl chloride resins. Briefly, an equimolar mixture of 19 of the common Fmoc AAs (excluding cysteine) was prepared for each synthesis and used for coupling in eight positions, whereas a single type of Fmoc AA (including cysteine) was used in one position. This position was changed in each synthesis starting with the N-terminus and ending with the C-terminus. In one synthesis, the AA pool was used in all nine positions. The library therefore consisted of $20 \times 9 + 1 = 181$ individual peptide libraries:

- 20 PSCPL sublibraries describing position 1: AX_8, CX_8, DX_8, … YX_8
- 20 PSCPL sublibraries describing position 2: XAX_7, XCX_7, XDX_7, … XYX_7
- etc.
- 20 PSCPL sublibraries describing position 9: X_8A, X_8C, X_8D, … X_8Y
- a completely random peptide library: X_9

X denotes the random incorporation of AA from the mixture, whereas the single-letter AA abbreviation is used to denote the identity of the fixed AA. Following synthesis, the peptides were cleaved from the resin in trifluoroacetic acid/1,2-ethanedithiol/triisopropylsilane/water 95:2:1:3 v/v/v/v, precipitated in cold diethyl ether and extracted with water before desalting on C18-columns, freeze drying and weighing.

ELISA for affinity of peptide binding

Peptides were tested for their ability to form complexes with the SLA-1*0401 and SLA-2*0401 proteins using a previously described immunosorbent assay (Sylvester-Hvid *et al.* 2002). Complexes of heavy chain with human β_2m and peptide were formed in 96-well plates (Thermo Scientific). All peptides were dissolved in 150 μl standard folding buffer [PBS, 0.1% pluriol (Lutrol F-68, BASF), pH 7.0] using sonication for 5 min. A fivefold dilution series of peptide in 12 consecutive points was performed in standard folding buffer. Following a 48-h incubation (18 °C), samples were transferred to streptavidine-coated plates (Nunc, DK-4000) and incubated for 3 h at 4 °C. Plates were washed in wash buffer (PBS, 0.05% Tween-20) and probed with a mouse anti-hβ_2m mAb (Brodsky *et al.* 1979), BBM1 (70 nM), for 1 h at room temperature. All wells were washed in wash buffer and detection antibody [HRP-conjugated goat-anti-mouse IgG (1.13 nM); Sigma] was added followed by a 1-h incubation at room temperature. Plates were washed and substrate (TMB; Kirkegaard & Perry Laboratories) was added to all wells. Reactions were stopped using H_2SO_4 (0.3 M) and plates read at 450 nm using a ELx808 Microplate reader (Biotek). Data were analyzed using EXCEL and PRISM software.

A pre-folded, biotinylated FLPSDYFPSV/HLA-A*02:01 (Kast *et al.* 1994) complex was used as a standard to convert OD_{450} values to the amount of complex formed using the second-order polynomial ($Y = a + bX + cX^2$), thereby enabling a direct conversion of the actual peptide concentration offered to the actual concentration of correctly formed pMHC complex. Because the effective concentration of MHC (2–5 nM) used in these assays is below the equilibrium dissociation constant (K_D) of most high-affinity peptide–MHC interactions, the peptide concentration, ED_{50}, leading to half-saturation of the MHC is a reasonable approximation of the affinity of the interaction.

Results

Analysis of the peptide-binding specificity of SLA-2*0401 with the PSCPL

The porcine MHC class I heavy chain, SLA-2*0401, was tested for binding PSCPL using human β_2m to support folding, as previously described (Stryhn *et al.* 1996; Pedersen *et al.* 2011). Similar to the SLA-1*0401 molecule (Pedersen *et al.* 2011), no differences were seen for the SLA-2*0401 allele when comparing human β_2m and porcine β_2m in supporting MHC peptide binding and complex folding (data not shown). Each peptide sublibrary was titrated to determine the EC50 (K_D) for SLA-2*0401. The peptide-binding preferences for the SLA-2*0401 heavy chain protein are shown in Table 1. Amino acids in each peptide position were assigned a RB value as described in Materials and Methods. Amino acid residues with RB values above 2 (shown in boldface, Table 1) indicate support of peptide binding, whereas AAs having RB values below 0.5 (shown in italics, Table 1) are considered disfavored. A

Published 2012. This article is a U.S. Government work and is in the public domain in the USA., doi: 10.1111/j.1365-2052.2012.02400.x

Table 1 SLA-2*0401-binding motif

	Amino acid position in peptide								
SLA-2*0401	1	2	3	4	5	6	7	8	9
A	*0.3*	*0.4*	1.3	1.9	0.8	0.6	**2.6**	0.8	*0.0*
C	*0.4*	*0.1*	0.6	0.9	*0.2*	*0.4*	*0.5*	1.0	*0.0*
D	*0.5*	*0.3*	0.7	*0.4*	1.5	**2.2**	1.3	1.5	*0.1*
E	0.7	*0.1*	1.1	0.8	0.8	*0.1*	**3.7**	**2.7**	*0.0*
F	**2.0**	*0.2*	*0.3*	0.9	1.3	1.5	*0.4*	0.8	**3.0**
G	*0.1*	0.9	*0.4*	*0.2*	1.0	*0.2*	*0.4*	1.6	*0.1*
H	1.0	*0.1*	*0.1*	*0.5*	0.9	**2.3**	*0.4*	0.7	*0.3*
I	1.2	0.7	0.6	0.5	1.2	0.8	1.7	0.6	*0.3*
K	*0.5*	*0.2*	*0.1*	1.1	*0.4*	*0.3*	*0.2*	0.6	*0.1*
L	*0.5*	*0.3*	0.9	0.8	0.8	1.0	0.7	0.7	*0.1*
M	**2.2**	*0.3*	1.4	0.8	1.1	1.5	1.2	1.0	*0.3*
N	0.8	**8.9**	1.6	0.7	1.8	*0.3*	0.8	0.7	*0.1*
P	*0.1*	*0.5*	0.7	**3.3**	1.4	1.6	0.6	0.8	*0.0*
Q	1.4	*0.2*	0.8	1.5	**3.3**	**2.5**	**2.8**	1.0	*0.0*
R	**2.2**	*0.2*	1.4	1.4	0.5	1.2	*0.4*	1.1	*0.1*
S	1.6	**3.3**	1.0	0.8	0.9	0.6	0.8	0.9	*0.1*
T	0.9	1.8	1.1	0.8	0.5	1.2	*0.4*	0.7	*0.1*
V	1.1	0.8	0.8	*0.4*	0.7	*0.2*	*0.3*	0.8	*0.0*
W	0.9	*0.2*	**2.1**	1.0	0.5	0.9	*0.3*	1.0	**11.2**
Y	1.9	*0.5*	**3.1**	1.3	0.6	0.6	*0.4*	1.1	**4.1**
Sum	20	20	20	20	20	20	20	20	20
AP value	9	77	10	9	8	10	19	5	132

Normalized relative binding (RB) values indicate whether an amino acid is favored (RB $\geq$ 2.0, bold numbers) or disfavored (RB $\leq$ 0.5, *italic* numbers) for binding of each position in the peptide. Anchor position (AP) values are given by the equation $\sum(\text{RB} - 1)^2$. Important AP values are underlined.
SLA, swine leukocyte antigen.

primary AP is characterized by AAs being strongly preferred, and many AAs were unaccepted by the class I molecule in question. Anchor position values of 15 or more indicate primary anchors (underlined values, Table 1) (Lamberth *et al.* 2008). Such anchors are of critical importance for peptide binding.

The PSCPL analysis of SLA-2*0401 identifies positions 2 and 9 as APs, as is commonly seen for many class I molecules (Sette & Sidney 1999; Lamberth *et al.* 2008). The motif in Table 1 shows that the AAs asparagine (N) and tryptophan (W) are favored for peptide binding in positions 2 and 9 respectively. The preference of AAs with larger side chains such as tryptophan (W), tyrosine (Y) and phenylalanine (F) in position 9 was revealed by RB values of 11.2, 4.1 and 3.0 respectively (Table 1). Such RB values indicate that this anchor must align with a large and deep F pocket. The B pocket responsible for binding the AA in position 2 of the peptide is most stable binding hydrophilic side chains, resulting in a preference for the AAs serine (S) and asparagine (N) with RB values of 3.3 and 8.9 respectively.

These preferences are illustrated in Fig. 1, where logos displaying single-letter AA codes were generated to compare the *in vitro* SLA-binding motifs for the PSCPL with those of *in silico* NetMHCpan-based peptide preference predictions. NetMHCpan is a mathematical algorithm developed for MHC peptide-binding predictions in several different species of interest (Nielsen *et al.* 2007; Hoof *et al.* 2009). For SLA-1*0401, the data show that the PSCPL-based matrix detected preferences only for aspartic acid (D) and glutamic acid (E) in position 3 of the peptide. Furthermore, the NetMHCpan-based logo had tyrosine (Y) preferred in position 9 with phenylalanine (F) second most preferred, whereas the PSCPL data indicate a preference of phenylalanine (F) over tyrosine (Y) (Fig. 1). The PSCPL showed the same preference for the SLA-2*0401 molecule regarding tyrosine (Y) and phenylalanine (F) in position 9 (Fig. 1). Additionally, a shared preference for serine (S) was seen between the two SLA-2*0401 logos in position 2, as well as a unique preference for asparagine (N) within the PSCPL matrix only. These differences between the NetMHCpan-based logo and the PSCPL-based logo likely reflect the limited amount of peptide-binding data available for the NetMHCpan algorithm-based predictions with regard to MHC molecules that share specificity with these two SLA molecules (Hoof *et al.* 2009). Increasing the data available

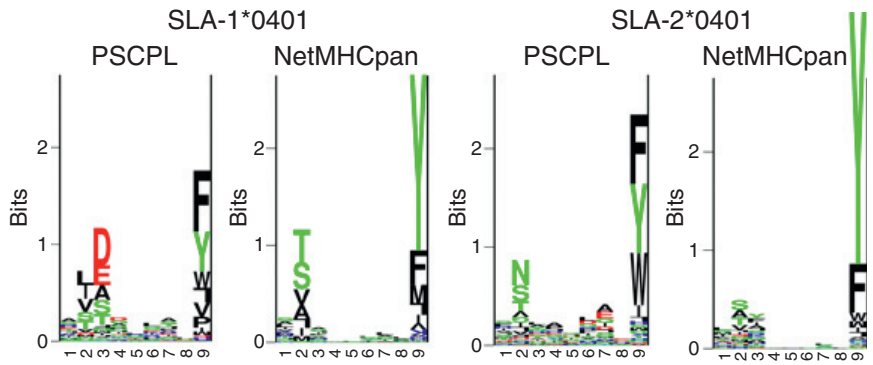

Figure 1 Sequence logo representations of the SLA-1*0401- and SLA-2*0401-binding motifs. The logos were calculated from the top 1% highest scoring peptides selected from a pool of 200 000 natural 9mer peptides using either the positional scanning combinatorial peptide library matrix or NetMHCpan as predictors. In the sequence logo, each peptide position is represented by a stack of letters indicating its significance for binding (information content) and the height of each letter (amino acid) is proportional to its relative frequency (Schneider & Stephens 1990). Acidic residues are displayed in red, basic in blue, neutral in green, and hydrophobic in black. Underrepresented amino acids are displayed upside down. SLA, swine leukocyte antigen.

Published 2012. This article is a U.S. Government work and is in the public domain in the USA., doi: 10.1111/j.1365-2052.2012.02400.x

for swine MHC class I proteins will improve the NetMHCpan algorithm prediction profile.

Identification of peptides derived from FMDV bound by SLA-1*0401 and SLA-2*0401 alleles

The P1 region of FMDV, which codes for the viral capsid or structural proteins, was screened for 9mer and 10mer peptides that would potentially bind SLA-1-*0401 and SLA-2*0401 using the NetMHCpan version 2.3 (Nielsen *et al.* 2007). Nine such peptides were identified for the SLA-1*0401 allele (four 9mers and five 10mers), and 10 peptides (five 9mers and five 10mers) were identified for SLA-2*0401 (Table 2). Selection of peptides was based on the NetMHCpan algorithm predictions and further analyzed for the AA preference in positions 2, 3 and 9 of the individual peptides based on the PSCPL-binding motifs (Table 1 and Pedersen *et al.* 2011). Some peptides were selected because of their NetMHCpan rank despite not satisfying one of the primary anchors according to the PSCPL motif. Others were left out despite expressing an anchor–residue match and a proper NetMHCpan rank because of in-house peptide limitations. Within a pool of 726 possible peptide combinations from the P1 region, eight of the nine peptides selected for either SLA-1*0401 or SLA-2*0401 were within the top 10 highest ranking peptides for predicted binding (Appendix S2). All chosen peptides had a NetMHCpan rank score of <2% (Erup *et al.* 2011), meaning that <2% of random natural peptides had a predicted binding affinity stronger than the selected peptides.

These peptides, predicted to be bound, were tested for actual binding by SLA-1 and SLA-2 in an *in vitro* ELISA binding assay. Five of the nine FMDV-derived peptides predicted to be bound by the SLA-1*0401 molecule tested positive in the assay. These peptides include four 9mers (TVYNGTSKY, MTAHITVPY, SSVGVTHGY and YLSGIAQYY) and one 10mer (NMTAHITVPY). Additionally, we observed that four of the 10 peptides predicted to be bound by SLA-2*0401 produced correctly folded peptide–MHC complexes. These included three 9mers (MTAHITVPY, SSVGVTHGY and YLSGIAQYY) and one 10mer (NTYLSGIAQY). The respective binding affinity (K_D) values for all bound peptides ranged between 0.8 and 433 nM. Peptides with K_D values below 500 nM are considered strong (50–500 nM) or very strong (0.1–50 nM) binders (Table 2).

Two additional peptides, from the VP35 region of the Sudan *Ebola* virus and from the conserved hypothetical protein of the *Vibrio cholera* bacteria respectively, also were tested for binding by the SLA-2*0401 protein for comparison (Table 2). These peptides previously have been shown to be bound by SLA-1*0401 with high affinity (Pedersen *et al.* 2011). As for SLA-1*0401, both peptides were found to be strongly bound by the SLA-2*0401 molecule with K_D values of 1 and 2 nM respectively (Table 2).

Discussion

Previously, we defined the peptide motifs that are bound by the class I MHC protein of swine, SLA-1*0401 (Pedersen *et al.* 2011). We now expand this analysis to an additional SLA protein, SLA-2*0401, and describe a method for the analysis of a virus proteome to identify the peptides that will be bound by porcine MHC I proteins. Peptides from the P1 region of the FMDV genome, which encodes the structural proteins of the virus, were identified using this method for the gene products of two class I alleles, SLA-1*0401 and SLA-2*0401. These two class I proteins are commonly expressed alleles in commercial pig breeds as well as in different porcine cell lines

Table 2 Peptide candidates for SLA-1*0401 and SLA-2*0401 affinity analysis

	FMDV peptides tested for SLA-1*0401			FMDV peptides tested for SLA-2*0401		
Peptide sequence	NetMHCpan predicted% rank score	K_D (nM)	Actual binding status	NetMHCpan predicted% rank score	K_D (nM)	Actual binding status
TVYNGTSKY	0.17	87	Intermediate	0.05	NB	Non-binder
MTAHITVPY	0.01	0.8	Strong	0.05	7	Strong
SSVGVTHGY	0.10	433	Intermediate	0.40	14	Strong
AAKHMSNTY	1.00	ND	ND	0.40	NB	Non-binder
YLSGIAQYY	1.50	17	Strong	0.25	42	Strong
LAAKHMSNTY	0.20	NB	Non-binder	0.12	NB	Non-binder
NMTAHITVPY	2.0	67	Strong	0.80	NB	Non-binder
NTYLSGIAQY	0.20	NB	Non-binder	0.12	22	Strong
ATVYNGTSKY	0.15	NB	Non-binder	0.80	NB	Non-binder
QSSVGVTHGY	0.80	NB	Non-binder	1.50	NB	Non-binder

Peptide sequence	SLA-2*0401 *Ebola*/Cholera peptides NetMHCpan predicted% rank score	K_D (nM)	Actual binding status
ASYQFQLPY	0.01	2	Strong
ATAAATEAY	1.00	1	Strong

ND, not determined; NB, non-binding peptide having a $K_D > 5000$ nM; FMDV, foot-and-mouth disease virus; SLA, swine leukocyte antigen.

Published 2012. This article is a U.S. Government work and is in the public domain in the USA., doi: 10.1111/j.1365-2052.2012.02400.x

used for experimental research (Smith *et al.* 2005; Ho *et al.* 2006, 2009). Hence, the determination of binding motifs for such proteins is of great value as a tool in the analysis of porcine immune responses and vaccine development.

A comparison of *in silico* predictions with *in vitro* analysis of peptide binding, expressed as the formation of correctly folded porcine MHC class I, supports previously published data describing the capacity of the NetMHCpan predictor to identify successful peptide/MHC binding beyond humans (Hoof *et al.* 2009; Pedersen *et al.* 2011). All 12 different peptides tested for the SLA-2*0401 molecule were predicted by the NetMHCpan to be bound, and six formed complexes with the SLA class I alpha chain and β_2m *in vitro* (Table 2). These data show the NetMHCpan predicted actual peptide binding at a rate of 50%, based on the limited data available to date. Of the nine peptides selected for SLA-1*0401-binding tests, all were predicted to be bound and five formed complexes with the heavy chain during the *in vitro* analysis. For the SLA-1*0401 molecule, 55.6% of the predictions were confirmed. These results were obtained using a prediction algorithm based on human MHC proteins. As such, they illuminate the value of using the extensive human database to apply to swine MHC peptide predictions to identify potential immune epitopes.

Of the 10 peptides from the sequence of the FMDV structural protein region identified by the algorithm, four of the six that failed to be bound by SLA-2*0401 have random binding scores. Contrarily, none of the four peptides that were bound by SLA-2*0401 have random binding scores calculated from the PSCPL matrix values and the approximation for longer peptide-binding prediction described by Lundegaard *et al.* (2008) (data not shown). This indicates that improvement could be achieved by adding quantitative SLA peptide-binding data derived using the PSCPL matrix for the NetMHCpan neural network to refine the algorithm and generate more accurate predictions (Nielsen *et al.* 2007; Hoof *et al.* 2009). In addition, one peptide (YLSGIAQYY) was predicted not to be bound by SLA-2*0401 but in fact was strongly bound. Considering several peptides predicted to be bound failed to do so *in vitro* illustrates the need for more data to enhance the NetMHCpan for species other than humans.

Differences in peptide motifs expressed by the two SLA alleles, SLA-1*0401 and SLA-2*0401, are illustrated by peptides bound by one allele but not by the other. The 10mer peptide, NTYLSGIAQY, was bound by SLA-2*0401 with an affinity (K_D) value of 22 nM but was not bound by the SLA-1*0401 alpha chain (Table 2). This supports the higher preference for the AA tyrosine (Y) in position 3 (RB = 3.1) by the SLA-2*0401 molecule and that the residue is disfavored in the same position for SLA-1*0401 (RB = 0.5) peptide binding. SLA-1*0401 is unique from most other alleles in that this alpha chain has a peptide-binding anchor in position 3 as well as in the more commonly observed APs 2 and 9 (Pedersen *et al.* 2011). Thus, the side chain of the AA in position 3 factors into peptide binding, and so the NTYLSGIAQY peptide does not bind despite the positions 2 and 9 anchors being satisfied (T: RB = 2.5 and Y: RB = 4.3 respectively). The opposite effect is seen for the 10mer peptide NMTAHITVPY. This peptide is readily bound by SLA-1*0401 with a K_D value of 67 nM but is not bound by SLA-2*0401. Methionine (M) is disfavored in position 2 in the SLA-2*0401 protein, whereas it is favored by the SLA-1*0401 peptide-binding motif (RB = 0.3 and 1.9 respectively). Furthermore, threonine (T) in position 3 is less favored for SLA-2*0401 than for SLA-1*0401.

As with the differences in binding preferences, similarities also are seen for the two SLA alpha chains analyzed when analyzing these viral peptides. Some of the identified binding peptides are shared, and this sharing can be explained by the identical preferences for tyrosine (Y) in the important position 9 anchor and for methionine (M) in position 1. There is also the shared preference for serine (S) and threonine (T) in the position 2 anchor (Table 1; Pedersen *et al.* 2011). In addition, our data show that both SLA proteins can bind 9mer peptides as well as 10mer peptides with similar affinities. This observation may indicate that peptide epitopes longer than nine AAs may be common for these MHC proteins. Such peptides would lead to different recognition patterns expressed by TCRs than the more often reported 9mers. The reason for this lies in the conformation of the peptide–MHC complex, which would differ in the way the peptide bulges away from the groove. This is caused by the bound peptide now having one or even two additional AAs in the center available for TCR recognition, depending on which peptide AA interacts with the respective anchors within the MHC groove (Fig. 2).

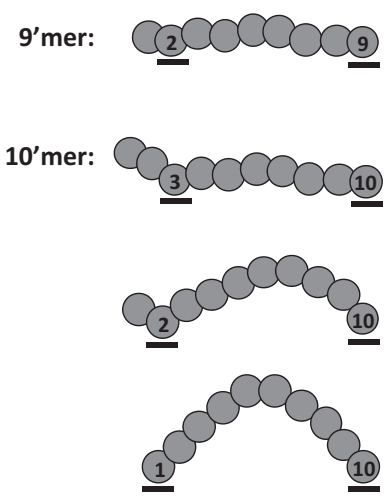

Figure 2 Illustration of commonly known 9mer peptide-binding vs. three different proposed 10mer peptide-binding scenarios and the effect on the exposure of the central amino acids. Black bars illustrate important interactions between the peptide and the anchor position residues in the B- and F-pockets of the major histocompatibility complex (MHC) class I-binding groove. Numbers indicate the peptide position of the primary MHC-interacting amino acids within the peptide.

Published 2012. This article is a U.S. Government work and is in the public domain in the USA., doi: 10.1111/j.1365-2052.2012.02400.x

To date, most analysis has focused on 9mer peptides as candidates for strong class I complex folding. Longer peptides, specifically the 10mers, were included in this study to expand the pool of possible peptides for analysis and, hence, possible T-cell epitope candidates. For human class I (Chen *et al.* 1994; Urban *et al.* 1994; Tynan *et al.* 2005), binding of peptides other than 9mers has been readily shown with resulting diverse peptide conformations within the HLA class I-binding groove. Longer peptides not only provide a larger pool of combinations of potential peptide sequences and binding configurations (Fig. 2), but also contribute to greater diversity in the center region of the peptide available for TCR recognition as a result of the peptide bulging away from the binding cleft. Hence, depending on the individual binding pattern of the peptide, binding of a 10mer peptide could include additional AAs between the anchors of the bound peptide available for TCR interactions. Such a change in conformation could have the potential to expand pMHC-mediated activation of virus-specific CTLs.

The ability of MHC molecules to bind the same peptide in different combinations, depending on the identity of the peptide anchor residues, would appear to have distinct advantages to the immune system. Based on the PSCPL RB values of the respective pockets expressed by the SLA-1*0401 and SLA-2*0401 molecules, and in combination with the respective 10 AA peptides bound, the model predicts that the two 10mer peptides bind by a position 2/position 10 (P2/P10) or P1/P10 anchor manner (NMTAHITVPY) for SLA-1*0401 and a P3/P10 anchor manner (NTYLSGIAQY) for SLA-2*0401 (Table 1; Pedersen *et al.* 2011). These binding patterns are only speculations and rely on a comparison of the AA in peptide positions 1–3 with the MHC preferences expressed for the individual AA in P1–3, combined with the comparison of the AA in peptide positions 9 and 10 with the preferences expressed for the individual AA in P9. Future mapping of MHC class I-binding motifs using an X10-based peptide library as compared to exclusively X9 will further illuminate which AA positions of the 10mer peptides account for binding interactions between the peptide residues and the anchors of the MHC class I protein groove.

In conclusion, we determined the binding motif of an additional swine MHC class I molecule, SLA-2*0401. Further, the NetMHCpan prediction algorithm based on human MHC proteins identified peptides from a viral proteome of interest. Based on *in silico* predictions and *in vitro* verifications, we identified four FMDV peptides bound by SLA-2*0401: MTAHITVPY, SSVGVTHGY, YLSGIAQYY and NTYLSGIAQY; and five FMDV peptides bound by SLA-1*0401: TVYNGTSKY, MTAHITVPY, SSVGVTHGY, YLSGIAQYY and NMTAHITVPY. Three of these peptides were observed to be commonly shared between the two heavy chain molecules (MTAHITVPY, SSVGVTHGY and YLSGIAQYY), whereas one peptide (NTYLSGIAQY) was bound only by the SLA-2*0401 protein and two peptides (TVYNGTSKY and NMTAHITVPY) were bound only by the SLA-1*0401 protein. All these peptides are candidate T-cell epitopes by virtue of being strongly bound by two of the most highly expressed porcine class I MHC proteins.

Analysis of antigen-specific, MHC I-restricted T cells using MHC tetramers made with the peptides identified here showed that at least one of these, MTAHITVPY bound by SLA-1*0401, reacts with FMDV-specific T cells (Patch *et al.* 2011). The reason for including *Ebola* and *V. cholera* peptides in this study was an ambition of adding the SLA-2*0401 molecule to the experimental setup of such tetramer staining analyses. FMDV-specific porcine CTLs should not recognize either *Ebola*- or *V. cholera*-derived peptides bound and presented by the SLA-2*0401 molecule, and hence, these peptides should make for good negative controls. Subsequent studies indicate that other peptides represented in the data presented here are T-cell epitopes, and confirmation of these preliminary results is underway, now also including the SLA-2*0401 molecule. Minimally, these data, together with our previous reports (Patch *et al.* 2011; Pedersen *et al.* 2011), show that the approach of using the NetMHCpan prediction algorithm, developed for human MHC molecules, can be effective in predicting MHC peptide interactions in other species.

Acknowledgements

This work was funded by CRIS #1940-32000-053-00D from the Agricultural Research Service, USDA (WTG); by the Danish Council for Independent Research, Technology and Production Sciences (274-09-0281) (GJ); and by the United States National Institutes of Health (NIH) (HHSN266200400025C) (SB).

Conflict of interest

The authors claim no conflict of interest in the publication of this information.

References

Bevan M.J. (1995) Antigen presentation to cytotoxic T lymphocytes *in vivo*. *Journal of Experimental Medicine* **182**, 639–41.

Brodsky F.M., Bodmer W.F. & Parham P. (1979) Characterization of a monoclonal anti-beta 2-microglobulin antibody and its use in the genetic and biochemical analysis of major histocompatibility antigens. *European Journal of Immunology* **9**, 536–45.

Chen Y., Sidney J., Southwood S., Cox A.L., Sakaguchi K., Henderson R.A., Appella E., Hunt D.F., Sette A. & Engelhard V. H. (1994) Naturally processed peptides longer than nine amino acid residues bind to the class I MHC molecule HLA-A2.1 with high affinity and in different conformations. *Journal of Immunology* **152**, 2874–81.

Doherty P.C. & Zinkernagel R.M. (1975) H-2 compatibility is required for T-cell-mediated lysis of target cells infected with lymphocytic choriomeningitis virus. *Journal of Experimental Medicine* **141**, 502–7.

Published 2012. This article is a U.S. Government work and is in the public domain in the USA., doi: 10.1111/j.1365-2052.2012.02400.x

Erup L.M., Kloverpris H., Stryhn A., Koofhethile C.K., Sims S., Ndung'u T., Goulder P., Buus S. & Nielsen M. (2011) HLARESTRICTOR—a tool for patient-specific predictions of HLA restriction elements and optimal epitopes within peptides. *Immunogenetics* **63**, 43–55.

Ferre H., Ruffet E., Blicher T., Sylvester-Hvid C., Nielsen L.L., Hobley T.J., Thomas O.R. & Buus S. (2003) Purification of correctly oxidized MHC class I heavy-chain molecules under denaturing conditions: a novel strategy exploiting disulfide assisted protein folding. *Protein Science* **12**, 551–9.

Hansen N.J., Pedersen L.O., Stryhn A. & Buus S. (2001) High-throughput polymerase chain reaction cleanup in microtiter format. *Analytical Biochemistry* **296**, 149–51.

Harty J.T., Tvinnereim A.R. & White D.W. (2000) CD8 + T cell effector mechanisms in resistance to infection. *Annual Review of Immunology* **18**, 275–308.

Ho C.S., Rochelle E.S., Martens G.W., Schook L.B. & Smith D.M. (2006) Characterization of swine leukocyte antigen polymorphism by sequence-based and PCR-SSP methods in Meishan pigs. *Immunogenetics* **58**, 873–82.

Ho C.S., Franzo-Romain M.H., Lee Y.J., Lee J.H. & Smith D.M. (2009) Sequence-based characterization of swine leucocyte antigen alleles in commercially available porcine cell lines. *International Journal of Immunogenetics* **36**, 231–4.

Ho C.S., Lunney J.K., Lee J.H., Franzo-Romain M.H., Martens G.W., Rowland R.R. & Smith D.M. (2010a) Molecular characterization of swine leucocyte antigen class II genes in outbred pig populations. *Animal Genetics* **41**, 428–32.

Ho C.S., Martens G.W., Amoss M.S. Jr, Gomez-Raya L., Beattie C.W. & Smith D.M. (2010b) Swine leukocyte antigen (SLA) diversity in Sinclair and Hanford swine. *Developmental and Comparative Immunology* **34**, 250–7.

Hoof I., Peters B., Sidney J., Pedersen L.E., Sette A., Lund O., Buus S. & Nielsen M. (2009) NetMHCpan, a method for MHC class I binding prediction beyond humans. *Immunogenetics* **61**, 1–13.

Kast W.M., Brandt R.M., Sidney J., Drijfhout J.W., Kubo R.T., Grey H. M., Melief C.J. & Sette A. (1994) Role of HLA-A motifs in identification of potential CTL epitopes in human papillomavirus type 16 E6 and E7 proteins. *Journal of Immunology* **152**, 3904–12.

Lamberth K., Roder G., Harndahl M., Nielsen M., Lundegaard C., Schafer-Nielsen C., Lund O. & Buus S. (2008) The peptide-binding specificity of HLA-A*3001 demonstrates membership of the HLA-A3 supertype. *Immunogenetics* **60**, 633–643.

Lundegaard C., Lund O. & Nielsen M. (2008) Accurate approximation method for prediction of class I MHC affinities for peptides of length 8, 10 and 11 using prediction tools trained on 9mers. *Bioinformatics* **24**, 1397–8.

Nielsen M., Lundegaard C., Blicher T. *et al.* (2007) NetMHCpan, a method for quantitative predictions of peptide binding to any HLA-A and -B locus protein of known sequence. *PLoS ONE* **2**, e796.

Ostergaard P.L., Nissen M.H., Hansen N.J., Nielsen L.L., Lauenmoller S.L., Blicher T., Nansen A., Sylvester-Hvid C., Thromsen A.R. & Buus S. (2001) Efficient assembly of recombinant major histocompatibility complex class I molecules with preformed disulfide bonds. *European Journal of Immunology* **31**, 2986–96.

Patch J.R., Pedersen L.E., Toka F.N., Moraes M., Grubman M.J., Nielsen M., Jungersen G., Buus S. & Golde W.T. (2011) Induction of foot-and-mouth disease virus-specific cytotoxic T cell killing by vaccination. *Clinical and Vaccine Immunology* **18**, 280–8.

Pedersen L.E., Harndahl M., Rasmussen M., Lamberth K., Golde W. T., Lund O., Nielsen M. & Buus S. (2011) Porcine major histocompatibility complex (MHC) class I molecules and analysis of their peptide-binding specificities. *Immunogenetics* **63**, 821–34.

Schmidt E.G., Buus S., Thorn M., Stryhn A., Leisner C. & Claesson M.H. (2009) Peptide specific expansion of CD8(+) T cells by recombinant plate bound MHC/peptide complexes. *Journal of Immunological Methods* **340**, 25–32.

Schneider T.D. & Stephens R.M. (1990) Sequence logos: a new way to display consensus sequences. *Nucleic Acids Research* **18**, 6097–100.

Sette A. & Sidney J. (1999) Nine major HLA class I supertypes account for the vast preponderance of HLA-A and -B polymorphism. *Immunogenetics* **50**, 201–12.

Smith D.M., Lunney J.K., Martens G.W., Ando A., Lee J.H., Ho C.S., Schook L., Renard C. & Chardon P. (2005) Nomenclature for factors of the SLA class-I system, 2004. *Tissue Antigens* **65**, 136–49.

Stryhn A., Pedersen L.O., Romme T., Holm C.B., Holm A. & Buus S. (1996) Peptide binding specificity of major histocompatibility complex class I resolved into an array of apparently independent subspecificities: quantitation by peptide libraries and improved prediction of binding. *European Journal of Immunology* **26**, 1911–8.

Sylvester-Hvid C., Kristensen N., Blicher T., Ferre H., Lauemoller S.L., Wolf X.A., Lamberth K., Nissen M.H., Pedersen L.O. & Buus S. (2002) Establishment of a quantitative ELISA capable of determining peptide–MHC class I interaction. *Tissue Antigens* **59**, 251–8.

Tynan F.E., Borg N.A., Miles J.J. *et al.* (2005) High resolution structures of highly bulged viral epitopes bound to major histocompatibility complex class I. Implications for T-cell receptor engagement and T-cell immunodominance. *Journal of Biological Chemistry* **280**, 23900–9.

Urban R.G., Chicz R.M., Lane W.S., Strominger J.L., Rehm A., Kenter M.J., UytdeHaag F.G., Ploegh H., Uchanska-Ziegler B. & Ziegler A. (1994) A subset of HLA-B27 molecules contains peptides much longer than nonamers. *Proceedings of the National Academy of Sciences of the United States of America* **91**, 1534–8.

Yeom S.C., Park C.G., Lee B.C. & Lee W.J. (2010) SLA typing using the PCR-SSP method and establishment of the SLA homozygote line in pedigreed SNU miniature pigs. *Animal Science Journal* **81**, 158–64.

Zinkernagel R.M. & Doherty P.C. (1975) H-2 compatibility requirement for T-cell-mediated lysis of target cells infected with lymphocytic choriomeningitis virus. Different cytotoxic T-cell specificities are associated with structures coded for in H-2K or H-2D. *Journal of Experimental Medicine* **141**, 1427–36.

Supporting information

Additional supporting information may be found in the online version of this article.

Appendix S1 The nucleic acid and amino acid sequence of SLA-2*0401 expressed in *E. coli*.

Appendix S2 NetMHCpan version 2.3 predictions

As a service to our authors and readers, this journal provides supporting information supplied by the authors. Such materials are peer-reviewed and may be re-organized for online delivery, but are not copy-edited or typeset. Technical support issues arising from supporting information (other than missing files) should be addressed to the authors.

Published 2012. This article is a U.S. Government work and is in the public domain in the USA., doi: 10.1111/j.1365-2052.2012.02400.x

5. Paper III

An analysis of affinity and stability in the identification of peptides bound by Swine Leukocyte Antigens (SLA) combining matrix- and NetMHCpan based peptide selection

Pedersen LE, Rasmussen M, Harndahl M, Nielsen M, Buus S, Jungersen G.

Manuscript ready for submission to Immunogenetics

In this study SLA:peptide complexes are analyzed with respect to both affinity and complex stability for the three SLA molecules, SLA-1*0401, SLA-2*0401 and SLA-3*0401. By combining PSCPL matrix- and *NetMHCpan* based peptide predictions we here illustrate a highly efficient approach for selection of potential T cell epitopes. Such combined predictions led to identification of more peptides bound with high affinity and stability than each prediction method alone. In addition, we describe a correlation between low affinity peptides and the production of pSLA complexes of low stability, and show that peptides bound with high affinity may produce both unstable as well as highly stable pSLA complexes.

Furthermore, these studies present the complete nonamer PSCPL binding matrix for the SLA-3*0401 molecule, introducing the use of a novel approach for screening of such SLA binding specificities based on pSLA complex stability instead of affinity.

An analysis of affinity and stability in the identification of peptides bound by Swine Leukocyte Antigens (SLA) combining matrix- and NetMHCpan based peptide selection

Lasse Eggers Pedersen[1], Michael Rasmussen[2], Mikkel Harndahl[2], Morten Nielsen[3], Søren Buus[2, 4], and Gregers Jungersen[1]

[1] National Veterinary Institute, Technical University of Denmark

[2] Laboratory of Experimental Immunology, Faculty of Health Sciences, University of Copenhagen

[3] Center for Biological Sequence Analysis, Technical University of Denmark

[4] Correspondence to professor Søren Buus, Department of International Health, Immunology and Microbiology, Blegdamsvej 3, 2200 Copenhagen N., Denmark, (s.buus@sund.ku.dk).

Abstract

The affinity and stability of peptides bound by major histocompatibility complex (MHC) class I molecules are important factors in presentation of viral epitopes to cytotoxic T lymphocytes (CTLs) of the adaptive immune system. In swine, such peptide presentations by swine leukocyte antigens (SLA) are crucial for immunity during most viral infections and diseases.

The identification of peptide candidates, derived from viral genomes of interest, for SLA binding and presentation continues to be an exhaustive task seeing hundreds and sometimes even thousands of different peptide sequences available within a single viral proteome.

In this study, we expand the analysis of SLA binding preferences by determining the complete nonamer SLA-3*0401 PSCPL (positional scanning combinatorial peptide library) binding matrix and suggest a method to facilitate the task of specific peptide selection. This was done by combining the ability of such a matrix, to predict peptide candidates for MHC binding, with that of the *in silico* prediction algorithm *NetMHCpan*. Analyses of such peptide binding predictions were performed for two additional SLA molecules, the SLA-1*0401 and SLA-2*0401, along with the identification of several virally derived peptide epitope candidates. In addition, a comparison of the affinity and stability of peptide-SLA (pSLA) complexes was performed and a significant observation of peptides being bound by low affinity also produce pSLA complexes of low stability was made. Furthermore, it was found that peptides bound with high affinity produce pSLA complexes of various stabilities ranging from 0 – 200 hours in half-life periods.

In conclusion, the combination of *NetMHCpan* and SLA PSCPL matrix prediction led to identification of more peptides with high affinity and stability than each prediction method alone. Applying these methods thus constitute a highly cost-effective guide for epitope discovery studies and MHC binding analysis, not only in the case of porcine immunology but for any species of interest.

Key words: MHC, binding predictions, peptide affinity, complex stability

Introduction

MHC class I molecules can be seen as tell-tales of the immune system displaying to the surroundings endogenously derived peptides from processed self- as well as non-self proteins. Recognition of such peptide MHC complexes (pMHC) by specific CTLs can lead to the activation of cytotoxic T cells. Cells infected by an intracellular pathogen will display non-self peptides on their cell surface hereby signaling a state of alert to circulating CTLs leading to subsequent elimination of the infected cells.

Peptide - MHC-I affinity is the primary criteria for presentation of peptides by MHC class I molecules. Once bound, the stability of the pMHC influence the timeframe in which peptides are displayed at the cell surface of antigen presenting cells (APCs), and hence the stability of individual pMHC has a proposed additional impact on the immunogenicity of the peptides, with stably bound peptides being the more immunogenic (Busch and Pamer 1998, Harndahl et al. 2012, van der Burg et al. 1996).

Knowledge about the MHC-I binding specificity is thus paramount in epitope discovery to limit the pool of peptides available for analysis. The peptide binding specificities of the human leukocyte antigen (HLA) molecule have been thoroughly studied and several high performance prediction servers, such as *NetMHCpan*, exist to predict peptide-HLA binding (Lundegaard et al. 2011, Nielsen et al. 2007, Nielsen et al. 2008, Zhang et al. 2009). However, knowledge of the peptide binding motifs of MHC-I molecules from other species such as livestock is limited, complicating epitope identification.

We recently reported the peptide binding motif of the porcine MHC-I molecules SLA-1*0401 and SLA-2*0401, identified by ELISA based positional scanning combinatorial peptide libraries (PSCPL) (Pedersen et al. 2011, Pedersen et al. 2012). Here, we describe the PSCPL derived peptide binding motif of the SLA-3*0401 molecule using a newly developed methodology based on pMHC-I complex dissociation (Rasmussen et al. 2012). Combining the peptide predictions of the individual binding matrices for SLA-1*0401, SLA-2*0401 and SLA-3*0401 with *in silico* peptide binding predictions using *NetMHCpan* (Hoof et al. 2009, Lundegaard et al. 2011) version 2.4, we predicted possible peptide binders from a library of more than 9000 nonameric peptides to investigate if combined predictions were more accurate than using either of the prediction tools alone. Predicted peptides were screened for binding and high affinity binders were identified for SLA-1*0401, SLA-2*0401 and SLA-3*0401. In addition, the stability of pSLA was measured for peptides identified to be bound with high affinity, showing that our recently published peptide-HLA stability assay can easily be modified to measure pMHC stability in other species (Harndahl et al. 2011, Rasmussen et al. 2012). Comparing affinity and stability data identified several high-affinity, and highly stable, peptide binders for all three SLA proteins, and a tendency of peptides being bound with high affinity also produce highly stable pSLA complexes. Despite this it was found that high affinity peptides in general produce pSLA complexes of various stabilities ranging from 0 – 200 hour half-life periods. Furthermore, these analyses revealed a clear correlation between peptides bound with low affinity also produce low stability pSLA complexes illustrating that high affinity peptide binding is indeed a prerequisite for stable interactions. Such data indicate that the methodology presented here is capable of identifying potential $CD8^+$ T-cell epitopes as well as pointing out peptides which are not suitable for the production of stable pSLA complexes.

All together these methods provide state-of-the-art tools for the prediction, analysis and selection of peptides for MHC class I binding, hereby paving the way to actual identification of strongly, and stably, bound peptides with the potential of being viral peptide epitopes. These experiments introduce an expansion of the field of pMHC analysis now to include livestock such as the pig.

Materials and methods

*Recombinant construct encoding the SLA-3*0401 protein*

Recombinant SLA-3*0401 protein was produced as described elsewhere (Pedersen et al. 2011). Briefly, DNA encoding residues 1 to 276 of the SLA-3*0401 alpha chain (purchased from Genscript) was cloned into a pET28a+ vector (Novagen) upstream of a polytag consisting of a FXa cleavage site, a biotinylation signal peptide (BSP) and a histidine affinity tag (HAT). Correct constructs were verified by sequencing (ABI Prism 3100Avant, Applied Biosystems) (Hansen et al. 2001). The validated construct of interest was transformed into *E. coli* BL21(DE3), containing the pACYC184 expression plasmid (Avidity, Denver, CO) encoding an IPTG inducible *BirA* gene to express biotin-ligase. This leads to almost complete in vivo biotinylation (85 – 100%) of the desired product (Leisner et al. 2008).

*Expression and purification of recombinant SLA-3*0401, human- and porcine beta-2 microglobulin (*β_2m)

SLA-3*0401 heavy chain proteins were produced recombinantly as previously described (Pedersen et al. 2011). *E. coli* BL21(DE3) cells containing the SLA proteins were lyzed in a cell-disrupter (Constant Cell Disruptor Systems set at 2300 bar) and the released inclusion bodies were isolated by centrifugation (Sorval RC6, 20 min, 17000 g). The inclusion bodies were washed twice in PBS, 0.5% NP-40 (Sigma), 0.1% deoxycholic acid (DOC, Sigma) and extracted into Urea-Tris buffer (8M urea, 25mM Tris, pH 8.0).

SLA-3*0401 heavy chain proteins extracted in 8 M urea were purified as previously described for the SLA-1*0401 molecule (Pedersen et al. 2011). In brief, this was done by successive immobilized metal adsorption, hydrophobic interaction-, and eventually Superdex-200 size exclusion chromatography. Throughout purification and storage the MHC-I heavy chain proteins were dissolved in 8 M Urea to ensure denaturation. The pre-oxidized, biotinylated and fully denatured proteins were stored at -20°C in Tris buffered 8 M urea.

Recombinant human- and porcine β_2m were expressed and purified as described elsewhere (Ferre et al. 2003, Ostergaard et al. 2001, Pedersen et al. 2011).

Peptides and peptide libraries

All peptides were purchased from Schafer-N, Denmark (www.schafer-n.com). Briefly, they were synthesized by standard 9-fluorenylmethyloxycarbonyl (Fmoc)-chemistry, purified by reversed-phase high-performance liquid chromatography (to at least >80% purity, frequently 95-99% purity), validated by mass spectrometry, and quantified by weight.

Positional scanning combinatorial peptide libraries (PSCPL) were used to determine the SLA-3*0401 binding motif. The experimental strategy of PSCPL has previously been described for both HLA (Stryhn et al. 1996) and SLA (Pedersen et al. 2011) proteins. The individual PSCPL peptide stability analysis was performed using ^{125}Iodine-labeled porcine β_2m (^{125}I- β_2m) in a FlashPlate® based proximity assay (Harndahl et al. 2011) explained below.

ELISA peptide affinity analysis

Affinity analysis of peptide interactions with the SLA-1*0401 was performed using a slightly modified version of a previously described immunosorbent assay (Sylvester-Hvid et al. 2002) most recently described by Pedersen et al. (Pedersen et al. 2012).

Luminescent oxygen channeling assay (LOCI) for peptide affinity analysis

Affinity analysis of peptide interactions with the SLA-3*0401 and SLA-2*0401 were performed using a conformation-dependent anti-SLA monoclonal antibody based LOCI technology as previously described for HLA (Harndahl et al. 2009). In brief, recombinant, biotinylated SLA heavy chains were diluted in buffer (0.1% Lutrol F 68 (BASF, Art. No. S30101. Ludwigshafen, Germany) in PBS, pH 7.2) to a concentration of 2 nM followed by addition of 15 times excess of porcine β_2m and a dose titration of peptide, and incubated at 18°C for 48 hours. pSLA complexes were detected using streptavidin (SA) donor beads and an anti-SLA monoclonal antibody (PT85A, VMRD, Pullman, Wash., USA) conjugated to acceptor beads. Beads and pSLA complexes were incubated at 18°C over night at a final bead concentration of 5 µg/ml, then equilibrated to room temperature 1 hour prior to detection by an EnVision multilabel reader (Perkin Elmer, Boston, USA).

*FlashPlate® scintillation proximity assay (SPA) for SLA-3*0401 motif mapping and pSLA stability measures*

The measurement of pSLA stability was done as previously described for HLA (Harndahl et al. 2011) using peptide and radiolabeled porcine β_2m in a mix with recombinant SLA heavy chain 100-fold diluted in (0.1% Lutrol F 68 (BASF, Art. No. S30101. Ludwigshafen, Germany) in PBS, pH 7.2) . pSLA folding reactions were carried out in streptavidin coated scintillation microplates (FlashPlate® PLUS, Perkin Elmer, Boston, USA). Steady-state of the folding reaction was reached by overnight incubation at 18°C at conditions of 30 nM SLA heavy chain, 1 nM (approximately 25,000 cpm) of ^{125}I-β_2m and 10 µM peptide. At steady-state unlabeled porcine β_2m was

added to a final concentration of 1 µM to prevent re-association of any dissociated ^{125}I-β_2m, and the temperature was raised to 37°C. Dissociation of pSLA was monitored continuously on a scintillation multiplate counter (TopCount NTX, Perkin Elmer) modified to operate at 37°C. PSCPL data were analyzed as described previously (Rasmussen et al. 2012) and the obtained binding matrix was visualized by the Seq2Logo server (Thomsen and Nielsen 2012) normalizing the values at each position to 1, using P-weighted Kullback-Leibler logo types and an even amino acid background distribution (0.05 for all amino acids).

Results

Mapping of the SLA-3*0401 peptide binding matrix using PSCPL

We have recently reported the peptide binding specificities of the swine leukocyte antigens, SLA-1*0401 and SLA-2*0401 (Pedersen et al. 2011, Pedersen et al. 2012). These peptide binding specificities were determined by nonameric PSCPL analysis using ELISA. Since then, we have introduced a new method to determine human MHC-I binding specificities (Rasmussen et al. 2012), based on a pMHC-I dissociation assay (Harndahl et al. 2011). This method is based on the dissociation of ^{125}I-radiolabeled human β_2m from *in situ* formed pHLA complexes. By ^{125}I-radiolabeling porcine β_2m, we adopted this methodology to allow PSCPL-based determination of the SLA-3*0401 binding matrix, illustrated in figure 1 and Table 1.

PSCPL analysis of the SLA-3*0401 molecule revealed a binding motif with a primary anchor in the position 2 (P2) of the peptide displaying preferences for asparagine (N) and arginine (R) with relative binding (RB) values of 5.6 and 2.3, respectively (Figure 1 and Table 1). This suggests a polar, acidic B-pocket within the SLA-3*0401 peptide binding groove. Auxiliary anchors were observed in P1, P3, P7 and P9 with anchor position (AP) values of 9, 11, 11 and 9, respectively. For P9 it was found that methionine (M), phenylalanine (F) and tyrosine (Y) were preferred with RB values of 2.4, 2.3 and 2.0, respectively (Table 1). Isoleucine (I) and aspartic acid (D) were also accepted in P9 having RB values of 1.8 and 1.5, respectively. Furthermore, it was observed that arginine (R), glutamine (Q), lysine (K) and proline (P) were all disfavored at P9 (RB values of 0.2, 0.3, 0.3 and 0.4, respectively). These results indicate the presence of a hydrophobic F-pocket within the binding groove of SLA-3*0401, although this pocket does not function as a primary anchor for peptide binding which again makes the binding motif for SLA-3*0401 rather atypical when compared to the dominating P2 and P9 anchors that are commonly observed for both SLA and HLA molecules (Kubo et al. 1994, Lamberth et al. 2008, Pedersen et al. 2011, Pedersen et al. 2012, Rammensee et al. 1999, Rapin et al. 2008, Sette and Sidney 1999, Yamada et al. 1999). Instead, a primary anchor was observed only in P2 (AP value of 27), with an auxiliary anchor expressing a preference for tryptophan (W), leucine (L), and phenylalanine (F) in P7 revealing a non-polar E-pocket. Altogether these results indicate that for SLA-3*0401 P2 is the most important peptide position in regard to peptide binding.

Analysis of peptide-SLA affinities

SLA-1*0401 peptide affinity studies were performed using a previously described ELISA (Pedersen et al. 2011), whereas affinity measurements for SLA-2*0401 and SLA-3*0401 were performed by a modified version of a previously published LOCI based MHC-I binding assay (Harndahl et al. 2009), using acceptor bead conjugated antibody PT85A which enable the capture of correctly folded pSLA on the surface of donor beads leading to a signal read-out once excited by laser (Figure 2). By using a combination of *NetMHCpan* (with a 2 % rank score threshold) and PSCPL matrix based predictions (with a threshold of 25 corresponding to 0.5 % percentile rank score threshold) a total of 157, 72, and 76 peptides were selected to be tested for their ability to be bound by SLA-1*0401, SLA-2*0401, and SLA-3*0401, respectively (Table 2 and Supporting Table 1 A - C). Note. that the *NetMHCpan*-2.4 prediction software has been trained on a limited set of SLA binding data consisting of 14 SLA-1*0401 and one SLA-2*0401 (all bound) peptides. From the 157 selected peptides

tested on SLA-1*0401, it was found that 67 peptides were bound with high affinity having K_D values of 50 nM or less, 45 peptides had intermediate binding affinities in the range of 50 – 500 nM, 20 peptides turned out to be bound with weak affinities of 500 – 5000 nM, and 25 peptides were identified as non-binding peptides with affinities >5000 nM (Table 2). In total, it was found that, of the 157 peptides chosen for binding studies, 112 (71.3 %) did bind with K_D values below 500 nM. It has previously been described that peptides with K_D affinity values below 500 nM are likely to be considered as immunological relevant (Assarsson et al. 2007). For the SLA-2*0401 molecule, 14 peptides (20%) of the predicted 72 were found to have K_D values lower than 500 nM, whereas 20 and 32 peptides respectively were in the range of being either weak or non-binding peptides. Finally, 76 peptides were tested for SLA-3*0401 binding identifying 20 strongly bound peptides, 9 intermediate and 9 weakly bound peptides, whereas 38 peptides were identified not to be bound by SLA-3*0401 (Table 2) leading to a total of 38 % of the peptides selected for the SLA-3*0401 molecule being bound with affinities stronger than 500 nM. Individual peptide sequences, origin, prediction rank scores, and K_D affinity values are shown in Supporting Table 1 A - C. Examples of LOCI dose titration curves for affinity analysis of two individual peptides, MTAASYARY and KRMMMMNLNY, bound by SLA-2*0401 and SLA-3*0401, respectively, are shown in Supporting Figure 1 and 2.

Combining PSCPL matrix- and *NetMHCpan* based predictions

To quantify the complementarities of the PSCPL matrix and *NetMHCpan* prediction methods, the individual predictions were split into subsets predicted by (a) *either* the matrix method *or* the *NetMHCpan* method, (b) by *both* the matrix and *NetMHCpan* methods, or (c) *exclusively* by one of the two. The result of this analysis is shown in Table 3. From this comparison, it is seen that the two methods are highly complementary when it comes to identification of SLA binding peptides. Depending on the given SLA molecule, only 45–59 % of the peptides validated to be bound by SLA are predicted by both methods (Table 3, Sensitivity). Also, it is apparent that not one method is consistently more accurate in identifying SLA peptide binders than the other. For SLA-2*0401 we found that only 2 of the 20 peptides (10 %), identified exclusively by the matrix-based method turned out to be bound. For the exclusive *NetMHCpan* predictions 9 of 25 (36%) were found to bind. In contrast to this, the exclusive matrix-based predictions for the SLA-3*0401 molecule identified 47 % binding peptides (8 of 17), whereas the *NetMHCpan* exclusive predictions for this SLA molecule only identified 11 % binding peptides (4 of 35). The predictive positive value (true positives divided with the predicted positive) for the two methods on the two SLA molecules (SLA-2*0401 and SLA-3*0401) is statistically significant ($p<0.05$ in both cases, comparison of ratia). That is, the predictive positive value of the *NetMHCpan* method is significantly higher for the SLA-2*0401 molecule compared to SLA-3*0401 and vice versa for the PSCPL matrix method emphasizing the complementarities of the two methods, and underlining the importance of including both to ensure optimal coverage of the binding repertoire of SLA molecules.

pSLA stability analysis

pMHC class stability has been proposed to be a better determinant of immunogenicity rather than binding affinity (Busch and Pamer 1998, Harndahl et al. 2012, Lazarski et al. 2005, Mullbacher et al. 1999, Sant et al. 2005, van der Burg et al. 1996). In order to investigate the stability of pSLA complexes, we modified an existing scintillation proximity assay (SPA) based pMHC dissociation assay (Harndahl et al. 2011) enabling us to measure pSLA stability. Peptides binding with an affinity better than 500 nM to SLA-1*0401, SLA-2*0401 or SLA-3*0401 were tested for their pSLA stability. The correlation between pSLA affinity and stability is shown for all three SLA molecules in Figure 3 A – C. It was found that the pSLA stability ranged from extremely stable (T½ of 158 hours) to fairly unstable (T½ of 0.18 hours). The correlation between binding affinity and stability was statistically significant for all three SLA molecules (Spearmans rank correlations of 0.39 (SLA-2*0401) to 0.78 (SLA-1*0401), and with $p<0.05$ in all cases, exact permutation test). In general, it was seen that

peptides bound with high affinities were also generating highly stable pSLA complexes with T½ ≥ 1 hour (Figure 3 A – B). It was observed that SLA-3*0401 complexes were more unstable than the equivalent pSLA-1*0401 and pSLA-2*0401, having only six peptides with stability T½ periods ranging between 1.1 and 6.7 hours (Figure 3 C + Supporting Table 1 C). In comparison, the SLA-1*0401 had 65 peptides with stabilities ranging from T½ of 1 hour to more than 158 hours, and several of those had T½ of more than 10 hours (Figure 3 A + Supporting Table 1 A). For SLA-2*0401, 18 of the 20 peptide with measured binding affinity stronger than 500 nM were shown to be stably bound with T½ of more than 1 hour (Supporting Table 1 B). This difference between fraction of stable binders between the SLA-3*0401 and the two other SLA molecules is highly statistical significant ($p<0.01$, comparison of ratia). Note, that analysis here for SLA-2*0401 and SLA-3*0401 is limited to relative few peptides identified with binding affinities stronger than 500 nM. Additional analyses including a larger number of peptides would be necessary to draw a more general conclusion in regard to those two molecules and their pSLA complex stabilities. Such analyses are likely to confirm the pattern observed here leading to the identification of several more highly stable pSLA-2*0401 but only a few additional stable pSLA-3*0401 due to the unique binding characteristics of the SLA-3*0401 molecule expressing only one dominating anchor in P2 (Table 1) as discussed below. Despite this, it was still possible to identify peptides that were bound by the SLA-3*0401 molecule with high affinity and producing highly stable pSLA, an example being the peptide sequence RNMSRIFPY, derived from *Encephalitozoon cuniculi* IEDB ID: 93734, (2011). This peptide is an almost perfect match for the SLA-3*0401 binding motif (Table 1) and was also predicted to be bound by both the matrix and *NetMHCpan* prediction rank scores (Supporting Table 1 C). Furthermore, *in vitro* analysis verified this sequence as an extremely strong and stable binding peptide with a K_D value of 1 nM and a stability half-life of T½ = 6.7 hours (Supporting Table 1 C). Such data confirm the ability of the prediction approach, combining specific PSCPL binding matrix and *in silico* predictions, to identify potential T cell epitopes.

Discussion

The mapping of the complete nonamer SLA-3*0401 peptide binding matrix revealed a single dominating anchor in P2 of the binding groove (Table 1). Instead of a dominating P9 anchor which is commonly seen for other SLA and HLA proteins (Lamberth et al. 2008, Pedersen et al. 2011, Pedersen et al. 2012, Rammensee et al. 1999, Rapin et al. 2008, Sette and Sidney 1999), it was found that this molecule displayed a rather atypical auxiliary peptide anchor for P7 within the E-pocket of the binding groove.

We here present state-of-the-art tools for peptide prediction, selection, and binding analysis – both in terms of affinity and stability. These analyses were based on combining individual SLA binding matrix predictions with those of *NetMHCpan*, and further test binding affinity and stability using homogenous, high throughput LOCI and SPA assays, respectively. The combination of the two individual prediction methods resulted in an enhancement of the overall peptide selection in the range of a 10 to 45 % increase in the final number of peptides identified to be bound (Supporting Table 1 A - C). Confirming the advantage gained by combining the two prediction tools is seen for peptides TSDGFINGW and ITDYIVGYY. These peptides were both identified to be bound with high affinity and to form highly stable pSLA but while TSDGFINGW only came out as a candidate ligand for SLA-1*0401 by the matrix-based predictions (matrix score of 195, NetMHCpan rank of 15.00), the ITDYIVGYY peptide was predicted exclusively by the *NetMHCpan* (matrix score of 0, NetMHCpan rank of 0.03), (Supporting Table 1 A). Hence, combining the two prediction tools resulted in inclusion of both peptides of which one of them would have been lost, were the predictions only performed by one of the predictors. Similar examples can be found in Supporting Table 1 A – C. We observe a general trend that the overlap between the *NetMHCpan* and PSCPL matrix-based predictions is highest for the SLA molecule where peptide-binding data form part of the training data for the *NetMHCpan* method. This is consistent with earlier findings (Rasmussen et al. 2012), and suggests that as data for constructing the pan-specific predictor are enriched with SLA peptide

binding measurements, identified as described here using both the PSCPL and pan-specific predictions, the *NetMHCpan* method will be able to learn the SLA binding repertoire described by both methods. By way of example is, that the correlation between predictions performed by the PSCPL matrix and *NetMHCpan* methods, increase by 33 % when the 76 SLA-3*0401 binding measurements obtained in this study are included in the training data (data not shown).

Analyzing the correlation between pSLA affinity and stability for the three SLA proteins revealed a general trend of peptides being bound with high affinity, were also producing high stability pSLA (Figure 3 A – C). Still it was found that the individual pSLA-3*0401 turned out to display significantly lower T½ values than those of both the pSLA-1*0401 and pSLA-2*0401. Several factors, which could cause such a tendency, remain to be addressed in detail. Factors such as the low number of peptides tested, limitations in regard to the diversity of peptides in the in-house peptide library (comprised of some 9000 different peptides, where no peptides have the pattern of N/R at P2 and D at P9, as compared to "the whole universe" of peptides) or the fact that SLA-3*0401 has a lack of the otherwise commonly expressed P9 anchor in regard to peptide binding, could all be causative for the production of low stability pSLA-3*0401 regardless of the peptide offered. As seen in Supporting Tables 1 A + B, a trend for peptides satisfying *both* the P2 and P9 anchor of SLA-1*0401 and SLA-2*0401, as well as the P3 anchor of SLA-1*0401, is that they are bound with higher stability, as compared to peptides that satisfy only *one* of the two anchors (or only *two* of the *three* anchors in regard to SLA-1*0401) which tend to be bound with lower stability. This observation is consistent with previous observations made for the human class I molecule, HLA-A*02:01 (Harndahl et al. 2012). Hence, for each anchor satisfied the stability of the bound peptide seems to increase, which could explain why the "one-anchor-only" molecule, SLA-3*0401, produces mostly low stable pSLA. Speculating the biological relevance, expression of a single major anchor for P2 could be a phenotypic preference in regard to SLA-3*0401 leading to faster turnover rates in the sense of peptide association and dissociation, which again would claim pSLA-3*0401 of lower stabilities as compared to other molecules showing slow peptide turnovers but higher stabilities. An SLA allele repertoire combining fast-unstable and slow-stable pSLA could be an advantage for the host in the sense of effective and diverse protection against intruding pathogens expressing both fast, and diverse, peptide turnovers as well as stable peptide presentation.

Having determined the SLA-3*0401 binding matrix and knowing how to specifically map such matrices can be of great value when screening for peptide candidates. Not only does it provide an overview and insight of specific biochemical features within the binding groove, it also contributes to the overall predictions of possible peptide candidates for binding. The prediction tool combination presented here prove extremely effective in the initial steps of identifying CTL peptide epitopes now adding swine to the list of species that can be addressed, screening virtually any pathogen of interest. Furthermore, improvement of the *NetMHCpan* alone, which has only been trained on a very limited number of peptides for SLA-1*0401 and SLA-2*0401 (15 and 1, respectively) and none for the SLA-3*0401 so far, could also benefit the process of selecting peptide candidates for pMHC binding studies – especially when studying MHC molecules for which peptide binding matrixes have not yet been defined. The data achieved in this study, as well as data recently obtained for cattle MHC-I (BoLA) by the group at the University of Copenhagen, will further contribute to the constant improvement of the *NetMHCpan* by data training.

Finally, we here present several peptides derived from bacteria and viruses such as foot-and-mouth disease virus (FMDV) and Influenza A virus which could have a great relevance for future studies in regard to disease in livestock animals, bound with both high affinity and stability by three of the most commonly expressed SLA molecules worldwide (Supporting Table 1 A - C). Such peptides can be categorized as potential CTL epitopes expressing the ability to generate stable pSLA, in that they are likely to be targets for circulating CTLs, eventually leading to

cell activation and elimination of pathogenic intruders. Clarifying details concerning the peptide binding properties of swine MHC class I molecules could contribute tremendously to epitope discoveries as well as to the overall validation and analysis of currently available or newly developed livestock vaccines. Furthermore, knowledge of SLA binding motifs could improve current studies and surveillance of porcine immune responses to agricultural threats such as foot-and-mouth disease virus (FMDV), porcine reproductive and respiratory syndrome virus (PRRSV), swine influenza virus and others, in what seems to be a continuous struggle to keep animals healthy and protected to avoid substantial outbreaks.

Ackowledgements

The authors would like to thank Lise Lotte Bruun Nielsen and Panchale Olsen for their expert experimental support. This work was supported by the Danish Council for Independent Research, Technology and Production Sciences (274-09-0281).

References

http://www.immuneepitope.org. 2011. Ref Type: Internet Communication

Assarsson E., Sidney J., Oseroff C., Pasquetto V., Bui H.H., Frahm N., Brander C., Peters B., Grey H. & Sette A. (2007) A quantitative analysis of the variables affecting the repertoire of T cell specificities recognized after vaccinia virus infection. *J. Immunol.* 178, 7890-7901.

Busch D.H., Pamer E.G. (1998) MHC class I/peptide stability: implications for immunodominance, in vitro proliferation, and diversity of responding CTL. *J. Immunol.* 160, 4441-4448.

Ferre H., Ruffet E., Blicher T., Sylvester-Hvid C., Nielsen L.L., Hobley T.J., Thomas O.R. & Buus S. (2003) Purification of correctly oxidized MHC class I heavy-chain molecules under denaturing conditions: a novel strategy exploiting disulfide assisted protein folding. *Protein Sci.* 12, 551-559.

Hansen N.J., Pedersen L.O., Stryhn A. & Buus S. (2001) High-throughput polymerase chain reaction cleanup in microtiter format. *Anal. Biochem.* 296, 149-151.

Harndahl M., Justesen S., Lamberth K., Roder G., Nielsen M. & Buus S. (2009) Peptide binding to HLA class I molecules: homogenous, high-throughput screening, and affinity assays. *J. Biomol. Screen.* 14, 173-180.

Harndahl M., Rasmussen M., Roder G. & Buus S. (2011) Real-time, high-throughput measurements of peptide-MHC-I dissociation using a scintillation proximity assay. *J. Immunol. Methods* 374, 5-12.

Harndahl M., Rasmussen M., Roder G., Dalgaard P., I, Sorensen M., Nielsen M. & Buus S. (2012) Peptide-MHC class I stability is a better predictor than peptide affinity of CTL immunogenicity. *Eur. J. Immunol.* 42, 1405-1416.

Hoof I., Peters B., Sidney J., Pedersen L.E., Sette A., Lund O., Buus S. & Nielsen M. (2009) NetMHCpan, a method for MHC class I binding prediction beyond humans. *Immunogenetics* 61, 1-13.

Kubo R.T., Sette A., Grey H.M., Appella E., Sakaguchi K., Zhu N.Z., Arnott D., Sherman N., Shabanowitz J., Michel H. & . (1994) Definition of specific peptide motifs for four major HLA-A alleles. *J. Immunol.* 152, 3913-3924.

Lamberth K., Roder G., Harndahl M., Nielsen M., Lundegaard C., Schafer-Nielsen C., Lund O. & Buus S. (2008) The peptide-binding specificity of HLA-A*3001 demonstrates membership of the HLA-A3 supertype. *Immunogenetics* 60, 633-643.

Lauemoller S.L., Holm A., Hilden J., Brunak S., Holst N.M., Stryhn A., Ostergaard P.L. & Buus S. (2001) Quantitative predictions of peptide binding to MHC class I molecules using specificity matrices and anchor-stratified calibrations. *Tissue Antigens* 57, 405-414.

Lazarski C.A., Chaves F.A., Jenks S.A., Wu S., Richards K.A., Weaver J.M. & Sant A.J. (2005) The kinetic stability of MHC class II:peptide complexes is a key parameter that dictates immunodominance. *Immunity.* 23, 29-40.

Leisner C., Loeth N., Lamberth K., Justesen S., Sylvester-Hvid C., Schmidt E.G., Claesson M., Buus S. & Stryhn A. (2008) One-pot, mix-and-read peptide-MHC tetramers. *PLoS. One.* 3, e1678.

Lundegaard C., Lund O. & Nielsen M. (2011) Prediction of epitopes using neural network based methods. *J. Immunol. Methods* 374, 26-34.

Mullbacher A., Lobigs M., Yewdell J.W., Bennink J.R., Tha H.R. & Blanden R.V. (1999) High peptide affinity for MHC class I does not correlate with immunodominance. *Scand. J. Immunol.* 50, 420-426.

Nielsen M., Lundegaard C., Blicher T., Lamberth K., Harndahl M., Justesen S., Roder G., Peters B., Sette A., Lund O. & Buus S. (2007) NetMHCpan, a method for quantitative predictions of peptide binding to any HLA-A and -B locus protein of known sequence. *PLoS. One.* 2, e796.

Nielsen M., Lundegaard C., Blicher T., Peters B., Sette A., Justesen S., Buus S. & Lund O. (2008) Quantitative predictions of peptide binding to any HLA-DR molecule of known sequence: NetMHCIIpan. *PLoS. Comput. Biol.* 4, e1000107.

Ostergaard P.L., Nissen M.H., Hansen N.J., Nielsen L.L., Lauenmoller S.L., Blicher T., Nansen A., Sylvester-Hvid C., Thromsen A.R. & Buus S. (2001) Efficient assembly of recombinant major histocompatibility complex class I molecules with preformed disulfide bonds. *Eur. J. Immunol.* 31, 2986-2996.

Pedersen L.E., Harndahl M., Nielsen M., Patch J.R., Jungersen G., Buus S. & Golde W.T. (2012) Identification of peptides from foot-and-mouth disease virus structural proteins bound by class I swine leukocyte antigen (SLA) alleles, SLA-1*0401 and SLA-2*0401. *Anim Genet.*

Pedersen L.E., Harndahl M., Rasmussen M., Lamberth K., Golde W.T., Lund O., Nielsen M. & Buus S. (2011) Porcine major histocompatibility complex (MHC) class I molecules and analysis of their peptide-binding specificities. *Immunogenetics* 63, 821-834.

Rammensee H., Bachmann J., Emmerich N.P., Bachor O.A. & Stevanovic S. (1999) SYFPEITHI: database for MHC ligands and peptide motifs. *Immunogenetics* 50, 213-219.

Rapin N., Hoof I., Lund O. & Nielsen M. (2008) MHC motif viewer. *Immunogenetics* 60, 759-765.

Rasmussen M., Harndahl M., Nielsen M. & Buus S. (2012) Uncovering the Peptide Binding Specificity of HLA-C. A generic approach/strategy for determining the specificity of MHC Class I molecules by combining experimentally determined matrices with artificial neural networks. *Manuscript in preparation*

Sant A.J., Chaves F.A., Jenks S.A., Richards K.A., Menges P., Weaver J.M. & Lazarski C.A. (2005) The relationship between immunodominance, DM editing, and the kinetic stability of MHC class II:peptide complexes. *Immunol. Rev.* 207, 261-278.

Sette A., Sidney J. (1999) Nine major HLA class I supertypes account for the vast preponderance of HLA-A and -B polymorphism. *Immunogenetics* 50, 201-212.

Stryhn A., Pedersen L.O., Romme T., Holm C.B., Holm A. & Buus S. (1996) Peptide binding specificity of major histocompatibility complex class I resolved into an array of apparently independent subspecificities: quantitation by peptide libraries and improved prediction of binding. *Eur. J. Immunol.* 26, 1911-1918.

Sylvester-Hvid C., Kristensen N., Blicher T., Ferre H., Lauemoller S.L., Wolf X.A., Lamberth K., Nissen M.H., Pedersen L.O. & Buus S. (2002) Establishment of a quantitative ELISA capable of determining peptide - MHC class I interaction. *Tissue Antigens* 59, 251-258.

Thomsen M.C., Nielsen M. (2012) Seq2Logo: a method for construction and visualization of amino acid binding motifs and sequence profiles including sequence weighting, pseudo counts and two-sided representation of amino acid enrichment and depletion. *Nucleic Acids Res.* 40, W281-W287.

van der Burg S.H., Visseren M.J., Brandt R.M., Kast W.M. & Melief C.J. (1996) Immunogenicity of peptides bound to MHC class I molecules depends on the MHC-peptide complex stability. *J. Immunol.* 156, 3308-3314.

Yamada N., Ishikawa Y., Dumrese T., Tokunaga K., Juji T., Nagatani T., Miwa K., Rammensee H.G. & Takiguchi M. (1999) Role of anchor residues in peptide binding to three HLA-A26 molecules. *Tissue Antigens* 54, 325-332.

Zhang H., Lundegaard C. & Nielsen M. (2009) Pan-specific MHC class I predictors: a benchmark of HLA class I pan-specific prediction methods. *Bioinformatics.* 25, 83-89.

Figures

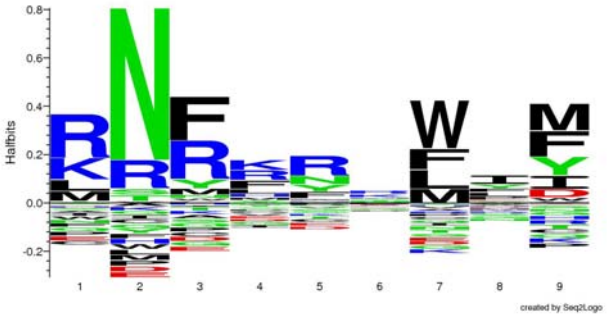

Figure 1 Binding motif of the SLA-3*0401 molecule determined by pMHC dissociation driven PSCPL analysis and displayed as logos. Each logo represents a single amino acid. The larger the size of the amino acid representative letter, the higher the affinity for binding. Positive amino acid logos indicate slow pMHC dissociation rates and high binding affinity. Negative amino acid logos indicate fast pMHC dissociation rates and low binding affinity. The visualization was performed by the Seq2Logo server (Thomsen and Nielsen 2012) normalizing scores for each peptide position to one, using P-weighted Kullback-Leibler logo types with an even amino acid background distribution (0.05 for all amino acids).

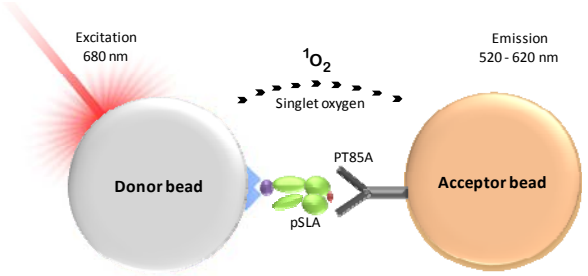

Figure 2 Illustration of the PT85A based LOCI principle for analysis of SLA-2*0401 and SLA-3*0401 peptide affinity. Streptavidin (blue) coated donor beads enable the capture of biotinylated pSLA (purple (biotin), green (MHC/β_2m), red (bound peptide)). Acceptor beads were coated with a mouse-anti-SLA monoclonal antibody, PT85A (carbon grey). Recognition of the pSLA by PT85A brings the donor and acceptor beads in close proximity leading to the transfer of singlet oxygen ($^1O_2$) from the excited donor bead to the acceptor bead, which results in detectable emission from the acceptor bead (orange).

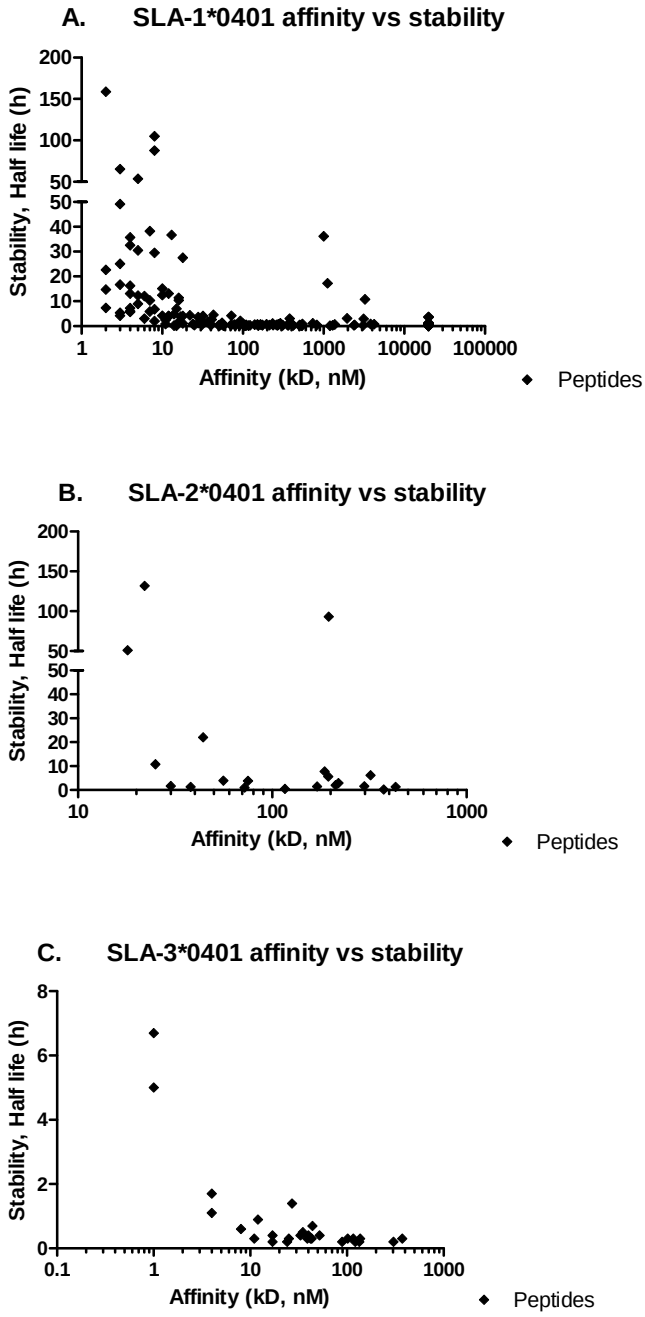

Figure 3 A - C pSLA affinity versus stability for predicted peptide candidates with measured K_D values below 500 nM. A: SLA-1*0401 (n: 110). B: SLA-2*0401 (n: 20). C: SLA-3*0401 (n: 29).

Supporting figures

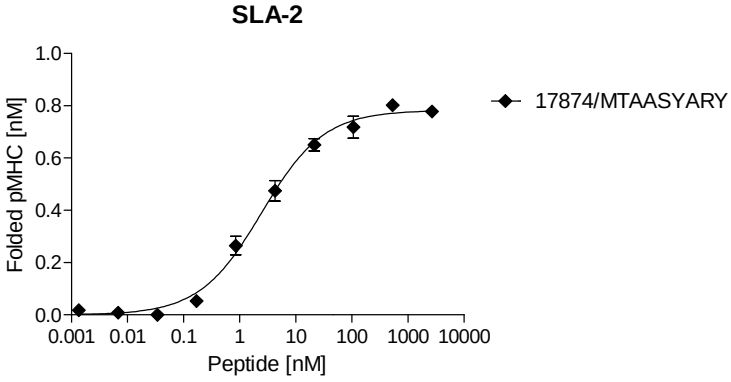

Supporting Figure 1 LOCI based titration curve for affinity analysis of the SLA-2*0401 binding of peptide MTAASYARY (K_D 75 nM, T½ of 3.8 hours).

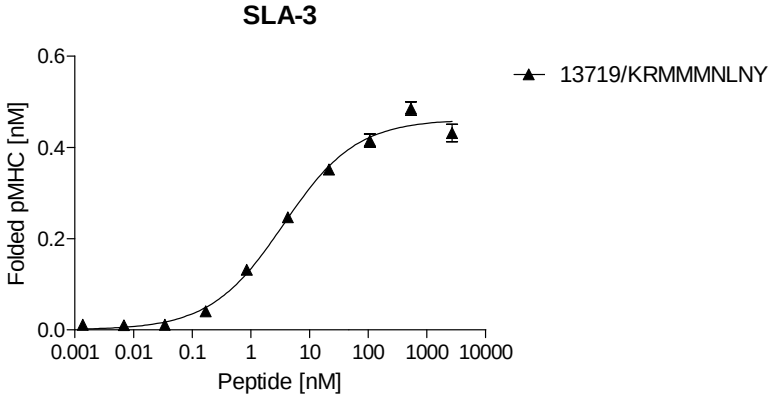

Supporting Figure 2 LOCI based titration curve for affinity analysis of the SLA-3*0401 binding of peptide KRMMMNLNY (K_D 4 nM, T½ of 1.1 hours).

Tables

SLA-3*0401	Amino acid position in peptide								
	1	2	3	4	5	6	7	8	9
A	0,8	0,7	0,6	0,8	0,9	1,0	0,7	0,9	0,9
C	*0,4*	0,6	*0,5*	0,7	*0,5*	0,5	0,7	0,9	*0,5*
D	0,9	*0,4*	*0,3*	0,5	*0,4*	0,7	0,5	0,8	1,5
E	*0,4*	*0,4*	*0,4*	0,6	*0,4*	0,9	0,5	1,2	0,9
F	0,6	0,5	**3,0**	1,7	1,6	0,8	**2,2**	1,5	**2,3**
G	0,9	0,6	*0,4*	*0,3*	0,7	0,6	*0,5*	0,5	0,6
H	0,8	0,5	0,8	1,3	1,1	1,0	0,8	0,8	0,6
I	0,7	0,7	0,8	*0,5*	1,1	1,0	0,6	1,9	1,8
K	**2,2**	0,7	0,6	1,8	0,7	1,5	*0,4*	0,7	*0,3*
L	1,7	*0,5*	1,1	1,4	0,9	1,1	**2,1**	1,4	0,9
M	1,6	*0,5*	1,4	1,3	1,1	1,2	1,9	0,7	**2,4**
N	0,6	**5,6**	1,2	0,9	1,7	1,1	0,6	*0,5*	0,7
P	*0,3*	*0,4*	*0,5*	0,7	0,9	0,9	0,7	1,4	*0,4*
Q	*0,5*	0,7	0,5	1,1	0,8	1,1	0,7	0,9	*0,3*
R	**3,1**	**2,3**	**2,8**	1,8	**2,4**	1,5	0,7	0,7	*0,2*
S	0,8	1,3	0,6	0,8	0,7	1,2	0,6	0,6	0,7
T	1,1	1,3	0,7	0,8	0,6	1,1	0,6	1,0	*0,5*
V	1,0	1,1	1,1	0,7	0,8	0,9	0,8	1,2	1,1
W	0,6	0,5	1,2	1,0	1,0	0,8	**3,4**	0,9	1,2
Y	0,9	0,6	1,6	1,2	1,6	1,0	0,8	1,5	**2,0**
Sum	20	20	20	20	20	20	20	20	20
AP-value	9	27	11	4	5	1	11	3	9

Table 1 The complete nonamer SLA-3*0401 binding matrix as determined by the PSCPL approach. RB values greater than 2 are defined as favored AAs for peptide binding (marked in bold), whereas values below 0.5 are defined as destabilizing (marked in italics), (Lauemoller et al. 2001, Stryhn et al. 1996). As previously defined, AP-values above 15 are considered as dominating anchors of importance illustrated by underlining (Lamberth et al. 2008).

	Peptide affinity (K_D, nM)			
Molecule	≤ 50	50 - 500	500 - 5000	≥ 5000
SLA-1*0401	67	45	20	25
SLA-2*0401	6	14	20	32
SLA-3*0401	20	9	9	38

Table 2 Peptide affinity analysis of peptides predicted for SLA binding by the *NetMHCpan* or PSCPL matrix prediction methods. The total numbers of identified strong (K_D ≤ 50 nM), intermediate (K_D 50 - 500 nM), and weak (K_D 500 - 5000) as well as non-binding (K_D ≥ 5000 nM) peptides are indicated for each SLA molecule.

PSCPL matrix *or* NetMHCpan prediction	**Peptides predicted by *either* PSCPL matrix *or* NetMHCpan**	**Peptides bound**		**Sensitivity**
SLA-1*0401	157	112	(71.3 %)	1.00
SLA-2*0401	72	20	(27.8 %)	1.00
SLA-3*0401	76	29	(38.2 %)	1.00
Combined prediction	**Peptides predicted by PSCPL matrix *and* NetMHCpan**	**Peptides bound**		**Sensitivity**
SLA-1*0401	61	53	(86.9 %)	0.473
SLA-2*0401	27	9	(33.3 %)	0.450
SLA-3*0401	24	17	(70.8 %)	0.586
NetMHCpan prediction	**Peptides predicted by NetMHCpan exclusively**	**Peptides bound**		**Sensitivity**
SLA-1*0401	76	44	(57.9 %)	0.393
SLA-2*0401	25	9	(36.0 %)	0.450
SLA-3*0401	35	4	(11.4 %)	0.138
PSCPL matrix prediction	**Peptides predicted by PSCPL matrix exclusively**	**Peptides bound**		**Sensitivity**
SLA-1*0401	20	15	(75.0 %)	0.134
SLA-2*0401	20	2	(10.0 %)	0.100
SLA-3*0401	17	8	(47.1 %)	0.276

Table 3 Comparing abilities of the PSCPL matrix- and *NetMHCpan* based prediction methods to identify true binding peptides for SLA-1*0401, SLA-2*0401 and SLA-3*0401. The sensitivity of each prediction scenario is given as (true positives)/(actual positives), i.e. the share of all peptides actually identified to be bound (from the pool of PSCPL matrix or *NetMHCpan* predicted candidates), that were also found to be so within the pool of peptides predicted by the respective method exclusively.

Supporting Tables

Supporting Table 1 A

SLA-1*0401 peptide binding analysis

		Prediction Affinity/Rank					
Peptide amino acid sequence	Origin/Uniprot ID/Position	PSCPL matrix	NetMHCpan	Affinity (K_D, nM)	Stability (T1/2, h)	Predicted by PSCPL matrix	Predicted by NetMHCpan
AVEDFLAFF	Andes virus/Q9E005/1037	679	2.00 (WB)	2	22,69	Yes	Yes
STAPTGSWF	NA	186	0.40 (SB)	2	7,30	Yes	Yes
GTDSGFAAY	SARS-like coronavirus/Q3I5J2/187	65	0.08 (SB)	2	158,75	Yes	Yes
MADSFKSDY	NA	170	1.00 (WB)	2	14,71	Yes	Yes
VLDKWNTNY	Variola virus/Q89167/164	81	0.80 (WB)	3	25,12	Yes	Yes
TIDKSSPLY	Vaccinia virus/Q85324/95	172	0.25 (SB)	3	16,68	Yes	Yes
MIDSDEWVY	Entamoeba histolytica/Q512E5/461	84	0.80 (WB)	3	49,13	Yes	Yes
TSDGFINGW	Yersinia pestis/A6BRR8/79	195	15,00	3	5,34	Yes	No
ITDITSPLW	Marburg virus/P35262/2017	185	0.80 (WB)	3	65,22	Yes	Yes
TQDLFLPFY	SARS-CoV/Q202H8/55	89	3,00	3	4,21	Yes	No
ITDYIVGYY	Escherichia coli/B3C476/239	0	0.03 (SB)	4	13,09	No	Yes
SVDGFRASY	NA	353	0.40 (SB)	4	35,71	Yes	Yes
KLDAWLLPF	Salmonella typhi/Q8Z2M9/132	230	1.00 (WB)	4	16,26	Yes	Yes
NTDAFSREY	Variola virus/Q0N575/184	171	0.40 (SB)	4	6,03	Yes	Yes
KLDPTNTLW	Machupo virus/Q8AZ68/370	240	3,00	4	32,59	Yes	No
GVEPGHAFY	Mycobacterium tuberculosis/A4KFR1/150	175	0.40 (SB)	4	5,74	Yes	Yes
MTAHITVPY	Foot-and-mouth disease virus strain A24 P1 protein	1	0.01 (SB)	4	7,23	No	Yes
SVEVKLPDY	Dengue virus type 4/Q2YHF0/449	93	2.00 (WB)	5	53,56	Yes	Yes
VTDPGGLYY		67	0.01 (SB)	5	12,33	Yes	Yes
HSDDALFIY	Sangassou virus/Q1L0R2/123	112	0.17 (SB)	5	8,98	Yes	Yes
RADSMMLGY	Pseudomonas mallei/Q62FQ6/356	131	0.10 (SB)	5	30,50	Yes	Yes
EVAGAGSGF	Mycobacterium tuberculosis/Q6MWX9/706	146	15,00	6	3,01	Yes	No
NIDNMCHLY	Vaccinia virus/Q49PZ6/18	184	1.00 (WB)	6	12,14	Yes	Yes
FTFWTFANY	NA	7	0.05 (SB)	7	38,25	No	Yes
LIDGRTSFY	Lassa virus/Q6Y630/140	213	0.30 (SB)	7	5,88	Yes	Yes
YTDKIAMSY	Francisella tularensis subsp. Tularensis/A7JE81/332	5	0.03 (SB)	7	10,34	No	Yes
ATDFKFAMY	NA	0	0.08 (SB)	8	104,90	No	Yes
RVERIKSEY	Yellow fever virus/Q9W9I1/281	85	1.50 (WB)	8	29,52	Yes	Yes
SSDLRSWTF		174	2.00 (WB)	8	2,07	Yes	Yes
TMDVNHPIY	Variola virus/Q0NIE/511	342	0.80 (WB)	8	6,80	Yes	Yes
VSDGPPTGY	Variola virus/Q89222/298	144	0.50 (WB)	8	87,80	Yes	Yes
ATEDPSSGY	Ebola virus/P60170/205	128	0.30 (SB)	10	4,15	Yes	Yes
VVDALRNIY	Tula virus/Q9YQR5/1005	120	0.80 (WB)	10	15,11	Yes	Yes
GTDSNGMLW	Mycobacterium tuberculosis/Q6MWX8/1587	226	2.00 (WB)	10	12,52	Yes	Yes
ASAAHLAAY	Shigella sonnei/Q3YTU7/42	80	0.03 (SB)	11	2,46	Yes	Yes
MTAASYARY	NA	4	0.01 (SB)	11	0,85	No	Yes
IVDCLTEMY	NA	145	0.40 (SB)	12	13,14	Yes	Yes
MIEPRTLQY	NA	93	0.17 (SB)	12	3,98	Yes	Yes
SVAMCRTPF	Yellow fever virus/Q1X881/2440	174	3,00	12	4,14	Yes	No
IVDINVKDY	Influenza A virus/genbank AY702454/107	75	3,00	12	3,89	Yes	No
QTDNDIWFW	Escherichia coli/B3BVD0/932	71	15,00	13	36,67	Yes	No
ITDITKYLY	Bacillus anthracis/B0ARG1/50	96	0.05 (SB)	14	4,78	Yes	Yes
YVYFYDLSY	Variola virus/Q0NLZ1/504	0	0.01 (SB)	14	0,21	No	Yes
ATAAATEAY	Ebola virus/Q05127/154	8	0.01 (SB)	15	6,97	No	Yes
KSNRIPFLY	Giardia lamblia/A8BAY0/318	5	0.80 (WB)	15	0,15	No	Yes
LTDDMIAAY	SARS-CoV/Q202H8/847	156	0.05 (SB)	16	11,41	Yes	Yes
LSDDAVVCY	SARS-like coronavirus/P0C6W6/5125	98	0.50 (WB)	16	10,38	Yes	Yes
RIARFHRPY	Brucella suis/Q8FVB3/115	92	0.80 (WB)	16	1,68	Yes	Yes
RVSTGLYRY	Mycobacterium tuberculosis/A4KJM5/1479	68	0.30 (SB)	17	3,86	Yes	Yes
EIAQHGAWY	Escherichia coli/B3BCL5/74	160	2.00 (WB)	18	1,14	Yes	Yes
LTDSDSPTY	Mycobacterium tuberculosis/A4KDY3/1298	87	0.80 (WB)	18	4,06	Yes	Yes
QTDNQLAVF	West Nile virus strain PTRoxo/A8KCE3/2252	135	1.50 (WB)	18	27,51	Yes	Yes
QTDPLWQKY	Vibrio vulnificus/Q8D5T5/90	76	0.40 (SB)	20	ND	Yes	Yes
LLDGLLAWY	Mycobacterium tuberculosis/A4KM19/247	252	1.00 (WB)	22	4,38	Yes	Yes

SLA-1*0401 peptide binding analysis

		Prediction Affinity/Rank					
Peptide amino acid sequence	Origin/Uniprot ID/Position	PSCPL matrix	NetMHCpan	Affinity (Kᴅ, nM)	Stability (T1/2, h)	Predicted by PSCPL matrix	Predicted by NetMHCpan
VVYRGTTTY	SARS-like coronavirus/P0C6W6/5508	4	0.08 (SB)	28	1,25	No	Yes
FTDNNELEF	Bacillus anthracis Tsiankovskii-I/B3J7Q9/95	149	0.50 (WB)	31	0,49	Yes	Yes
CSDETTLYY	Francisella tularensis subsp. Tularensis/A7JDX6/88	5	0.03 (SB)	32	1,48	No	Yes
RVFPGDHFY	Mycobacterium tuberculosis/A4KKI8/230	3	0.05 (SB)	32	4,07	No	Yes
VSDGGPNLY	Influenza A virus (A/duck/Guangdong/173/04(H5 N1))/genbank AY737302/591	190	0.08 (SB)	37	1,72	Yes	Yes
SSDISFIKY	Vaccinia virus/Q80HY4/66	63	0.40 (SB)	40	0,77	Yes	Yes
ASYAGAGAY	Artificially designed sequence	0	0.03 (SB)	40	0,36	No	Yes
EVDQTKIQY	Yellow fever virus/Q9WN82/22	103	4,00	41	2,70	Yes	No
CTDDNALAY	SARS-like coronavirus/P0C6T7/4138	74	0.03 (SB)	43	4,59	Yes	Yes
ATVKGMQSY	NA	2	0.05 (SB)	50	0,36	No	Yes
FTIRDVLAY	Yersinia enterocolitica/A1JNP9/275	0	0.03 (SB)	52	0,36	No	Yes
ASYQFQLPY	Vibrio cholerae/A6Y7B0/208	4	0.01 (SB)	53	0,61	No	Yes
RTDAWSYPV	Escherichia coli/B3BD85/110	112	0.80 (WB)	55	1,28	Yes	Yes
RSNDTELNY	Marburg virus/P35262/1181	68	0.17 (SB)	57	0,24	Yes	Yes
MTSGSSSGF	Mycobacterium tuberculosis/Q6MWX9/2924	125	0.40 (SB)	57	0,62	Yes	Yes
RLASYGLYY	Variola virus/Q9PXS2/560	9	0.05 (SB)	71	0,38	No	Yes
RTWAYHGSY	Dengue virus type 4/Q2YHF0/2788	0	0.08 (SB)	72	0,62	No	Yes
SSDDIPPRW	Variola virus/Q9PXS3/58	326	5,00	72	4,16	Yes	No
KSDGTGTIY	SARS-like coronavirus/P0C6T7/4173	296	0.40 (SB)	78	0,59	Yes	Yes
RSADGSPPY	Mycobacterium tuberculosis/A4KJ56/29	296	0.08 (SB)	82	0,50	Yes	Yes
RTWNYHGSY	West Nile virus strain PTRoxo/A8KCE3/2831	0	0.08 (SB)	91	0,43	No	Yes
QTEENLLDF	NA	141	3,00	92	1,03	Yes	No
ALTDLGLIY	Lassa virus/Q9IMI9/201	63	0.15 (SB)	93	2,08	Yes	Yes
KSDLQPPNY	NA	104	1.00 (WB)	100	0,97	Yes	Yes
KMFHGGLRY	Mycobacterium tuberculosis/A4KLJ6/79	1	0.08 (SB)	105	0,18	No	Yes
VVAANRSAF	Mycobacterium tuberculosis/A4KJA4/104	78	3,00	109	0,23	Yes	No
AVEGGLYPV	NA	76	15,00	109	0,39	Yes	No
ETESVNSNY	Giardia lamblia/A8BQ55/260	79	2.00 (WB)	110	0,48	Yes	Yes
RTLASGLIY	Yersinia pestis/A6BRM7/395	4	0.05 (SB)	117	0,24	No	Yes
FLYPSWSLY	Cryptosporidium parvum Iowa II/Q5CTZ8/176	3	0.05 (SB)	122	0,34	No	Yes
YAQMWTLMY	Dengue virus type 3/P27915/3248	0	0.08 (SB)	140	0,56	No	Yes
FTYAPAGMY	Listeria monocytogenes/A3FVB4/508	0	0.01 (SB)	151	0,69	No	Yes
ATTFARFLY	Salmonella typhi/Q8Z4W4/505	0	0.10 (SB)	155	0,26	No	Yes
KTAVVVTRY	Yersinia enterocolitica/A1JJ64/43	5	0.05 (SB)	165	0,72	No	Yes
ASYAAAAAY	Artificially designed sequence	3	0.03 (SB)	174	0,31	No	Yes
ATAWRTGGY	Pseudomonas mallei/Q62HR4/293	0	0.05 (SB)	174	0,51	No	Yes
DTEDNVPPW	NA	114	32,00	196	0,79	Yes	No
YTASVVAAY	NA	7	0.01 (SB)	213	0,40	No	Yes
KVFFGPIYY	Variola virus/Q0N679/1007	0	0.05 (SB)	234	1,07	No	Yes
AVSFRNLAY	NA	0	0.05 (SB)	236	0,38	No	Yes
MSWESTAEY	Bacillus anthracis Tsiankovskii-I/B3J8I0/10	1	0.01 (SB)	261	0,54	No	Yes
YTSDYFISY	NA	8	0.01 (SB)	265	0,40	No	Yes
MSAIVSCRY	Salmonella typhi/Q8Z5E5/93	8	0.10 (SB)	268	0,36	No	Yes
KTFEWGVFY	Entamoeba histolytica/Q50Y27/4	8	0.01 (SB)	272	0,60	No	Yes
YTYPCIPEY	NA	8	0.01 (SB)	279	0,80	No	Yes
FTAMQALDY	Salmonella typhi/Q8Z404/38	3	0.08 (SB)	290	1,16	No	Yes
RTWFHGSLY	Cryptosporidium parvum Iowa II/Q5CQR9/77	0	0.01 (SB)	310	0,40	No	Yes
ESDMEVFDY	NA	241	2.00 (WB)	312	0,36	Yes	Yes
EISGSSARY	Yellow fever virus/Q9YRV3/1420	63	1.50 (WB)	324	ND	Yes	Yes
GSDGGLDDY	NA	100	2.00 (WB)	359	0,43	Yes	Yes
QTWHGDAPY	Vibrio parahaemolyticus/A6B1M3/64	0	0.08 (SB)	365	0,34	No	Yes
QTNLYNLLY	Salmonella typhi/Q8Z632/273	2	0.03 (SB)	380	3,05	No	Yes
ISAYTHWYY	Francisella tularensis subsp. Tularensis/A7JES6/146	6	0.05 (SB)	384	1,53	No	Yes
AMYDPQTYY	Rickettsia sibirica/Q7P8Y1/1874	2	0.05 (SB)	417	0,29	No	Yes

SLA-1*0401 peptide binding analysis

		Prediction Affinity/Rank					
Peptide amino acid sequence	Origin/Uniprot ID/Position	PSCPL matrix	NetMHCpan	Affinity (KD, nM)	Stability (T1/2, h)	Predicted by PSCPL matrix	Predicted by NetMHCpan
HSNASTLLY	NA	2	0.03 (SB)	507	ND	No	Yes
KSTDSESDW	NA	156	6,00	521	ND	Yes	No
YIFFASFYY	NA	0	0.08 (SB)	541	ND	No	Yes
RTWHYCGSY	NA	0	0.08 (SB)	546	ND	No	Yes
HMMAVTLFY	NA	2	0.03 (SB)	734	ND	No	Yes
YTFEPHYFY	NA	6	0.01 (SB)	823	ND	No	Yes
DSDDWLNKY	NA	102	5,00	1001	ND	Yes	No
ESSDDELPY	NA	82	1.50 (WB)	1117	ND	Yes	Yes
VSYAAAAAY	NA	2	0.03 (SB)	1200	ND	No	Yes
GTTEVNGLY	NA	0	0.08 (SB)	1293	ND	No	Yes
ITMVNSLTY	NA	8	0.01 (SB)	1375	ND	No	Yes
WVAGVQLLY	NA	4	0.08 (SB)	1950	ND	No	Yes
YANMWSLMY	NA	3	0.05 (SB)	2385	ND	No	Yes
VSALRLFNY	NA	92	0.40 (SB)	2429	ND	Yes	Yes
QTYMYTGQY	NA	0	0.05 (SB)	3098	ND	No	Yes
ITTFFTFAY	NA	0	0.03 (SB)	3134	ND	No	Yes
MTRGLLGSY	NA	0	0.15 (SB)	3248	ND	No	Yes
CTLNKSHLY	NA	1	0.08 (SB)	3831	ND	No	Yes
VTIGNAYIY	NA	5	0.10 (SB)	4233	ND	No	Yes
LTFLDCLYY	NA	1	0.05 (SB)	20000	ND	No	Yes
MTRVLPFTY	NA	1	0.15 (SB)	20000	ND	No	Yes
MTRGILGSY	NA	0	0.12 (SB)	20000	ND	No	Yes
YSYIFLSSY	NA	4	0.03 (SB)	20000	ND	No	Yes
VTRGAVLMY	NA	1	0.10 (SB)	20000	ND	No	Yes
STFTFPGIY	NA	0	0.05 (SB)	20000	ND	No	Yes
ATIMPHNLY	NA	9	0.08 (SB)	20000	ND	No	Yes
MTRVTNNVY	NA	0	0.25 (SB)	20000	ND	No	Yes
ITFQSILGY	NA	4	0.03 (SB)	20000	ND	No	Yes
FSIPVTFSY	NA	0	0.05 (SB)	20000	ND	No	Yes
ITAGYNRYY	NA	2	0.10 (SB)	20000	ND	No	Yes
MTAAQIRRY	NA	7	0.15 (SB)	20000	ND	No	Yes
SAYERGLRY	NA	3	0.05 (SB)	20000	ND	No	Yes
GSQYVSLAY	NA	1	0.08 (SB)	20000	ND	No	Yes
ASFAAQLFY	NA	5	0.03 (SB)	20000	ND	No	Yes
GTEYRLTLY	NA	191	0.25 (SB)	20000	ND	Yes	Yes
ESENISEPY	NA	83	2.00 (WB)	20000	ND	Yes	Yes
TTSDFFVNY	NA	105	0.08 (SB)	20000	ND	Yes	Yes
NQDLNGNWY	NA	93	15,00	20000	ND	Yes	No
MSDIFHALV	NA	98	0.80 (WB)	20000	ND	Yes	Yes
QSAANMYIY	NA	69	0.17 (SB)	20000	ND	Yes	Yes
LTMDREMLY	NA	66	0.01 (SB)	20000	ND	Yes	Yes
TSSARSSEW	NA	189	3,00	20000	ND	Yes	No
NMAPEKVDF	NA	76	32,00	20000	ND	Yes	No
LTAHYCFLY	NA	1	0.01 (SB)	20000	ND	No	Yes

Supporting Table 1 B

SLA-2*0401 peptide binding analysis

		Prediction Affinity/Rank					
Peptide amino acid sequence	Origin/Uniprot ID/Position	PSCPL matrix	NetMHCpan	Affinity (KD, nM)	Stability (T1/2, h)	Predicted by PSCPL matrix	Predicted by NetMHCpan
ASYQFQLPY	Vibrio cholerae/A6Y7B0/208	30	0.01 (SB)	18	51,00	Yes	Yes
MNYAAAAAY	NA	456	0.03 (SB)	22	131,70	Yes	Yes
YTIGIGAFY	NA	1	0.03 (SB)	25	10,80	No	Yes
SSLPSYAAY	SARS-like coronavirus/P0C6T7/3924	60	0.15 (SB)	30	1,70	Yes	Yes
IIYYQLAGY	Variola virus/Q0N4Z8/220	174	0.40 (SB)	38	1,30	Yes	Yes
ITLKVFAGY	Salmonella typhi/Q83T18/304	36	0.12 (SB)	44	22,00	Yes	Yes
MVASQLARY	Yersinia enterocolitica/A1JQV7/564	66	0.08 (SB)	56	3,90	Yes	Yes
MTRGLLGSY	West Nile virus strain PTRoxo/A8KCE3/1531	1	0.03 (SB)	72	1,00	No	Yes
MTAASYARY	NA	55	0.01 (SB)	75	3,80	Yes	Yes
QQYHRFGLY	Variola virus/Q89107/120	0	0.01 (SB)	116	0,50	No	Yes
YTASVVAAY	NA	4	0.01 (SB)	170	1,50	No	Yes
VSYAAAAAY	NA	89	0.03 (SB)	186	7,80	Yes	Yes
VSIPVTNTW	Brucella melitensis/Q9L772/174	37	2.00 (WB)	194	5,60	Yes	Yes
ESLLHQASW	Ebola virus/A3RCD1/57	89	4.00	195	93,00	Yes	No
FTFWTFANY	NA	7	0.01 (SB)	212	2,00	No	Yes
HTSALSLGY	Vibrio vulnificus/Q8DEM6/164	7	0.05 (SB)	219	2,90	No	Yes
YTSDYFISY	NA	7	0.03 (SB)	298	1,60	No	Yes
MVFQNYALY	Listeria monocytogenes/A3FZ93/80	5	0.01 (SB)	321	6,20	No	Yes
RSVWIPGRW	Pseudomonas mallei/Q62BF8/186	59	4.0	375	0,20	Yes	No
FTIRDVLAY	Yersinia enterocolitica/A1JNP9/275	2	0.03 (SB)	431	1,30	No	Yes
RVYNNTARY	NA	101	0.08 (SB)	525	ND	Yes	Yes
ESPSSDEDY	NA	47	32.00	718	ND	Yes	No
YSSPHLLRY	NA	51	0.03 (SB)	729	ND	Yes	Yes
KSWPAAIDW	NA	138	8.00	790	ND	Yes	No
SLRPNDIVY	NA	44	1.50 (WB)	1143	ND	Yes	Yes
ISRQIHWCW	NA	77	6.00	1464	ND	Yes	No

SLA-2*0401 peptide binding analysis

		Prediction Affinity/Rank					
Peptide amino acid sequence	Origin/Uniprot ID/Position	PSCPL matrix	NetMHCpan	Affinity (KD, nM)	Stability (T1/2, h)	Predicted by PSCPL matrix	Predicted by NetMHCpan
QTYMYTGQY	NA	9	0.01 (SB)	1713	ND	No	Yes
RYQAQQVEW	NA	108	8.00	1740	ND	Yes	No
YANMWSLMY	NA	1	0.01 (SB)	1829	ND	No	Yes
LTEAQDQFY	NA	119	3.00	2120	ND	Yes	No
YTITYHDDW	NA	46	5.00	2158	ND	Yes	No
YTNPQFNVY	NA	225	0.03 (SB)	2846	ND	Yes	Yes
ITMVNSLTY	NA	3	0.03 (SB)	3147	ND	No	Yes
DTRAIDQFF	NA	39	5.00	3652	ND	Yes	No
YSRMLYIEF	NA	48	1.00 (WB)	3654	ND	Yes	Yes
VTEPGTAQY	NA	102	1.50 (WB)	4093	ND	Yes	Yes
MLYPRVWPY	NA	1	0.03 (SB)	4427	ND	No	Yes
YTGPDHQEW	NA	1277	8.00	5198	ND	Yes	No
MMAWRMMRY	NA	4	0.01 (SB)	5323	ND	No	Yes
HTAEIQQFF	NA	35	0.80 (WB)	6677	ND	Yes	Yes
STFATVLEY	NA	1	0.01 (SB)	7274	ND	No	Yes
ATAVNQECW	NA	56	15.00	7405	ND	Yes	No
SSMNSDAAY	NA	83	0.40 (SB)	9871	ND	Yes	Yes
FAHDDRYLY	NA	0	0.05 (SB)	20000	ND	No	Yes
FQMDYSLEY	NA	1	0.03 (SB)	20000	ND	No	Yes
HQYPANLFY	NA	1	0.01 (SB)	20000	ND	No	Yes
YAYNSSLLY	NA	2	0.01 (SB)	20000	ND	No	Yes
FSSQLGLFY	NA	4	0.05 (SB)	20000	ND	No	Yes
MTRVTNNVY	NA	1	0.05 (SB)	20000	ND	No	Yes
HMMAVTLFY	NA	1	0.01 (SB)	20000	ND	No	Yes
MANIFRGSY	NA	2	0.05 (SB)	20000	ND	No	Yes
YAQMWSLMY	NA	0	0.03 (SB)	20000	ND	No	Yes
ISVQPLWEW	NA	54	6.00	20000	ND	Yes	No
MTAAQIRRY	NA	45	0.30 (SB)	20000	ND	Yes	Yes
FSVPLDEGF	NA	586	5.00	20000	ND	Yes	No
HSNLNDATY	NA	132	0.40 (SB)	20000	ND	Yes	Yes
STEPPMLNY	NA	44	1.00 (WB)	20000	ND	Yes	Yes
FGMPNPEGY	NA	622	2.00 (WB)	20000	ND	Yes	Yes
YSYIFLSSY	NA	39	0.01 (SB)	20000	ND	Yes	Yes
KSLDNYQEW	NA	45	6.00	20000	ND	Yes	No
RVYPNPEVY	NA	590	0.80 (WB)	20000	ND	Yes	Yes
SSVSSFERF	NA	50	3.00	20000	ND	Yes	No
VSRLEHQMW	NA	257	5.00	20000	ND	Yes	No
SAYYLDIGF	NA	39	1.50 (WB)	20000	ND	Yes	Yes
QTWHGDAPY	NA	48	0.25 (SB)	20000	ND	Yes	Yes
SSNPVMSRF	NA	73	0.80 (WB)	20000	ND	Yes	Yes
SSNAKNSEW	NA	43	5.00	20000	ND	Yes	No
KSAAIDGEY	NA	50	1.50 (WB)	20000	ND	Yes	Yes
MYADDTAGW	NA	44	5.00	20000	ND	Yes	No

Supporting Table 1 C

SLA-3*0401 peptide binding analysis

		Prediction Affinity/Rank					
Peptide amino acid sequence	Origin/Uniprot ID/Position	PSCPL matrix	NetMHCpan	Affinity (KD, nM)	Stability (T1/2, h)	Predicted by PSCPL matrix	Predicted by NetMHCpan
RNMSRIFPY	Encephalitozoon cuniculi/Q8SSE7/755	287	0.10 (SB)	1	6,70	Yes	Yes
RVFNNYMPY	SARS-CoV/Q19QX2/2140	85	0.01 (SB)	1	5,00	Yes	Yes
KRMMMNLNY	Rift valley fever virus/A2SZV2/1030	23	1.50 (WB)	4	1,10	No	Yes
RRMATTFTF	Variola virus/Q0NBG5/290	31	0.80 (WB)	4	1,10	Yes	Yes
RRARYWLTY	Giardia lamblia/A8BPJ1/256	43	0.50 (WB)	4	1,70	Yes	Yes
RAYRNALSM	Yellow fever virus/Q89318/36	34	0.03 (SB)	8	0,60	Yes	Yes
RARKRGITM	Mycobacterium tuberculosis/A4KI89/219	27	0.50 (WB)	11	0,30	Yes	Yes
KNNFWFWEY	Entamoeba histolytica/Q50ND6/107	169	0.80 (WB)	12	0,90	Yes	Yes
RRSRRSLTV	West Nile virus strain PTRoxo/A8KCE3/211	54	32,00	17	0,40	Yes	No
RIRAANLPI	Mycobacterium tuberculosis/A4KJM5/1391	28	3,00	17	0,20	Yes	No
KSFFSRLNW	Influenza A virus (A/Northern Ireland/44233/2003(H3N2))/genbank AY738729/55	21	0.30 (SB)	24	0,20	No	Yes
SARRRHLVF	Mycobacterium tuberculosis/A4KH94/44	40	0.40 (SB)	25	0,30	Yes	Yes
KRIRLKHIF	Cryptosporidium parvum Iowa II/Q5CXD6/25	40	6,00	27	1,40	Yes	No
YRFRFRSVY	Variola virus/Q9PXS7/740	38	1.00 (WB)	33	0,40	Yes	Yes
YSRPWNWTF	Giardia lamblia/A8BGW5/121	24	0.30 (SB)	35	0,50	No	Yes
RRFFPYYVY	NA	65	0.80 (WB)	39	0,30	Yes	Yes
RRRQWASCM	Salmonella typhimurium/P26474/262	27	15,00	40	0,40	Yes	No
TSFASSWIY	Rickettsia rickettsii/B0BWV4/130	44	0.40 (SB)	42	0,30	Yes	Yes
RVRRLNWAA	Pseudomonas mallei/Q62BN5/105	50	32,00	43	0,30	Yes	No
RRLHRLLLM	NA	187	1.50 (WB)	44	0,70	Yes	Yes
RMFKRVFNM	Yersinia pestis/A6BP81/183	43	0.03 (SB)	52	0,40	Yes	Yes
LNIMNKLNI	Variola virus/Q89231/129	46	32,00	89	0,20	Yes	No

SLA-3*0401 peptide binding analysis

		Prediction Affinity/Rank					
Peptide amino acid sequence	Origin/Uniprot ID/Position	PSCPL matrix	NetMHCpan	Affinity (Kᴅ, nM)	Stability (T1/2, h)	Predicted by PSCPL matrix	Predicted by NetMHCpan
MARWITWAM	Shigella flexneri/Q7UCA1/179	29	1.50 (WB)	122	0,20	Yes	Yes
KTLKGGWFF	Vibrio vulnificus/Q8DF54/110	31	0.25 (SB)	134	0,20	Yes	Yes
KSYEHQTPF	SARS-like coronavirus/P0C6T7/247	7	0.01 (SB)	137	0,30	No	Yes
KARARLLSM	Salmonella typhi/Q935J1/915	30	0.25 (SB)	302	0,20	Yes	Yes
RRFKYLLNV	Machupo virus/Q6XQI0/691	75	9,00	373	0,30	Yes	No
RRFNRTKPM	NA	75	6,00	554	ND	Yes	No
SRWSRKMLM	NA	37	50,00	912	ND	Yes	No
LNWFEIWIV	NA	60	50,00	1318	ND	Yes	No
RIYSHIAPY	NA	6	0.01 (SB)	1506	ND	No	Yes
RNNDPTLPY	NA	75	1.50 (WB)	1659	ND	Yes	Yes
GMFANRWII	NA	34	2.00 (WB)	2514	ND	Yes	Yes
RWFVRNPFF	NA	22	0.17 (SB)	3034	ND	No	Yes
RVFKETLFL	NA	27	0.80 (WB)	3758	ND	Yes	Yes
VTFWGFWLF	NA	23	0.25 (SB)	4911	ND	No	Yes
RTFDRFFEE	NA	31	32,00	20000	ND	Yes	No
RRVRRRVLV	NA	66	32,00	20000	ND	Yes	No
RLFFIDWEY	NA	55	0.25 (SB)	20000	ND	Yes	Yes
YTFFFTQYF	NA	27	0.20 (SB)	20000	ND	Yes	Yes
RSFRIHILF	NA	55	0.01 (SB)	20000	ND	Yes	Yes
RYFTVAFLF	NA	23	0.20 (SB)	20000	ND	No	Yes
TVFYNIPPM	NA	19	0.30 (SB)	20000	ND	No	Yes
RRRRRRAAL	NA	82	7,00	20000	ND	Yes	No
LSNFMLWQF	NA	44	4,00	20000	ND	Yes	No
RLRRRRHPL	NA	31	3,00	20000	ND	Yes	No
RVFYFAIFY	NA	38	0.05 (SB)	20000	ND	Yes	Yes
TTRHRKPTY	NA	30	10,00	20000	ND	Yes	No
SMFDSWGPF	NA	1	0.01 (SB)	20000	ND	No	Yes
SQYHRFPIY	NA	6	0.01 (SB)	20000	ND	No	Yes
YMIGYTAYY	NA	0	0.03 (SB)	20000	ND	No	Yes
RVYPNPEVY	NA	7	0.03 (SB)	20000	ND	No	Yes
AMYDPQTYY	NA	1	0.05 (SB)	20000	ND	No	Yes
FLYPSWSLY	NA	0	0.05 (SB)	20000	ND	No	Yes
RQHPGLFPF	NA	7	0.01 (SB)	20000	ND	No	Yes
VMFRNASEY	NA	6	0.03 (SB)	20000	ND	No	Yes
HQYPANLFY	NA	4	0.01 (SB)	20000	ND	No	Yes
YSYIFLSSY	NA	1	0.03 (SB)	20000	ND	No	Yes
ASYAAAAAY	NA	2	0.05 (SB)	20000	ND	No	Yes
VSYAAAAAY	NA	2	0.05 (SB)	20000	ND	No	Yes
YAYNSSLLY	NA	5	0.01 (SB)	20000	ND	No	Yes
RTLDTLALY	NA	3	0.03 (SB)	20000	ND	No	Yes
FQMDYSLEY	NA	3	0.03 (SB)	20000	ND	No	Yes
YTYATRGIY	NA	3	0.05 (SB)	20000	ND	No	Yes
RLYPFGSYY	NA	3	0.01 (SB)	20000	ND	No	Yes
HMMAVTLFY	NA	3	0.01 (SB)	20000	ND	No	Yes
GMFSWNLAY	NA	4	0.01 (SB)	20000	ND	No	Yes
SSMNSFLLY	NA	5	0.01 (SB)	20000	ND	No	Yes
RMFLAMITY	NA	10	0.01 (SB)	20000	ND	No	Yes
MQYLNPPPY	NA	7	0.01 (SB)	20000	ND	No	Yes
KMFHGGLRY	NA	6	0.01 (SB)	20000	ND	No	Yes
RLASYGLYY	NA	4	0.03 (SB)	20000	ND	No	Yes
ITMVNSLTY	NA	8	0.01 (SB)	20000	ND	No	Yes
MMHASTSPF	NA	1	0.01 (SB)	20000	ND	No	Yes

Supporting Table 1 A - C SLA-1, -2, and -3*0401 peptide prediction, affinity and stability analysis as well as successful predictions. Stability analysis (T½) was performed for peptides with a KD of 500 nM or less. Affinity (KD) is given in nano molar (nM). Stability (T½) periods are given in hours (h). NetMHCpan rank thresholds are 0.500 for strong binders (SB) and 2.00 for weak binders (WB). Peptides with NetMHCpan rank values above 2.00 were considered as predicted non-binders. PSCPL matrix scores were calculated as the multiplication of all RB values for each of the nine amino acids in the peptide. A matrix score threshold of >25 was set for peptides considered as PSCPL matrix predicted binders. Peptides with KD affinities of >500 nM are shaded (grey).
ND: Not Determined. NA: Not Assigned.

MHC molecule / total peptides tested	PSCPL Binding Matrix	Affinity Measures (K_D)	Stability Measures (T½)
SLA-1*0401 / 157 peptides	Determined by ELISA (Pedersen et al. 2011)	Determined by ELISA	Determined by SPA
SLA-2*0401 / 72 peptides	Determined by ELISA (Pedersen et al. 2012)	Determined by LOCI	Determined by SPA
SLA-3*0401 / 76 peptides	Determined by SPA	Determined by LOCI	Determined by SPA

Supporting Table 2 Methods used to determine the respective SLA heavy chain binding matrices as well as peptide affinities and stabilities. Enzyme-Linked Immunosorbent Assay (ELISA). Scintillation Proximity Assay (SPA). Luminiscent Oxygen Channeling Assay (LOCI).

6. Paper IV

Induction of foot-and-mouth disease virus-specific cytotoxic T cell killing by vaccination

Patch JR, Pedersen LE, Toka FN, Moraes M, Grubman MJ, Nielsen M, Jungersen G, Buus S, Golde W.T.

Clin Vaccine Immunol. 2011 Feb:18(2):280-8

The work presented in this manuscript addresses the potential induction of FMDV-specific $CD8^+$ CTLs as a result of vaccination against FMDV. We hypothesize that using a recombinant human adenovirus vector based vaccine, delivering FMDV antigens in a T cell-directed manner, would enhance cytolytic activity and effectively increase pSLA peptide concentration for stimulation of a CTL response.

The results confirm the hypothesis and show the induction of FMDV-specific CTLs capable of killing MHC-matched target cells. These data were further confirmed by specific SLA tetramer staining of activated PBMCs.

In this manuscript we present the first demonstration of FMDV-specific CTL killing and confirmation by MHC tetramer staining in response to vaccination against FMDV.

CLINICAL AND VACCINE IMMUNOLOGY, Feb. 2011, p. 280–288 Vol. 18, No. 2
1556-6811/11/$12.00 doi:10.1128/CVI.00417-10

Induction of Foot-and-Mouth Disease Virus-Specific Cytotoxic T Cell Killing by Vaccination▽§

Jared R. Patch,[1] Lasse E. Pedersen,[1,2,3] Felix N. Toka,[1] Mauro Moraes,[1] Marvin J. Grubman,[1] Morten Nielsen,[2] Gregers Jungersen,[2] Soren Buus,[3] and William T. Golde[1]*

Plum Island Animal Disease Center, Agricultural Research Service, USDA, Greenport, New York[1]; National Veterinary Institute and Center for Biological Sequence Analysis, Technical University of Denmark, Copenhagen, Denmark[2]; and Laboratory of Experimental Immunology, Faculty of Health Sciences, University of Copenhagen, Copenhagen, Denmark[3]

Received 28 September 2010/Returned for modification 5 November 2010/Accepted 10 December 2010

Foot-and-mouth disease (FMD) continues to be a significant threat to the health and economic value of livestock species. This acute infection is caused by the highly contagious FMD virus (FMDV), which infects cloven-hoofed animals, including large and small ruminants and swine. Current vaccine strategies are all directed toward the induction of neutralizing antibody responses. However, the role of cytotoxic T lymphocytes (CTLs) has not received a great deal of attention, in part because of the technical difficulties associated with establishing a reliable assay of cell killing for this highly cytopathic virus. Here, we have used recombinant human adenovirus vectors as a means of delivering FMDV antigens in a T cell-directed vaccine in pigs. We tested the hypothesis that impaired processing of the FMDV capsid would enhance cytolytic activity, presumably by targeting all proteins for degradation and effectively increasing the class I major histocompatibility complex (MHC)/FMDV peptide concentration for stimulation of a CTL response. We compared such a T cell-targeting vaccine with the parental vaccine, previously shown to effectively induce a neutralizing antibody response. Our results show induction of FMDV-specific $CD8^+$ CTL killing of MHC-matched target cells in an antigen-specific manner. Further, we confirm these results by MHC tetramer staining. This work presents the first demonstration of FMDV-specific CTL killing and confirmation by MHC tetramer staining in response to vaccination against FMDV.

Foot-and-mouth disease (FMD) is a highly infectious viral disease that affects cloven-hoofed animals and remains an important threat to livestock throughout much of the world (reviewed in reference 18). Many species of wild animals are susceptible to infection, but agricultural concerns are particularly focused on swine, cattle, sheep, and goats. This acute disease is characterized by fever and viremia that last 1 to 2 days, the formation of vesicular lesions in the mouth and on the feet and teats, lethargy, lameness, and loss of meat and milk production. Clinical signs of disease resolve within 7 to 10 days; however, an asymptomatic persistent infection (carrier state) can develop, particularly in previously vaccinated cattle (14, 17). The etiological cause of disease is FMD virus (FMDV), which has a single-stranded, positive-sense RNA genome of 8 kb. FMDV is a member of the *Picornaviridae* family, genus *Aphthovirus*. Following entry of the virus into the cell and uncoating, the released viral genome serves as an mRNA for the translation of viral proteins. Initially synthesized as a single polypeptide, the protein is subsequently cleaved by viral proteases, including leader (L^{pro}) and $3C^{pro}$, into mature structural and nonstructural proteins (53).

FMDV is highly cytopathic, and several viral proteins are known to play a role in disrupting the host immune response (reviewed in reference 19). L^{pro} cleaves the host translation initiation factor eIF4G, which plays a critical role in cap-dependent mRNA translation (12). An internal ribosomal entry site (IRES) in the 5′ untranslated region of the FMDV genome allows synthesis of viral proteins to continue while effectively shutting down host protein synthesis (2, 27). L^{pro} also promotes the degradation of NF-κB, a regulator of beta interferon (IFN-β) transcription (10). The combined actions of L^{pro} allow FMDV to block synthesis of the antiviral proteins IFN-α and -β, to which FMDV is sensitive (7, 9). In addition to the role of $3C^{pro}$ in cleaving the viral polyprotein into mature protein products, it has been shown to induce the cleavage of eIF4A and eIF4G (3). This protease has also been implicated in the cleavage of histone H3 (15, 54), thus further inhibiting host transcription and translation. In addition, both the precursor protein 2BC and the coexpressed mature products, 2B and 2C, are involved in disruption of the cellular secretory pathway (33, 34). Combined with the loss of host protein synthesis, this disruption of the secretory pathway appears to be responsible for inhibition of new MHC class I translation and surface expression in FMDV-infected cells (51).

The immunopathology of this acute infection includes a transient lymphopenia (1, 13). Viral infection was shown to lead to inhibition of the type I IFN response of multiple populations of dendritic cells (36, 37). *In vitro*, natural killer (NK) cells have been shown to lyse FMDV-infected cells (56). However, analysis of cells from FMDV-infected animals shows a loss of NK cell function during the acute phase of infection (55) (reviewed in reference 16).

The development of neutralizing antibodies plays a central

* Corresponding author. Mailing address: Plum Island Animal Disease Center, Agricultural Research Service, USDA, P.O. Box 848, Greenport, NY 11944. Phone: (631) 323-3249. Fax: (631) 323-3006. E-mail: william.golde@ars.usda.gov.

§ Supplemental material for this article may be found at http://cvi.asm.org/.

▽ Published ahead of print on 22 December 2010.

role in FMDV immunity and often correlates with protection of vaccinated animals against live virus challenge (32). Currently available vaccines consist of killed virus in adjuvant and are effective at providing protection but do not allow for the "differentiation of infected from vaccinated animals" (DIVA) (48). A leading candidate for a next-generation FMDV vaccine is a replication-defective human adenovirus 5 (Ad5) viral vector delivering FMDV capsid precursor (P1) and $3C^{pro}$, an "empty capsid" vaccine. This platform has DIVA capability and is very compatible with diagnostic tests in use at present. The parent polypeptide is processed by the $3C^{pro}$ into the protein components of the capsid (reviewed in references 20 and 48). This vaccine strategy is effective in swine (30, 31, 35) and cattle (39). However, like the killed-virus vaccine and natural infection, neutralizing antibodies raised against the vaccine strain do not provide cross-serotype protection. This limits the value of vaccination during an FMDV outbreak or in disease eradication (48), as virus strain matching is required for vaccine efficacy.

$CD8^+$ cytotoxic T lymphocytes (CTLs) play an important role in adaptive immunity and are capable of directly killing virus-infected cells in an antigen-specific manner through the release of perforin and granzymes as well as through Fas-Fas ligand interactions (reviewed in references 5 and 58). Unlike antibodies which recognize complex antigens, CTLs recognize antigens that have been processed and cleaved into 8- to 12-amino-acid peptides by the proteasome and then loaded into MHC class I molecules in the lumen of the endoplasmic reticulum (reviewed in reference 46). These peptide/MHC complexes are then transported to the surface of the infected cell, where they are displayed to T cell surveillance. CTL recognition occurs when an appropriate T cell receptor (TCR), in association with the CD8 molecule, stably binds to the peptide/MHC complex, resulting in stimulatory signaling cascades within the CTL (58). The ability of CTLs to recognize epitopes that remain hidden to neutralizing antibodies makes them attractive candidates for enhancing FMDV immunity.

In contrast to the focus on neutralizing antibodies, the role of CTLs in FMDV immunity has gone largely unexplored. The ability of the virus to inhibit MHC synthesis and transport and the speed with which the virus is cleared presumably result in limited antigen exposure for MHC class I-restricted T cells. In addition to the virus-induced lymphopenia, data from *in vitro* studies would predict that FMDV-specific CTLs are not elicited by natural FMDV infection if MHC class I expression is blocked *in vivo* as has been described *in vitro* (51). This would make FMDV-infected cells invisible to class I-restricted CTLs. Given the cytopathic nature of the virus, this hypothesis has gone largely untested, as FMDV-infected cells are rapidly lysed *in vitro* and cannot be used as target cells in assays for antigen-specific cell lysis.

We have overcome these limitations with two alternative approaches. First, we employed recombinant Ad5 FMDV vaccine technology as a method for delivering FMDV antigens to both stimulating and target cells for the *in vitro* CTL killing assay. Here, we describe our development of an assay using swine leukocyte antigen (SLA) homozygous pigs and the MHC-matched PK (15) cells as target cells. Second, in order to maximize the CTL response, we used a vaccine construct containing a mutation in $3C^{pro}$ that inhibits its ability to process P1 into mature capsids. This approach tests the hypothesis that one result of reduced processing of the primary polypeptide precursor would be an increase in the pool of FMDV proteins available for loading of FMDV-derived peptides into MHC class I molecules. This is then predicted to enhance stimulation of CTLs specific for FMDV peptides.

Further, to confirm that CTL killing was antigen specific and MHC restricted, we developed class I MHC tetramers using the NetMHCpan prediction algorithm developed for human class I MHC (38) and extended to other species, including swine (reference 25 and this report). Here we report that the T cell-targeting vaccine elicited a greater overall CTL killing response than the parental vaccine and correlated with the induction of FMDV-specific CTLs by MHC tetramer staining.

MATERIALS AND METHODS

Cell lines. Porcine kidney [PK(15)] cells (ATCC CCL-33) and PK(15)-EGFP cells (described below) were maintained in minimal essential medium (MEM) (Invitrogen, Carlsbad, CA) supplemented with 10% fetal bovine serum (FBS) (Thermo Fisher Scientific, Waltham, MA) and 3.4 mM L-glutamine, 3 mM dextrose, 1 mM sodium pyruvate, 5% sodium bicarbonate, nonessential and essential amino acids, 2-mercaptoethanol, and antibiotics (MEM-10). Baby hamster kidney (BHK-21) cells (ATCC CCL-10) were maintained in basal medium Eagle (BME) (Invitrogen, Carlsbad, CA) supplemented with 10% FBS, 10% tryptose phosphate broth, 2 mM L-glutamine, and antibiotics (BME-10). Human 293 cells (ATCC CRL-1573) were maintained in MEM supplemented with 10% FBS, 2 mM L-glutamine, and antibiotics. Peripheral blood mononuclear cells (PBMCs) were maintained in Roswell Park Memorial Institute (RPMI)-1640 medium (Invitrogen, Carlsbad, CA) supplemented with 10% FBS, 3.4 mM L-glutamine, 3 mM dextrose, 1 mM sodium pyruvate, 5% sodium bicarbonate, nonessential and essential amino acids, 2-mercaptoethanol, and antibiotics. IBRS2 (swine kidney) cells were maintained in MEM supplemented with 10% FBS, 2 mM L-glutamine, and antibiotics.

Animals. Yucatan 4b.0/4b.0 (24) pigs were obtained from Sinclair Research, Inc., Columbia, MO. Animals were held for at least 1 week before being entered into a study. All animal procedures were reviewed and approved by the Plum Island Institutional Animal Care and Use Committee.

Antibodies. A mouse monoclonal antibody (MAb) against porcine CD6, clone MIL8, was purchased from AbD Serotec (Raleigh, NC). Mouse MAbs against porcine CD8 (R-phycoerythrin [RPE], clone 76-2-11) and CD4 (fluorescein isothiocyanate [FITC], clone 74-12-4) were purchased from BD Biosciences (San Jose, CA). Monoclonal anti-FMDV-VP1 (clone 6HC4.1.3 [45]) and anti-VP2 (VP0) (clone F1412SA [57]) were used in combination to probe for Western blotting. In addition, a mixture of rabbit polyclonal antibodies raised against the FMDV capsid proteins (VP1, VP2, and VP3) were used for Western blotting (43). Anti-tubulin-α MAb was used for control staining of the Western blot (clone DM1A from Thermo Scientific, Fremont, CA).

Viruses. The production of viruses Ad5A24 (Ad5-FMDV-B), Ad5VSV-G (Ad5-VSV-G) (35), and Ad5-Blue (Ad5-Empty) (35) have been previously described. A mutation in the active site of the $3C^{pro}$ gene (21) was subcloned into pAd5-A24, replacing the parental, wild-type $3C^{pro}$, and was termed pAd5A24-3C-mut. Production of this new adenovirus, Ad5A24-3C-mut (Ad5-FMDV-T), was otherwise identical to that of the parental virus. All adenoviruses were grown in 293 cells. FMDV, strain A24 Cruzeiro, was propagated in BHK-21 cells.

Western blotting. IBRS2 cells were seeded in a 96-well microplate at 20,000 cells/well in 50 μl supplemented, phenol red-free MEM and incubated for 24 h at 37°C. Following attachment, cells were infected with adenovirus constructs at a multiplicity of infection (MOI) of 20, or with FMDV A24 at an MOI of 10, and then incubated for 24 h or 5 h, respectively. Whole-cell lysates were prepared, and protein expression was evaluated by separation by SDS-PAGE followed by Western blotting.

Vaccination. Six Yucatan 4b.0/4b.0 pigs were divided into two groups of three pigs each and vaccinated with either Ad5-FMDV-B or Ad5-FMDV-T. PBS was administered to one additional pig as a negative control. For both vaccination and boosting, animals were given a total of 5×10^9 PFU of the appropriate adenovirus. Virus was delivered intradermally in a total of 2 ml to four sites on the neck (0.5 ml/site) using the DERMA-VAC NF needle-free system (Merial, Duluth, GA). Pigs were boosted 12 weeks postvaccination and again 11 or 13 months postvaccination.

Isolation of PBMCs. Porcine blood was collected in Vacutainer tubes containing heparin. Typically, 20 ml of blood was diluted with 14 ml of phosphate-buffered saline (PBS), followed by the addition of a 12-ml underlay of Lymphoprep (Axis-Shield, Oslo, Norway), and then centrifuged at 1,000 × *g* for 20 min at room temperature. The band of peripheral blood mononuclear cells (PBMCs) was harvested and washed three times with PBS, followed by suspension in RPMI.

Stimulator/target cell preparation. PK(15) cells were chosen because they are MHC haplotype 4b.0/4.b0 (23), matching the MHC locus of the Yucatan swine under study. To prepare stimulator cells, PK(15) cells were seeded into 24-well plates and allowed to attach overnight. Cell medium was removed and cells were infected with adenovirus at an MOI of 10 in 0.2 ml of RPMI 1640 (nonsupplemented) for 1 h at 37°C with occasional rocking. For target cells, we developed PK(15)-EGFP cells. pEGFP-C1 (Clontec, Mountain View, CA) was linearized by digestion with PciI (New England BioLabs, Ipswich, MA) and transfected into PK(15) cells using the ProFection mammalian transfection system (Promega, Madison, WI). Stably transfected cells were selected by growth in the presence of Geneticin (500 μg/ml) (Invitrogen, Carlsbad, CA) and cloned by two rounds of limiting dilution. For the assay, 2×10^6 cells were infected with the appropriate virus at an MOI of 10 for 1 h in a low volume of MEM. Target cells were then given MEM-10 and incubated overnight at 37°C.

CD6$^+$ purification. PBMCs isolated from vaccinated pigs were suspended at a concentration of 10^7 cells/ml, and 1 ml was added to each well of infected PK(15) cells (typically 10 to 16 replicate wells), followed by the addition of 1 ml/well of RPMI 1640 (supplemented). Plates were incubated at 37°C for 3 to 5 days. Stimulated PBMCs were recovered from wells and reisolated on Lymphoprep in order to remove dead cells. To positively select CD6$^+$ cells, purified PBMCs were labeled with mouse anti-porcine CD6 MAb (1 μl/10^6 cells) followed by MACS goat anti-mouse IgG microbeads and separated on LS columns using a MidiMACS magnetic separator (Miltenyi Biotec, Gladbach, Germany), according to the manufacturer's instructions, resulting in approximately 95% CD6$^+$ cells (data not shown).

Cytotoxic T lymphocyte killing assay. *In vitro* expanded, CD6$^+$-enriched cells were suspended in supplemented RPMI 1640 at a concentration of 10^7 cells/ml, plated (100 μl/well) in a low-binding 96-well plate (Thermo Fisher Scientific, Waltham, MA), and diluted 2-fold to obtain final effector-to-target-cell (E:T) ratios of 50:1, 25:1, 12:1, and 6:1. Trypsinized PK(15)-EGFP target cells were suspended at 10^5 cells/ml and added to the effector cells (100 μl/well). In order to discriminate dead target cells from live cells, 5 μl of 7-amino-actinomycin D (7-AAD) (BD Biosciences, San Jose, CA) was added to each well. The plate was centrifuged at 233 × *g* for 1 min and then incubated at 37°C for 4 h. Following incubation, cells were resuspended and data were acquired by a FACSCalibur flow cytometer with a high-throughput sampler (HTS) (BD Biosciences, San Jose, CA). Data were analyzed using CellQuest Pro software (BD Biosciences, San Jose, CA) by gating on PK(15)-EGFP cells and determining the percentage of 7-AAD-positive (lysed) cells. Background lysis was determined by 7-AAD staining of target cells in the absence of effectors, and this percentage was subtracted from all groups.

Serum neutralization assay. Endpoint titers of serum neutralization of FMDV A24 were determined according to the procedure described by Pacheco and coworkers (40). Briefly, 4-fold serum dilutions were incubated at 37°C with 100 50% tissue culture infective doses ($TCID_{50}$) of FMDV serotype A24 for 1 h in a microtiter plate, after which BHK-21 cells were added (10^4 cells/well). Following incubation for 3 days, wells were scored for cytopathic effect and endpoint titers were calculated, which represent the reciprocal of the log dilution of serum able to neutralize 100 $TCID_{50}$ of virus.

Tetramer construction and staining. Peptides and recombinant SLA-1*0401 and human β_2-microglobulin (β_2m) were produced and complexed into tetramers as described previously (28) with minor modifications. Briefly, recombinant β_2m and peptides were added to 10-fold and 40-fold excesses, respectively, of SLA-1*0401 in a reaction buffer containing a cocktail of protease inhibitors [0.68 mM EDTA, 4.8 μM pepstatin A, 94.4 μM 1-10 phenanthroline, 0.1 mM *N*-ethylmaleimide, 8.9 μM tosyl-L-lysine chloromethyl ketone (TLCK), 9.3 μM tosyl-L-phenylalanine chloromethyl ketone (TPCK), 66.8 μM phenylmethylsulfonyl fluoride (PMSF)] followed by the addition of streptavidin-allophycocyanin (SA-APC). For tetramer staining, 2×10^5 to 5×10^5 cells were washed with cold FACS buffer (PBS, 0.3% bovine serum albumin, 0.1% sodium azide) and resuspended in solution containing tetramer previously mixed 1:1 with 2× FACS buffer. Cells were incubated at room temperature with rocking for 20 min and then washed three times in cold FACS buffer. Cells were resuspended in FACS buffer containing fluorescent MAbs against porcine CD8 and CD4 and then incubated at room temperature for 20 min. After being washed three times in FACS buffer, cells were fixed in PBS containing 1% formaldehyde and stored at 4°C until being analyzed by flow cytometry.

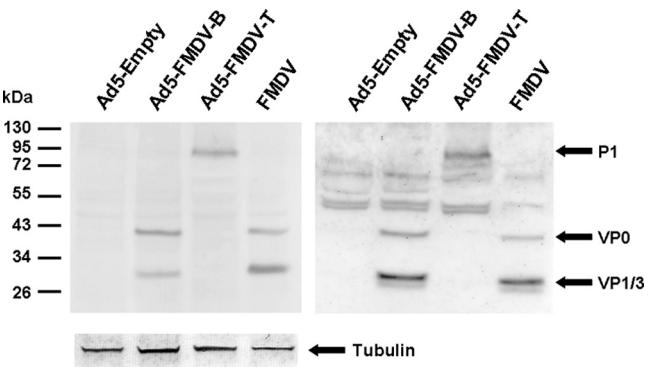

FIG. 1. Reduced capsid processing of Ad5-FMDV-T. IBRS2 cells were infected with the indicated virus as described in Materials and Methods. Following infection, cell lysates were made and proteins were separated by SDS-PAGE and visualized by Western blotting using either MAbs against VP2 (visualized as the VP0 precursor) and VP1 (left) or a mix of rabbit polyclonal antibodies against FMDV capsid proteins (right).

RESULTS

Mutation of FMDV 3C protease results in reduced capsid processing and production of anti-FMDV antibodies. Previous work by Moraes and coworkers demonstrated that vaccination of swine with Ad5A24 (Ad5-FMDV-B) resulted in the generation of a protective anti-FMDV antibody response (35). Mutation of the 3C protease resulting in an amino acid change (C163S) is known to inhibit processing of P1 into mature capsid proteins (21). A second adenovirus construct with the same P1 polyprotein derived from FMDV strain A24 and the mutated 3C protease was made, which we designate Ad5-FMDV-T. This construct was predicted to provide enhanced stimulation of a CTL response based on previous work that demonstrated a lack of antibody response to a similar construct made for FMDV strain A12 (31).

To demonstrate the reduced activity of 3C in this new construct, IBRS2 cells were infected with Ad5-FMDV-B, Ad5-FMDV-T, Ad5-Empty, or FMDV strain A24. Cell lysates were analyzed by SDS-PAGE followed by Western blotting. We detected the presence of P1 cleavage products VP0, VP3, and VP1 in the lysates of cells infected with either FMDV or Ad5-FMDV-B, with little or no P1 precursor (Fig. 1). In contrast, cells infected with Ad5-FMDV-T showed a significant decrease in the presence of VP0, VP3, and VP1, with significantly more unprocessed P1 (Fig. 1), suggesting a reduction of $3C^{pro}$ activity and consequent accumulation of P1.

Sera from pigs vaccinated and boosted with Ad5-FMDV-B and Ad5-FMDV-T were tested for FMDV neutralizing antibodies as described in Materials and Methods. All three pigs vaccinated with Ad5-FMDV-B generated neutralizing antibodies following priming, with elevated titers following two rounds of boosting (Fig. 2). In contrast, of the three pigs vaccinated with Ad5-FMDV-T, only p945 generated detectable neutralizing antibodies following priming. Both p945 and p947 had serum neutralizing antibodies following boost, with the titer for p947 remaining relatively low. Neutralizing antibodies were

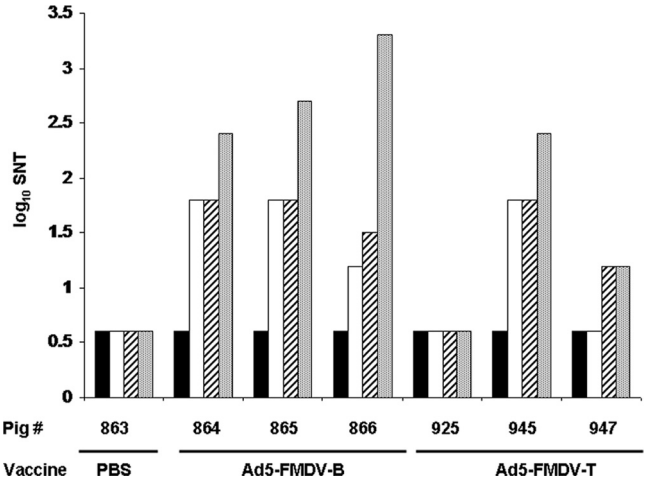

FIG. 2. Reduced neutralizing antibodies in Ad5-FMDV-T-vaccinated animals. Serum samples from pigs vaccinated with PBS, Ad5-FMDV-B, or Ad5-FMDV-T were collected before and following priming and boosting (solid bars, prevaccination; open bars, preboost; striped bars, pre-second boost; shaded bars, final). Serum neutralizing titers (SNT) were determined as described in Materials and Methods. Final serum was collected 26 days or more postboost.

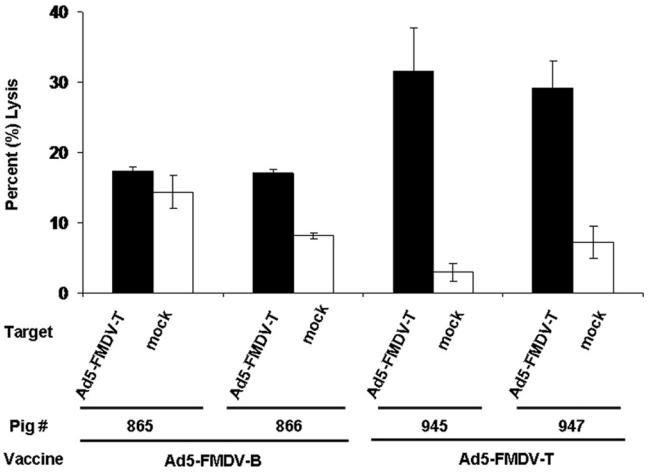

FIG. 3. Elevated CTL activity in Ad5-FMDV-T-vaccinated animals. PBMCs were isolated from vaccinated animals, stimulated in the presence of Ad5-FMDV-T-infected PK(15) cells for 5 days, and then assayed for cytolytic activity against Ad5-FMDV-T-infected or mock-infected target cells, as described in Materials and Methods. The mean and standard deviation of results for duplicate wells of an E:T ratio of 50:1 are shown.

never detected in serum from p925 or from the PBS negative control, p863. These data suggest that Ad5-FMDV-T is less effective than Ad5-FMDV-B at eliciting neutralizing antibodies, presumably due to less efficient processing of P1 by $3C^{pro}$.

Establishment of an FMDV CTL assay. The animals vaccinated with either Ad5-FMDV-T, Ad5-FMDV-B, or PBS were boosted 12 weeks postvaccination and analyzed. PBMCs were collected 24 days postboost and stimulated for 5 days in the presence of PK(15) cells infected with Ad5-FMDV-T and then tested for cytolytic activity against target cells that were either mock infected or infected with Ad5-FMDV-T. Consistent with our hypothesis, we observed the greatest antigen-specific cytolysis by cells derived from pigs vaccinated with Ad5-FMDV-T (Fig. 3). Due to low effector cell numbers, we were unable to evaluate the response against mock-infected cells for p864 and p925, and thus we omitted data from these two animals from Fig. 3. In spite of the observed elevation of antigen-specific cytolysis, with the exception of p945 we observed poor titration of target cell killing across several effector-to-target-cell (E:T) ratios (data not shown). A similar lack of titration of cytolysis by bulk PBMCs was previously observed by Denyer and coworkers, who demonstrated that purification of $CD6^+$ cells by positive selection prior to incubating with target cells resulted in titration of cytolytic activity across E:T ratios (11).

Based on this information, we enriched for $CD6^+$ cells following antigen stimulation in all further experiments, as described in Materials and Methods. PBMCs isolated from pigs vaccinated with Ad5-FMDV-T and enriched for CD6 expression exhibited enhanced cytolysis of Ad5-FMDV-T-infected target cells that titrated across E:T ratios, compared to mock or Ad5-Empty-infected cells (Fig. 4). The level of killing detected by this refined assay was slightly reduced, likely due to the elimination of NK cells from the responding population. The animal vaccinated with PBS showed no specific killing (see Fig. S1 in the supplemental material). In subsequent figures, we show the data for the 50:1 E:T ratio only, with the cytolysis of Ad5-Empty-infected cells subtracted from each group, though all four E:T ratios were always run. Finally, with this new assay, we tested the kinetics of the expansion culture over the course of 5 days and found that the highest level of killing,

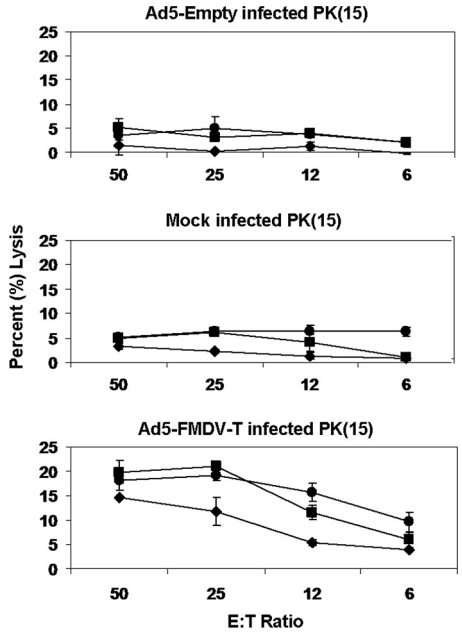

FIG. 4. Titration of $CD6^+$ CTL activity. PBMCs isolated from pigs vaccinated with Ad5-FMDV-T (◆, p925; ■, p945; ●, p947) were stimulated with Ad5-FMDV-T-infected cells for 3 days and then enriched for CD6 surface expression. Effector and target cells were mixed at E:T ratios of 50:1, 25:1, 12:1, and 6:1. Cytolysis of target cells was measured by flow cytometry with target cells mock infected or infected with Ad5-Empty or Ad5-FMDV-T. All error bars represent the standard deviation of results for duplicate wells.

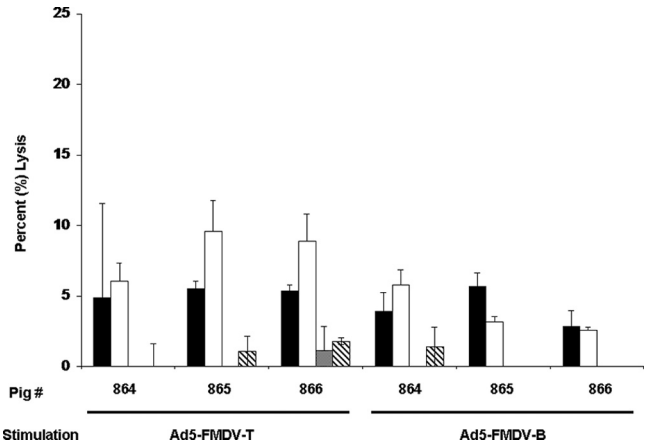

FIG. 5. Differential antigen stimulation. PBMCs from Ad5-FMDV-B-vaccinated pigs were isolated 4 days postboost and stimulated for 3 days with PK(15) cells infected with either Ad5-FMDV-T or Ad5-FMDV-B. Following $CD6^+$ purification, effector cells were assayed for cytolysis of target cells infected with Ad5-FMDV-T (solid bars), Ad5-FMDV-B (open bars), or Ad5-VSV-G (shaded bars) or mock-infected (striped bars) cells. Data are shown relative to Ad5-Empty. The mean and standard deviation of results for triplicate wells are indicated.

with minimum background, was detected on day 3 (data not shown), so all expansion cultures were done for 3 days.

Specificity of CTL cytolytic activity for FMDV P1. The development of this CTL assay was achieved with these vaccinated and boosted animals such that by 9 months following the first boost, antigen-specific cytolysis was difficult to detect, suggesting a waning of CTL immunity. Therefore, all pigs were boosted a second time with the vaccinating virus construct (p864 to p866 with Ad5-FMDV-B and p925, p945, and p947 with Ad5-FMDV-T) and activation of CTL killing was tracked using the assay.

In order to test the ability of the different adenovirus constructs to stimulate CTLs, PBMCs isolated from pigs 4 days after boosting with Ad5-FMDV-B were stimulated with cells infected with either Ad5-FMDV-B or Ad5-FMDV-T. Following enrichment for $CD6^+$ cells, the effector cells were mixed with target cells infected with either Ad5-FMDV-B, Ad5-FMDV-T, Ad5-Empty, or Ad5-VSV-G or mock infected. Ad5-VSV-G contains the gene for glycoprotein G of vesicular stomatitis virus, strain New Jersey (VSV-NJ), and served as a negative-control antigen. $CD6^+$ cells stimulated with Ad5-FMDV-B, compared to those stimulated with Ad5-FMDV-T, appeared to show less overall target cell killing, but there was no statistical difference between these groups (Fig. 5). Specificity for FMDV P1 was shown by little or no cytolysis of target cells infected with Ad5-VSV-G or mock infected (Fig. 5), eliminating the possibility that expression of any adenovirus-delivered transgene may contribute to cell lysis independent of antigen specificity.

Vaccine targeting T cells induces an enhanced CTL response. Following the second boost of animals, PBMCs were obtained on days 4, 8, 14, and 28 and CTL killing activity for each pig was assayed. Antigen-specific cytolysis remained low throughout the experiment in animals vaccinated with the Ad5-FMDV-B construct. In Fig. 6, a small rise in antigen-specific killing on day 4 after the second boost is apparent. Low CTL lysis was observed when analyzing cells taken the day of the boost or 8 and 14 days following the boost. These data suggest that Ad5-FMDV-B is a poor inducer of CTLs. Data from all time points are shown relative to Ad5-Empty, except for data for day 14, which are shown relative to Ad5-VSV-G because small numbers of effector cells isolated necessitated omitting mock and Ad5-Empty target groups.

PBMCs from pigs boosted with Ad5-FMDV-T and stimulated *ex vivo* with Ad5-FMDV-T-infected cells were tested for lysis of target cells infected with Ad5-FMDV-T, Ad5-Empty, or mock infected. In contrast to cells from the Ad5-FMDV-B-vaccinated animals, here we observed increased levels of antigen-specific cytolysis 4 days following the boost that waned to preboost levels by day 14 or 28 (Fig. 6). In all three animals, a high level of specific killing of PK(15) cells infected with the Ad5-FMDV-T construct was observed. Pig 925 had little killing activity 8 days after vaccine boost but good activity (equivalent to the day 4 result) when assayed 14 days after boost. This may indicate a technical problem with that day's sample from that animal (day 8, p925). As shown above, this animal (p925) showed no detectable neutralizing antibody either (Fig. 2). With that exception, the Ad5-FMDV-T-vaccinated animals had higher levels of target cell killing than the Ad5-FMDV-B-vaccinated animals through 14 days following the boost.

Animals vaccinated and boosted with Ad5-FMDV-T showed elevated mean killing of Ad5-FMDV-T-infected target cells compared to that of those vaccinated and boosted with Ad5-FMDV-B when cells isolated 4 days after the respective final boost were analyzed. This enhanced killing was statistically significant ($P < 0.05$; Fig. 7). As described above, the animal that was given PBS as a negative control never showed antigen-specific killing of target cells (see Fig. S1 in the supplemental material).

CTL cytolytic activity correlates with staining by an FMDV peptide-SLA-1 tetramer. In order to further characterize the effector cells, we developed pMHC tetramers for the SLA-1 molecule expressed by these animals, SLA-1*0401. The MHC class I peptide binding prediction algorithm NetMHCpan has previously been demonstrated to accurately capture the binding specificity of SLA class I molecules (25). Using this prediction method, we identified a peptide (MTAHITVPY) derived from the P1 capsid precursor of FMDV strain A24 that binds SLA-1*0401 at a low K_d (dissociation constant) (L. E. Pedersen, M. N. Harndahl, K. Lamberth, W. T. Golde, O. Lund, M. Nielsen, and S. Buus, unpublished data). As a negative control, a second SLA-1 tetramer was used that contained a peptide (ATAAATEAY) derived from the Ebola virus VP35 protein, which also binds to SLA-1*0401. For the experiments associated with the second boost (Fig. 6), a portion of the PBMCs isolated for evaluation of CTL killing were set aside for SLA-1 tetramer staining.

Cells were stained with antibodies specific for CD4 and CD8 and with the tetramers. Analysis by flow cytometry was carried out by gating on the $CD4^-/CD8^+$ cell population and determining the percentage of tetramer-positive ($tetramer^+$) cells (see Fig. S2 in the supplemental material). For pigs vaccinated with Ad5-FMDV-B, little tetramer staining was detected from samples taken 4 days following the second boost (Fig. 8) or thereafter (data not shown). This result correlated with low levels of cytolytic activity from the same samples (Fig. 6). In contrast, pigs vaccinated with Ad5-FMDV-T had a 2- to 3-fold

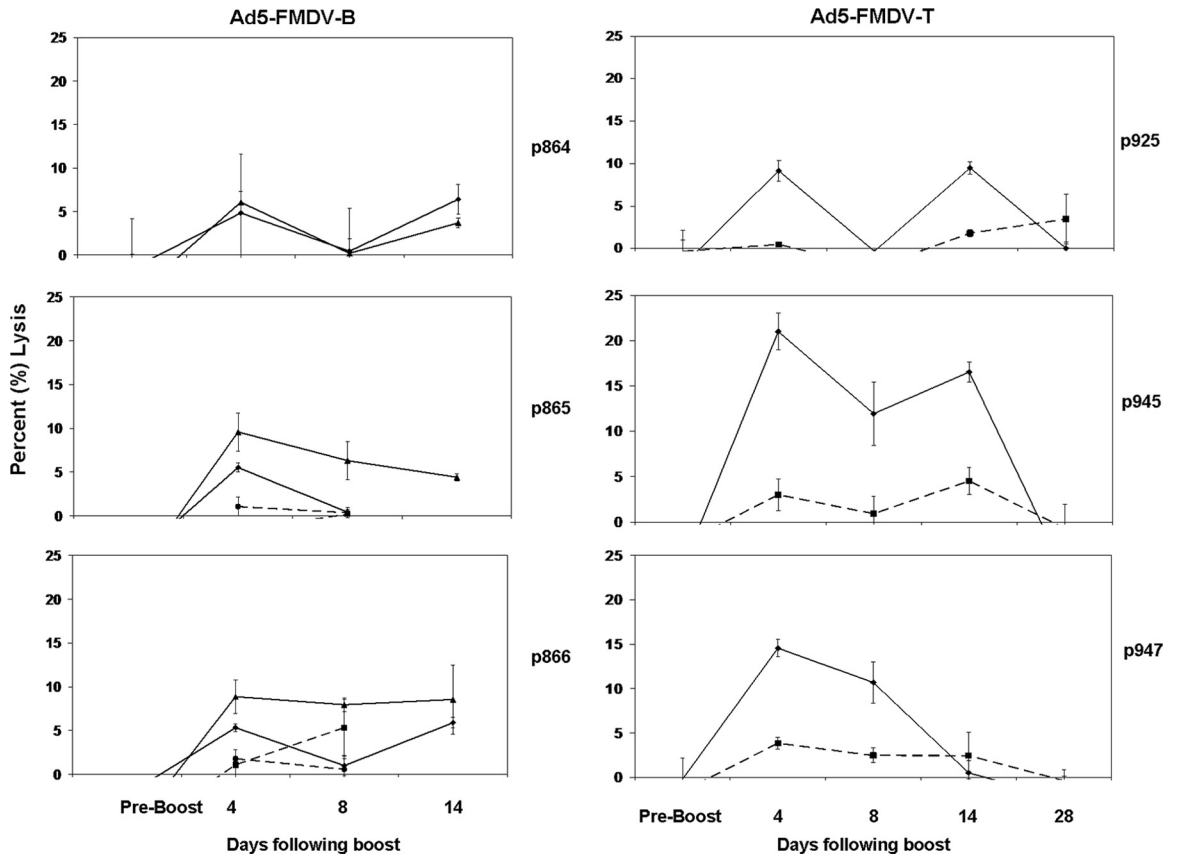

FIG. 6. CD6$^+$ CTL activity generated following second boost. PBMCs from Ad5-FMDV-B (p864, p865, and p866)- or Ad5-FMDV-T (p925, p945 and p947)-vaccinated pigs were isolated before and following boosting and treated as described in the legend to Fig. 5, except that only data from Ad5-FMDV-T secondary antigen stimulation are shown. Target cells: ◆, Ad5-FMDV-T; ■, mock. Additionally, pigs 864, 865, and 866 were tested on target cells: ▲, Ad5-FMDV-B; ●, Ad5-VSV-G. Data from all time points are shown relative to Ad5-Empty. Error bars represent the standard deviation of results for duplicate wells.

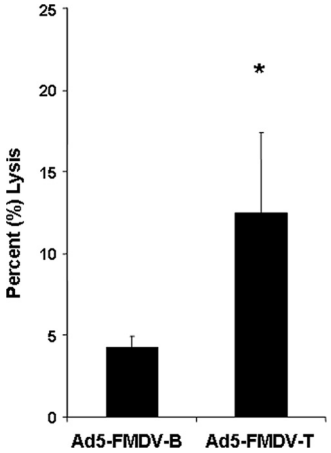

FIG. 7. CD6$^+$ CTL activity generated by Ad5-FMDV-T vaccination. Mean CTL cytolysis activity on day 4 following final boost of pigs vaccinated with Ad5-FMDV-B or Ad5-FMDV-T was determined after subtracting percentage of lysis of the highest negative-control target cell group from that of Ad5-FMDV-T target cells for each individual pig. Error bars represent the standard deviations ($n = 3$), and the asterisk indicates statistical significance ($P < 0.05$) as determined by an unpaired, one-tailed Student's t test with unequal variances.

increase, compared to preboost levels, in tetramer staining of the CD8$^+$ population isolated 4 days following the second boost (Fig. 8). Increased tetramer staining was correlated with peak cytolysis (compare Fig. 6 and Fig. 8) and was no longer detectable by 8 days after the boost. These data show that FMDV peptide MTAHITVPY is presented by SLA-1*0401 molecules *in vivo* and serve as confirmation of the presence of anti-FMDV, MHC-restricted CTLs.

A number of other peptides from the viral capsid precursor protein, P1, were also shown to bind the SLA-1 MHC class I protein. In addition, more peptides were identified that bind SLA-2 of these Yucatan pigs (SLA-2*040201) (L. E. Pedersen, M. Harndahl, M. Nielsen, J. R. Patch, G. Jungersen, S. Buus, and W. T. Golde, unpublished data). We also prepared tetramers from these combinations and tested them on CD8$^+$ T cells from the vaccinated pigs in this study. All of these tetramers were negative for staining cells taken 4 days after boost and all other time points tested. Only the SLA-1*0401/MTAHITVPY tetramer stained cells from the Ad5-FMDV-T vaccinated animals.

DISCUSSION

In the present study, we tested the ability of two nonreplicating adenovirus vectors to generate a CTL cytolytic response

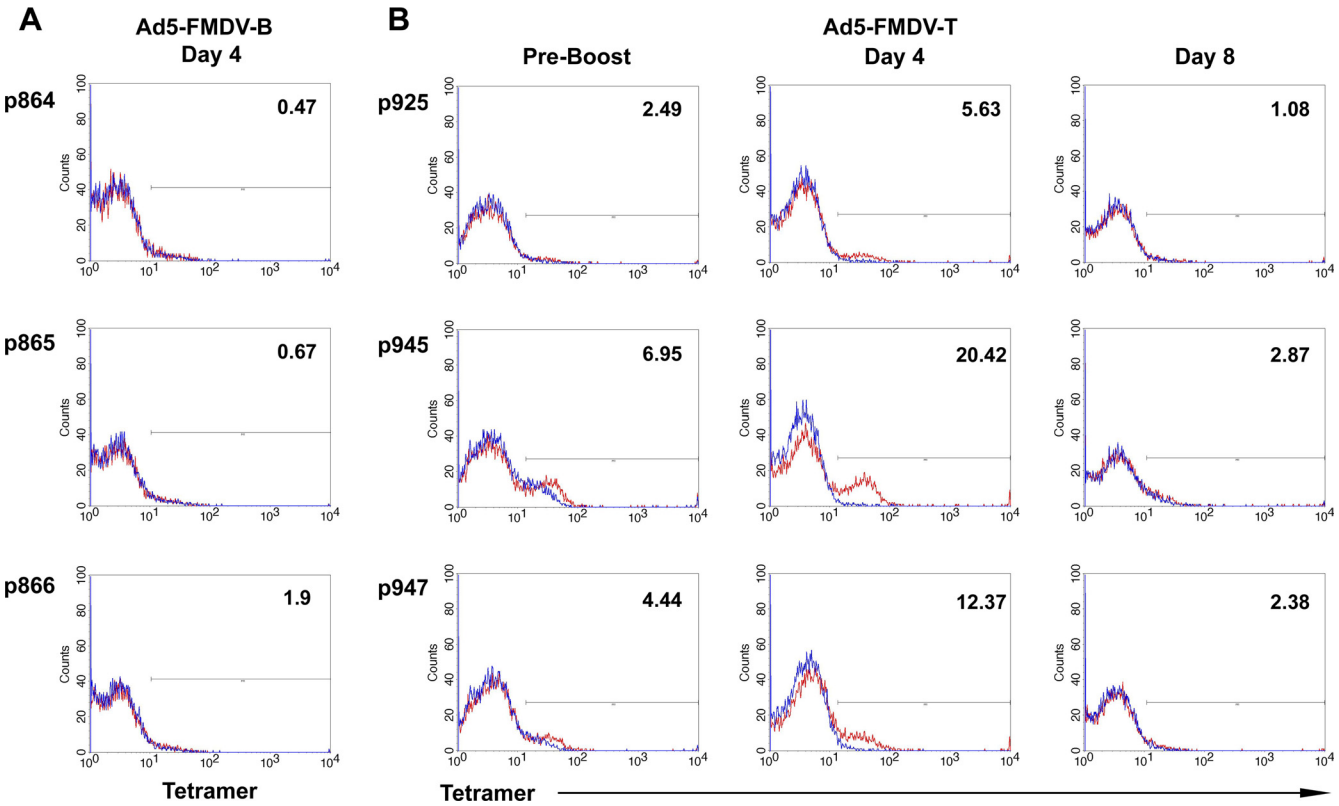

FIG. 8. Tetramer staining of $CD4^-/CD8^+$ CTLs. For time points shown in Fig. 6, PBMCs were stained with antibodies against CD4 and CD8 and costained with SLA-1*0401 tetramers bound to either an FMDV (red) or Ebola virus (blue) peptide. Histograms of tetramer-positive CTLs from Ad5-FMDV-B (A)- or Ad5-FMDV-T (B)-vaccinated animals are shown. Numbers indicate percent FMDV tetramer-positive cells from the $CD8^+$, $CD4^-$ gate and were calculated by subtracting the percentage of cells stained with the negative-control tetramer.

in swine to FMDV epitopes. The ability of this vaccine platform to induce the production of neutralizing antibodies to empty FMDV capsids in both swine (30, 31, 35, 43) and cattle (39) is well established. However, its ability to stimulate an antigen-specific CTL response has not been addressed. We hypothesized that the parental adenovirus-based empty capsid vaccine would provide relatively poor stimulation of CTLs because of the efficiency of capsid processing and formation. We reasoned that inhibited processing of FMDV P1 would enhance CTL activation, presumably as a result of enhanced degradation of P1 and subsequent loading of peptides onto class I MHC molecules. Swine were vaccinated with a T cell-directed adenovirus-based vaccine for FMDV (Ad5-FMDV-T), which contained a mutant $3C^{pro}$ that processes P1 poorly. The decreased processing of P1 by Ad5-FMDV-T was evident in Western blot analysis, as well as in the titers of virus-neutralizing antibodies in serum.

Whole PBMCs isolated from vaccinated animals demonstrated cytolytic activity against appropriate target cells. However, enriching for $CD6^+$ cells before mixing the effector and target cells improved the analysis of CTL activity. These results are in agreement with those of Denyer and coworkers, who demonstrated improved titration of antigen-specific, MHC-restricted cytolysis by enriching for the $CD6^+$ population of swine T cells (11). The $CD6^+$ cell population has been characterized as consisting of MHC-restricted CTLs and helper T cells, including $CD4^+/CD8^-$, $CD4^-/CD8^+$, and $CD4^+/CD8^+$ populations (8, 11, 41, 42, 49). Thus, an additional advantage of positively selecting for $CD6^+$ cells is the elimination of non-MHC-restricted cytolytic cells such as NK cells and γδ T cells, which do not express CD6 (44).

The MHC restriction of this CTL response was strongly supported by SLA-1 tetramer staining of cells derived from these animals. When peripheral blood cells derived from pigs vaccinated with Ad5-FMDV-T were analyzed, an increase in $tetramer^+/CD4^-/CD8^+$ cells was detected. The increase in tetramer-positive cells correlated with the peak of cytolytic activity, consistent with MHC-restricted cytolytic activity. We also noted that for pigs vaccinated with Ad5-FMDV-T, the relative tetramer staining of samples taken 4 days after the second boost correlates with the relative level of CTL killing activity. However, given the small number of animals in the group, this correlation is not statistically significant.

The enhanced cytolysis and tetramer staining of cells derived from pigs vaccinated with Ad5-FMDV-T relative to those vaccinated with Ad5-FMDV-B are supportive of our hypothesis that decreased capsid processing enhances CTL activity. However, it is possible that the precursor and mature capsid proteins are cleaved differently by the proteasome, resulting in a lack of MTAHITVPY peptides displayed in MHC molecules of the Ad5-FMDV-B-infected cells. This could explain why few tetramer-positive cells were detected in animals vaccinated with Ad5-FMDV-B. At minimum, this peptide from the C-terminal half of the VP2 region of P1 is not near the cleavage site at the

junction of VP2 and VP3. Differential tetramer staining cannot, therefore, be attributed to a loss of this peptide due to precursor cleavage by $3C^{pro}$.

Although CTLs play a central role in the adaptive immune response to intracellular antigens, their role in FMDV immunity has received little attention, in part because of the technical difficulties in establishing appropriate assays with which to measure their activity. In addition to the requirement for genetic matching of MHC class I alleles between effector and target cells, the cytopathic nature of FMDV has hampered development of a cytolytic assay. As a consequence, investigators have measured other biological properties of $CD8^+$ cells, such as proliferation (6, 26, 47, 50) or IFN-γ secretion (22), as proxies for CTL killing activity. The present report describes an alternative strategy for directly assessing CTL killing in response to FMDV antigens and relies on recombinant expression of FMDV proteins. In an earlier report, Li and coworkers described vaccination of swine with an attenuated pseudorabies virus containing a gene for the FMDV P1 capsid precursor that was effective at generating CTL killing activity (29). However, these investigators did not address MHC restriction, characterization of the cells responsible for killing, or antigen specificity of the reported CTL activity. In contrast, we now present data describing the first description of using MHC tetramers to identify antigen-specific CTLs in swine in general and the first time that anti-FMDV CTL killing in any livestock species has been correlated with tetramer staining.

Whether CTLs can play a significant role in FMDV protection and vaccination strategies remains to be determined. Previous work in swine found that a complete lack of capsid processing resulted in a failure to generate neutralizing antibodies, and challenged animals developed clinical signs comparable to those of unvaccinated animals (30, 31). However, the dose of vaccine used was more than a log lower than the dose used here. Reports using higher doses of a P1-based vaccine in swine resulted in partial protection in the absence of FMDV-specific antibodies (50). Similar results were obtained in cattle by the same investigators (52).

In vitro, FMDV inhibition of MHC class I surface expression begins in as little as 30 min postinfection (51). Thus, even under ideal conditions where anti-FMDV CTLs are primed and expanded, control of infection by CTLs depends on host cells infected by wild-type virus *in vivo* processing and displaying FMDV peptides leading to the CTL response before inhibition of new MHC class I protein expression is blocked by viral proteases. Although neutralizing antibodies are likely to remain the principal focus of FMDV vaccination, CTLs may be able to contribute to cross-serotype and subtype immunity because potential T cell epitopes are not limited to the structural proteins, where most of the immune-driven diversity is located (4). Whereas antibody epitopes are large and three dimensional, the T cell epitopes are linear and extremely small (8 to 12 amino acids) and have the potential to be highly conserved over the different serotypes of FMDV. Further work directed toward refining the induction and measuring of the CTL response, as well as evaluating protection from challenge, is needed to determine if induction of CTL immunity can yield protection across serotypes in diverse breeds of pigs and other species of interest, especially cattle.

ACKNOWLEDGMENTS

We thank Mary Kenney and Mital Pandya (Plum Island Animal Disease Center, ARS, USDA) for their support and assistance with these studies. We also thank staff of the Animal Resources Unit (Plum Island Animal Disease Center, DHS) for their professional work with the animals used in these experiments.

This work was funded by CRIS grant no. 1940-32000-052-00D from the Agricultural Research Service, USDA (W.T.G.). In addition, this work was partially cofunded by the Danish Council for Independent Research, Technology and Production Sciences grant no. 274-09-0281 (G.J.). L. E. Pedersen was the recipient of a Plum Island Animal Disease Center Research Participation Program fellowship, administered by the Oak Ridge Institute for Science and Education (ORISE) through an interagency agreement between the U.S. Department of Energy (DOE) and the U.S. Department of Agriculture (USDA).

REFERENCES

1. **Bautista, E. M., G. S. Ferman, and W. T. Golde.** 2003. Induction of lymphopenia and inhibition of T cell function during acute infection of swine with foot and mouth disease virus (FMDV). Vet. Immunol. Immunopathol. **92:**61–73.
2. **Belsham, G. J., and J. K. Brangwyn.** 1990. A region of the 5′ noncoding region of foot-and-mouth disease virus RNA directs efficient internal initiation of protein synthesis within cells: involvement with the role of L protease in translational control. J. Virol. **64:**5389–5395.
3. **Belsham, G. J., G. M. McInerney, and N. Ross-Smith.** 2000. Foot-and-mouth disease virus 3C protease induces cleavage of translation initiation factors eIF4A and eIF4G within infected cells. J. Virol. **74:**272–280.
4. **Carrillo, C., et al.** 2005. Comparative genomics of foot-and-mouth disease virus. J. Virol. **79:**6487–6504.
5. **Chavez-Galan, L., M. C. Arenas-Del Angel, E. Zenteno, R. Chavez, and R. Lascurain.** 2009. Cell death mechanisms induced by cytotoxic lymphocytes. Cell Mol. Immunol. **6:**15–25.
6. **Childerstone, A., L. Cedillo-Baron, M. Foster-Cuevas, and R. Parkhouse.** 1999. Demonstration of bovine CD8+ T-cell responses to foot-and-mouth disease virus. J. Gen. Virol. **80:**663–669.
7. **Chinsangaram, J., M. Koster, and M. J. Grubman.** 2001. Inhibition of L-deleted foot-and-mouth disease virus replication by alpha/beta interferon involves double-stranded RNA-dependent protein kinase. J. Virol. **75:**5498–5503.
8. **de Bruin, T. G., et al.** 2000. Discrimination of different subsets of cytolytic cells in pseudorabies virus-immune and naive pigs. J. Gen. Virol. **81:**1529–1537.
9. **de Los Santos, T., S. de Avila Botton, R. Weiblen, and M. J. Grubman.** 2006. The leader proteinase of foot-and-mouth disease virus inhibits the induction of beta interferon mRNA and blocks the host innate immune response. J. Virol. **80:**1906–1914.
10. **de Los Santos, T., F. Diaz-San Segundo, and M. J. Grubman.** 2007. Degradation of nuclear factor kappa B during foot-and-mouth disease virus infection. J. Virol. **81:**12803–12815.
11. **Denyer, M. S., T. E. Wileman, C. M. Stirling, B. Zuber, and H. H. Takamatsu.** 2006. Perforin expression can define CD8 positive lymphocyte subsets in pigs allowing phenotypic and functional analysis of natural killer, cytotoxic T, natural killer T and MHC un-restricted cytotoxic T-cells. Vet. Immunol. Immunopathol. **110:**279–292.
12. **Devaney, M. A., V. N. Vakharia, R. E. Lloyd, E. Ehrenfeld, and M. J. Grubman.** 1988. Leader protein of foot-and-mouth disease virus is required for cleavage of the p220 component of the cap-binding protein complex. J. Virol. **62:**4407–4409.
13. **Diaz-San Segundo, F., et al.** 2006. Selective lymphocyte depletion during the early stage of the immune response to foot-and-mouth disease virus infection in swine. J. Virol. **80:**2369–2379.
14. **Doel, T. R., L. Williams, and P. V. Barnett.** 1994. Emergency vaccination against foot-and-mouth disease: rate of development of immunity and its implications for the carrier state. Vaccine **12:**592–600.
15. **Falk, M. M., et al.** 1990. Foot-and-mouth disease virus protease 3C induces specific proteolytic cleavage of host cell histone H3. J. Virol. **64:**748–756.
16. **Golde, W. T., C. K. Nfon, and F. N. Toka.** 2008. Immune evasion during foot-and-mouth disease virus infection of swine. Immunol. Rev. **225:**85–95.
17. **Golde, W. T., et al.** 2005. Vaccination against foot-and-mouth disease virus confers complete clinical protection in 7 days and partial protection in 4 days: use in emergency outbreak response. Vaccine **23:**5775–5782.
18. **Grubman, M. J., and B. Baxt.** 2004. Foot-and-mouth disease. Clin. Microbiol. Rev. **17:**465–493.
19. **Grubman, M. J., M. P. Moraes, F. Diaz-San Segundo, L. Pena, and T. de los Santos.** 2008. Evading the host immune response: how foot-and-mouth disease virus has become an effective pathogen. FEMS Immunol. Med. Microbiol. **53:**8–17.

20. **Grubman, M. J., et al.** 2010. Adenovirus serotype 5-vectored foot-and-mouth disease subunit vaccines: the first decade. Future Virol. **5:**51–64.
21. **Grubman, M. J., M. Zellner, G. Bablanian, P. W. Mason, and M. E. Piccone.** 1995. Identification of the active-site residues of the 3C proteinase of foot-and-mouth disease virus. Virology **213:**581–589.
22. **Guzman, E., G. Taylor, B. Charleston, M. A. Skinner, and S. A. Ellis.** 2008. An MHC-restricted CD8+ T-cell response is induced in cattle by foot-and-mouth disease virus (FMDV) infection and also following vaccination with inactivated FMDV. J. Gen. Virol. **89:**667–675.
23. **Ho, C. S., M. H. Franzo-Romain, Y. J. Lee, J. H. Lee, and D. M. Smith.** 2009. Sequence-based characterization of swine leucocyte antigen alleles in commercially available porcine cell lines. Int. J. Immunogenet. **36:**231–234.
24. **Ho, C. S., et al.** 2009. Nomenclature for factors of the SLA system, update 2008. Tissue Antigens **73:**307–315.
25. **Hoof, I., et al.** 2009. NetMHCpan, a method for MHC class I binding prediction beyond humans. Immunogenetics **61:**1–13.
26. **Joshi, G., R. Sharma, and N. K. Kakker.** 2009. Phenotypic and functional characterization of T-cells and in vitro replication of FMDV serotypes in bovine lymphocytes. Vaccine **27:**6656–6661.
27. **Kuhn, R., N. Luz, and E. Beck.** 1990. Functional analysis of the internal translation initiation site of foot-and-mouth disease virus. J. Virol. **64:**4625–4631.
28. **Leisner, C., et al.** 2008. One-pot, mix-and-read peptide-MHC tetramers. PLoS One **3:**e1678.
29. **Li, X., et al.** 2008. Induction of protective immunity in swine by immunization with live attenuated recombinant pseudorabies virus expressing the capsid precursor encoding regions of foot-and-mouth disease virus. Vaccine **26:**2714–2722.
30. **Mayr, G. A., J. Chinsangaram, and M. J. Grubman.** 1999. Development of replication-defective adenovirus serotype 5 containing the capsid and 3C protease coding regions of foot-and-mouth disease virus as a vaccine candidate. Virology **263:**496–506.
31. **Mayr, G. A., V. O'Donnell, J. Chinsangaram, P. W. Mason, and M. J. Grubman.** 2001. Immune responses and protection against foot-and-mouth disease virus (FMDV) challenge in swine vaccinated with adenovirus-FMDV constructs. Vaccine **19:**2152–2162.
32. **McCullough, K. C., et al.** 1992. Relationship between the anti-FMD virus antibody reaction as measured by different assays, and protection in vivo against challenge infection. Vet. Microbiol. **30:**99–112.
33. **Moffat, K., et al.** 2005. Effects of foot-and-mouth disease virus nonstructural proteins on the structure and function of the early secretory pathway: 2BC but not 3A blocks endoplasmic reticulum-to-Golgi transport. J. Virol. **79:**4382–4395.
34. **Moffat, K., et al.** 2007. Inhibition of the secretory pathway by foot-and-mouth disease virus 2BC protein is reproduced by coexpression of 2B with 2C, and the site of inhibition is determined by the subcellular location of 2C. J. Virol. **81:**1129–1139.
35. **Moraes, M. P., G. A. Mayr, P. W. Mason, and M. J. Grubman.** 2002. Early protection against homologous challenge after a single dose of replication-defective human adenovirus type 5 expressing capsid proteins of foot-and-mouth disease virus (FMDV) strain A24. Vaccine **20:**1631–1639.
36. **Nfon, C. K., G. S. Ferman, F. N. Toka, D. A. Gregg, and W. T. Golde.** 2008. Interferon-alpha production by swine dendritic cells is inhibited during acute infection with foot-and-mouth disease virus. Viral Immunol. **21:**68–77.
37. **Nfon, C. K., F. N. Toka, M. Kenney, J. M. Pacheco, and W. T. Golde.** 2010. Loss of plasmacytoid dendritic cell function coincides with lymphopenia and viremia during foot-and-mouth disease virus infection. Viral Immunol. **23:**29–41.
38. **Nielsen, M., et al.** 2007. NetMHCpan, a method for quantitative predictions of peptide binding to any HLA-A and -B locus protein of known sequence. PLoS One **2:**e796.
39. **Pacheco, J. M., M. C. Brum, M. P. Moraes, W. T. Golde, and M. J. Grubman.** 2005. Rapid protection of cattle from direct challenge with foot-and-mouth disease virus (FMDV) by a single inoculation with an adenovirus-vectored FMDV subunit vaccine. Virology **337:**205–209.
40. **Pacheco, J. M., et al.** 2010. IgA antibody response of swine to foot-and-mouth disease virus infection and vaccination. Clin. Vaccine Immunol. **17:**550–558.
41. **Pauly, T., et al.** 1995. Classical swine fever virus-specific cytotoxic T lymphocytes and identification of a T cell epitope. J. Gen. Virol. **76**(pt. 12)**:**3039–3049.
42. **Pauly, T., et al.** 1996. Differentiation between MHC-restricted and non-MHC-restricted porcine cytolytic T lymphocytes. Immunology **88:**238–246.
43. **Pena, L., et al.** 2008. Delivery of a foot-and-mouth disease virus empty capsid subunit antigen with nonstructural protein 2B improves protection of swine. Vaccine **26:**5689–5699.
44. **Piriou-Guzylack, L., and H. Salmon.** 2008. Membrane markers of the immune cells in swine: an update. Vet. Res. **39:**54.
45. **Robertson, B. H., D. O. Morgan, and D. M. Moore.** 1984. Location of neutralizing epitopes defined by monoclonal antibodies generated against the outer capsid polypeptide, VP1, of foot-and-mouth disease virus A12. Virus Res. **1:**489–500.
46. **Rock, K. L., D. J. Farfan-Arribas, and L. Shen.** 2010. Proteases in MHC class I presentation and cross-presentation. J. Immunol. **184:**9–15.
47. **Rodriguez, A., et al.** 1996. A porcine CD8+ T cell clone with heterotypic specificity for foot-and-mouth disease virus. J. Gen. Virol. **77**(pt. 9)**:**2089–2096.
48. **Rodriguez, L. L., and M. J. Grubman.** 2009. Foot and mouth disease virus vaccines. Vaccine **27**(suppl. 4)**:**D90–D94.
49. **Saalmuller, A., T. Pauly, B. J. Hohlich, and E. Pfaff.** 1999. Characterization of porcine T lymphocytes and their immune response against viral antigens. J. Biotechnol. **73:**223–233.
50. **Sanz-Parra, A., et al.** 1999. Recombinant viruses expressing the foot-and-mouth disease virus capsid precursor polypeptide (P1) induce cellular but not humoral antiviral immunity and partial protection in pigs. Virology **259:**129–134.
51. **Sanz-Parra, A., F. Sobrino, and V. Ley.** 1998. Infection with foot-and-mouth disease virus results in a rapid reduction of MHC class I surface expression. J. Gen. Virol. **79**(pt. 3)**:**433–436.
52. **Sanz-Parra, A., et al.** 1999. Evidence of partial protection against foot-and-mouth disease in cattle immunized with a recombinant adenovirus vector expressing the precursor polypeptide (P1) of foot-and-mouth disease virus capsid proteins. J. Gen. Virol. **80**(pt. 3)**:**671–679.
53. **Stanway, G., et al.** 2005. Virus taxonomy: classification and nomenclature of viruses: eighth report of the International Committee on the Taxonomy of Viruses. Elsevier Academic Press, San Diego, CA.
54. **Tesar, M., and O. Marquardt.** 1990. Foot-and-mouth disease virus protease 3C inhibits cellular transcription and mediates cleavage of histone H3. Virology **174:**364–374.
55. **Toka, F. N., C. Nfon, H. Dawson, and W. T. Golde.** 2009. Natural killer cell dysfunction during acute infection with foot-and-mouth disease virus. Clin. Vaccine Immunol. **16:**1738–1749.
56. **Toka, F. N., C. K. Nfon, H. Dawson, D. M. Estes, and W. T. Golde.** 2009. Activation of porcine natural killer cells and lysis of foot-and-mouth disease virus infected cells. J. Interferon Cytokine Res. **29:**179–192.
57. **Yang, M., A. Clavijo, R. Suarez-Banmann, and R. Avalo.** 2007. Production and characterization of two serotype independent monoclonal antibodies against foot-and-mouth disease virus. Vet. Immunol. Immunopathol. **115:**126–134.
58. **Yewdell, J. W., and S. M. Haeryfar.** 2005. Understanding presentation of viral antigens to CD8+ T cells in vivo: the key to rational vaccine design. Annu. Rev. Immunol. **23:**651–682.

7. SLA Tetramers

The identification of peptides strongly bound by SLA molecules, and producing stable pSLA complexes, was performed in regard to (i) achieving knowledge about the individual SLA binding profiles, and (ii) producing stable pSLA complex based tetramers for staining of porcine PBMCs.

7.1. FMDV TETRAMER STAINING

pSLA tetramer studies were performed at PIADC as part of this PhD project using FMDV derived peptides, followed by staining of PBMCs isolated from six animals previously vaccinated and boosted against FMDV. These studies resulted in the identification of an FMDV T cell epitope (Figure 13). General results and findings of the overall study are fully discussed in Paper IV, and presents the first demonstration of FMDV-specific CTL killing of infected porcine kidney (PK15) cells with confirmation by SLA allele matched tetramer staining.

My primary focus will be on the tetramer part of the studies presented in Paper IV, in that it constitutes a general section of the overall PhD project. Hence, the killing analysis and results are only briefly discussed.

To date the role of CTLs in FMDV immunity has gone largely unexplored partly due to the role of neutralizing Abs been proven dominating in the establishment of protection against the virus as described above. Furthermore, the ability of the virus to inhibit MHC synthesis and transport to the surface has previously been described *in vitro* (Sanz-Parra et al. 1998). The inhibited MHC synthesis and transport combined with the virus-induced lymphopenia, predict FMDV-specific CTLs to play a minor role in clearing natural FMDV infection, if the MHC class I expression is as well obstructed *in vivo*. Further complicating the analysis of specific CTLs and their role during FMDV infection is that FMDV infected cells are rapidly lysed *in vitro*, and hence cannot be used as targets in assays for antigen-specific cell lysis.

We developed an assay using available strains of pigs homozygous for SLA-1*0401, -2*0401, and -3*0401. Further, the porcine fibroblast cell line, PK15, cells are a genetic match to the SLA class I genes expressed in these pigs and thus are appropriate targets for the *in vitro* killing

assay. Using the replication defective Ad5 virus vector expressing FMDV P1 protein, we were able to infect PK15 target cells without lysis and thus test CTLs from vaccinated, MHC matched pigs for killing of the infected PK15 cells. A vaccine construct containing a mutation in the protease $3C^{pro}$ (Ad5-FMDV-T) enabled us to test a hypothesis that an increase in the intracellular pool of FMDV proteins available for degradation and loading of FMDV-derived peptides into SLA class I molecules would enhance stimulation of FMDV peptide specific CTLs. To confirm that the observed CTL induced killing was antigen specific, and MHC restricted, FMDV pSLA complex based tetramers were produced and used to stain PBMCs isolated from the vaccinated animals at identical time points post vaccine boost as for the PBMCs used to kill infected PK15 targets. A comparison of animals vaccinated using the Ad5-FMDV-T vaccine with animals vaccinated with a $3C^{pro}$ *intact* vaccine (Ad5-FMDV-B) was performed, to verify the hypothesis of enhanced CTL stimulation due to inactive $3C^{pro}$ (Figure 13 A versus B, Day 4).

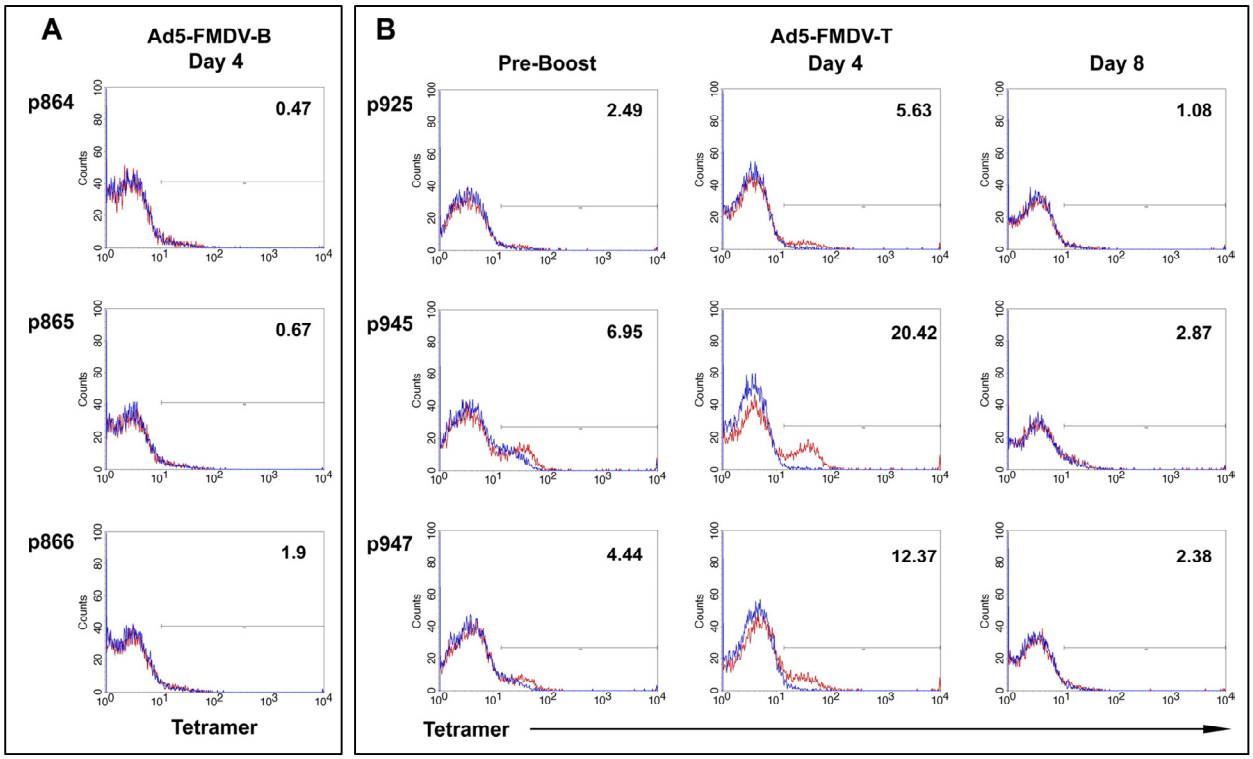

Figure 13. Tetramer staining of $CD8^{+}CD4^{-}$ PBMCs using two tetramers produced with either an FMDV (red) or *Ebola* (blue) virus-derived peptide. Histograms of tetramer stained $CD8^{+}CD4^{-}$ PBMCs from Ad5-FMDV-B (**A**) or Ad5-FMDV-T (**B**) –vaccinated animals are shown. Numbers indicate the individual percentage FMDV tetramer positive cells within the $CD8^{+}CD4^{-}$ population of PBMCs after subtracting the percentage of cells stained with the negative-control *Ebola*-tetramer. The figure shows responses for three Ad5-FMDV-B vaccinated pigs (p864, 865, 866) and three Ad5-FMDV-T vaccinated pigs (p925, 945, 947). The figure is taken from Paper IV of this thesis.

As illustrated in Figure 13, animals vaccinated with the Ad5-FMDV-T construct stained clearly positive with tetramer at day 4 post vaccine boost (Figure 13B), whereas the Ad5-FMDV-B vaccinated animals showed no staining for samples taken at the same time point (Figure 13A). Similar staining was seen for the Ad5-FMDV-B vaccinated group of animals pre-boost and on day 8 (not shown). These data confirm the hypothesis stated above and classifies the Ad5-FMDV-T construct as a CTL inducing vaccination approach against FMDV, and identify the FMDV derived peptide of the positive tetramer (MTAHITVPY) as a CTL epitope capable of being recognized by a significant number of activated CTLs within the $CD8^{+}CD4^{-}$ population (ranging from 5.63 – 20.42 % between different animals). An increase in tetramer staining in the scale of 2- to 3-fold was seen for Ad5-FMDV-T vaccinated animals on day 4 post boost as compared to pre-boost levels (Figure 13B) and correlated with peak cytolysis of adenovirus infected PK15 target cells observed at day 4 post boost (Figure 6, Paper IV). In a previous study performed in cattle, it was found that bovine leukocyte antigen (BoLA) class II tetramers (DRB3*1201-P16-7) positively stained between 10 and 15.5 % of bovine $CD4^{+}$ T cells derived from cattle previously immunized once (Norimine et al. 2006). Instead of boosting their animals with antigen, Norimine et al. used *in vitro* stimulation of positively selected $CD4^{+}$ lymphocytes for one week with peptide P16-7 to achieve proliferation of the peptide specific cell population. We observed a decrease in cytolysis and absence of positive tetramer staining at day 8 post boost (Figure 13B and Paper IV, Figure 6), which might be an indication of the dose and duration of the Ad5 antigen expression not being efficient enough to create a durable response for longer periods without further boosting. A certain level of pre-boost staining was observed for p945 and p947 (Figure 13B) which was likely due to previous vaccination of the animals followed by a primary boost 12 weeks post vaccination. The tetramer staining presented in Figure 13 was performed following a second boost at 11 (FMDV-T) and 13 (FMDV-B) months post vaccination. Altogether these data serve as confirmation of the presence of anti-FMDV, SLA-restricted CTLs and illustrate the ability of the methods, developed in this project to fit the porcine model, in the identification of CTL epitopes and monitoring of immune responses induced by vaccination.

7.2. INFLUENZA TETRAMER STAINING

Approaching the end of the PhD project, having established in-house SLA molecules with several identified high affinity peptide binders derived from Influenza along with the tools available to specifically monitor activated porcine CTLs, I got the opportunity to get fresh blood samples from 20 animals which were part of another project. These animals had been immunized five times against swine influenza A with three week intervals. Unfortunately, once I got knowledge about their existence they had just received their fifth and final immunization and faced elimination. Hence I only had one chance to try and identify any influenza epitopes.

The animals had received chemically ($C_3H_4O_2$) inactivated TCID50/ml doses between 2.32 x 10^5 and 2.32 x 10^7 of various swine influenza A strains divided into different groups of pigs and delivered intramuscularly in the ratio of 1:1 in *Freunds Incomplete* adjuvant (Table 2). Blood samples were collected from all 20 pigs and each of them was SLA allele typed using the PCR-SSP typing method and custom SLA class I designed high resolution primers. Of the 20 animals typed, 16 turned out to express the allele of interest (SLA-1*0401) for which we had previously identified four influenza peptides, CTELKLSDY, GTEKLTITY, SSSFSFGGF, and YVFVGTSRY, bound with high affinities. These influenza peptides were predicted to be bound by *NetMHCpan* in conjunction with the SLA-1*0401 binding matrix criteria, and identified as strongly bound peptides by *in vitro* analysis in the same way as described for the FMDV derived peptides presented in Paper II.

Tetramer peptides and positions in Influenza viral genome				**Immunization strains 1 - 6**					
				1	**2**	**3**	**4**	**5**	**6**
Peptide	**Viral protein of origin**	**AA position* in virus**	**Nucleotide position* in virus**	**A/swine/Denmark/101310-1/2011 (H1N1pdm09)**	**A/swine/Denmark/101568-1/2011 (H1pdm09†)**	**A/swine/Denmark/19126/1993 (H1N1)**	**A/swine/Denmark/101490-3/2011 (H1N1)**	**A/swine/Denmark/1037-2/2011 (H1N2†)**	**A/swine/Denmark/101116-3/2011 (H1N2‡)**
CTELKLSDY	NP	44 - 52	130-156	+	+	CTELQLSDY	CTELQLSDY	CTELQLSDY	+
GTEKLTITY	PB2	523 - 531	1567-1593	+	+	+	+	+	+
SSSFSFGGF	PB2	320 - 328	958-984	+	+	+	+	+	+
YVFVGTSRY	HA	215 - 223	643-669	+	+	YVSVESSKY	YVSVVSSKY	YVSVVSSKY	YVSVGSSKY
				Animal ID for pigs immunized by the respective viral strains 1 - 6					
				1 + 2	4	6	8	15 + **16**	17

Table 2. Comparison of influenza peptide sequences within the different strains used for immunizations. Only animals with cells found to positively stain with tetramer are shown (pigs 1, 2, 4, 6, 8 and 16) along with pig 17 which represents the 10 non-responding animals. (+) Peptide sequence present in the viral strain used for immunization. (*) Position relative to start codon in virus A/swine/Denmark/12687/2003 (Breum 2012). (†) Reassortant swine influenza virus encoding a different N2 gene (Breum 2012). (‡) Reassortant influenza virus strain

with NP gene from H1N1pdm09 virus (Breum 2012). Amino acids in bold (grey), mark substitutions in the peptide sequence coded for in the immunization strain as compared to the peptide used for tetramer production.

PBMCs isolated from the 16 animals positive for SLA-1*0401 were initially frozen and later analyzed by influenza pSLA-1*0401 complex based tetramer staining using four different influenza peptides and two different fluorochrome tetramer labels (allophycocyanin (APC) and brilliant violet (BV421)), which enable the identification of tetramer double positive cell populations as illustrated in Figure 14A (Pig 4, (GTEKLTITY)). A negative control peptide (ASYGAGAGY) was included for comparison. The experimental setup for these immunizations was designed for other purposes than tetramer staining, which left us with no non-vaccinated or SLA mismatched pigs as negative controls. Hence, I decided to use a human PBMC sample stained with tetramers as an additional negative control. Such a control has to be included with caution in that it is not a definite negative control. Still, it is capable of proving that the tetramers we use are not just staining whatever cells they are offered regardless of their species of origin.

Of the 16 correctly SLA matched animals it was found that six pigs (Pig 1, 2, 4, 6, 8, and 16) displayed positive signals above background for one or more of the influenza tetramers in the staining assay (Table 3). A study examining influenza virus specific $CD8^+$ T cell responses in Macaques has recently been performed using macaque MHC class I, *Mane-A1*08401*, tetramers produced with an influenza epitope; RA9 (Jegaskanda et al. 2012). In this study animals were infected intranasal and intratracheal at day 0 and day 28, followed by administration of a third infection dose 2 to 10 months later using recombinant influenza virus. PBMCs were collected from blood and frozen. The results of these experiments showed distinct staining of thawed RA9-specific $CD8^+$ T cells by 0.14 % of the $CD8^+$ T cell population compared to 0.02 % negative control staining of an influenza naïve *Mane-A1*08401*-RA9 negative animal, corresponding to a 7-fold increase in tetramer staining signal between positive and negative samples.

From our studies, tetramer cell staining examples of double positively stained (SLA matched, responding animal 4), no staining (SLA matched, non-responding animal 17) and additional negative control staining of human PBMCs with SLA tetramers (SLA mismatched, non-

responding human) are shown in Figure 14 for one swine influenza A peptide (GTEKLTITY) and the negative control peptide (ASYGAGAGY). Here illustrating a 5.4-fold increase in tetramer staining signal between positive and negative samples (Figure 14A). A 32.5-fold increase in positive tetramer staining was seen for PBMCs derived from pig 4 and stained with the influenza tetramer (GTEKLTITY) compared with the same tetramer staining of completely mismatched human PBMCs (Figure 14A + C). Comparing the influenza-tetramer data for the six pigs with those of the macaque study performed by Jegaskanda et al., it is demonstrated that our positive tetramer staining percentages are generally 11 to 46-folds higher, but with similar ratios to the negative control samples, and with some variation between different animals and peptides. These tetramer staining percentages are generally higher than previously observed for fresh *ex vivo* staining of $CD8^+$ PBMCs responding to vaccination against (or infection with) yellow fever (Co et al. 2009) in humans, *M. tuberculosis* (Wei et al. 2009) in macaque monkeys, and hepatitis C (He et al. 1999) in humans, and could be due to a higher degree of auto-fluorescent cells when studying porcine PBMCs or as a result of a higher level of non-specific, false positive tetramer background staining using SLA tetramers. Most of the responses reported in humans and macaques were shown to increase in tetramer positive percentage scores once stimulated with antigen, hereby reaching numbers around (or above) what is reported here for staining of porcine PBMCs.

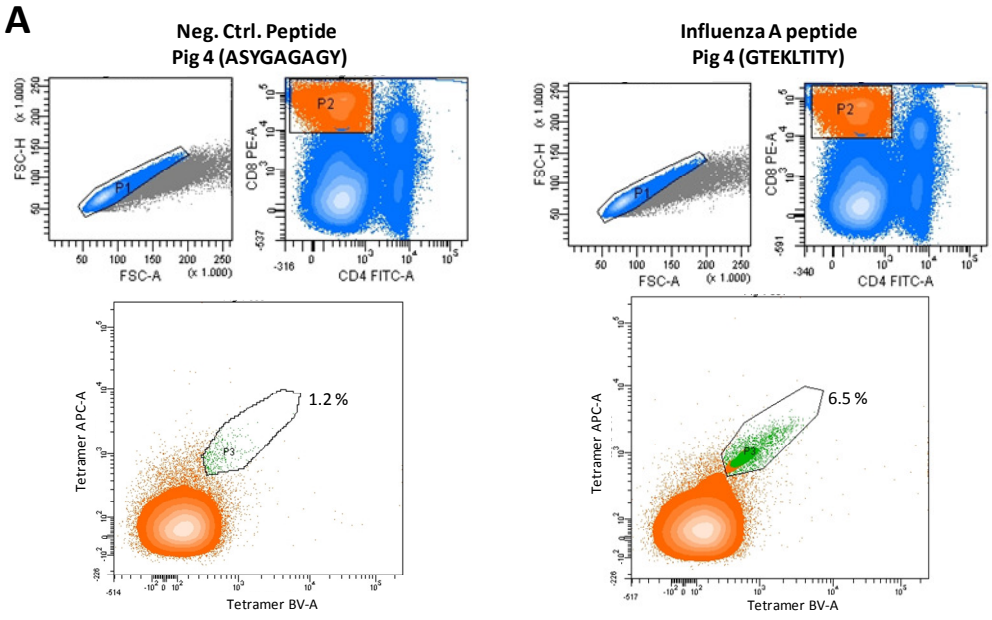

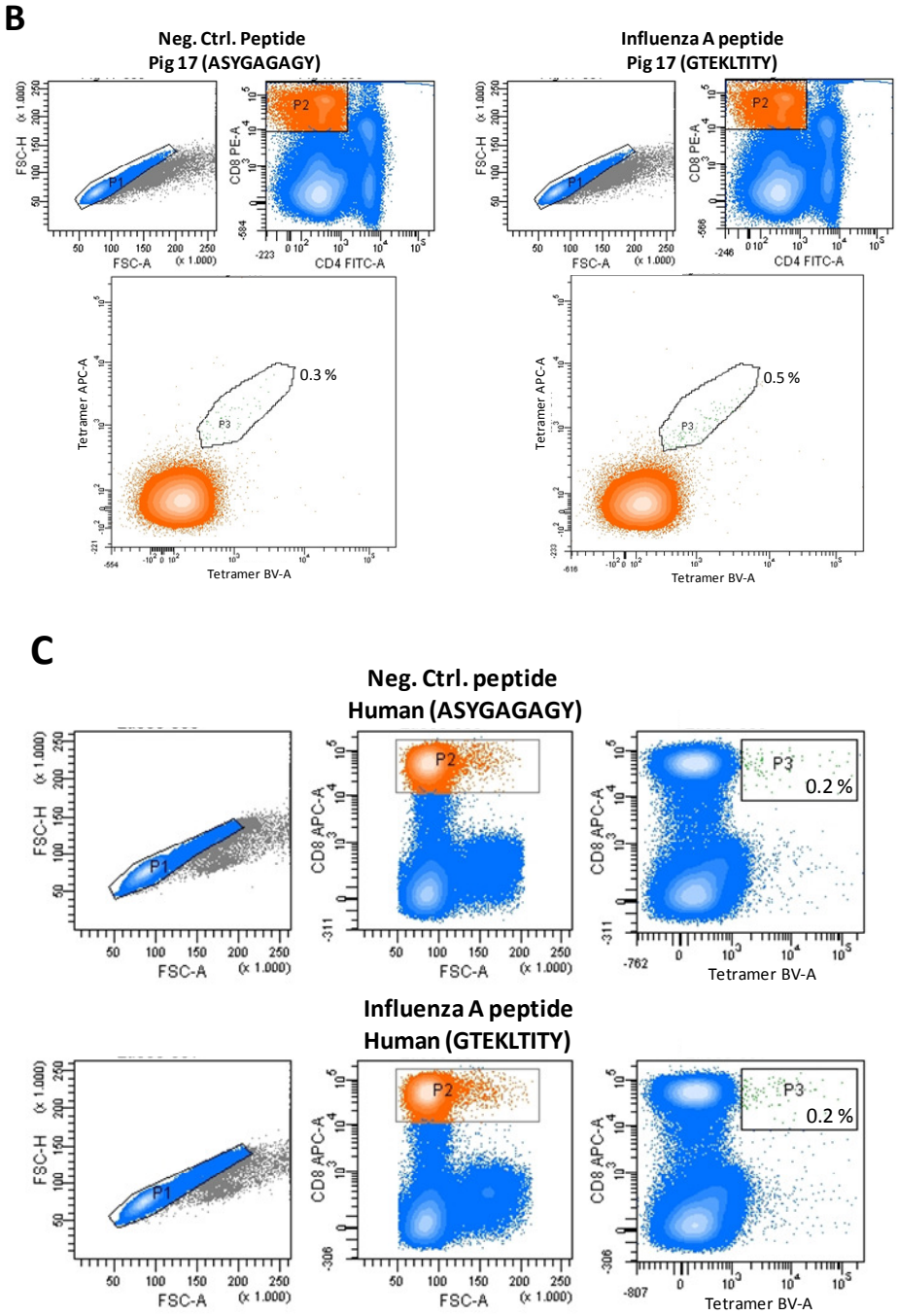

Figure 14. Tetramer staining of PBMCs. (**A** + **B**): PBMCs from animals previously vaccinated and boosted against swine influenza A. (**C**): Human PBMCs. Individual samples were stained by a negative control peptide (ASYGAGAGY) tetramer and a swine influenza A derived peptide (GTEKLTITY) tetramer. Singlet PBMCs were gated in P1 (blue). $CD8^{+}$(high)$CD4^{-}$ cells were gated in P2 (orange), and $CD8^{+}$(high)$CD4^{-}APC^{+}BV^{+}$ double tetramer positive cells were gated in P3 (green) for Pig 4 and Pig 17 (A + B). For the human control samples, singlet PBMCs were gated in P1 (blue), $CD8^{+}$(high) cells were gated in P2 (orange) and $CD8^{+}$(high)BV^{+} tetramer single positive cells were gated in P3 (green) (C). Percentages of tetramer positive cells within the $CD8^{+}$(high)$CD4^{-}$ population are shown for each sample in the figure. Individual staining percentages for all animals and tetramers are given in Table 3.

The influenza tetramer studies presented here revealed four influenza derived peptide epitopes (CTELKLSDY, GTEKLTITY, SSSFSFGGF, YVFVGTSRY) which were recognized in complex with the SLA-1*0401 molecule by porcine CTLs activated by immunization against swine influenza as illustrated in Figure 15 for Pig 4. Not all animals were responsive towards every influenza tetramer as positive staining was only seen for one of the four tetramers for pigs 1 and 2 (Table 3) using a threshold of 1 % positive staining of the $CD8hi^{+}$ PBMC population post negative background subtraction, which corresponds to a 2-fold higher staining percentage than measured for the negative control tetramer stained cells. Such a 2-fold higher threshold has previously been set by others (Ferrari et al. 2004). Furthermore, it was found that 10 of the 16 animals did not stain positive with any of the tetramers, as illustrated by Pig 17 (Figure 14B + 15, and Table 3), despite being correctly SLA matched. Such non-responsiveness illustrates how SLA bound peptides are not necessarily recognized as epitopes in all animals. Similar observations have previously been made for HLA tetramers and yellow fever peptides as well (Stryhn 2012). Collectively, the differences in individual peptide responses of animals with identical SLA alleles indicate that the SLA-1*0401 tetramers were not just staining any activated CTL derived from a correctly matched animal, but only CTLs with the right specificity, and that although peptide binding to the SLA molecule may be predicted and verified in advance, this is no guarantee for development of a CTL specific immune response to this particular peptide.

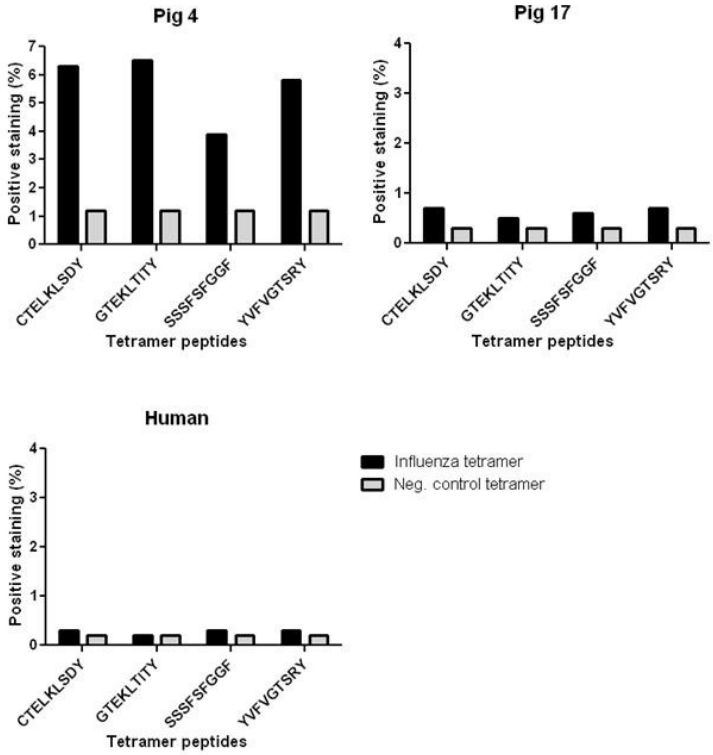

Figure 15. Percentages of tetramer positive cells within the $CD8^{+}$(high)$CD4^{-}$ population stained by each of the four influenza tetramers. Cell populations and individual percentages are shown in Figure 14 and Table 3, respectively. All four influenza tetramer peptides tested, along with the negative control tetramer (ASYGAGAGY), are shown (black and grey bars, respectively).

An interesting observation was made for Pigs 6, 8 and 16 which had all received viral immunization strains that differ in the NP and HA protein regions coding for two of the peptide sequences used to produce the tetramers (Table 2). The peptide CTELKLSDY had a single substitution in P5 of the peptide (K48Q) compared to the viral strains used for immunization of animals 6, 8 and 16, whereas peptide YVFVGTSRY had up to four substitutions (F217S, G219E, T220S, R222K) for peptide residues P3, P5, P6, and P8. Still, positive tetramer staining of CTLs was seen for all three pigs using these peptides. Such observations could be explained by CTL cross-reactivity suggesting that CTL clones can recognize different peptides, some even sharing no obvious sequence identity (Frankild et al. 2008). In addition to this, looking at the nature of the AAs involved in the substitutions could explain why the CTELKLSDY based tetramers were recognized by the porcine CTLs in that lysine (K) features a basic, positively charged $-NH_3^+$ side chain and glutamine (Q) features a neutral amide $-CONH_2$ side chain, making both AAs hydrophilic and capable of protrude toward the solvent. From a peptide:SLA-1*0401 affinity

point of view it is also seen that both K and Q are bound with almost similar RB values of 0.4 and 0.5, respectively (Paper I, Table 1). For the tetramers produced with the YVFVGTSRY peptide, the positive staining could be reasoned by similarities between the different AA residues responsible for the substitutions and the respective AA residues within the peptides derived from the viral strains. According to the SLA-1*0401 binding matrix it can be seen that no major differences exist between the different AA substitutions when it comes to binding affinity RB values, slightly favoring the viral strain derived peptide sequences (YVSVESSKY, YVSVVSSKY, YVSVGSSKY) for binding compared to the tetramer peptide sequence (Paper I, Table 1). Both phenylalanine (F) and serine (S) are being hidden within the D-pocket of the SLA-1*0401 peptide binding groove responsible for binding residue P3, with neither of them being disfavored for binding according to the binding matrix (Paper I, Table 1). Hence, despite their overall structural diversity, it could be speculated that such substitution plays a minor role in the matter of tetramer staining, in that these residues are not available for recognition by the TCR. Furthermore, the only difference seen between threonine (T) and serine in P6 is the methyl group of threonine, seeing both AAs as nucleophilic and hydrophilic which makes them more or less alike in terms of interacting with the surroundings. For residue P8 the AAs arginine (R) and lysine (K) share common features in being positively charged, basic and hydrophilic enabling almost similar recognition, whereas the AAs in P5 truly differ in glycine (G) being small and hydrophobic and glutamic acid (E) is acidic and hence hydrophilic. Comparing the other P5 substitution of (G219V) it is noteworthy that both AAs are hydrophobic, with valine (V) being somewhat larger in the presentation of a dimethyl group to the solvent. These P5 AA residues point away from the groove of the MHC enabling them to interact with the TCR of specific CTLs. When that is said, glycine being the smallest existing AA available might enable TCR recognition of the YVFVGTSRY-based tetramers, in that it is likely that the glycine P5 residue does not play a significant role in this particular TCR:pSLA interaction, or at least is unlikely to interfere with such. Nevertheless, further experiments including further negative controls such as non-vaccinated and SLA mismatched animals, as well as pre-vaccination and pre-boost samples for comparison, would be needed for conclusively confirmation of the specific influenza tetramer staining data presented in this section.

Pig #	Tetramer influenza peptide	Peptide present in immunization strain used	% Tetramer+ cells within the CD8+CD4- population	% Tetramer+ cells within the CD8+CD4- population (background subtracted)
1	ASYGAGAGY	No	0,80	*0,00*
	CTELKLSDY	Yes	1,70	*0,90*
	GTEKLTITY	Yes	1,90	**1,10**
	SSSFSFGGF	Yes	1,70	*0,90*
	YVFVGTSRY	Yes	1,60	*0,80*
2	ASYGAGAGY	No	0,60	*0,00*
	CTELKLSDY	Yes	1,70	**1,10**
	GTEKLTITY	Yes	1,50	*0,90*
	SSSFSFGGF	Yes	1,40	*0,80*
	YVFVGTSRY	Yes	1,50	*0,90*
4	ASYGAGAGY	No	1,20	*0,00*
	CTELKLSDY	Yes	6,30	**5,10**
	GTEKLTITY	Yes	6,50	**5,30**
	SSSFSFGGF	Yes	3,90	**2,70**
	YVFVGTSRY	Yes	5,80	**4,60**
6	ASYGAGAGY	No	2,60	*0,00*
	CTELKLSDY	No	5,80	**3,20**
	GTEKLTITY	Yes	5,80	**3,20**
	SSSFSFGGF	Yes	4,90	**2,30**
	YVFVGTSRY	No	5,90	**3,30**
8	ASYGAGAGY	No	0,90	*0,00*
	CTELKLSDY	No	3,00	**2,10**
	GTEKLTITY	Yes	2,40	**1,50**
	SSSFSFGGF	Yes	1,90	**1,00**
	YVFVGTSRY	No	2,70	**1,80**
16	ASYGAGAGY	No	1,10	*0,00*
	CTELKLSDY	No	2,80	**1,70**
	GTEKLTITY	Yes	2,50	**1,40**
	SSSFSFGGF	Yes	2,30	**1,20**
	YVFVGTSRY	No	2,70	**1,60**
17	ASYGAGAGY	No	0,30	*0,00*
	CTELKLSDY	Yes	0,70	*0,40*
	GTEKLTITY	Yes	0,50	*0,20*
	SSSFSFGGF	Yes	0,60	*0,30*
	YVFVGTSRY	No	0,70	*0,40*
Human	ASYGAGAGY	-	0,20	*0,00*
	CTELKLSDY	-	0,30	*0,10*
	GTEKLTITY	-	0,20	*0,00*
	SSSFSFGGF	-	0,30	*0,10*
	YVFVGTSRY	-	0,30	*0,10*

Table 3. Specific staining of porcine $CD8^{+}$(high)$CD4^{-}$ PBMCs using four different influenza peptide-based tetramers. Percentages in bold illustrate positive tetramer staining based on a threshold of 1.0 % post background subtraction. Italic numbers illustrate no specific binding whereas grey highlights point out positive staining with peptides that are not 100 % identical in sequence with those of the respective vaccine constructs used. ASYGAGAGY is a designed negative control peptide for defining the relative false-positive background signal. Animal ID 17 was included as an example of a non-responding animal. ID Human: Human PBMCs included as an additional negative control for comparison.

8. Conclusions and Perspectives

Throughout this PhD project, the fully developed large-scale technology to produce, analyze, and validate peptide–MHC interactions, which was pioneered over three decades for mice and humans (Ferre et al. 2003, Harndahl et al. 2009, Ostergaard et al. 2001, Pedersen et al. 1995,

Stryhn et al. 1996), has been applied to analysis of porcine MHC molecules. By doing so, instigation of knowledge on potential T cell epitopes in this particular species, has been made possible further allowing *in silico* prediction servers, that identify specific peptides for MHC binding, such as the *NetMHCpan*, also to successfully include swine (Hoof et al. 2009, Larsen et al. 2005, Lundegaard et al. 2011, Nielsen et al. 2007, Pedersen et al. 2011, Pedersen et al. 2012a). Combined with the tetramer technology described in this thesis for specific T cell analysis this has enabled fast, accurate "one-pot, mix-and-read" analyses of MHC restricted $CD8^+$ T cell reactivity following vaccination. In pigs, *in silico* prediction of virus derived peptides bound by SLA class I molecules has been verified by *in vitro* analysis of specific peptide binding, leading to the identification of strongly bound viral peptides (Pedersen et al. 2011, Pedersen et al. 2012a). In addition, the analysis of pSLA stability was included hereby identifying peptides, which were not only bound with high affinity but further produce pSLA complexes of high stability (Pedersen et al. 2012b). Furthermore, the effects of T cell specific vaccination have been investigated by monitoring $CD8^+$ T cell responses post vaccination (Patch et al. 2011). Such reverse immunology proposals should be expected to become important in the contribution to, as well as support of, the study of livestock immune responses.

As part of the project, SLA molecules have been produced and their peptide-binding profiles analyzed. All SLA alleles were initially identified by PCR-SSP allele specific tissue typing (or previously reported in the literature) to be commonly expressed among swine herds. Following these approaches, I predicted and identified several peptides which were bound with high affinity and generate highly stable pSLA complexes with one or more of the newly produced SLA proteins. This was done by using the *NetMHCpan* prediction tool in concert with individual SLA peptide binding matrix predictions, and followed by *in vitro* peptide affinity and stability measures (Hoof et al. 2009, Pedersen et al. 2011, Pedersen et al. 2012b, Pedersen et al. 2012a). Having identified such possible peptide epitopes led to SLA based tetramer staining experiments in an attempt to positively stain PBMCs from animals previously vaccinated against either FMDV (Patch et al. 2011) or swine influenza A. These experiments ultimately led to the identification of T cell epitopes as presented in this thesis (Figure 13 and 15).

Altogether, the assays and experimental approaches presented and discussed here provide new tools to (i) identify commonly expressed SLA class I alleles within herds, (ii) analyze the diverse

peptide binding profiles of individual SLA proteins, and (iii) identify antigenic peptide ligands bound with high affinity and stability by such MHC molecules of interest. These results lead to the production of pSLA tetramers, which, when combined with cytokine release and staining assays, as well as measuring target cell killing, are capable of (i) providing a tool for the enumeration and determination of the relative frequencies of epitope-specific, cytokine-secreting CTLs in a sample, (ii) evaluating the effector function of such CTLs, i.e. their ability to specifically kill infected targets and the identification of specific cytokines and chemokines produced, and (iii) identifying viral as well as tumor derived peptide T cell epitopes (Patch et al. 2011, Romero et al. 1998, Romero et al. 2004).

Some future perspectives and suggested ideas for new projects based on the assays, approaches and results presented in this thesis are illuminated in the sub sections 8.1. – 8.3.

8.1. SIMULTANEOUS ANALYSIS OF MULTIPLE SPECIFICITIES

An interesting approach for future studies would be the establishment of assays capable of simultaneously analyzing porcine CTLs with different specificities based on differently labeled pMHC complex multimers such as the systemically organized dextramers. Dextramers are fluorescently labeled MHC class I oligomers based on dextran backbones, which are capable of binding ten times more biotinylated pMHC complexes, and the conjugation of four to five times more fluorescein than the conventional tetramers (Batard et al. 2006). They have been shown to produce similar or stronger signal than their tetramer counterparts partly due to stronger pMHC:TCR avidity, and particularly because of the higher level of fluorescent labeling. Hence, in contrast to tetramers, MHC dextramers are not restricted to only the brightest fluorochromes for optimal detection. Such features make dextramers interesting alternatives in the identification and labeling of minor populations of antigen specific CTLs using higher order multicolor flow cytometry, and enabling the use of a broad range of fluorochrome conjugates including the ones that are less fluorescent (Batard et al. 2006). Using multicolor staining with either dextramers or tetramers would further improve the cell staining assays and approaches described in this thesis. Such multicolor staining could enable simultaneous identification and enumeration of separate cell populations specific for individual pMHC complexes even after

surface-marker gating. This could be done using two different pMHC multimers each with their own fluorochrome conjugate. In such ways, single (and dual) specificities of activated CTLs can be demonstrated and the cell staining assay itself validated. The scenario of having dual specificities expressed simultaneously by a single population of CTLs would be expected to require almost identical pMHC complex based tetramers or cross-reactive CTLs. Applying such pSLA tetramer or dextramer based multicolor staining assays to swine prove promising for future studies of livestock diseases, and could turn out to become valuable tools, eventually leading to advanced and high specific validation of the functions of existing vaccines, as well as accelerated development of future vaccines.

8.2. SYNTHETIC IMMUNOGENIC PROTEIN (SIP) VACCINES

By use of the different assays and techniques presented throughout this thesis, it should be possible to deliver a new and innovative approach for tailoring synthetic protein vaccines to specifically induce an efficient CTL immune response against some of the most important infectious diseases currently known to threat the swine production worldwide. Evaluation of the different approaches to induce CTL responses with currently available adjuvants would be facilitated by tetramer assessment of different vaccine formulations. An approach described for, and tested in, mice more than a decade ago (Suhrbier 1997, Thomson et al. 1998) and later followed up in regard to enhanced CTL responses using supporting adjuvant (Li et al. 2005), make it reasonable to suggest novel vaccines can be designed of a synthetic string of conserved sub-dominant, well-defined SLA class I CTL epitopes of viruses such as FMDV, PRRSV and swine influenza A virus. Furthermore, it could be suggested that such a vaccine delivered either in a CD8 activating adjuvant or in a live non-replicating vector, would be able to induce an efficient and sustained CTL response against current viral strains as well as forthcoming virus mutations. As described above, the recently developed SLA tetramers could be used to identify important peptide epitopes (such as those highly conserved among viral strains) capable of activating CTLs, followed by transformation of such identified peptides into a designed string of tandem repeated peptides in a synthetic immunogenic protein (SIP) encoded by a carefully designed DNA construct. Once the SIP is delivered, degraded and finally presented as peptides by antigen presenting cells, the porcine adaptive immune system of vaccinated animals should become

activated in a highly specific manner leading to generation of immunologic memory and CTL mediated protection against the virus represented by the SIP (Figure 16). Such SIP vaccines could turn out to be a novelty with the potential to revolutionize current protein and subunit-based vaccine approaches and development.

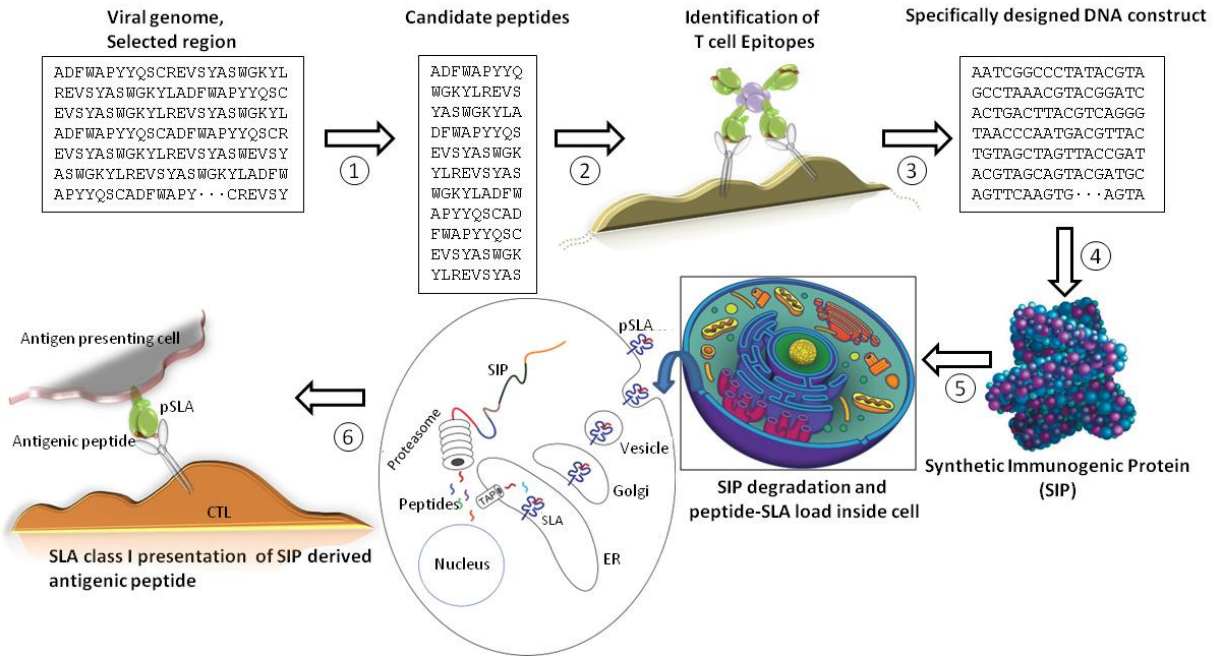

Figure 16. From genome to SIP vaccine to protection. **1:** Selected genomic regions of the virus of interest is screened for peptide candidates with the ability to form complexes with SLA class I molecules using combined *in silico* NetMHCpan and PSCPL matrix predictions followed by *in vitro* verification. **2:** Production of correctly folded pSLA tetramers and the identification of T cell epitope peptides capable of being recognized by cytotoxic T cells. **3:** Design of DNA construct encoding tandem repeats of sequences encoding all identified viral epitopes. **4:** Recombinant production of the SIP directly from the DNA construct. **5:** SIP-based vaccine formulation and adjuvant non-vectored/vectored vaccine delivery of SIP proteins/construct. **6:** Intracellular degradation of SIPs into peptides and SIP peptide load onto SLA class I molecules, followed by cell surface presentation of SIP-pSLA complexes to circulating CTLs ultimately leading to adaptive immune activation and protection against the virus of interest.

Investigation of the induction of CTL responses following live non-replicating adenovirus vaccine vectored SIP (Ad-SIP) vaccination, or vaccination with the SIP formulated into different adjuvants would be highly relevant in the search for optimal adjuvant-based co-delivery and immune activation. Such novel adjuvants, with the potential to induce CTL responses, could arise from modifications of the cationic adjuvant system (CAF) adjuvant family (Nordly et al. 2011), immune stimulatory complexes (ISCOMs) (Schiott et al. 2011), *Cholera* toxin (Olvera-Gomez et al. 2012) or other new formulations (Heegaard et al. 2011). Succeeding in designing

functionally SIP vaccines would tremendously accelerate vaccine development against viral infections which require a high quality host CTL response for elimination and establishment of protection.

A potential drawback of the SIP based vaccination approach would be the challenge of getting whole SIPs successfully delivered into the cytoplasm of antigen presenting cells, which make protein-adjuvant vaccination a substantial task to deal with. This may be overcome by using the Ad-SIP construct for the synthesis and delivery of SIPs inside the cells. Still, if the use of adenovirus vectors is to be avoided, another solution could be adding “opsonization tags” in the construct encoding the SIP, leading to specific glycosylation of the SIP, for example with mannose, making it recognizable by mannose-binding lectins at the surface of antigen presenting cells.

Most pork producers are likely to select breeding stock for quality and quantity of meat. Hence, vaccine makers will have to customize vaccines to the strains of pigs favored by the producers. If vaccines based on the most frequent SLA alleles are successful, however, it is likely that they will also introduce selection towards an undesired reduction in SLA diversity. Thus, it will be important to include a broad range of SLA specificities in the design of corresponding vaccine polyepitopes.

8.3. MULTIMER BASED CANCER TREATMENT

Using swine as an animal model, it would be possible to validate the effects of human cancer vaccines, by monitoring the specificity and status of activation of different cell populations via pSLA multimers based on peptides derived from the cancer type of interest. Furthermore, pMHC multimers could potentially be used *in vivo* to label tumor cells for elimination by already existing CTLs of the host specific to common viruses such as *Epstein-Barr* virus (EBV), *Cytomegalo* virus (CMV), and influenza, from which the tetramer peptides should be derived. Hereby tetramers would resemble antigen presenting cells bound to the cell surface of tumor cells by an anti-tumor specific mAb directly coupled to streptavidin of the tetramer (Figure 17), enabling the activation of host CTLs and leading to elimination of the tumor cell.

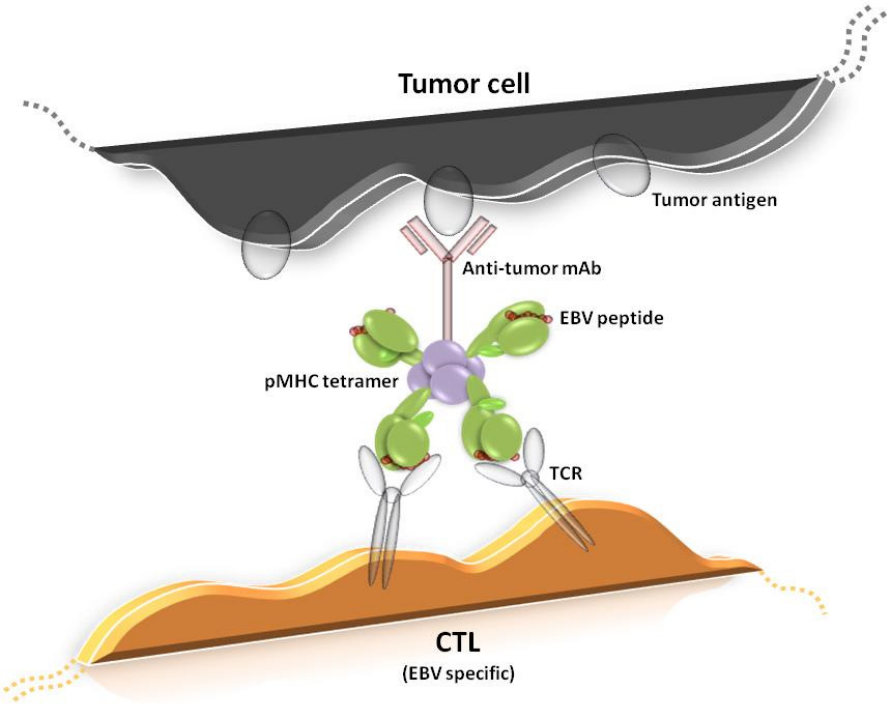

Figure 17. Redirected killing of a tumor cell by an EBV specific CTL. EBV peptides (red) are presented by a pMHC tetramer (green/purple), which is attached to the cell surface of a tumor cell (black) via an anti-tumor mAb (pink) that recognize tumor antigens (grey).

In vitro studies have shown such Ab-pMHC tetramers to sensitize tumor cells to lysis by specific CTLs (Ogg et al. 2000, Robert et al. 2000) making further refinement and development of this technique for *in vivo* utilization an interesting approach for future immunological therapy of cancer.

8.4. ANSWERS LEAD TO QUESTIONS

The approaches, assays and proposals presented in this PhD thesis could ultimately lead to a better agriculture in terms of a more productive farming industry and overall greater animal health. Still the questions are many, and the greatly accelerated evolution in the field of immunology within the past two decades, has now made curiosity-driven research possible at a scale not previously imaginable. It is often so in science that most answers tend to bring several new questions. Hence, knowing what we do today forces us to strive for more. Could the distribution of SLA molecules, such as the commonly expressed SLA-1*0401, be of any interest in the susceptibility to, or protection against, certain viruses in swine? Would one commonly

occurring class I molecule cover for most of the pSLA complex mediated CTL immune response, or would a symphony of several more or less common alleles be a criteria for the induction of strong and durable adaptive immune protection? How important are the individual peptide anchor requirements and peptide lengths for SLA class I ligand binding, and the corresponding level of immunogenicity, and how does pSLA complex stability affect TCR activation? Would high peptide turn-overs and a great variety in peptide presentation be beneficial to effective protection against disease, or would a low number of a few highly stable pSLA complexes be more capable of sufficiently activating CTLs? Would it be possible to specifically monitor immune responses in outbred populations, leading to the identification of several conserved peptide epitopes from viruses that are constantly mutating to achieve immune evasion? Could such epitopes turn out to be potentially valuable vaccine candidates in the design and development of highly specific subunit vaccines, and how should such a vaccine be delivered for optimal effect? Would it be possible to effectively validate different vaccines and vaccine delivery approaches for humans, using the pig as an experimental model, hereby improving our understanding of targeting various cancers as well as of the pathogenesis and immune elimination of disease in both humans and livestock animals?

Final Thoughts

To get a full – or at least better – understanding on what is going on in our field of veterinary immunology, we need to step back and take yet another look, share and use the technologies and approaches available to us in research laboratories around the globe; discard a lot, re-think some, use a few, and finally have the courage to go down different alleys embracing whatever complexities that we might find.

Reference List

Addo M.M., Yu X.G., Rathod A., Cohen D., Eldridge R.L., Strick D., Johnston M.N., Corcoran C., Wurcel A.G., Fitzpatrick C.A., Feeney M.E., Rodriguez W.R., Basgoz N., Draenert R., Stone D.R., Brander C., Goulder P.J., Rosenberg E.S., Altfeld M. & Walker B.D. (2003) Comprehensive epitope analysis of human immunodeficiency virus type 1 (HIV-1)-specific T-cell responses directed against the entire expressed HIV-1 genome demonstrate broadly directed responses, but no correlation to viral load. *J. Virol.* 77, 2081-2092.

Altman J.D., Davis M.M. (2003) MHC-peptide tetramers to visualize antigen-specific T cells. *Curr. Protoc. Immunol.* Chapter 17, Unit.

Altman J.D., Moss P.A., Goulder P.J., Barouch D.H., Heyzer-Williams M.G., Bell J.I., McMichael A.J. & Davis M.M. (1996) Phenotypic analysis of antigen-specific T lymphocytes. *Science* 274, 94-96.

Anderson G., Takahama Y. (2012) Thymic epithelial cells: working class heroes for T cell development and repertoire selection. *Trends Immunol.* 33, 256-263.

Banchereau J., Pascual V. & O'Garra A. (2012) From IL-2 to IL-37: the expanding spectrum of anti-inflammatory cytokines. *Nat. Immunol.* 13, 925-931.

Baranov O.K., Eppel' M.S. (1984) [Genetic bases of antibody diversity]. *Genetika* 20, 1397-1413.

Batard P., Peterson D.A., Devevre E., Guillaume P., Cerottini J.C., Rimoldi D., Speiser D.E., Winther L. & Romero P. (2006) Dextramers: new generation of fluorescent MHC class I/peptide multimers for visualization of antigen-specific CD8+ T cells. *J. Immunol. Methods* 310, 136-148.

Beigel J., Bray M. (2008) Current and future antiviral therapy of severe seasonal and avian influenza. *Antiviral Res.* 78, 91-102.

Bevan M.J. (1977) In a radiation chimaera, host H-2 antigens determine immune responsiveness of donor cytotoxic cells. *Nature* 269, 417-418.

Bevan M.J. (1995) Antigen presentation to cytotoxic T lymphocytes in vivo. *J. Exp. Med.* 182, 639-641.

Bjorkman P.J., Saper M.A., Samraoui B., Bennett W.S., Strominger J.L. & Wiley D.C. (1987a) Structure of the human class I histocompatibility antigen, HLA-A2. *Nature* 329, 506-512.

Bjorkman P.J., Saper M.A., Samraoui B., Bennett W.S., Strominger J.L. & Wiley D.C. (1987b) The foreign antigen binding site and T cell recognition regions of class I histocompatibility antigens. *Nature* 329, 512-518.

Breum S.Ø. Novel Influenza A viral strains and sequence analysis. 20-9-2012.
Ref Type: Personal Communication

Brocchi E., Bergmann I.E., Dekker A., Paton D.J., Sammin D.J., Greiner M., Grazioli S., De S.F., Yadin H., Haas B., Bulut N., Malirat V., Neitzert E., Goris N., Parida S., Sorensen K. & de C.K. (2006) Comparative evaluation of six ELISAs for the detection of antibodies to the non-structural proteins of foot-and-mouth disease virus. *Vaccine* 24, 6966-6979.

Brown I.H., Ludwig S., Olsen C.W., Hannoun C., Scholtissek C., Hinshaw V.S., Harris P.A., McCauley J.W., Strong I. & Alexander D.J. (1997) Antigenic and genetic analyses of H1N1 influenza A viruses from European pigs. *J. Gen. Virol.* 78 (Pt 3), 553-562.

Busch D.H., Pamer E.G. (1998) MHC class I/peptide stability: implications for immunodominance, in vitro proliferation, and diversity of responding CTL. *J. Immunol.* 160, 4441-4448.

Campanini G., Piralla A., Paolucci S., Rovida F., Percivalle E., Maga G. & Baldanti F. (2010) Genetic divergence of influenza A NS1 gene in pandemic 2009 H1N1 isolates with respect to H1N1 and H3N2 isolates from previous seasonal epidemics. *Virol. J.* 7, 209.

Chardon P., Renard C., Gaillard C.R. & Vaiman M. (2000) The porcine major histocompatibility complex and related paralogous regions: a review. *Genet. Sel Evol.* 32, 109-128.

Chardon P., Rogel-Gaillard C., Cattolico L., Duprat S., Vaiman M. & Renard C. (2001) Sequence of the swine major histocompatibility complex region containing all non-classical class I genes. *Tissue Antigens* 57, 55-65.

Choi E.M., Palmowski M., Chen J. & Cerundolo V. (2002) The use of chimeric A2K(b) tetramers to monitor HLA A2 immune responses in HLA A2 transgenic mice. *J. Immunol. Methods* 268, 35-41.

Clavijo A., Wright P. & Kitching P. (2004) Developments in diagnostic techniques for differentiating infection from vaccination in foot-and-mouth disease. *Vet. J.* 167, 9-22.

Co M.D., Kilpatrick E.D. & Rothman A.L. (2009) Dynamics of the CD8 T-cell response following yellow fever virus 17D immunization. *Immunology* 128, e718-e727.

Cobbold M., Khan N., Pourgheysari B., Tauro S., McDonald D., Osman H., Assenmacher M., Billingham L., Steward C., Crawley C., Olavarria E., Goldman J., Chakraverty R., Mahendra P., Craddock C. & Moss P.A. (2005) Adoptive transfer of cytomegalovirus-specific CTL to stem cell transplant patients after selection by HLA-peptide tetramers. *J. Exp. Med.* 202, 379-386.

Cresswell P., Bangia N., Dick T. & Diedrich G. (1999) The nature of the MHC class I peptide loading complex. *Immunol. Rev.* 172, 21-28.

Cresswell P., Turner M.J. & Strominger J.L. (1973) Papain-solubilized HL-A antigens from cultured human lymphocytes contain two peptide fragments. *Proc. Natl. Acad. Sci. U. S. A* 70, 1603-1607.

Dalchau N., Phillips A., Goldstein L.D., Howarth M., Cardelli L., Emmott S., Elliott T. & Werner J.M. (2011) A peptide filtering relation quantifies MHC class I peptide optimization. *PLoS. Comput. Biol.* 7, e1002144.

Danilova N. (2012) The evolution of adaptive immunity. *Adv. Exp. Med. Biol.* 738, 218-235.

Davis M.M., Bjorkman P.J. (1988) T-cell antigen receptor genes and T-cell recognition. *Nature* 334, 395-402.

Doel T.R. (2003) FMD vaccines. *Virus Res.* 91, 81-99.

Doherty P.C., Zinkernagel R.M. (1975) H-2 compatibility is required for T-cell-mediated lysis of target cells infected with lymphocytic choriomeningitis virus. *J. Exp. Med.* 141, 502-507.

Dunbar P.R., Ogg G.S., Chen J., Rust N., van der B.P. & Cerundolo V. (1998) Direct isolation, phenotyping and cloning of low-frequency antigen-specific cytotoxic T lymphocytes from peripheral blood. *Curr. Biol.* 8, 413-416.

Elliott T., Cerundolo V., Elvin J. & Townsend A. (1991) Peptide-induced conformational change of the class I heavy chain. *Nature* 351, 402-406.

Elliott T., Williams A. (2005) The optimization of peptide cargo bound to MHC class I molecules by the peptide-loading complex. *Immunol. Rev.* 207, 89-99.

Engvall E., Perlmann P. (1971) Enzyme-linked immunosorbent assay (ELISA). Quantitative assay of immunoglobulin G. *Immunochemistry.* 8, 871-874.

Essler S.E., Ertl W., Deutsch J., Ruetgen B.C., Groiss S., Stadler M., Wysoudil B., Gerner W., Ho C.S. & Saalmueller A. (2012) Molecular characterization of swine leukocyte antigen gene diversity in purebred Pietrain pigs. *Anim Genet.*

Ferrari G., Neal W., Ottinger J., Jones A.M., Edwards B.H., Goepfert P., Betts M.R., Koup R.A., Buchbinder S., McElrath M.J., Tartaglia J. & Weinhold K.J. (2004) Absence of immunodominant anti-Gag p17 (SL9) responses among Gag CTL-positive, HIV-uninfected vaccine recipients expressing the HLA-A*0201 allele. *J. Immunol.* 173, 2126-2133.

Ferre H., Ruffet E., Blicher T., Sylvester-Hvid C., Nielsen L.L., Hobley T.J., Thomas O.R. & Buus S. (2003) Purification of correctly oxidized MHC class I heavy-chain molecules under denaturing conditions: a novel strategy exploiting disulfide assisted protein folding. *Protein Sci.* 12, 551-559.

Frankild S., de Boer R.J., Lund O., Nielsen M. & Kesmir C. (2008) Amino acid similarity accounts for T cell cross-reactivity and for "holes" in the T cell repertoire. *PLoS. One.* 3, e1831.

Gao M., Zhang R., Li M., Li S., Cao Y., Ma B. & Wang J. (2012) An ELISA based on the repeated foot-and-mouth disease virus 3B epitope peptide can distinguish infected and vaccinated cattle. *Appl. Microbiol. Biotechnol.* 93, 1271-1279.

Gay D., Saunders T., Camper S. & Weigert M. (1993) Receptor editing: an approach by autoreactive B cells to escape tolerance. *J. Exp. Med.* 177, 999-1008.

Germain R.N. (2012) Maintaining system homeostasis: the third law of Newtonian immunology. *Nat. Immunol.* 13, 902-906.

Golde W.T., Pacheco J.M., Duque H., Doel T., Penfold B., Ferman G.S., Gregg D.R. & Rodriguez L.L. (2005) Vaccination against foot-and-mouth disease virus confers complete clinical protection in 7 days and partial protection in 4 days: Use in emergency outbreak response. *Vaccine* 23, 5775-5782.

Goldszmid R.S., Trinchieri G. (2012) The price of immunity. *Nat. Immunol.* 13, 932-938.

Gorer P.A., Lyman S. & Snell G.D. (1948) Studies on the Genetic and Antigenic Basis of Tumour Transplantation. Linkage between a Histocompatibility Gene and 'Fused' in Mice. *Proc. R. Soc. Lond. B.* 135, 499-505.

Grey H.M., Kubo R.T., Colon S.M., Poulik M.D., Cresswell P., Springer T., Turner M. & Strominger J.L. (1973) The small subunit of HL-A antigens is beta 2-microglobulin. *J. Exp. Med.* 138, 1608-1612.

Grubman M.J., Baxt B. (2004) Foot-and-mouth disease. *Clin. Microbiol. Rev.* 17, 465-493.

Grubman M.J., Moraes M., Schutta C., Barrera J., Neilan J., Ettyreddy D., Butman B.T., Brough D.E. & Brake D.A. (2010) Adenovirus serotype 5-vectored foot-and-mouth disease subunit vaccines: the first decade. *Future Virol.* 5:51-64.,

Grubman M.J., Zellner M., Bablanian G., Mason P.W. & Piccone M.E. (1995) Identification of the active-site residues of the 3C proteinase of foot-and-mouth disease virus. *Virology* 213, 581-589.

Guzman E., Taylor G., Charleston B., Skinner M.A. & Ellis S.A. (2008) An MHC-restricted CD8+ T-cell response is induced in cattle by foot-and-mouth disease virus (FMDV) infection and also following vaccination with inactivated FMDV. *J. Gen. Virol.* 89, 667-675.

Harndahl M., Justesen S., Lamberth K., Roder G., Nielsen M. & Buus S. (2009) Peptide binding to HLA class I molecules: homogenous, high-throughput screening, and affinity assays. *J. Biomol. Screen.* 14, 173-180.

Harndahl M., Rasmussen M., Roder G., Dalgaard P., I, Sorensen M., Nielsen M. & Buus S. (2012) Peptide-MHC class I stability is a better predictor than peptide affinity of CTL immunogenicity. *Eur. J. Immunol.* 42, 1405-1416.

Hart H.E., Greenwald E.B. (1979a) Scintillation proximity assay (SPA)--a new method of immunoassay. Direct and inhibition mode detection with human albumin and rabbit antihuman albumin. *Mol. Immunol.* 16, 265-267.

Hart H.E., Greenwald E.B. (1979b) Scintillation-proximity assay of antigen-antibody binding kinetics: concise communication. *J. Nucl. Med.* 20, 1062-1065.

Hartley S.B., Cooke M.P., Fulcher D.A., Harris A.W., Cory S., Basten A. & Goodnow C.C. (1993) Elimination of self-reactive B lymphocytes proceeds in two stages: arrested development and cell death. *Cell* 72, 325-335.

Harty J.T., Tvinnereim A.R. & White D.W. (2000) CD8+ T cell effector mechanisms in resistance to infection. *Annu. Rev. Immunol.* 18, 275-308.

He X.S., Rehermann B., Lopez-Labrador F.X., Boisvert J., Cheung R., Mumm J., Wedemeyer H., Berenguer M., Wright T.L., Davis M.M. & Greenberg H.B. (1999) Quantitative analysis of hepatitis C virus-specific CD8(+) T cells in peripheral blood and liver using peptide-MHC tetramers. *Proc. Natl. Acad. Sci. U. S. A* 96, 5692-5697.

Heegaard P.M., Dedieu L., Johnson N., Le Potier M.F., Mockey M., Mutinelli F., Vahlenkamp T., Vascellari M. & Sorensen N.S. (2011) Adjuvants and delivery systems in veterinary vaccinology: current state and future developments. *Arch. Virol.* 156, 183-202.

Ho C.S., Ando A., Essler S.E., Rogel-Gaillard C., Lee J.H., Lunney J.K., Schook L. & Smith D.M. The Swine Leukocyte Antigen (SLA) Nomenclature System: Current Status after 10 Years of its Establishment. Conference of the International Society for Animal Genetics. [33rd.]. 20-7-2012.
Ref Type: Conference Proceeding

Ho C.S., Franzo-Romain M.H., Lee Y.J., Lee J.H. & Smith D.M. (2009a) Sequence-based characterization of swine leucocyte antigen alleles in commercially available porcine cell lines. *Int. J. Immunogenet.* 36, 231-234.

Ho C.S., Lunney J.K., Ando A., Rogel-Gaillard C., Lee J.H., Schook L.B. & Smith D.M. (2009b) Nomenclature for factors of the SLA system, update 2008. *Tissue Antigens* 73, 307-315.

Ho C.S., Lunney J.K., Franzo-Romain M.H., Martens G.W., Lee Y.J., Lee J.H., Wysocki M., Rowland R.R. & Smith D.M. (2009c) Molecular characterization of swine leucocyte antigen class I genes in outbred pig populations. *Anim Genet.* 40, 468-478.

Ho C.S., Lunney J.K., Lee J.H., Franzo-Romain M.H., Martens G.W., Rowland R.R. & Smith D.M. (2010a) Molecular characterization of swine leucocyte antigen class II genes in outbred pig populations. *Anim Genet.* 41, 428-432.

Ho C.S., Martens G.W., Amoss M.S., Jr., Gomez-Raya L., Beattie C.W. & Smith D.M. (2010b) Swine leukocyte antigen (SLA) diversity in Sinclair and Hanford swine. *Dev. Comp Immunol.* 34, 250-257.

Ho C.S., Rochelle E.S., Martens G.W., Schook L.B. & Smith D.M. (2006) Characterization of swine leukocyte antigen polymorphism by sequence-based and PCR-SSP methods in Meishan pigs. *Immunogenetics* 58, 873-882.

Hoof I., Peters B., Sidney J., Pedersen L.E., Sette A., Lund O., Buus S. & Nielsen M. (2009) NetMHCpan, a method for MHC class I binding prediction beyond humans. *Immunogenetics* 61, 1-13.

Horton R., Wilming L., Rand V., Lovering R.C., Bruford E.A., Khodiyar V.K., Lush M.J., Povey S., Talbot C.C., Jr., Wright M.W., Wain H.M., Trowsdale J., Ziegler A. & Beck S. (2004) Gene map of the extended human MHC. *Nat. Rev. Genet.* 5, 889-899.

Hunt D.F., Henderson R.A., Shabanowitz J., Sakaguchi K., Michel H., Sevilir N., Cox A.L., Appella E. & Engelhard V.H. (1992) Characterization of peptides bound to the class I MHC molecule HLA-A2.1 by mass spectrometry. *Science* 255, 1261-1263.

Hutchings P.R., Cambridge G., Tite J.P., Meager T. & Cooke A. (1989) The detection and enumeration of cytokine-secreting cells in mice and man and the clinical application of these assays. *J. Immunol. Methods* 120, 1-8.

Janeway C.A., Jr. (1989) Approaching the asymptote? Evolution and revolution in immunology. *Cold Spring Harb. Symp. Quant. Biol.* 54 Pt 1, 1-13.

Jegaskanda S., Reece J.C., De R.R., Stambas J., Sullivan L., Brooks A.G., Kent S.J. & Sexton A. (2012) Comparison of influenza and SIV specific CD8 T cell responses in macaques. *PLoS. One.* 7, e32431.

Jo S.K., Kim H.S., Cho S.W. & Seo S.H. (2007) Pathogenesis and inflammatory responses of swine H1N2 influenza viruses in pigs. *Virus Res.* 129, 64-70.

Kelley J., Walter L. & Trowsdale J. (2005) Comparative genomics of major histocompatibility complexes. *Immunogenetics* 56, 683-695.

Kida H., Ito T., Yasuda J., Shimizu Y., Itakura C., Shortridge K.F., Kawaoka Y. & Webster R.G. (1994) Potential for transmission of avian influenza viruses to pigs. *J. Gen. Virol.* 75 (Pt 9), 2183-2188.

Kiepiela P., Leslie A.J., Honeyborne I., Ramduth D., Thobakgale C., Chetty S., Rathnavalu P., Moore C., Pfafferott K.J., Hilton L., Zimbwa P., Moore S., Allen T., Brander C., Addo M.M., Altfeld M., James I., Mallal S., Bunce M., Barber L.D., Szinger J., Day C., Klenerman P., Mullins J., Korber B., Coovadia H.M., Walker B.D. & Goulder P.J. (2004) Dominant influence of HLA-B in mediating the potential co-evolution of HIV and HLA. *Nature* 432, 769-775.

Kisielow P., Bluthmann H., Staerz U.D., Steinmetz M. & von B.H. (1988) Tolerance in T-cell-receptor transgenic mice involves deletion of nonmature CD4+8+ thymocytes. *Nature* 333, 742-746.

Klenerman P., Cerundolo V. & Dunbar P.R. (2002) Tracking T cells with tetramers: new tales from new tools. *Nat. Rev. Immunol.* 2, 263-272.

Kristensen B. (1988) Current Status of SLA Class I and II Serology. In: Improving Genetic Disease Resistance in Farm Animals. Kluwer Academic Publishers., Brussels, Belgium, pp 23-32

Kubo R.T., Sette A., Grey H.M., Appella E., Sakaguchi K., Zhu N.Z., Arnott D., Sherman N., Shabanowitz J., Michel H. & . (1994) Definition of specific peptide motifs for four major HLA-A alleles. *J. Immunol.* 152, 3913-3924.

Kundin W.D. (1970) Hong Kong A-2 influenza virus infection among swine during a human epidemic in Taiwan. *Nature* 228, 857.

Kusza S., Flori L., Gao Y., Teillaud A., Hu R., Lemonnier G., Bosze Z., Bourneuf E., Vincent-Naulleau S. & Rogel-Gaillard C. (2011) Transcription specificity of the class Ib genes SLA-6, SLA-7 and SLA-8 of the swine major histocompatibility complex and comparison with class Ia genes. *Anim Genet.* 42, 510-520.

Lacey C., Wilkie B.N., Kennedy B.W. & Mallard B.A. (1989) Genetic and other effects on bacterial phagocytosis and killing by cultured peripheral blood monocytes of SLA-defined miniature pigs. *Anim Genet.* 20, 371-381.

Larsen M.V., Lundegaard C., Lamberth K., Buus S., Brunak S., Lund O. & Nielsen M. (2005) An integrative approach to CTL epitope prediction: a combined algorithm integrating MHC class I binding, TAP transport efficiency, and proteasomal cleavage predictions. *Eur. J. Immunol.* 35, 2295-2303.

Leisner C., Loeth N., Lamberth K., Justesen S., Sylvester-Hvid C., Schmidt E.G., Claesson M., Buus S. & Stryhn A. (2008) One-pot, mix-and-read peptide-MHC tetramers. *PLoS. One.* 3, e1678.

Lemke C.D., Graham J.B., Lubaroff D.M. & Salem A.K. (2011) Development of an MHC class I L(d)-restricted PSA peptide-loaded tetramer for detection of PSA-specific CD8+ T cells in the mouse. *Prostate Cancer Prostatic. Dis.* 14, 118-121.

Li X., Yang X., Jiang Y. & Liu J. (2005) A novel HBV DNA vaccine based on T cell epitopes and its potential therapeutic effect in HBV transgenic mice. *Int. Immunol.* 17, 1293-1302.

Lumsden J.S., Kennedy B.W., Mallard B.A. & Wilkie B.N. (1993) The influence of the swine major histocompatibility genes on antibody and cell-mediated immune responses to immunization with an aromatic-dependent mutant of Salmonella typhimurium. *Can. J. Vet. Res.* 57, 14-18.

Lundegaard C., Lund O. & Nielsen M. (2011) Prediction of epitopes using neural network based methods. *J. Immunol. Methods* 374, 26-34.

Lunney J.K., Ho C.S., Wysocki M. & Smith D.M. (2009) Molecular genetics of the swine major histocompatibility complex, the SLA complex. *Dev. Comp Immunol.* 33, 362-374.

Madden D.R. (1995) The three-dimensional structure of peptide-MHC complexes. *Annu. Rev. Immunol.* 13, 587-622.

Madden D.R., Gorga J.C., Strominger J.L. & Wiley D.C. (1992) The three-dimensional structure of HLA-B27 at 2.1 A resolution suggests a general mechanism for tight peptide binding to MHC. *Cell* 70, 1035-1048.

Madden K.B., Murrell K.D. & Lunney J.K. (1990) Trichinella spiralis: major histocompatibility complex-associated elimination of encysted muscle larvae in swine. *Exp. Parasitol.* 70, 443-451.

Mallard B.A., Wilkie B.N. & Kennedy B.W. (1989a) Influence of major histocompatibility genes on serum hemolytic complement activity in miniature swine. *Am. J. Vet. Res.* 50, 359-363.

Mallard B.A., Wilkie B.N. & Kennedy B.W. (1989b) The influence of the swine major histocompatibility genes (SLA) on variation in serum immunoglobulin (Ig) concentration. *Vet. Immunol. Immunopathol.* 21, 139-151.

Malyguine A., Strobl S., Zaritskaya L., Baseler M. & Shafer-Weaver K. (2007) New approaches for monitoring CTL activity in clinical trials. *Adv. Exp. Med. Biol.* 601, 273-284.

Martens G.W., Lunney J.K., Baker J.E. & Smith D.M. (2003) Rapid assignment of swine leukocyte antigen haplotypes in pedigreed herds using a polymerase chain reaction-based assay. *Immunogenetics* 55, 395-401.

Matsumura M., Fremont D.H., Peterson P.A. & Wilson I.A. (1992) Emerging principles for the recognition of peptide antigens by MHC class I molecules. *Science* 257, 927-934.

Mayr G.A., Chinsangaram J. & Grubman M.J. (1999) Development of replication-defective adenovirus serotype 5 containing the capsid and 3C protease coding regions of foot-and-mouth disease virus as a vaccine candidate. *Virology* 263, 496-506.

Mayr G.A., O'Donnell V., Chinsangaram J., Mason P.W. & Grubman M.J. (2001) Immune responses and protection against foot-and-mouth disease virus (FMDV) challenge in swine vaccinated with adenovirus-FMDV constructs. *Vaccine* 19, 2152-2162.

Medzhitov R. (2007) Recognition of microorganisms and activation of the immune response. *Nature* 449, 819-826.

Mescher M.F., Curtsinger J.M., Agarwal P., Casey K.A., Gerner M., Hammerbeck C.D., Popescu F. & Xiao Z. (2006) Signals required for programming effector and memory development by CD8+ T cells. *Immunol. Rev.* 211, 81-92.

Messaoudi I., Estep R., Robinson B. & Wong S.W. (2011) Nonhuman primate models of human immunology. *Antioxid. Redox. Signal.* 14, 261-273.

Moraes M.P., Mayr G.A., Mason P.W. & Grubman M.J. (2002) Early protection against homologous challenge after a single dose of replication-defective human adenovirus type 5 expressing capsid proteins of foot-and-mouth disease virus (FMDV) strain A24. *Vaccine* 20, 1631-1639.

Mullbacher A., Lobigs M., Yewdell J.W., Bennink J.R., Tha H.R. & Blanden R.V. (1999) High peptide affinity for MHC class I does not correlate with immunodominance. *Scand. J. Immunol.* 50, 420-426.

Muller J.D., Wilkins M., Foord A.J., Dolezal O., Yu M., Heine H.G. & Wang L.F. (2010) Improvement of a recombinant antibody-based serological assay for foot-and-mouth disease virus. *J. Immunol. Methods* 352, 81-88.

Murphy K., Travers P. & Walport M. (2008) Innate Immunnity. In: Immuno Biology. Garland Science, Taylor & Francis Group, New York, pp 39-108

Murray P.J., Smale S.T. (2012) Restraint of inflammatory signaling by interdependent strata of negative regulatory pathways. *Nat. Immunol.* 13, 916-924.

Nielsen M., Lundegaard C., Blicher T., Lamberth K., Harndahl M., Justesen S., Roder G., Peters B., Sette A., Lund O. & Buus S. (2007) NetMHCpan, a method for quantitative predictions of peptide binding to any HLA-A and -B locus protein of known sequence. *PLoS. One.* 2, e796.

Nordly P., Rose F., Christensen D., Nielsen H.M., Andersen P., Agger E.M. & Foged C. (2011) Immunity by formulation design: induction of high CD8+ T-cell responses by poly(I:C) incorporated into the CAF01 adjuvant via a double emulsion method. *J. Control Release* 150, 307-317.

Norimine J., Han S. & Brown W.C. (2006) Quantitation of Anaplasma marginale major surface protein (MSP)1a and MSP2 epitope-specific CD4+ T lymphocytes using bovine DRB3*1101 and DRB3*1201 tetramers. *Immunogenetics* 58, 726-739.

Ogg G.S., Dunbar P.R., Cerundolo V., McMichael A.J., Lemoine N.R. & Savage P. (2000) Sensitization of tumour cells to lysis by virus-specific CTL using antibody-targeted MHC class I/peptide complexes. *Br. J. Cancer* 82, 1058-1062.

Olsen C.W. (2002) The emergence of novel swine influenza viruses in North America. *Virus Res.* 85, 199-210.

Olvera-Gomez I., Hamilton S.E., Xiao Z., Guimaraes C.P., Ploegh H.L., Hogquist K.A., Wang L. & Jameson S.C. (2012) Cholera toxin activates nonconventional adjuvant pathways that induce protective CD8 T-cell responses after epicutaneous vaccination. *Proc. Natl. Acad. Sci. U. S. A* 109, 2072-2077.

Orr H.T., Lancet D., Robb R.J., Lopez de Castro J.A. & Strominger J.L. (1979) The heavy chain of human histocompatibility antigen HLA-B7 contains an immunoglobulin-like region. *Nature* 282, 266-270.

Ostergaard P.L., Nissen M.H., Hansen N.J., Nielsen L.L., Lauenmoller S.L., Blicher T., Nansen A., Sylvester-Hvid C., Thromsen A.R. & Buus S. (2001) Efficient assembly of recombinant major histocompatibility complex class I molecules with preformed disulfide bonds. *Eur. J. Immunol.* 31, 2986-2996.

Pacheco J.M., Brum M.C., Moraes M.P., Golde W.T. & Grubman M.J. (2005) Rapid protection of cattle from direct challenge with foot-and-mouth disease virus (FMDV) by a single inoculation with an adenovirus-vectored FMDV subunit vaccine. *Virology* 337, 205-209.

Parish I.A., Kaech S.M. (2009) Diversity in CD8(+) T cell differentiation. *Curr. Opin. Immunol.* 21, 291-297.

Patch J.R., Pedersen L.E., Toka F.N., Moraes M., Grubman M.J., Nielsen M., Jungersen G., Buus S. & Golde W.T. (2011) Induction of foot-and-mouth disease virus-specific cytotoxic T cell killing by vaccination. *Clin. Vaccine Immunol.* 18, 280-288.

Pedersen L.E., Harndahl M., Nielsen M., Patch J.R., Jungersen G., Buus S. & Golde W.T. (2012a) Identification of peptides from foot-and-mouth disease virus structural proteins bound by class I swine leukocyte antigen (SLA) alleles, SLA-1*0401 and SLA-2*0401. *Anim Genet.*

Pedersen L.E., Harndahl M., Rasmussen M., Lamberth K., Golde W.T., Lund O., Nielsen M. & Buus S. (2011) Porcine major histocompatibility complex (MHC) class I molecules and analysis of their peptide-binding specificities. *Immunogenetics* 63, 821-834.

Pedersen L.E., Rasmussen M., Harndahl M., Nielsen M., Buus S. & Jungersen G. (2012b) An analysis of affinity and stability in the identification of peptides bound by Swine Leukocyte Antigens (SLA) combining matrix- and NetMHCpan based peptide selection. *Immunogenetics* Manuscript ready for submisssion.,

Pedersen L.O., Stryhn A., Holter T.L., Etzerodt M., Gerwien J., Nissen M.H., Thogersen H.C. & Buus S. (1995) The interaction of beta 2-microglobulin (beta 2m) with mouse class I major histocompatibility antigens and its ability to support peptide binding. A comparison of human and mouse beta 2m. *Eur. J. Immunol.* 25, 1609-1616.

Penn D.J., Damjanovich K. & Potts W.K. (2002) MHC heterozygosity confers a selective advantage against multiple-strain infections. *Proc. Natl. Acad. Sci. U. S. A* 99, 11260-11264.

Racaniello V.R. (2006) Picornaviridae: the viruses and their replication. In: Fields Virology, 5th edn. Lippincott Williams & Wilkins, Philidelphia, PA, pp 795-838.

Renard C., Kristensen B., Gautschi C., Hruban V., Fredholm M. & Vaiman M. (1988) Joint report of the first international comparison test on swine lymphocyte alloantigens (SLA). *Anim Genet.* 19, 63-72.

Richt J.A., Lager K.M., Janke B.H., Woods R.D., Webster R.G. & Webby R.J. (2003) Pathogenic and antigenic properties of phylogenetically distinct reassortant H3N2 swine influenza viruses cocirculating in the United States. *J. Clin. Microbiol.* 41, 3198-3205.

Robert B., Guillaume P., Luescher I., Romero P. & Mach J.P. (2000) Antibody-conjugated MHC class I tetramers can target tumor cells for specific lysis by T lymphocytes. *Eur. J. Immunol.* 30, 3165-3170.

Robins H.S., Campregher P.V., Srivastava S.K., Wacher A., Turtle C.J., Kahsai O., Riddell S.R., Warren E.H. & Carlson C.S. (2009) Comprehensive assessment of T-cell receptor beta-chain diversity in alphabeta T cells. *Blood* 114, 4099-4107.

Rodriguez L.L., Grubman M.J. (2009) Foot and mouth disease virus vaccines. *Vaccine* 27 Suppl 4, D90-D94.

Romero P., Cerottini J.C. & Speiser D.E. (2004) Monitoring tumor antigen specific T-cell responses in cancer patients and phase I clinical trials of peptide-based vaccination. *Cancer Immunol. Immunother.* 53, 249-255.

Romero P., Dunbar P.R., Valmori D., Pittet M., Ogg G.S., Rimoldi D., Chen J.L., Lienard D., Cerottini J.C. & Cerundolo V. (1998) Ex vivo staining of metastatic lymph nodes by class I major histocompatibility

complex tetramers reveals high numbers of antigen-experienced tumor-specific cytolytic T lymphocytes. *J. Exp. Med.* 188, 1641-1650.

Rothschild M.F., Chen H.L., Christian L.L., Lie W.R., Venier L., Cooper M., Briggs C. & Warner C.M. (1984) Breed and swine lymphocyte antigen haplotype differences in agglutination titers following vaccination with B. bronchiseptica. *J. Anim Sci.* 59, 643-649.

Rueckert R.R., Wimmer E. (1984) Systematic nomenclature of picornavirus proteins. *J. Virol.* 50, 957-959.

Saalmuller A. (2006) New understanding of immunological mechanisms. *Vet. Microbiol.* 117, 32-38.

Salter R.D., Norment A.M., Chen B.P., Clayberger C., Krensky A.M., Littman D.R. & Parham P. (1989) Polymorphism in the alpha 3 domain of HLA-A molecules affects binding to CD8. *Nature* 338, 345-347.

Sanz-Parra A., Sobrino F. & Ley V. (1998) Infection with foot-and-mouth disease virus results in a rapid reduction of MHC class I surface expression. *J. Gen. Virol.* 79 (Pt 3), 433-436.

Saxena R.K., Tripathi P. & Rawat G. (2012) Pandemism of swine flu and its prospective drug therapy. *Eur. J. Clin. Microbiol. Infect. Dis.*

Schatz D.G. (2004) V(D)J recombination. *Immunol. Rev.* 200, 5-11.

Schiott A., Larsson K., Manniche S., Kalliomaki S., Heydenreich A.V., Dalsgaard K. & Kirkby N. (2011) Posintro-HBsAg, a modified ISCOM including HBsAg, induces strong cellular and humoral responses. *Int. J. Pharm.* 414, 312-320.

Schmidt E.G., Buus S., Thorn M., Stryhn A., Leisner C. & Claesson M.H. (2009) Peptide specific expansion of CD8(+) T cells by recombinant plate bound MHC/peptide complexes. *J. Immunol. Methods* 340, 25-32.

Scudamore J.M., Harris D.M. (2002) Control of foot and mouth disease: lessons from the experience of the outbreak in Great Britain in 2001. *Rev. Sci. Tech.* 21, 699-710.

Seder R.A., Darrah P.A. & Roederer M. (2008) T-cell quality in memory and protection: implications for vaccine design. *Nat. Rev. Immunol.* 8, 247-258.

Shapiro-Shelef M., Calame K. (2005) Regulation of plasma-cell development. *Nat. Rev. Immunol.* 5, 230-242.

Singer D.S., Mozes E., Kirshner S. & Kohn L.D. (1997) Role of MHC class I molecules in autoimmune disease. *Crit Rev. Immunol.* 17, 463-468.

Smith D.M., Lunney J.K., Martens G.W., Ando A., Lee J.H., Ho C.S., Schook L., Renard C. & Chardon P. (2005) Nomenclature for factors of the SLA class-I system, 2004. *Tissue Antigens* 65, 136-149.

Sorensen K.J., de S.K., Dyrting K.C., Grazioli S. & Haas B. (2005) Differentiation of foot-and-mouth disease virus infected animals from vaccinated animals using a blocking ELISA based on baculovirus expressed FMDV 3ABC antigen and a 3ABC monoclonal antibody. *Arch. Virol.* 150, 805-814.

Stanway G., Brown F., Christian P., Hovi T., Hyypiä T., King A.M.Q., Knowles N.J., Lemon S.M., Minor P.D., Pallansch M.A., Palmenberg A.C. & Skern T. (2005) Virus taxonomy: classification and nomenclature of

viruses: eighth report of the International Committee on Taxonomy of Viruses. Elsevier Academic Press, San Diego, CA, pp 757-778.

Stryhn A. Yellow fever peptides identified to be epitopes in some donors but not others, despite sharing a certain HLA allele susceptible for peptide binding. Only very few epitopes are dominant in all donors. 27-11-2012.
Ref Type: Personal Communication

Stryhn A., Pedersen L.O., Romme T., Holm C.B., Holm A. & Buus S. (1996) Peptide binding specificity of major histocompatibility complex class I resolved into an array of apparently independent subspecificities: quantitation by peptide libraries and improved prediction of binding. *Eur. J. Immunol.* 26, 1911-1918.

Suhrbier A. (1997) Multi-epitope DNA vaccines. *Immunol. Cell Biol.* 75, 402-408.

Sylvester-Hvid C., Kristensen N., Blicher T., Ferre H., Lauemoller S.L., Wolf X.A., Lamberth K., Nissen M.H., Pedersen L.O. & Buus S. (2002) Establishment of a quantitative ELISA capable of determining peptide - MHC class I interaction. *Tissue Antigens* 59, 251-258.

Tanaka-Matsuda M., Ando A., Rogel-Gaillard C., Chardon P. & Uenishi H. (2009) Difference in number of loci of swine leukocyte antigen classical class I genes among haplotypes. *Genomics* 93, 261-273.

Thakur A., Pedersen L.E. & Jungersen G. (2012) Immune markers and correlates of protection for vaccine induced immune responses. *Vaccine* 30, 4907-4920.

Thompson D., Muriel P., Russell D., Osborne P., Bromley A., Rowland M., Creigh-Tyte S. & Brown C. (2002) Economic costs of the foot and mouth disease outbreak in the United Kingdom in 2001. *Rev. Sci. Tech.* 21, 675-687.

Thomson S.A., Sherritt M.A., Medveczky J., Elliott S.L., Moss D.J., Fernando G.J., Brown L.E. & Suhrbier A. (1998) Delivery of multiple CD8 cytotoxic T cell epitopes by DNA vaccination. *J. Immunol.* 160, 1717-1723.

thor Straten P., Kirkin A.F., Siim E., Dahlstrom K., Drzewiecki K.T., Seremet T., Zeuthen J., Becker J.C. & Guldberg P. (2000) Tumor infiltrating lymphocytes in melanoma comprise high numbers of T-cell clonotypes that are lost during in vitro culture. *Clin. Immunol.* 96, 94-99.

Tonegawa S. (1983) Somatic generation of antibody diversity. *Nature* 302, 575-581.

Torremorell M., Allerson M., Corzo C., Diaz A. & Gramer M. (2012) Transmission of Influenza A Virus in Pigs. *Transbound. Emerg. Dis.*

Trebbien R., Larsen L.E. & Viuff B.M. (2011) Distribution of sialic acid receptors and influenza A virus of avian and swine origin in experimentally infected pigs. *Virol. J.* 8, 434.

Ujvari B., Belov K. (2011) Major histocompatibility complex (MHC) markers in conservation biology. *Int. J. Mol. Sci.* 12, 5168-5186.

Ullman E.F., Kirakossian H., Singh S., Wu Z.P., Irvin B.R., Pease J.S., Switchenko A.C., Irvine J.D., Dafforn A., Skold C.N. & . (1994) Luminescent oxygen channeling immunoassay: measurement of particle binding kinetics by chemiluminescence. *Proc. Natl. Acad. Sci. U. S. A* 91, 5426-5430.

Ullman E.F., Kirakossian H., Switchenko A.C., Ishkanian J., Ericson M., Wartchow C.A., Pirio M., Pease J., Irvin B.R., Singh S., Singh R., Patel R., Dafforn A., Davalian D., Skold C., Kurn N. & Wagner D.B. (1996) Luminescent oxygen channeling assay (LOCI): sensitive, broadly applicable homogeneous immunoassay method. *Clin. Chem.* 42, 1518-1526.

Vaiman M., Renard C., LaFage P., Ameteau J. & Nizza P. (1970) Evidence for a histocompatibility system in swine (SL-A). *Transplantation* 10, 155-164.

van der Burg S.H., Visseren M.J., Brandt R.M., Kast W.M. & Melief C.J. (1996) Immunogenicity of peptides bound to MHC class I molecules depends on the MHC-peptide complex stability. *J. Immunol.* 156, 3308-3314.

Van Weemen B.K., Schuurs A.H. (1971) Immunoassay using antigen-enzyme conjugates. *FEBS Lett.* 15, 232-236.

Viza D., Sugar J.R. & Binns R.M. (1970) Lymphocyte stimulation in pigs: evidence for the existence of a single major histocompatibility locus, PL-A. *Nature* 227, 949-950.

Webster R.G., Bean W.J., Gorman O.T., Chambers T.M. & Kawaoka Y. (1992) Evolution and ecology of influenza A viruses. *Microbiol. Rev.* 56, 152-179.

Wei H., Wang R., Yuan Z., Chen C.Y., Huang D., Halliday L., Zhong W., Zeng G., Shen Y., Shen L., Wang Y. & Chen Z.W. (2009) DR*W201/P65 tetramer visualization of epitope-specific CD4 T-cell during M. tuberculosis infection and its resting memory pool after BCG vaccination. *PLoS. One.* 4, e6905.

Wijdeven R.H., Bakker J.M., Paul P. & Neefjes J. (2012) Exploring genome-wide datasets of MHC class II antigen presentation. *Mol. Immunol.*

Wooldridge L., Lissina A., Cole D.K., van den Berg H.A., Price D.A. & Sewell A.K. (2009) Tricks with tetramers: how to get the most from multimeric peptide-MHC. *Immunology* 126, 147-164.

Xu X.N., Screaton G.R. (2002) MHC/peptide tetramer-based studies of T cell function. *J. Immunol. Methods* 268, 21-28.

Zhang N., Qi J., Feng S., Gao F., Liu J., Pan X., Chen R., Li Q., Chen Z., Li X., Xia C. & Gao G.F. (2011) Crystal structure of swine major histocompatibility complex class I SLA-1 0401 and identification of 2009 pandemic swine-origin influenza A H1N1 virus cytotoxic T lymphocyte epitope peptides. *J. Virol.* 85, 11709-11724.

Zuber B., Levitsky V., Jonsson G., Paulie S., Samarina A., Grundstrom S., Metkar S., Norell H., Callender G.G., Froelich C. & Ahlborg N. (2005) Detection of human perforin by ELISpot and ELISA: ex vivo identification of virus-specific cells. *J. Immunol. Methods* 302, 13-25.

PhD thesis
Lasse Eggers Pedersen

DTU Veterinærinstituttet
Danmarks Tekniske Universitet

Bülowsvej 27
1870 Frederiksberg C.
Tlf. 35 88 60 00
www.vet.dtu.dk